

**Physical Characterization and Benthic Megafauna Distribution and Species**

**Composition on Orphan Knoll and Orphan Seamount, NW Atlantic**

by

© Shawn P. Meredyk

A Thesis submitted to the

School of Graduate Studies

in partial fulfillment of the requirements for the degree of

**Master of Science**

**Environmental Science Program**

Memorial University of Newfoundland

**January 18, 2017**

St. John's

Newfoundland

## Abstract

Orphan Knoll (OK) is an 'orphaned' fragment of the North American continental crust that contains ~250 mounds of unknown composition ranging from 60 to 600 m of meters tall and 1 to 3 km wide. The adjacent “Orphan Seamount” (OS) is located 9 km NE of the SE portion of OK and is a volcanic seamount. The purpose of this study was to: determine the age and composition of the enigmatic OK mounds and OS, in an effort to better understand their origin and thus physical deep-sea habitat; to identify the distribution and abundance of the benthic megafauna of OK and OS; to examine the effects of bathymetry, oceanography and geology on deep-sea community composition.

A multipurpose survey using the remotely operated vehicle (ROV) ROPOS was used to collect geological substrate samples, biological presence data (HD video), oceanographic data (conductivity, temperature and density (CTD)) and high and low resolution multibeam imagery.

Rock samples on OS were identified as basaltic bedrock with limestone-filled vesicles (mid-Miocene aged through identification of *Globigerina* spp. and *Orbulina* spp. of pelagic foraminifera); thereby, identifying the OS as a volcanic seamount having been formed between the lower Cretaceous and the mid Miocene. Rock samples from the OK mounds identified mid-Miocene bedded pelagic limestone bedrock as the upper layer of limestone on top of the OK mounds. An unconformity was discovered between units 2 and 3 of the bedded OK mound limestone, identifying tilting of the faulted-blocks that are the Orphan Knoll mounds.

The formation of the OK mounds possibly occurred through Neogene faulting through plate movements along the White Sail fault and quaternary faulting along the Charlie Gibbs Fracture Zone (CGFZ).

On six ROV dives, 18 identified species of coral, 4 species of sponges, and 10 species of other deep-sea megafauna were identified. Amongst all of the recorded megafaunal species, 10 large concentrations (>20% area coverage) were grouped in an effort to further examine community turnover factors.

Statistical analysis using gradientForest identified that bathymetry data of an intermediate scale (100 m spatial resolution) was the most accurate data to collect to explain megafaunal distribution and abundance through examining changes in community turnover along driver gradients in the deep-sea megafaunal species; however, surficial geology and oceanographic data were also important drivers in distribution and abundance of deep-sea megafauna. The variables depth, slope and aspect were found as being the most accurate descriptors when assessing changes in deep-sea megafaunal community turnover.

## ACKNOWLEDGEMENTS

Interdisciplinary research is always a collaborative affair and this research could not have been possible without the help of the support of the Department of Fisheries and Oceans (DFO), Canadian Coastguard Ship *Hudson* (CCGS), Natural Resources Canada (NRCAN) and the Geological Survey of Canada (GSC). Collaborations between DFO, NRCAN /GSC, Memorial University of Newfoundland (MUN), Dalhousie University, L'Université du Québec à Montréal (UQAM) were necessary due to the financial and physical involvement needed to undertake a mission of this nature (e.g. ROV operations to the deep-sea). The support crew for the Remotely Operated Platform for Oceanographic Science (ROPOS) was pushed to perform at their best and I am thankful for their hard work. I need to thank Paul Fraser (GSC) for his expert help with many of my ArcGIS woes; Pim Kuus (Ocean Mapping Group (OMG) / University of New Brunswick (UNB)) for helping me edit /cleanup multibeam data; Nicole Debond (MUN) and Dr. Susan Zeigler (MUN) for their help with XRD sample preparation; Dr. David Mosher (GSC) for access to use the Kommander Jack (NRCAN) multibeam data for the predictive biological models for the entire Orphan Knoll and Seamount areas; Dr. Brian MacLean (GSC) for his help with some IRD identification; Dr. Graham Layne (MUN) and Michael Schaffer (MUN) for their help in rock type identification and petrographic microscope use; Dr. Wanda Aylward (MUN) for her assistance with XRD sample processing; Allan Ruffman (GeoMarine Inc.) for his help with strike and dips and Orphan Knoll geology; Dr. David Scott (DAL), Dr. Pierro Ascoli (GSC) and Dr. Kevin Cooper

(RPS Energy) for helping out with the micro and nanofossils identification. I especially need to thank my supervisors Dr. Evan Edinger (MUN) and Dr. David J.W. Piper (GSC /NRCAN, DAL) for their expertise, guidance and patience throughout this project.

# Table of Contents

<b>1</b>	<b>INTRODUCTION</b>	<b>1</b>
<b>1.1</b>	<b>Geology of Volcanic and Non-Volcanic Mounds</b>	<b>3</b>
1.1.1	Seamount Geology	3
1.1.2	Deep-Sea Mound / Knoll Geology	4
1.1.3	Enigmatic Mounds of Orphan Knoll	5
<b>1.2</b>	<b>Drivers of Deep-Sea Megafaunal Species Distributions</b>	<b>6</b>
1.2.1	Bathymetry	6
1.2.2	Oceanography	7
1.2.3	Geology	7
<b>1.3</b>	<b>Executive Summary</b>	<b>8</b>
<b>2</b>	<b>GEOLOGICAL INSIGHTS INTO BATHYAL ENIGMATIC MOUNDS THROUGH INVESTIGATION OF THE ENIGMATIC MOUNDS FROM ORPHAN KNOLL, NORTHWEST ATLANTIC OCEAN</b>	<b>9</b>
	<b>Abstract</b>	<b>9</b>
<b>2.1</b>	<b>Introduction</b>	<b>10</b>
2.1.1	Geological Setting of the Enigmatic Mounds of Orphan Knoll	11
2.1.2	Study Objectives	15
<b>2.2</b>	<b>Methods</b>	<b>18</b>

2.2.1	Geological Survey Planning	18
2.2.1.1	Historical Acoustic Imagery	18
	Seismic Profiles	18
	Side scan Imagery	19
	Multibeam Bathymetry	19
2.2.1.2	Cruise Collected Acoustic Imagery	20
2.2.2	ROV Dive Planning	22
2.2.3	Geological Sampling	24
2.2.4	Thin Section Analysis	25
2.2.5	XRD Analysis	26
2.2.6	Data Collection through HD Video Analysis	26
2.2.7	Calibration of the Estimate of Geological Coverage	29
2.2.8	Surficial Geology Mapping	31
2.2.9	ROV Imagenex Multibeam Bathymetry Collection and Processing	32
2.2.9.1	GIS Mapping Note	33
2.2.10	Measurements of Strikes and Dips	33
2.2.11	Dataset Integration / Database Management	35
<b>2.3</b>	<b>Results: Orphan Knoll (D1341- 46) Geological Survey</b>	<b>36</b>
2.3.1	SE Orphan Knoll (Dive 1341)	36
2.3.1.1	Geological Sample Characteristics	36
	Eocene Ooze	36
2.3.1.2	Manganese Nodules and Crusts	42
	Mn Nodules	42
	Mn Crusts	42
2.3.1.3	Limestone	44

2.3.1.4	Characteristics of the Surficial Geological Units (SGU)	48
2.3.2	NE Orphan Knoll (Dive 1343)	48
2.3.2.1	Geological Sample Characteristics	48
2.3.2.2	Characteristics of the Surficial Geological Segments	55
2.3.2.3	Geomorphological Characteristics	58
<b>2.4</b>	<b>Discussion</b>	<b>62</b>
2.4.1	Were previous interpretations of “bedrock” based on IRD?	62
2.4.2	The role of faults in the formation of enigmatic mounds	62
2.4.2.1	Strike and Dip Evidence of Block Faulting	65
2.4.3	Evidence for Sea-floor Dissolution of Carbonate	66
2.4.4	Evidence of Bedded Limestone	67
<b>2.5</b>	<b>Conclusions</b>	<b>70</b>
<b>2.6</b>	<b>Bibliography</b>	<b>72</b>
<b>2.7</b>	<b>Appendix</b>	<b>86</b>
<b>3</b>	<b>COMPOSITIONAL FACIES, AGE AND ORIGIN OF ORPHAN SEAMOUNT</b>	<b>89</b>
<b>3.1</b>	<b>Introduction</b>	<b>90</b>
3.1.1	Study Objectives	91
<b>3.2</b>	<b>Methods</b>	<b>92</b>
<b>3.3</b>	<b>Results</b>	<b>92</b>
3.3.1	Seismic Data Collection	92
3.3.2	Geological Sample Characteristics	92

3.3.2.1	Granites	92
3.3.2.2	Basalt	93
3.3.2.3	Limestone	95
3.3.3	Surficial Geological Segment Characteristics	98
<b>3.4</b>	<b>Discussion</b>	<b>106</b>
<b>3.5</b>	<b>Conclusion</b>	<b>108</b>
<b>3.6</b>	<b>Bibliography</b>	<b>109</b>
<b>4</b>	<b>ENVIRONMENTAL DRIVERS OF COMMUNITY COMPOSITION, ABUNDANCE AND DISTRIBUTION OF DEEP-SEA MEGAFUNA FROM THE ORPHAN KNOLL AND ORPHAN SEAMOUNT</b>	<b>123</b>
<b>4.1</b>	<b>Introduction</b>	<b>124</b>
4.1.1	Study Area	126
4.1.1.1	Orphan Knoll	126
4.1.1.2	Orphan Seamount	127
4.1.1.3	Oceanographic Characteristics of Orphan Knoll and Orphan Seamount	128
4.1.1.4	Anthropogenic Activities on Orphan Knoll and Orphan Seamount	130
4.1.1.5	Conservation- Preservation Measures for Orphan Knoll	130
4.1.1.6	Deep Sea Habitats	130
4.1.2	Study Summary	131
<b>4.2</b>	<b>Methods</b>	<b>132</b>
4.2.1	ROV Oceanographic Data Collection	132
4.2.2	Benthic Terrain Characterization	133

4.2.3	Dataset Integration / Database Management	134
4.2.4	Species Distribution	134
4.2.5	Community Analysis	134
	Community Analysis Plotting	136
	gradientForest Predictions	136
<b>4.3</b>	<b>Results</b>	<b>138</b>
4.3.1	Distribution and Abundance of Deep-Sea Megafauna on Three Deep-Sea Habitat Types (Seamount, Mounds, Flats)	138
4.3.1.1	Identified Megafauna	138
4.3.1.2	Coral Species Identified	139
4.3.1.3	Sponge Species Identified	140
4.3.1.4	Non-Coral and Non-Sponge Species Identified	141
4.3.2	Habitat 1 - Orphan Seamount (D1340)	142
4.3.2.1	Coral	142
4.3.2.2	Sponge	142
4.3.2.3	Other Invertebrates	144
4.3.2.4	Concentrations of Megafauna	144
4.3.3	Habitat 2 - Orphan Knoll Enigmatic Mounds (D1341 and D1343)	145
4.3.3.1	SE Mounds (D1341)	145
	Coral	145
	Sponges	145
	Other Invertebrates	145
	Concentrations of Megafauna	147
4.3.3.2	NE Mounds (D1343)	147
	Coral	147
		X

Sponge	147
Other Invertebrates	149
Concentrations of Megafauna	149
4.3.4 Habitat 3 – Orphan Knoll Deep-Sea Flats (D1342, 1345, 1346)	150
4.3.4.1 South OK (D1342)	150
Coral	150
Sponge	150
Other Invertebrates	150
4.3.4.2 Eastern OK (D1345)	152
Coral	152
Sponge	152
Other Invertebrates	152
4.3.4.3 Western OK (D1346)	154
Coral	154
Sponge	154
Other Invertebrates	154
<b>4.4 Community Composition Results</b>	<b>156</b>
4.4.1 Deep-Sea Benthic Coral Community	156
4.4.1.1 Coral Predictor Importance	156
4.4.1.2 Coral Predictor Importance Gradients	156
Coral Species Cumulative Importance (SPI)	4-159
Geographic clustering of important predictors relative to species abundance	164
4.4.1.3 Sponge Predictor Importance	167
4.4.1.4 Sponge Predictor Importance Gradients	167
Sponge Species Cumulative Importance (SPI)	170

Geographic clustering of important predictors relative to species abundance	174
4.4.1.5    Non-Coral and Non-Sponge Megafaunal Predictor Importance	177
4.4.1.6    Non-Coral and Non-Sponge Megafaunal Predictor Importance Gradients	177
Non-Coral and Non-Sponge Megafaunal Species Cumulative Importance (SPI)	181
Geographic clustering of important predictors relative to species abundance	185
4.4.1.7    Concentrated Megafaunal Predictor Importance	188
4.4.1.8    Concentrated Megafaunal Predictor Importance Gradients	188
Concentrated Megafaunal Species Cumulative Importance (SPI)	192
Geographic clustering of important predictors relative to species abundance	196
<b>4.5 Discussion</b>	<b>199</b>
4.5.1    Environmental Mechanisms Driving Deep-Sea Megafaunal Abundance and Distribution	200
4.5.1.1    Bathymetry (Depth, Slope, Aspect)	200
Depth	200
Slope	201
Aspect	201
4.5.1.2    Oceanography	202
4.5.1.3    Surficial Geology	205
4.5.1.4    Not a Typical Continental Margin	206
4.5.1.5    Community Ecology Analysis	209
<b>4.6 Conclusions</b>	<b>211</b>
<b>4.7 Bibliography</b>	<b>212</b>
<b>4.8 Appendices</b>	<b>227</b>

<b>5</b>	<b>CONCLUDING STATEMENTS</b>	<b>233</b>
<b>5.1</b>	<b>Physical Characterization of Orphan Knoll and Orphan Seamount</b>	<b>233</b>
<b>5.2</b>	<b>Deep-Sea Megafaunal Community Analysis</b>	<b>234</b>
<b>5.3</b>	<b>Emerging Issues</b>	<b>235</b>
5.3.1	Climate Change and the Deep-Sea	235
5.3.2	Conservation and Preservation	235

## **List of Figures**

- Figure 1-1. Orphan Knoll(yellow circle) and Orphan Seamount (white dot) locations relative to Newfoundland and the Grand Banks of Newfoundland. Prominent faults near the Orphan Knoll area are also identified (Charlie Gibbs Fracture Zone (CBFZ) and Charlie Gibbs Transfer Zone (CBTZ and White Sail fault. Chron 34 is ~100 Km eastward of Orphan Knoll. 6
- Figure 2-1. Orphan Knoll (yellow circle) and Orphan Seamount (white dot) locations relative to Newfoundland and the Grand Banks of Newfoundland. Prominent faults near the Orphan Knoll area are also identified (Charlie Gibbs Fracture Zone (CBFZ) and Charlie Gibbs Transfer Zone (CBTZ and White Sail fault. Chron 34 is ~100 Km eastward of Orphan Knoll. 12
- Figure 2-2. Orphan Knoll and Orphan Seamount with historical and new enigmatic mound (green) locations identified through historical compilation and interpretation of seismic reflection profiles (Bathymetry : GEBCO) 14
- Figure 2-3. 2D Seismic Profile of SW OK Mound (Nader) showing the SW flank of OK and SE extent of Orphan Basin (Horizons and Faults interpreted by Dr. Enachescu 2004)); (FGP-MUN) 16
- Figure 2-4. Huntec sub-bottom profile from CCGS Hudson cruise 2004-024 of a NE OK Mound at the 1978 dredge location (GSC-NRCAN, Piper, 2004) 17
- Figure 2-5. M /V Kommandor Jack (Fugro) multibeam imagery overlain by M /V Healy multibeam imagery; inset images of 3D view of the Orphan Knoll from various directions

and a zoomed in view of the enigmatic mounds on the NE slope of Orphan Knoll (7x exaggerated)	21
Figure 2-6. M /V Kommander Jack (Fugro) multibeam imagery overlain by M /V Healy multibeam imagery (base layer bathymetry : GEBCO )	23
Figure 2-7. ROPOS using jack hammer attachment to attempting to fracture bedrock from Orphan Seamount (D1340); green dots are 10 cm apart	25
Figure 2-8. HD video display (Left) with ClassActMapper Graphical User-Interface (GUI) (right)	27
Figure 2-9. HD video frame grab (Top), showing the progression of image changes to determine % coverage area; non-granule features removed (middle) and the final area of granules coverage (bottom)	30
Figure 2-10. Dive 1341, SE Orphan Knoll Mounds Surficial Geology (% Coverage) separated into surficial geological units (pink features)	31
Figure 2-11. Strike and dip locations on Orphan Knoll bedrock outcrop (mound); including rock collection locations. Delta T multibeam data collected from ROPOS. Multibeam data was manually processed in CARIS's HIPS & SIPS.	34
Figure 2-12. Geological Data Extraction and Processing Flow Diagram	35
Figure 2-13. ROPOS dive 1341, Calcareous ooze outcrop with Mn nodules on top of and at the base of the outcrop (Top) Scooping of calcareous ooze outcrop (bottom);green lasers are 10 cm apart; 2886 m depth	38
Figure 2-14. ROPOS Dive 1341 on SE Orphan Knoll mounds with inset 3D image of dive track relative to sampling locations	39

Figure 2-15. Smear slide of Calcareous Ooze from SE Orphan Knoll showing nannofossil Discoaster spp. (early Eocene, viewed at 50x)	40
Figure 2-16. XRD results of Calcareous Ooze sample R1341-4 from SE Ok, identifying the top five matching minerals in two different viewable formats	41
Figure 2-17. Mn-oxide crust (R1341-19) collected from a bedrock outcrop by ROPOS (green lasers are 10 cm apart)	43
Figure 2-18. Sample collection (R1341-7) pulled from bedrock outcrop on SE Orphan Knoll by ROPOS (green lasers are 10 cm apart)	45
Figure 2-19. Sample collection (R1341-10) from a bedrock outcrop on SE Orphan Knoll by ROPOS (green lasers are 10 cm apart)	45
Figure 2-20. Ice-Rafted Argillaceous Limestone (R1341-20) collected from a bedrock outcrop by ROPOS (green lasers are 10 cm)	46
Figure 2-21. R1341-20 Argillaceous Limestone collected from SE Orphan Knoll (Late Ordovician, IRD, viewed at 1.6x)	47
Figure 2-22. Rock sampling locations (red) for dive 1343 overlain with ROPOS collected multibeam data; inset 3D image of the latest multibeam imagery for the Orphan Knoll with the ROPOS dive track overlain.	49
Figure 2-23. Pelagic Limestone (R1343-3) collected by ROPOS from a bedrock outcrop covered by extensive Mn oxidation	50
Figure 2-24. Fe-Mn Oxide crust (R1343-4) collected by ROPOS from a bedrock outcrop	51

Figure 2-25. Fe-Mn oxide crust (R1343-10) collected by ROPOS from a bedrock outcrop (green lasers are 10 cm apart)	52
Figure 2-26. Fe-Mn oxide crust (R1343-14) collected by ROPOS from a bedrock outcrop (green lasers are 10 cm apart)	53
Figure 2-27. Fe-Mn oxide crust (R1343-15) collected by ROPOS from a bedrock outcrop (green lasers are 10 cm apart)	54
Figure 2-28. Surficial Geology (% Coverage) units from an Orphan Knoll NE Mound (D1343), divided into surficial Geological Segments (SGUs)	55
Figure 2-29. ROPOS HD video frame grabs as ROPOS travels down the exposed SW side of the NE OK mound. The picture ID is labeled 'Pic' and the heading of ROPOS is shown below the picture ID. Units 1 and 2 are of the same strike and dip; however Unit 2 has thicker bedded layers than Unit 1. Unit 3 is of a different strike, than Units 1 and 2, and has no apparent dip.	57
Figure 2-30. SE wall of Orphan Knoll mound showing Antipatharian Cold-Water corals and a 'graveyard' of sub-fossil <i>Desmophyllum dianthus</i> (Scleractinian) found within a mixture of fine sediment and IRD at the base of the exposed bedded limestone bedrock outcrop	58
Figure 2-31. 2D rendering of 3D imagery from ROPOS Delta T multibeam survey on NE Orphan Knoll mound, dive (D1343), north and south faces.	59
Figure 2-32. Dive 1343 (NE OK mound) ROPOS headings (colored arrows indicating heading) with strikes and dips (white); Fig. 2-28 inset, identifying the 'Pic' ID (black) relative to the stratigraphic Unit number.	60

- Figure 2-33. Orphan Knoll NE mound imagery of depression feature and eroded wall surface from dive 1343. Green dots are 10cm apart for scale reference (bottom center placement). 61
- Figure 2-34. Inset TGS 2D seismic profile providing a cross sectional view WSW -ENE across the Orphan Knoll (right with 3x exaggeration), passing just north of the DSDP site 111 (red cross) and south of the historical dredge locations (yellow cross) and ROPOS 2010-029 rock sample sites (blue dot). Contact TGS for more information on seismic line placements. 64
- Figure 2-35. Gas injection (GI) air gun seismic profile from Hudson 2004-024 cruise, at the location of the 1978 dredge location, identifying ponded sediment between NE OK mounds (GSC-NRCAN) 68
- Figure 2-36. Theoretical throw fault calculations (Pythagorean formula) for a 150 m throw dipping at 30 degrees resulting in a 260 m heave (i.e. NE OK mound) 70
- Figure 3-1. Orphan Knoll (pink circle) and Orphan Seamount (orange) locations relative to Newfoundland and the Grand Banks of Newfoundland. Prominent faults near the Orphan Knoll area are also identified (Charlie Gibbs Fracture Zone (CBFZ) and Charlie Gibbs Transfer Zone (CBTZ and White Sail fault). Chron 34 is ~100 Km eastward of Orphan Knoll. 91
- Figure 3-2. Thin Section of Granodiorite sample (R1340-13) from Orphan Seamount talus and IRD facies (Cross Polarized View at 1.6x Mag.) 93
- Figure 3-3. Basalt sample R1340-26 extracted by ROPOS from a lava outcrop amongst Isididae coral (bamboo coral); green dots are 10 cm apart (visible on ROV armature). 94

Figure 3-4. Thin Section of Orphan Seamount Basalt with geopetal structures (R1340-26B)(left) (1x); zoomed thin section views (right)(5x); carbonate fill within geopetal areas within weathered basalt; bottom right image is the cross polarized view of the above thin section (5x mag.)	95
Figure 3-5. ROPOS extracting rock sample R1340-14 from lava outcrop on Orphan Seamount	96
Figure 3-6. ROPOS extracting rock sample R1340-19 from lava outcrop from Orphan Seamount (green dots are 10 cm apart)	97
Figure 3-7. Thin Section (10x) of Pelagic Cenozoic limestone sample from Orphan Seamount (R1340-19), identifying foraminifera <i>Globigerina</i> spp. and <i>Orbulina</i> spp. foraminifera fossils.	97
Figure 3-8. Pillow Lava (bedrock), talus and IRD from the low-mid slope (3000 m) of Orphan Seamount (D1340).	99
Figure 3-9. Granule dominated facies on Orphan Seamount with <i>Enteropneusta</i> spp. (Acorn Worm); green dots are 10 cm apart	100
Figure 3-10. Fine grained sediment dominated facies found near the top of Orphan Seamount; unknown <i>Isididae</i> spp. Cold-Water Coral( <i>Gorgonian</i> -white box); green dots are 10 cm apart (center of image)	101
Figure 3-11. Lava tubes with talus and IRD filling the depressions in between the lava tubes; Cold-Water Coral <i>Paramuricea</i> spp. ( <i>Gorgonian</i> ) is seen growing on the lava tube on the right; green dots are 10 cm apart (center of image)	102

Figure 3-12. Collapsed Lava Tubes from Orphan Seamount rather covered by Fe-Mn crust, talus, IRD, several unknown sponges (Hexactinellidae) and Chrysogorgia spp. and other unknown Isididae spp. coral (bottom).	103
Figure 3-13. Pillow Basalt from Orphan Knoll covered by several unknown species of Hexactinellidae sponges (glass sponges).	104
Figure 3-14. Talus, IRD and hemi-pelagic sediment from Orphan Seamount slopes in between lava tube outcrops	104
Figure 3-15. Pillow lava and Fe-Mn oxide crust from Orphan Seamount; covered in Crinoidea, Hexactinellidae, Isididae Zoantharia and Chrysogorgia spp. benthic megafauna.	105
Figure 3-16. Thin Section of Fe-Mn Crust from Orphan Seamount (1.6x)	106
Figure 4-1. Orphan Knoll and Orphan Seamount locations relative to Newfoundland, Canada	127
Figure 4-2. Patterns of benthic current flow above Orphan Knoll. Arrows indicate direction of flow (Greenan et al. 2010) .	129
Figure 4-3. Orphan Seamount Surficial Geology and Megafauna Abundance and Distributions Maps (colour gradients in maps have been individually optimized for ease of viewing): Surficial Geology (A), Coral Species Distribution (B), Sponge Distribution (C), Coral Group Distribution by Taxonomic Order (D), Non-Coral or Sponge Invertebrates Distribution (E), Concentrations (>20% surficial coverage) of Megafaunal Groups Distributions (F).	143

Figure 4-4. SE Orphan Knoll Mounds' Surficial Geology , Megafauna Abundance and Distributions Maps (colour gradients in maps have been individually optimized for ease of viewing): Surficial Geology (A), Coral Species Distribution (B), Concentrations (>30% surficial coverage) of Megafaunal Groups Distributions (C), , Non-Coral or Sponge Invertebrates Distribution (D), Sponge Distribution (E). 146

Figure 4-5. NE Orphan Knoll Mound Surficial Geology , Megafauna Abundance and Distributions Maps (colour gradients in maps have been individually optimized for ease of viewing): Surficial Geology (A), Coral Species Distribution (B), Coral Species Distribution just on the mound top (C), Sponge Distribution (D), Non-Coral or Sponge Invertebrates Distribution (E), Concentrations (>30% surficial coverage) of Megafaunal Groups Distributions (F) . 148

Figure 4-6. Southern Orphan Knoll Flats Surficial Geology , Megafauna Abundance and Distributions Maps (colour gradients in maps have been individually optimized for ease of viewing): Surficial Geology (A), Coral Species Distribution (B), Sponge Distribution (C), Non-Coral or Sponge Invertebrates Distribution (D). 151

Figure 4-7. Eastern Orphan Knoll Flats Surficial Geology , Megafauna Abundance and Distributions Maps (colour gradients in maps have been individually optimized for ease of viewing): Surficial Geology (A), Coral Species Distribution (B), Sponge Distribution (C), Non-Coral or Sponge Invertebrates Distribution (D). 153

Figure 4-8. Western Orphan Knoll Flats Surficial Geology, Megafauna Abundance and Distributions Maps (colour gradients in maps have been individually optimized for ease

of viewing): Surficial Geology (A), Coral Species Distribution (B), Sponge Distribution (C), Non-Coral or Sponge Invertebrates Distribution (D). 155

Figure 4-9. gradientForest overall accuracy of community turnover predictors for all coral species (left); species-weighted importance analysis of predictors for coral species (right) from Orphan Seamount and Orphan Knoll. 157

Figure 4-10. Kernel density plots of surrogate gradient changes affecting coral presence from Orphan Seamount and Orphan Knoll 158

Figure 4-11. Cumulative importance (CI)(top) and Overall CI (bottom) plots for coral types for the OK and OS areas; showing change in abundance of individual species, where changes occur on the gradient and the species changing most on each gradient. The top 5 (from 11) species responses are noted within the individual plots. 160

Figure 4-12. Principal Components Analysis of the first two dimensions and the most important predictors as vectors; red crosses identify the most responsive coral fauna; colored and numbered clusters represent inferred assemblages, rather than a continuous representation of coral biodiversity at Orphan Seamount and Orphan Knoll. 165

Figure 4-13. Geospatial cluster occurrences of PCA scores. Dive ID (e.g. D1340) is shown below the actual dive location; Arrows are not vectors, but rather labeling arrows for the most responsive coral fauna and the most important environmental drivers relative to a specific dive site. 166

Figure 4-14. gradientForest overall importance analysis of predictors for all sponge species (left); species-weighted importance analysis of predictors for coral species (right) from Orphan Seamount and Orphan Knoll 168

Figure 4-15. Kernel density analysis plots of surrogate gradient change for sponge presence from Orphan Seamount and Orphan Knoll (blue peaks are standardised by observation density). 169

Figure 4-16. Cumulative importance (CI)(top) and Overall CI (bottom) plots for sponge types for the OK and OS areas; showing change in abundance of individual species, where changes occur on the gradient and the species changing most on each gradient. 173

Figure 4-17. Principal Components Analysis of the first two dimensions and the most important predictors as vectors; red crosses identify the most responsive sponge fauna; colored and numbered clusters represent inferred assemblages, rather than a continuous representation of coral biodiversity at Orphan Seamount and Orphan Knoll. 175

Figure 4-18. Geospatial cluster occurrences of PCA scores. Dive ID (e.g. D1340) is shown below the actual dive location; Arrows are not vectors, but rather labeling arrows for the most responsive sponge fauna and the most important environmental drivers relative to a specific dive site. 176

Figure 4-19. gradientForest overall importance analysis of predictors for all non-coral and non-sponge megafaunal species (left); species-weighted importance analysis of predictors for coral species (right) from Orphan Seamount and Orphan Knoll 179

Figure 4-20. Kernel density plots of surrogate gradient changes affecting non-coral and non-sponge presence from Orphan Seamount and Orphan Knoll 180

Figure 4-21. Cumulative importance plot (top) and Overall CI for non-coral and non-sponge megafaunal species for the OK and OS areas; showing change in abundance of

individual species, where changes occur on the gradient and the species changing most on each gradient. 184

Figure 4-22. Principal Components Analysis of the first two dimensions and the most important predictors as vectors; red crosses identify the most responsive coral fauna; colored and numbered clusters represent inferred assemblages, rather than a continuous representation of non-coral and non-sponge biodiversity at Orphan Seamount and Orphan Knoll. 186

Figure 4-23. Geospatial cluster occurrences of PCA scores. Dive ID (e.g. D1340) is shown below the actual dive location; Arrows are not vectors, but rather labeling arrows for the most responsive non-coral and non-sponge megafauna and the most important environmental drivers relative to a specific dive site. 187

Figure 4-24. gradientForest overall importance analysis of predictors for all concentrations (>20% area coverage) of megafaunal species (left); species-weighted importance analysis of predictors for coral species (right) from Orphan Seamount and Orphan Knoll 190

Figure 4-25. Kernel density analysis plots of surrogate gradient change for concentrations (>20% area coverage) of megafaunal species presence from Orphan Seamount and Orphan Knoll 191

Figure 4-26. Cumulative importance (CI)(top) and Overall CI plots for concentrations (>20% area coverage) of megafaunal species for the OK and OS areas; showing change in abundance of individual species, where changes occur on the gradient and the species changing most on each gradient. 195

Figure 4-27. Principal Components Analysis of the first two dimensions and the most important predictors as vectors; red crosses identify the most responsive coral fauna; colored and numbered clusters represent inferred assemblages, rather than a continuous representation of concentrations (>20% area coverage) biodiversity at Orphan Seamount and Orphan Knoll. 197

Figure 4-28. Geospatial cluster occurrences of PCA scores. Dive ID (e.g. D1340) is shown below the actual dive location; Arrows are not vectors, but rather labeling arrows for the most responsive concentrations (>20% area coverage) megafauna and the most important environmental drivers relative to a specific dive site. 198

## List of Appendices

Appendix 2-1. Rock collection Summary from CCGS Hudson 2010-029 cruise to Orphan Knoll and Orphan Seamount.....	86
Appendix 2-2. Rock Samples from Orphan Knoll and Orphan Seamount on Hudson 2010-029 Cruise.....	87
Appendix 2-3. Surficial Geology in % Coverage separated by Surficial Geological Unit (SGU).....	88
Photo Plate 4-1. Coral fauna from Orphan Seamount and Orphan Knoll; Gorgonian corals (top left), Black-wire coral (bottom-left), Stony coral (green box), Sea Pen (pink box), Soft coral (bottom-right) and Hexacorallia (top-right). ....	139
Photo Plate 4-2. Sponge fauna from Orphan Seamount and Orphan Knoll; Polymastia spp (top left), Euplectella spp. (A and B), Hexactinellidae (Mid and right columns: A-E) except an unknown sponge (top right).....	140
Photo Plate 4-3. Non-Coral and non-Sponge Megafaunal from Orphan Seamount and Orphan Knoll (green dots = 10cm scale); black box (Holothuroidea), red box (Munidopsis spp.), green box (Ophiuroidea), teal blue box (Enteropneusta), pink box (Actinaria), purple box (Echinoidea), magenta box (Crinoidea: stalked (top two images) and unstalked (bottom two images)).....	141
Appendix 4-4. Coral megafauna recorded on Orphan Knoll and Orphan Seamount (D1340). O = order, G = genus, F = family, C = class. rF_Overall_Perf indicates which	

coral fauna performed well enough during RandomForest (rF) analysis to be used for gradientForest analysis.....230

Appendix 4-5. Sponge megafauna recorded on Orphan Knoll and Orphan Seamount (D1340). O = order, G = genus, F = family, C = class. rF\_Overall\_Perf indicates which coral fauna performed well enough during RandomForest (rF) analysis to be used for gradientForest analysis.....231

Appendix 4-6. Other non-coral nor sponge megafauna recorded on Orphan Knoll and Orphan Seamount (D1340). O = order, G = genus, F = family, C = class. rF\_Overall\_Perf indicates which coral fauna performed well enough during RandomForest (rF) analysis to be used for gradientForest analysis. ....231

Appendix 4-7. Grouped concentrations of megafauna recorded on Orphan Knoll and Orphan Seamount (D1340). O = order, G = genus, F = family, C = class. rF\_Overall\_Perf indicates which coral fauna performed well enough during RandomForest (rF) analysis to be used for gradientForest analysis. ....232

# List of Abbreviations

## B

BTM

Benthic Terrain Modeller, 133

## C

Canadian Coastguard Ship

CCGS, iv

CI

Cummulative Importance, 4-159, 160, 161, 162,

163, 164, 170, 171, 172, 173, 181, 182, 183,

184, 192, 193, 194, 195, 201, 209

cumulative importance, 4-159, 170, 181, 192, 193

CITES

Convention on International Trade in Endangered

Species, 2, 130

COB

Continental-Oceanic Boundary, 5, 11

conductivity, temperature and density

CTD, 132

CSIRO

Commonwealth Scientific and Industrial Research

Organisation, 236

## D

Department of Fisheries and Oceans

DFO, iv

DIC

dissolved Inorganic Carbon, 7, 208

DSDP.

Deep-Sea Drilling Platform, 5, 13, 26, 37, 42, 48,

63, 64, 66, 67, 69, 96

## G

GDM

Generalized Dissimilarity Model, 134, 135, 236

Geological Long Range Inclined Asdic

GLORIA, 19

Geological Survey of Canada

GSC, iv

## I

IRD

Ice-Rafted Debris, iv, 24, 47, 48, 56, 58, 62, 70, 71,

86, 93, 98, 99, 102, 103, 104, 108, 130, 205,

206, 207, 233

## J

JDayGMT, 132

## M

Megapixel

MP, 26

Memorial University of Newfoundland

MUN, iv

MTD

Mass Transport Deposit, 70

## N

NAMOC

NW Atlantic Mid-Ocean Channel, 11, 62

Natural Resources Canada

NRCAN, iv

North Atlantic Fisheries Organization

NAFO, 1, 130

NVRM

non-volcanic rifted margin, 90

## O

Ocean Mapping Group

OMG, iv

Orphan Knoll

OK, ii, iv, 1, 9, 19, 86, 130

Orphan Seamount

OS, 86, 93, 123

## P

PCA

Principal Component Analysis, 137, 166, 176, 187,  
198, 204, 229

POM

Particulate Organic Matter, 7

## R

Remotely-Operated Platform for Oceanographic

Science

ROPOS, iv

ROV

Remotely-Operated Vehicle, ii, iii, iv, 15, 22, 24,  
32, 91, 94, 131, 132

## S

SPI

Species Cumulative Importance, 4-159, 161, 162,  
163, 164, 170, 171, 181, 182, 183, 192, 193,  
194

## U

UNCLOS

United Nations Convention on the Law of the Sea,  
19, 199

University of New Brunswick

UNB, iv

USGS

United States Geological Survey, 22

**X**

**V**

XRD

vulnerable marine ecosystem

X-Ray Diffraction, iv, xvii, xviii, 26, 41

VME, 1, 130

## Co-Authorship Statement

**Chapters 2** co-authors in order of contribution, detailing their individual contributions.

1. Shawn Meredyk, primary author. Collected historical imagery (seismic data profiles at GSC-A and MUN, multibeam and GLORIA imagery), recorded and plotted new mound locations, designed the ROPOS dive plans, collected the data during the research mission (3.5 kHz, ClassActMapper, HD video, rock samples), created the thin sections, did the thin section analysis, prepared the ooze for XRD, ran the XRD analysis, post-processed the HD video for all Orphan Knoll dives, edited the multibeam data in CARIS, created all of the images and maps, wrote the entire chapter.
2. Dr. David J.W. Piper, second author. Provided access to historical imagery (GSC-A) and helped with seismic interpretation of mound features, contributed feedback on manuscript structure and flow, and provided in-depth knowledge of marine geology and tectonics of the Orphan Knoll area.
3. Dr. Evan Edinger, third author. Helped in creating the ROPOS dive plans, collecting the data during the research mission ( 3.5 kHz, ClassActMapper, HD video, rock samples and preliminary on-board multibeam editing in CARIS), helped with thin section analysis, contributed to manuscript structure and flow, and provided knowledge of marine geology.
4. Alan Ruffman, fourth author. Helped in pre-cruise planning, helped with strike and dip measurements on Orphan Knoll enigmatic mound, contributed in-depth

knowledge of the geological information collected on Orphan Knoll from the DSDP site 111 Glomar Challenger research cruise.

**Chapter 3** focuses solely on the Orphan Seamount geology and bathymetry. Shawn Meredyk provided preliminary geological and bathymetric analysis along with additional physical samples that were used in the 2013 publication: “Petrology and tectonic significance of seamounts within transitional crust east of Orphan Knoll, offshore eastern Canada” in the journal *Geo-Marine Letters* (Pe-Piper, Georgia; Meredyk, Shawn; Zhang, Yuanyuan; Piper, David; Edinger, Evan). However, the text from this chapter is not the same as the *Geo-Marine Letters* publication.

**Chapter 4** co-authors in order of contribution, detailing their individual contributions.

1. Shawn Meredyk, primary author. Collected historical imagery (seismic data profiles at GSC-A and MUN, multibeam and GLORIA imagery), recorded and plotted new mound locations, designed the ROPOS dive plans, collected the data during the research mission (3.5 kHz, ClassActMapper, HD video, rock samples), created the thin sections, did the thin section analysis, prepared the ooze for XRD, ran the XRD analysis, post-processed the HD video for all Orphan Knoll dives, edited the multibeam data in CARIS, created all of the images and maps, wrote the entire chapter.
2. Dr. Evan Edinger, second author. Helped in creating the ROPOS dive plans, collecting the data during the research mission ( 3.5 kHz, ClassActMapper, HD video, rock samples and preliminary on-board multibeam editing in CARIS),

contributed to manuscript structure and flow, and provided knowledge of Deep-Sea megafauna (e.g. coral, sponge, etc.).

3. Dr. David J.W. Piper, third author. Provided access to historical imagery (GSC-A), contributed feedback on manuscript structure and flow, and provided in-depth knowledge of marine geology of the Orphan Knoll area.

# 1 Introduction

The deep sea is the last frontier on this planet and the geological and especially the biological elements in the deep-sea largely remain mysterious and unexplored (Wright & Goodchild 1997). Deep-sea bathymetric highs, such as knolls and mounds have been explored for their unique biodiversity (Richer-de-Forges et al. 2000; Davies et al. 2007; O'Hara et al. 2008; Burton & Lundsten 2008; Baillon et al. 2014) and also for the natural resource extraction potential (i.e. Oil/Gas, Mn nodules, etc.) (Colman et al. 2005; Fitzgerald & Gillis 2006; Cronan et al. 2010; Moscardelli et al. 2013).

Over time, some stony coral colonies (e.g. *Lophelia pertusa*) can form complex reef-like structures, which provide habitat for a variety of megafauna (Roberts et al. 2006; Althaus et al. 2009). Reefs and seamounts are hotspots of biodiversity (Hall-spencer et al. 2007; Levin et al. 2009; Buhl-Mortensen et al. 2010) and the possibility that mounds on Orphan Knoll were carbonate reef mounds was an exciting possibility to discover a variety of unique and possibly unknown deep-sea megafauna (Laughton et al. 1972; van Hinte et al. 1995; Enachescu 2004; Hall-spencer et al. 2007; O'Hara et al. 2008; Christiansen & Wolff 2009).

The Orphan Knoll was designated as a vulnerable marine ecosystem (VME) area in 2007 and will be protected until 2020, by the North Atlantic Fisheries Organization (NAFO) and the Canadian Department of Fisheries and Oceans (DFO) (Mortensen et al. 2006; ICES 2007; NAFO 2015). Orphan Knoll was protected due to its potential for containing abundant endangered reef-building corals and associated fauna, found within

the Convention on International Trade in Endangered Species (CITES) Appendix II list of endangered species (Mortensen et al. 2006; NAFO SCS 2008).

The current state of deep-sea coral and sponges around the world is entering a threatened state (Davies et al. 2007; Carpenter et al. 2008; Boutillier et al. 2008; Hoffmann et al. 2010). CITES has already placed corals on the appendix II list of endangered species to control the trade in tropical corals as curios (NAFO SCS 2008). Millennial (Roark et al. 2009) to centuries-old (Sherwood & Edinger 2009) cold-water coral have been found in a variety of locations around the world and can be abundant on slopes of a variety of substrates such as continental shelves, canyons, knolls, seamounts, cliffs, fault zones, etc. (Bailey et al. 2003; Colman et al. 2005; Wareham & Edinger 2007).

### **Study Objectives**

The identified research objectives were: [1] determine the age and composition of the enigmatic Orphan Knoll mounds (OK) and Orphan Seamount (OS), in an effort to better understand their origin and thus physical deep-sea habitat; [2] to identify the distribution and abundance of the megafauna of OK and OS; [3] to examine the effects of bathymetry, oceanography and geology on deep-sea community turnover.

Chapter 2 and 3 present the physical characterization results from the geological samples and multibeam imagery. Chapter 4 examines the biological / ecological objectives, which were to identify the distribution and abundance of the megafauna of OK and OS; and to determine the most important environmental drivers on deep-sea benthic megafaunal community composition.

## 1.1 Geology of Volcanic and Non-Volcanic Mounds

### 1.1.1 Seamount Geology

Seamounts, under-water bathymetric highs, are classified as solitary marine features that are taller than 1000m. Seamounts are generally found on oceanic crust and are generally consisting of a volcanic basalt (Moore et al. 1982; Paduan et al. 2007; Pe-Piper et al. 2013), though seamounts aren't all volcanic / basaltic (Fryer & Fryer 1987; Quilty 1997). They are also found at tectonic plate boundaries including oceanic ridges and sometimes at failed rifted margins (i.e. Orphan Knoll) (Etnoyer 2005; Yesson et al. 2011). Seamounts can be found all over the world and can be active or dormant depending on their proximity to mantle hotspots and active tectonic boundaries (Paduan et al. 2007). Active seamounts have been observed having hydrothermal activity (Alt 1988; Barrett et al. 1988; Curewitz & Karson 1997) with sometimes specialist megafaunal species (Richer-de-Forges et al. 2000; Burton & Lundsten 2008; O'Hara et al. 2008). The OS was studied primarily due to its close proximity to the Orphan Knoll, which was the primary area of study for this manuscript and because the OS was an unexplored seamount, possibly within the new Canadian UNCLOS defined exclusive economic zone (EEZ), which required a baseline biological and geological investigation.

## 1.1.2 Deep-Sea Mound / Knoll Geology

Benthic mounds (< 1000m tall features) and knolls (flat shoaling tops sub-sea hills < 1000m tall) are features that are commonly found in either seismic profiles or using other acoustic imaging machinery (e.g. side-scan, multibeam, etc.) during bathymetric and seismic exploration. Offshore bathymetric highs created by foundered continental fragments are one type of submarine knoll and are found in various locations in the world, two examples being in Canada (Orphan Knoll) and Norway (Cromer Knoll) (Hart 1976; Moscardelli et al. 2013). Foundered continental fragments are formed through tectonic forcing and can sometimes contain superficial mounds, which can form through a variety of processes (i.e. faulting, hydrothermal, etc.).

Deep-sea mounds / knolls were historically associated in and around petroleum basins and were sentinel bathyal features for exploration petroleum geologists (Bailey et al. 2003; Huuse & Feary 2005; Colman et al. 2005; Rüggeberg et al. 2005).

There are a variety of deep-sea mound types that can develop in a variety of ways (Pautot et al. 1970):

1. Carbonate reef mounds, principally derived sub-fossil Scleractinian coral skeletons growing on top of each other (Hovland et al. 1994; van Hinte et al. 1995; Roberts et al. 2003; Rüggeberg et al. 2005).
2. Mud Mounds, formed by biosedimentary buildup of metazoans (bryozoans, sponges, crinoids, etc.) and microbial benthic communities (Dronov 1993; Wendt et al. 1997; Long et al. 2003; Farrand & Lane 2007; Rodríguez-Martínez 2011).

3. Mounds, formed by subsurface fluid and gas escape (Barrett et al. 1988; Bolton et al. 1988; Enachescu 2004; Burton-Ferguson et al. 2006)
4. Mounds formed by diapiric action of evaporites (Laughton et al. 1972; Parson et al. 1984; Enachescu 2004; Ruffman 2011)
5. Mounds formed by diapiric action of igneous rock (Laughton et al. 1972)
6. Mounds formed of resistant sedimentary rock (Laughton et al. 1972; Sibuet 1992; Moscardelli et al. 2013)
7. Mounds formed by dissolution of carbonate (karst) (Laughton et al. 1972; Hart 1977; Parson et al. 1984; Ruffman 1989; Ford & Williams 1989; Dronov 1993; Immenhauser & Rameil 2011)

### 1.1.3 Enigmatic Mounds of Orphan Knoll

In international waters, 550 km East of St. John's, NL, Canada, a rifted fragment of continental crust, the Orphan Knoll (OK) measures 190 km long (NW-SE), 90 Km wide (SW-NE) with a depth range between 1533 m to 4130 m (Fig.1-1). The OK is at the continental-oceanic boundary (COB) of an oceanic-continental transition zone that extends eastward to Chron 34 (~200 Km) (Chian et al. 2001).

Mounds discovered on the Orphan Knoll in 1969 are 'enigmatic' despite several dredging efforts (1971), seismic exploration (1970 and 2003) and deep-sea drilling (DSDP site 111, 1970). The possibility that the OK mounds were deep-sea carbonate reefs, theorized from dredge samples of *D. dianthus* coral skeletons, was an exciting prospect worth investigating.

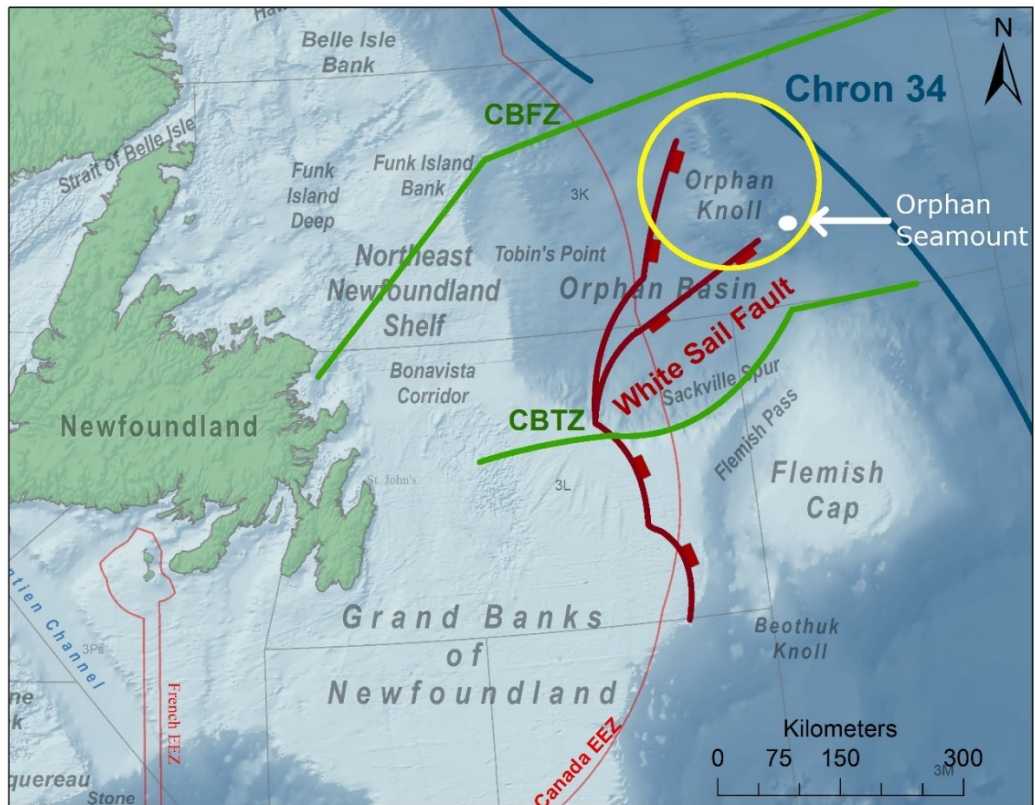


Figure 1-1. Orphan Knoll (yellow circle) and Orphan Seamount (white dot) locations relative to Newfoundland and the Grand Banks of Newfoundland. Prominent faults near the Orphan Knoll area are also identified (Charlie Gibbs Fracture Zone (CBFZ) and Charlie Gibbs Transfer Zone (CBTZ and White Sail fault. Chron 34 is ~100 Km eastward of Orphan Knoll.

## 1.2 Drivers of Deep-Sea Megafaunal Species Distributions

### 1.2.1 Bathymetry

Deep-sea megafauna, are aptly named due to the often deep depths at which these many species are found (Breeze et al. 1997; Davies et al. 2009). Bathymetry (depth and slope) has been known to drive the distribution and abundance of deep-sea megafaunal

species, especially cold-water coral and sponge communities (Madi et al. 1996; Davies & Guinotte 2011; Miller et al. 2011; Baker et al. 2012; Neves et al. 2014).

### 1.2.2 Oceanography

Ocean currents at the surface and at depth bring food to the deep-sea in the form of Particulate Organic Matter (POM) and Dissolved Inorganic Carbon (DIC) (Carmack & Wassmann 2006; Reidenbach et al. 2006; Christiansen & Wolff 2009; Levin et al. 2009; Henriot et al. 2010; Logerwell et al. 2011). Changes in deep-water circulation will play a vital role in the distribution and abundance of deep-sea megafauna through food source restrictions.

Some less motile megafaunal species are also restricted by temperature. Climate change (warming oceans) seen between glacial events have shown that large decreases in abundance and diversity of deep-sea benthic megafauna have occurred when a temperature change of  $>5^{\circ}\text{C}$  was sustained for 50-100 year period (Smith et al. 1997; Yasuhara et al. 2008).

### 1.2.3 Geology

Substrate type is of special importance when describing the attachment / anchoring method of certain megafaunal species such as cold-water corals (Barrie & Conway 2008; Edinger et al. 2011). Many hard cold-water coral species (i.e. Gorgonian, Stony, Black-Wire) require a method to anchor their structure within or near food (deep-water currents or ample detrital flux from the surface layer) (Roberts et al. 2006; Baillon et al. 2014). The hold-fast of some hard cold-water coral need a solid substrate to anchor-

to, but there are some hard corals (i.e. *Acanella* sp) that, along with soft coral species (i.e. Sea Pens) can create hold-fasts within soft sediment (van Hinte et al. 1995). Therefore, suitable geological substrate can also restrict where certain deep-sea megafaunal species are found.

### **1.3 Executive Summary**

This study was designed to test the various theories of the origins of the ‘enigmatic’ mounds of Orphan Knoll, to lead the first ROV exploration of the Orphan Knoll and its neighbouring seamount (Orphan Seamount), and to understand the most important mechanisms of community composition by investigation of bathymetric, oceanographic and geological influences of deep-sea benthic megafauna, such as deep-sea coral and sponges.

## **2 Geological Insights into Bathyal Enigmatic Mounds through Investigation of the Enigmatic Mounds from Orphan Knoll, Northwest Atlantic Ocean**

Meredyk, S., Piper, D.J.W., Edinger, E., Ruffman, A.

*1. Eventually to be submitted to the Canadian Journal of Earth Sciences*

### **Abstract**

Orphan Knoll is an 'orphaned' fragment of the North American continental crust that contains ~250 mounds, of unknown composition, that range from 60 to 600 m tall and 1 to 3 km wide. The Deep-Sea Drilling Project drilled the Orphan Knoll in 1970 and determined that the Orphan Knoll was continental crust but could not determine the composition and age of the enigmatic mounds on the Orphan Knoll. The principal objective of the study was to determine the age and composition of the enigmatic Orphan Knoll mounds in an effort to better understand their possible origins. Rock samples from the Orphan Knoll mounds identified mid-Miocene bedded pelagic limestone bedrock as the upper layer of limestone on top of the Orphan Knoll mounds. The formation of the Orphan Knoll mounds was possibly initially formed through listric faulting during rifting events (extension) and again by reactivated faulting during the Neogene and Quaternary, possibly through plate movements originating from the White Sail fault, Dover fault and /or the Charlie Gibbs Fracture Zone (CGFZ).

## 2.1 Introduction

Deep-sea mounds are commonly found in and around petroleum basins around the world (Pautot et al. 1970; Roberts et al. 2003) or areas of hydrocarbon seeps (Enachescu 2004; Colman et al. 2005; Pohlman et al. 2009), where the mounds are usually diapiric in nature (e.g. salt domes) (Pautot et al. 1970; Long et al. 2003; Rüggeberg et al. 2005; Huuse & Feary 2005), or have fluid or gas escaping from the subsurface (i.e. methane) (Levin et al. 2009; Jauer & Budkewitsch 2010).

Identifying the composition and age of detected enigmatic mounds is a necessity for oil and gas extraction companies, as salt diapirs can help explain the restriction of major petroleum reserves and therefore, potential indicators of a petroleum reservoir (Roberts & Nunn 1995). Alternatively, enigmatic mounds could be active carbonate reef mounds with unique cold-water coral growing on top of a sub-fossil coral matrix (Roberts et al. 2003; Roberts et al. 2006; Davies et al. 2008), or hydrothermal vents or the other varieties of mounds mentioned above; which are hotspots of biodiversity in the deep sea (Roberts et al. 2003; O'Hara et al. 2008; Buhl-Mortensen et al. 2010).

### 2.1.1 Geological Setting of the Enigmatic Mounds of Orphan Knoll

In international waters, 550 km East of St. John's, NL, Canada, a rifted fragment of continental crust, the Orphan Knoll (OK) measures 190 km long (NW-SE), 90 km wide (SW-NE) with a depth range between 1533 m to 4130 m (Fig. 2-1). The OK is on a non-volcanic rifted margin (NVRM) (Sibuet 1992) at the continental-oceanic boundary (COB) of an oceanic-continental transition zone that extends eastward to Chron 34 (~150 km east of OK) (NW Atlantic Mid-Ocean Channel (NAMOC))(Chian et al. 2001). The Charlie Gibbs Fracture Zone (CGFZ) and Dover Fault are ~100 km north of the northern tip of OK (Smee et al. 2003; Burton-Ferguson et al. 2006), while the White Sail Fault, in the mid Orphan Basin, is ~100 km to the west of OK (Burton-Ferguson et al. 2006; Enachescu 2009).

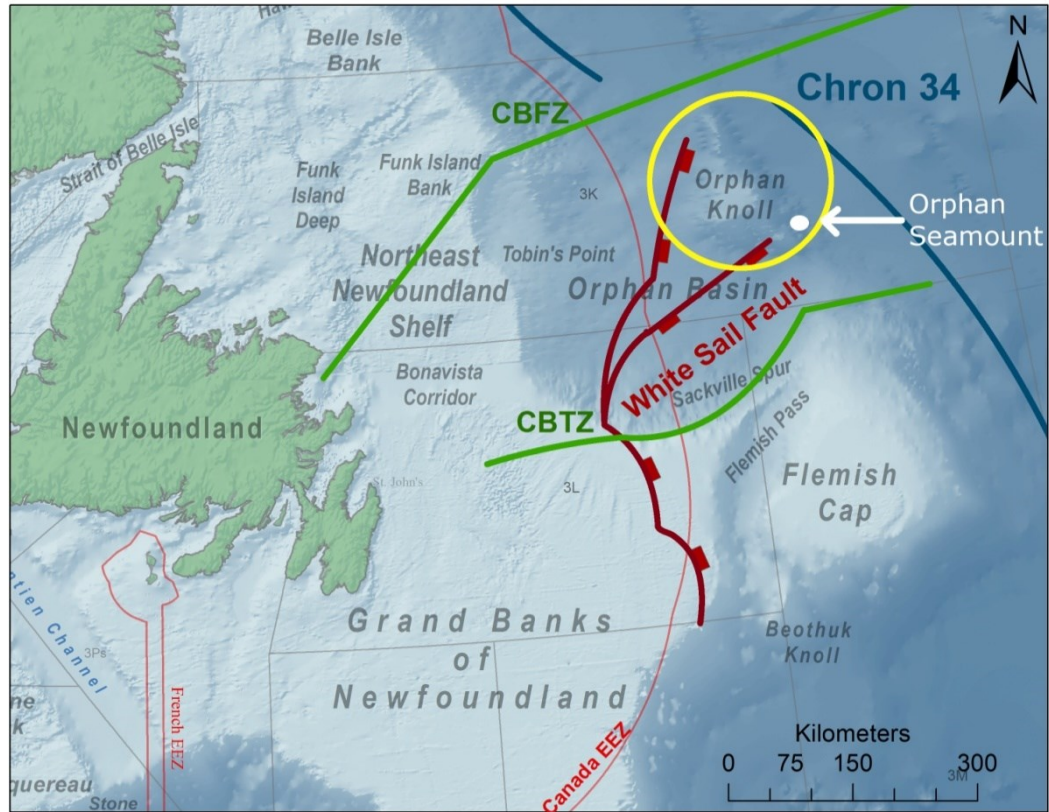


Figure 2-1. Orphan Knoll (yellow circle) and Orphan Seamount (white dot) locations relative to Newfoundland and the Grand Banks of Newfoundland. Prominent faults near the Orphan Knoll area are also identified (Charlie Gibbs Fracture Zone (CBFZ) and Charlie Gibbs Transfer Zone (CBTZ and White Sail fault. Chron 34 is ~100 Km eastward of Orphan Knoll.

In 1969 the M/V *Charcot* collected seismic reflection and magnetic anomaly profiles that identified mounds (buried and exposed) on the NW-SW side of Orphan Knoll, and the increasing positive magnetic anomaly indicated the presence of oceanic crust on the eastern edge of OK (Laughton et al. 1972). The OK mounds at this point

were thought to be linear ridges of outcropping bedrock (Laughton et al. 1972; van Hinte et al. 1995).

In 1970 the Deep-Sea Drilling Program (DSDP) and the research vessel *Glomar Challenger* drilled a 250 m core at DSDP site 111 (Fig. 2-2). The core stratigraphy identified the upper 182 m being a thick drape of Cenozoic hemipelagic sediment (zeolitic clay, foraminiferal ooze and nanoplankton marl) overlying 68 m of Mesozoic sediment (glauconitic limestone, dark sandstone and shale) on top of a 10 m Jurassic anthracitic coal layer, that was proposed to overly the supposed crystalline basement (Laughton et al. 1972; Berggren & Aubert 1976). In 1971, dredging data from the OK by the M/V *Lynch*, near the DSDP drill site 111; Devonian aged ostracods lead to the theory that the OK mounds were possibly folded dyke ridges that had been subaerial highs, weathered during the Jurassic – Cretaceous, and had subsided to their present bathyal depth between the Aptian and Thanetian (Laughton et al. 1972; Ruffman & van Hinte 1973; van Hinte et al. 1995).

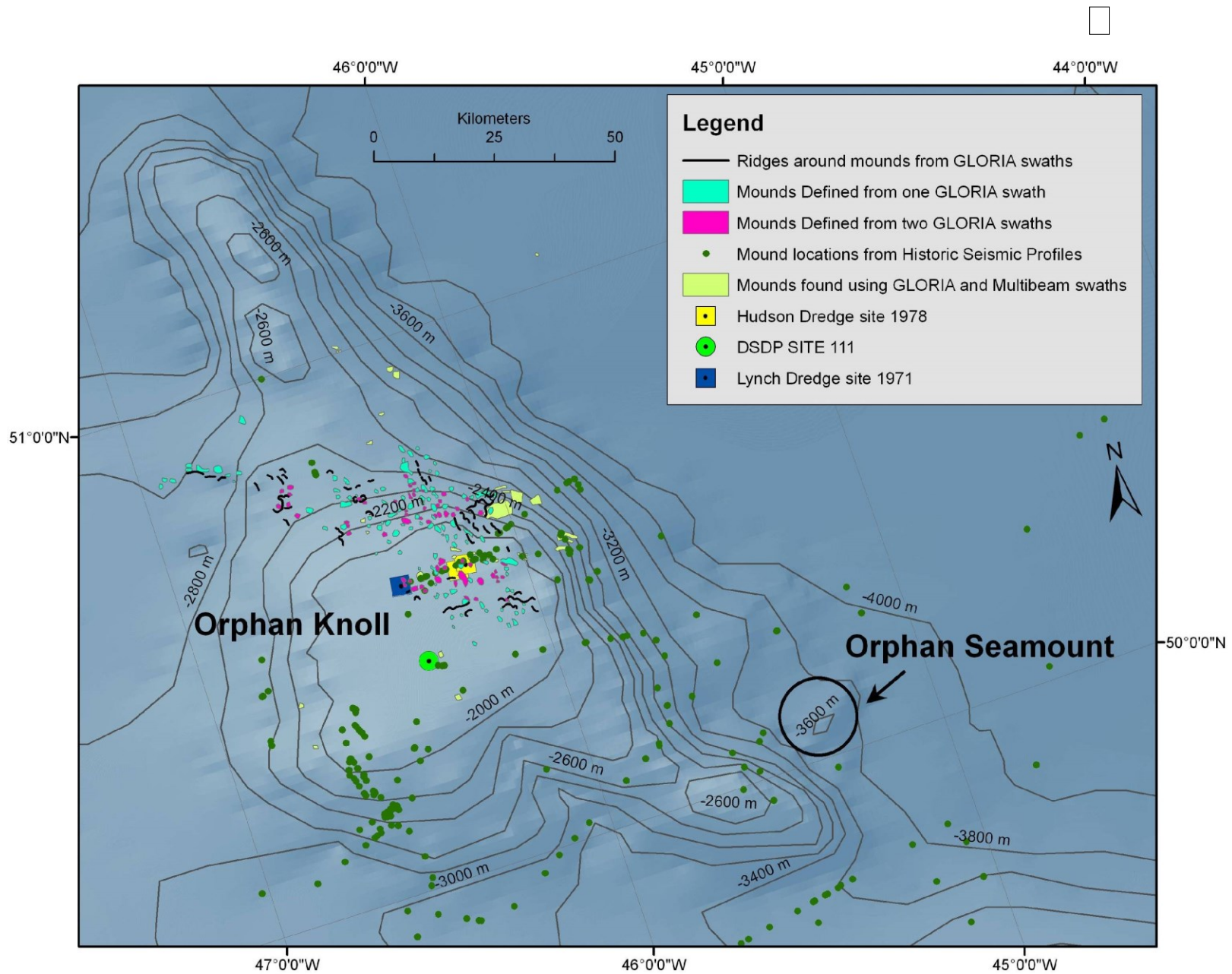


Figure 2-2. Orphan Knoll and Orphan Seamount with historical and new enigmatic mound (green) locations identified through historical compilation and interpretation of seismic reflection profiles (Bathymetry : GEBCO)

The possibility of the enigmatic mounds being carbonate reef mounds was theorized by Enachescu (2004) whereby he postulated that through faulting and / or diapiric action, the enigmatic mounds of OK were possibly bioherms, much like the mounds found in the NE Atlantic (i.e. Porcupine Seabight Basin), that thrived biologically through hydro-thermal vents or hydrothermal fluid escape (Enachescu 2004) (Fig. 4-3).

In 2004 the CCGS *Hudson* cruise 024 recovered several piston cores from a potential SW OK mound and from the Integrated Ocean Drilling Program (IODP) site U1302 and site U1303 (SE Orphan Knoll) (Toews & Piper 2002; Piper 2005). The results from the 2004 Huntec seismic profiles identified bedding on the NE OK mounds (Fig. 2-4); however, the piston core from a SW mound produced only mud and no coral was visible in the drop camera imagery (Piper 2005). Therefore, the results from CCGS *Hudson* cruise 024 were inconclusive, as to the composition of the OK mounds, and to be certain of the mounds' composition, bedrock samples would be needed to eliminate the variety of compositional theories.

### 2.1.2 Study Objectives

Using a remotely operated vehicle (ROV) equipped with high-definition (HD) video and high-resolution multibeam imagery, the collection of *in-situ* bedrock and detailed bathymetry were collected to verify the facies and petrology of these bedrock samples, in an effort to determine the composition, age and origin of the 'enigmatic' mounds of Orphan Knoll.

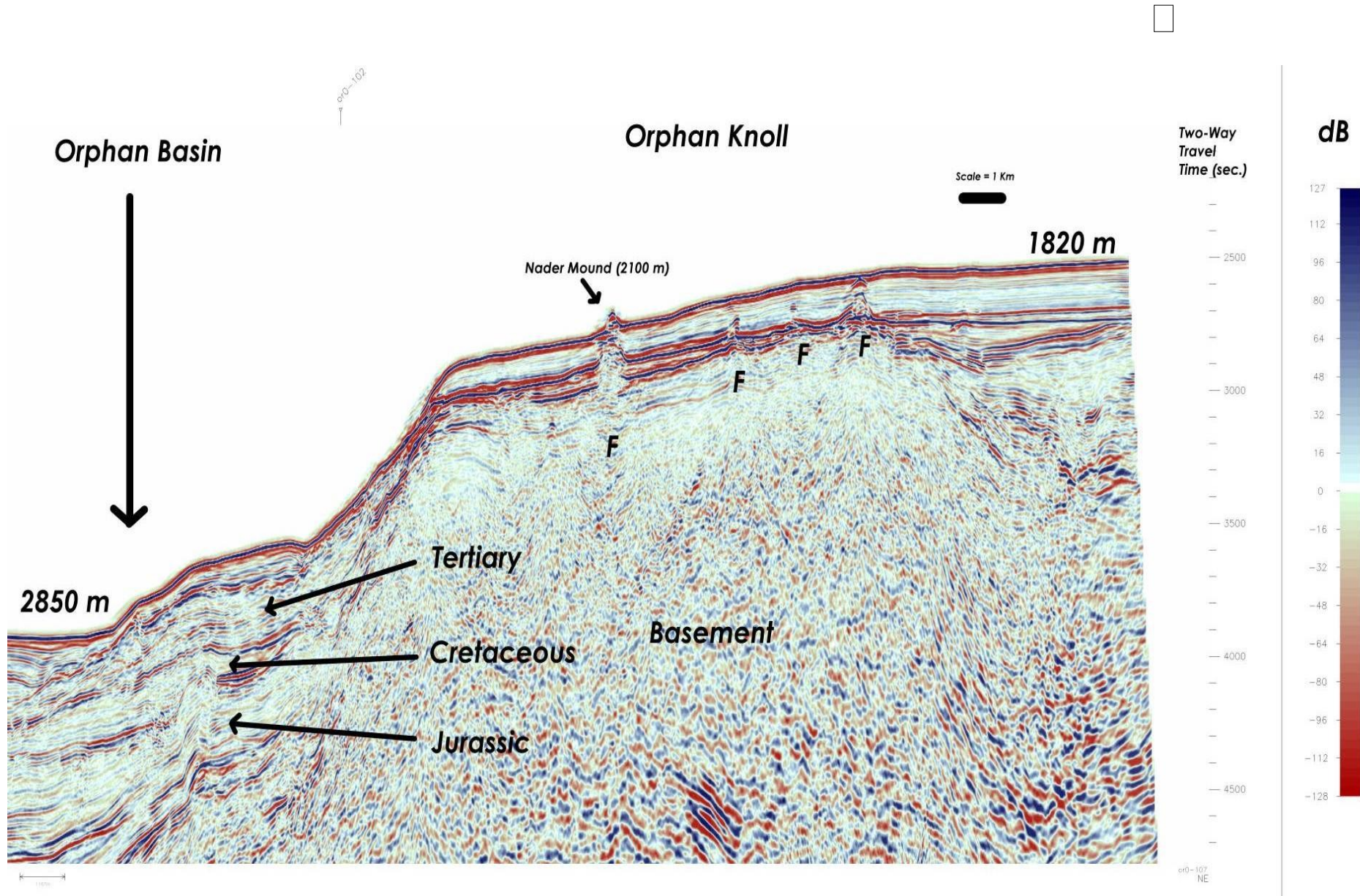


Figure 2-3. 2D Seismic Profile of SW OK Mound (Nader) showing the SW flank of OK and SE extent of Orphan Basin (Horizons and Faults interpreted by Dr. Enachescu 2004)); (FGP-MUN)

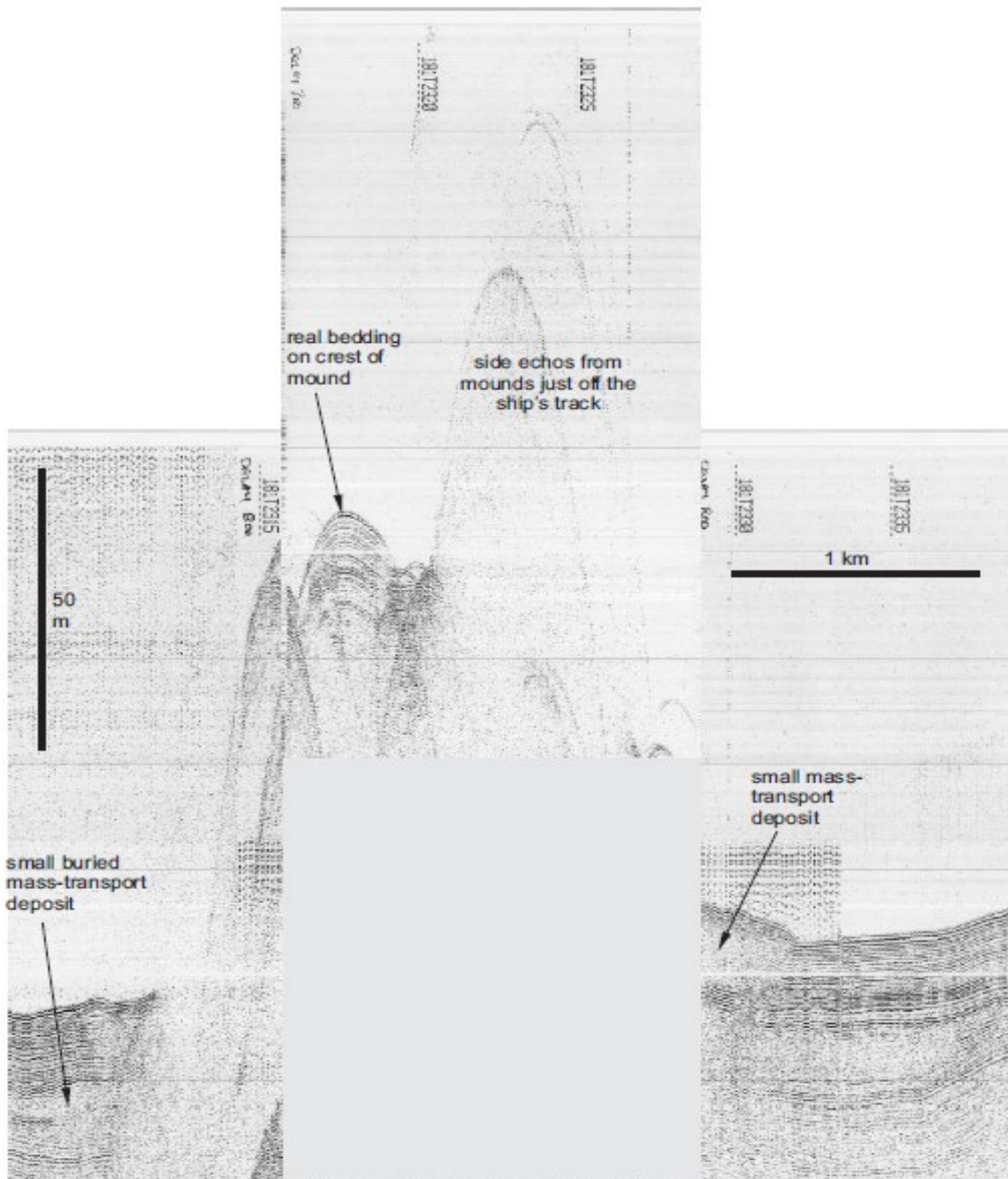


Figure 2-4. Hunttec sub-bottom profile from CCGS Hudson cruise 2004-024 of a NE OK Mound at the 1978 dredge location (GSC-NRCAN, Piper, 2004)

## **2.2 Methods**

### 2.2.1 Geological Survey Planning

#### **2.2.1.1 *Historical Acoustic Imagery***

Raw survey data (seismic reflection profiles, side-scan sonar and multibeam sonar) from historical cruises were compiled into an ArcGIS project to aid in survey planning and data interpretation.

#### **Seismic Profiles**

Hull-mounted Knudsen 3.5 kHz seismic profiles were collected from cruises: 78-020, 86-013, 90-007, 2001-043, 2003-033, 2004-024; 3.5 kHz Knudsen and 3.5 kHz Hunttec ® seismic profiles were collected from CCGS *Hudson* cruises: 2003-033, 2004-024 and 2010-029; 3.5 kHz airgun seismic profiles were collected from CSS *Hudson* cruise 69-041; LITHOPROBE deep seismic data from line FGP 84-3D, TGS line 107 and GSI lines ORO-111 and ORO-129 were examined and new enigmatic mounds (high slope (>45°)) were recorded and plotted in a ArcGIS project (Fig. 2-2).

## **Side scan Imagery**

GLORIA (Geological Long Range Inclined Asdic) 6.5 kHz side-scan imagery collected on the *Starella* (1979) and *Farnella* (1981) cruises covered ~40% of the Orphan Knoll, focused on the northern section of the Orphan Knoll (Parson et al. 1984). Ridge and mound features were created by geopositioning GLORIA imagery and manually digitizing the mounds and ridges seen in the imagery (Fig. 2-2).

## **Multibeam Bathymetry**

In 2000, the United States Coast Guard Cutter (USCGC) *Healy* used a Seabeam 2112 multibeam sonar (12 kHz) and collected bathymetry (gridded to 100 m res.) over the SE-W OK; this data was made available from the Geological Survey of Canada (GSC).

In 2006, the Fugro vessel *Kommander Jack*, (Kmdr. Jack) was commissioned by NRCan to collect data for Canada's claim for extended jurisdiction under the United Nations Convention on the Law of the Sea 's (UNCLOS) Commission on the Limits of the Continental Shelf (CLCS), re-defining areas of the Canadian continental shelf, in an effort to extend Canada's Exclusive Economic Zone (EEZ) . The *Kmdr. Jack* used a Kongsberg EM 122 12 kHz multibeam unit and collected bathymetry gridded to 100 m resolution over the SE OK; this data was made available from the Geological Survey of Canada – Atlantic (GSC-A). The *Kmdr. Jack* multibeam raster was overlain by *Healy* multibeam raster, due to raster merging inaccuracies (the *Kmdr. Jack* data was less 'clean' (increased interpolation variance) than the *Healy* data) within ArcGIS (inaccuracies were visualized in 3D, using GlobalMapper ver. 11); therefore, rather than merging the rasters,

the *Healy* data overlays the *Kmdr. Jack* data (Fig. 2-5), to get the most accurate raster for point-sampling statistical purposes.

### **2.2.1.2 *Cruise Collected Acoustic Imagery***

Before each dive, the CCGS *Hudson* used a hull-mounted Knudsen 3.5 kHz chirp system to collect sub-bottom profiles that diagonally traversed the dive plan (start to finish).

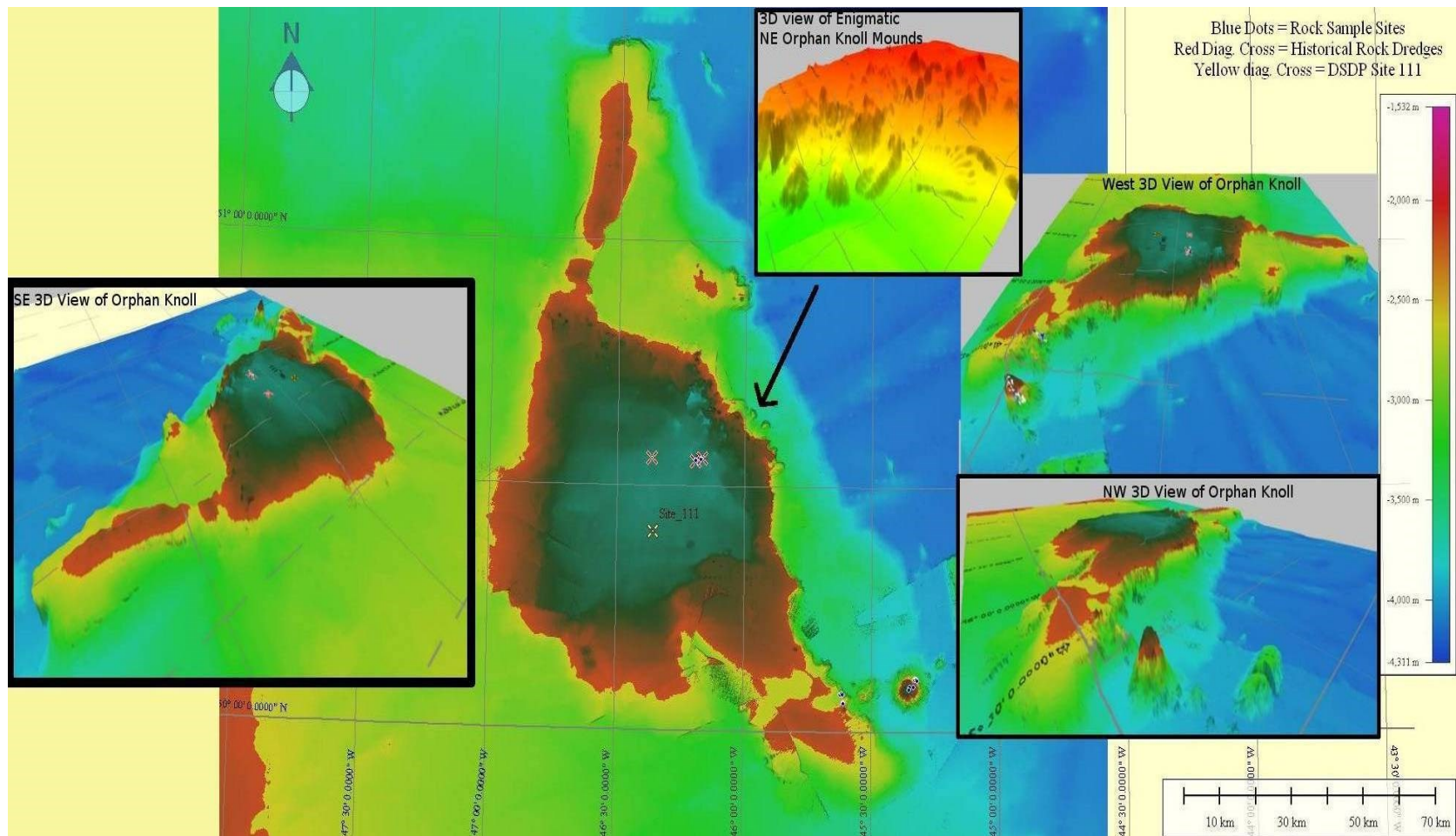


Figure 2-5. M /V Kommandor Jack (Fugro) multibeam imagery overlain by M /V Healy multibeam imagery; inset images of 3D view of the Orphan Knoll from various directions and a zoomed in view of the enigmatic mounds on the NE slope of Orphan Knoll (7x exaggerated)

## 2.2.2 ROV Dive Planning

Dive plans (sub-sea navigation routes) were designed to examine surficial geological heterogeneity and presumed coral and sponge habitat heterogeneity. The dive plans covered varying depths, presumed flat terrain and bathymetric highs or mounds seen in seismic profiles, GLORIA and USGS *Healy* Seabeam 2112 multibeam data (Fig. 2-6). Five creeping line dive plans were made for a 6 day sampling period (D1341, D1342, D1343, D1345 and D1346), to maximize surface area coverage, collect variable substrate types and to avoid duplication of observed geological features. Three of the six dives (D1340, D1341 and D1343) were designed with the sole purpose of collecting a diverse range of biological and geological samples from presumed steeply sloping terrain as previous studies have indicated that slopes and depth are indicators of where coral assemblages are most likely to be found (Austin 2002; Leverette & Metaxas 2004; Hall-spencer et al. 2007; Buhl-Mortensen, Buhl-Mortensen, et al. 2009; Davies & Guinotte 2011; Buhl-Mortensen et al. 2012; Neves et al. 2014). Dives (D1342, D1345 and D1346) were designed to retrieve oceanographic moorings deployed by DFO in 2008 and 2009, and to collect biological and geological data from the area surrounding the moorings.

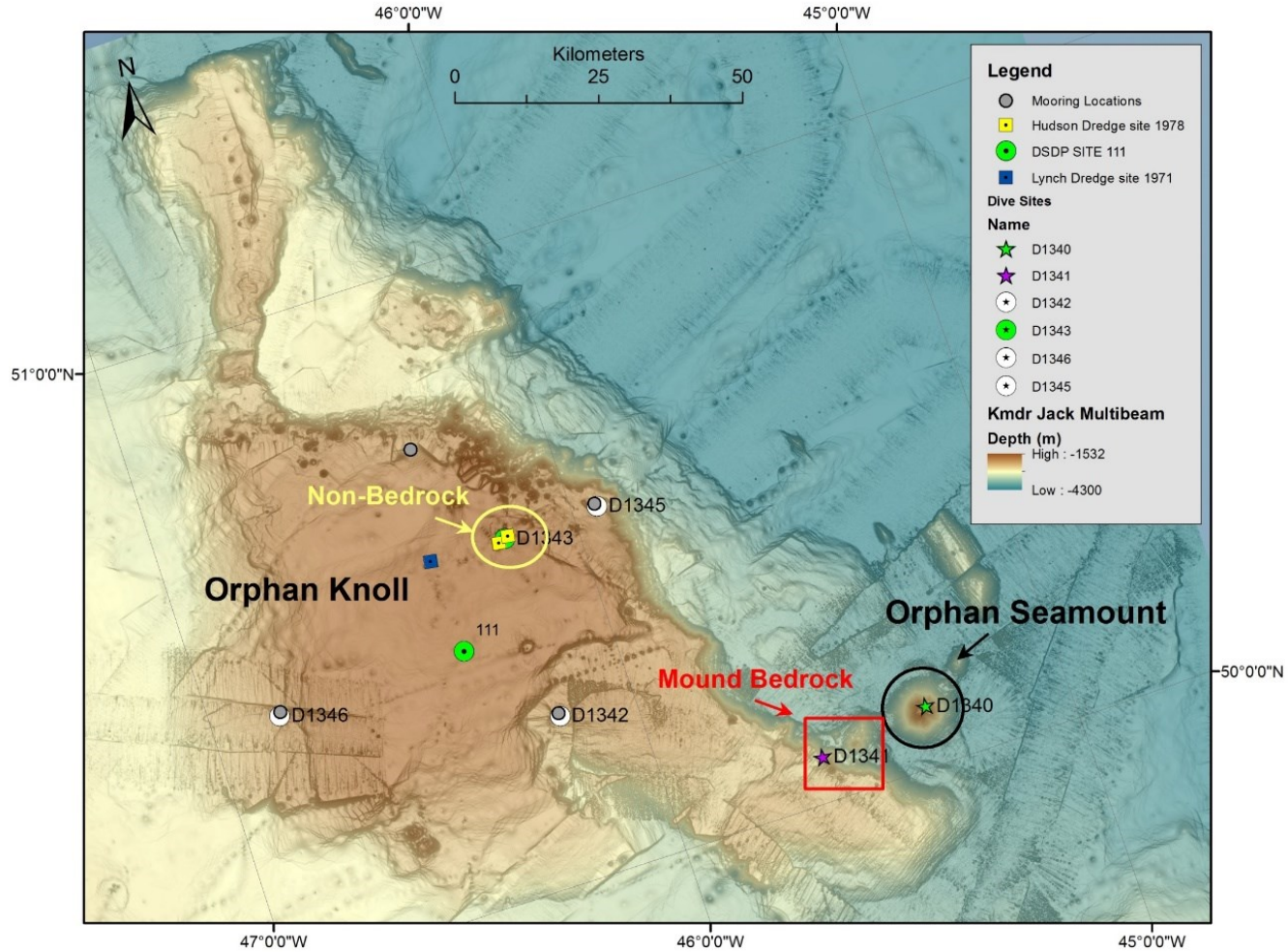


Figure 2-6. M/V Kommander Jack (Fugro) multibeam imagery overlain by M/V Healy multibeam imagery (base layer bathymetry : GEBCO )

### 2.2.3 Geological Sampling

Ice-rafted debris (IRD) has rained-down on the OK since the initiation of glaciations in the North Atlantic Ocean (Piacenzian (~3 Ma))(Shaw et al. 2006); therefore, positive discrimination of bedrock from ice-rafted boulders could only be verified through *in-situ* video, photographs and substrate samples.

Bedrock samples were collected by ROPOS when bedrock outcrops were physically accessible to the ROV and when there was enough room for rock storage within the collection boxes on ROPOS. A CH-15 Stanley underwater chipping hammer clamped to spring-loaded metal rods was installed onto ROPOS for the purpose of chipping sections of bedrock without over-stressing the manipulating arms of ROPOS and to allow ROPOS to collect the sample with its restricted manipulator arm gape (cobble sized rock samples) (Fig. 2-7).



*Figure 2-7. ROPOS using jack hammer attachment to attempting to fracture bedrock from Orphan Seamount (D1340); green dots are 10 cm apart*

## 2.2.4 Thin Section Analysis

The collected rock samples were cut into cross-sectional slabs and made into polished (800 grit) uncovered  $30\mu\text{m}$  thick thin sections (4.7cm x 2.7cm) by the lapidary lab at Memorial University of Newfoundland (MUN). A smear slide was made from the single calcareous ooze sample and was dated using nanno-fossils by Kevin Cooper (RPS Energy, United Kingdom). The thin sections were analyzed using a Leica<sup>®</sup> petrographic microscope with and without cross-polarization filters, at various magnifications (1.6 x, 5x, 10x, 20x and 50x) at MUN. Rock types of samples were visually identified through recognizable mineral and matrix composition.

## 2.2.5 XRD Analysis

XRD analysis was carried out to determine if the SE OK ooze sample (R1341-4) contained zeolite, in an effort to correlate recovered calcareous ooze from SE OK to a section of zeolitic ooze recovered from the DSDP site 111 core 6 (northern OK).

Two sub-samples were randomly selected from the dried calcareous ooze sample. The ooze sub-samples (R1341-4) were prepared for XRD analysis by digesting the organic material following the method outlined by Anderson, 1961, followed by freeze drying the digested powder for 24 hours and re-powderizing the sub-samples before XRD analysis.

A Rigaku Ultima IV X-Ray Diffraction (XRD) machine using a Cu, 40 kV, 44 mA X-ray with a 0.02 degree step width and a 2 second count time, was used to analyse an oriented smear slide of the ooze sample (R1341-4). Jade version 9 powder diffraction analysis software, from Materials Data, Inc., was used to provide quantitative analysis of polycrystalline materials within the ooze sample.

## 2.2.6 Data Collection through HD Video Analysis

ROPOS was equipped with two high-definition (HD) (forward facing 1080p HD camera and a downward facing 1080i HD camera) and one 5 Megapixel (MP) digital still camera. Both HD cameras had zooming capabilities with green laser sights 10 cm apart to provide scale at variable zoom distances. The forward facing camera had pan and tilt capabilities while the downward facing camera was affixed to the frame with only tilt functionality.

The HD video was geo-referenced using a Geostamp ® device, which audio-encoded the geographic position into the HD video signal / stream. The time-stamped geo-referenced HD video allowed for accurate (1m spatial resolution) positioning of species relative to surficial geology percentages *in-situ* and during re-processing of the HD video. The video annotation program ClassActMapper (CAM) was used during the cruise and in the post-processing of the HD video data to collect geospatial positioning of species relative to surficial geology percentages *in-situ* and during re-processing of the HD video. CAM is a graphical user-interface (GUI), whereby the user pressed custom-made species labeled buttons for each instance that a species was seen within the video. The resulting MS Access database contained when and where a species was observed relative to the surficial geology percentages *in-situ* and during re-processing of the HD video (e.g. *D. dianthus* is spotted on 100% bedrock (Fig. 2-8).

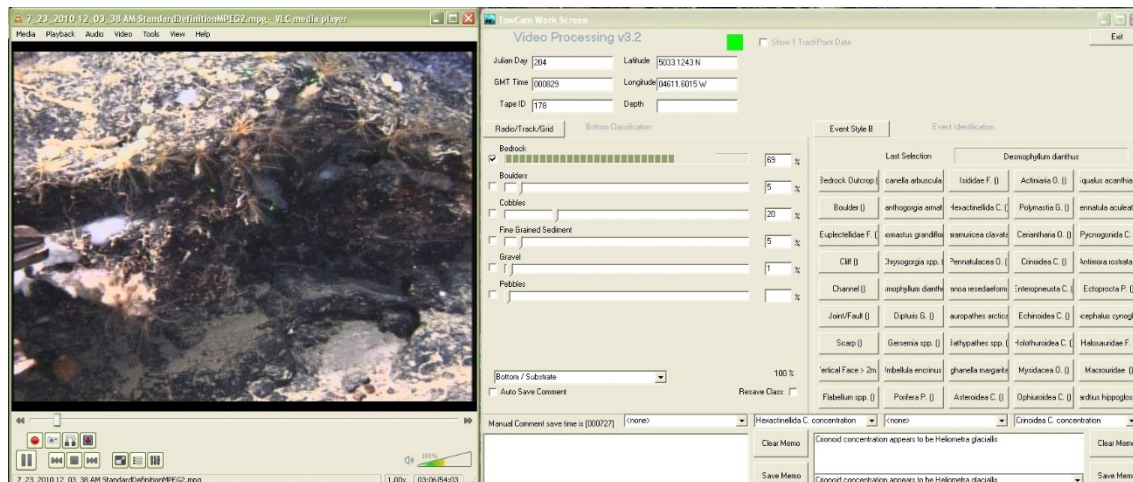


Figure 2-8. HD video display (Left) with ClassActMapper Graphical User-Interface (GUI) (right)

CAM was also able to record extra features when needed. Such as, when there were too many individual species to count *in-situ*. In such an instance the ‘comments’ field was manually labeled with any one megafauna species’ concentration greater than 20% (i.e. *Gersemia* spp.>20%) and added to the continuous 1 second data polling, which occurred independently to when a polling event occurred, by pressing of any one of the custom species presence buttons. During the cruise, CAM is programmed to poll a serial port every second and each instance a button is pressed, for the latitude, longitude and depth of ROPOS (during cruise via fiber-optic gyroscope (FOG) and during post-processing via Geostamp ®).

The collective (totaling 100% coverage) surficial geology was polled /recorded every second by CAM using visual estimates and a slider bar of the following sediment size classes, based on the Wentworth scale: bedrock, boulders, cobbles, pebbles, granules and fine-grained sediment (Sand-Mud). Sand and mud were undistinguishable by eye and were therefore grouped as fine-grained sediment.

The annotations were stored in a MS Access ® 97-2003 database and are linked through a post-processing field (JDayGMT) that combines Julian Day and Universal Coordinated Time (UCT). A secondary post-processing of the HD video was performed by a single user to eliminate multi-person estimation variation. The user performed a self-calibration (10 random frame grabs were analyzed using area sampling within ImageJ and compared to the user’s estimates to ensure accuracy and precision of their estimates) to determine the offset between the computer calculated percentage and the user’s estimate (see next section 2.1.9).

## 2.2.7 Calibration of the Estimate of Geological Coverage

The surficial area data was estimated by the user. To understand the percentage of user error associated with the user estimates, each sediment size class (coverage) was first quantified by using ten random screenshots of HD video collected from ROPOS and the percentage of area covered was estimated based on diagrams from the book '*Geology in the Field*' (Compton 1985). Then to determine the offset between the user's estimate and the computer generated coverage, the image processing software ImageJ (ver. 1.44f) was used. A histogram threshold filter in ImageJ was used to determine the area of estimated surface type (i.e. granules, fine sediment, etc.) from manually excluded interfering elements (water column and boulders) (Fig. 2-9). The area was divided by the total surface area of the image, which exports the percentage cover of a specific surface type within a single image (Fig. 2-9). The preliminary human estimates were compared to the actual ImageJ quantified surficial area and the user was over consistently estimating by 10%. Therefore, the data was collected compensating for the 10% over-estimation by the user.

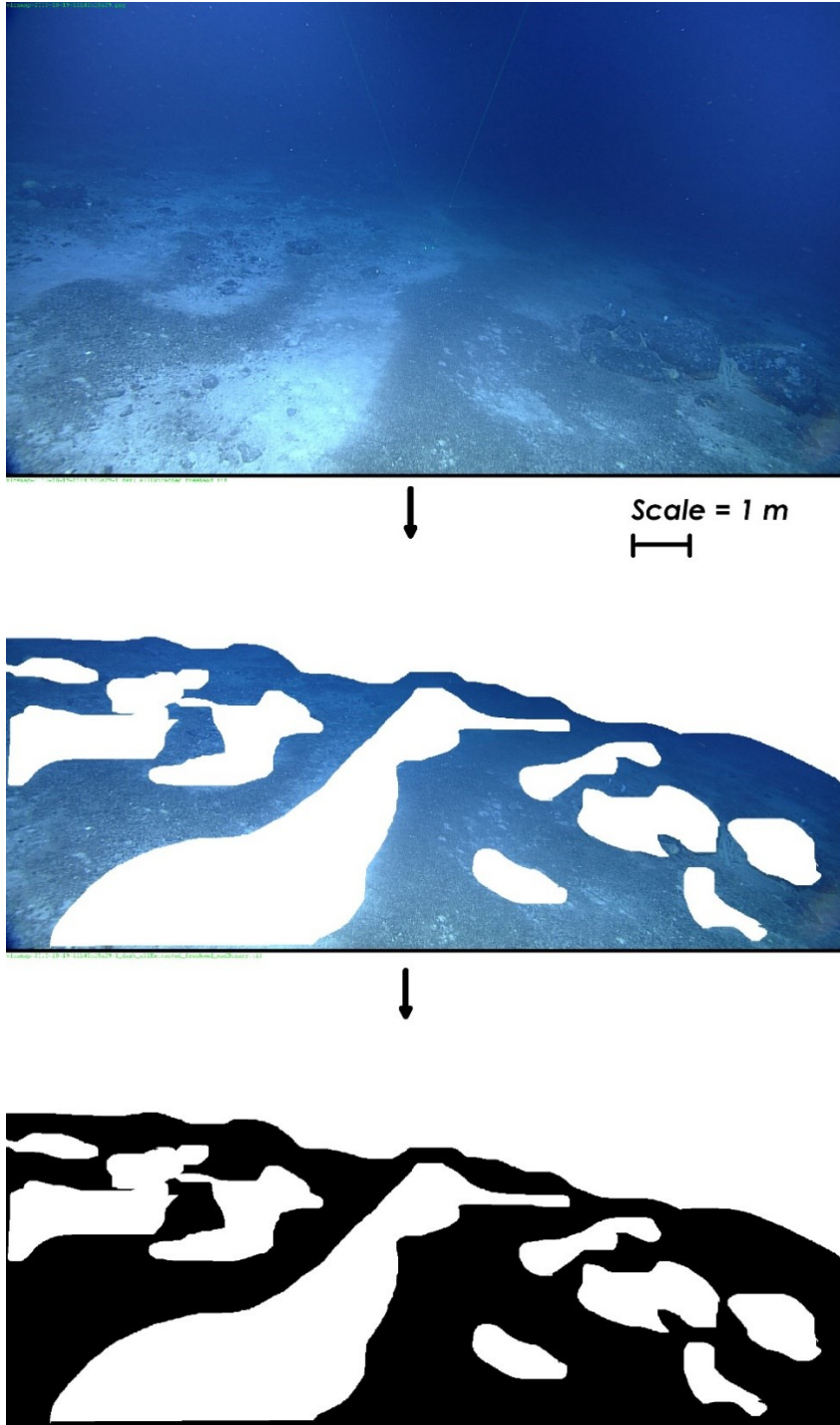


*Figure 2-9. HD video frame grab (Top), showing the progression of image changes to determine % coverage area; non-granule features removed (middle) and the final area of granules coverage (bottom)*

## 2.2.8 Surficial Geology Mapping

The post-processed CAM data, collected in the lab, was used to create surficial geology maps in an effort to remove multiple user biases found within the *in-situ* dataset (collected at sea). The size of plotted points, representing different sediment size classes within the surficial geological maps, are not coincidental for each sediment size class; thereby, allowing each sediment class layer to be overlain by another substrate type (Fig. 2-10). The surficial geology was divided into distinct surficial geological units (SGUs) for each dive and is summarized in Appendix 2-3.

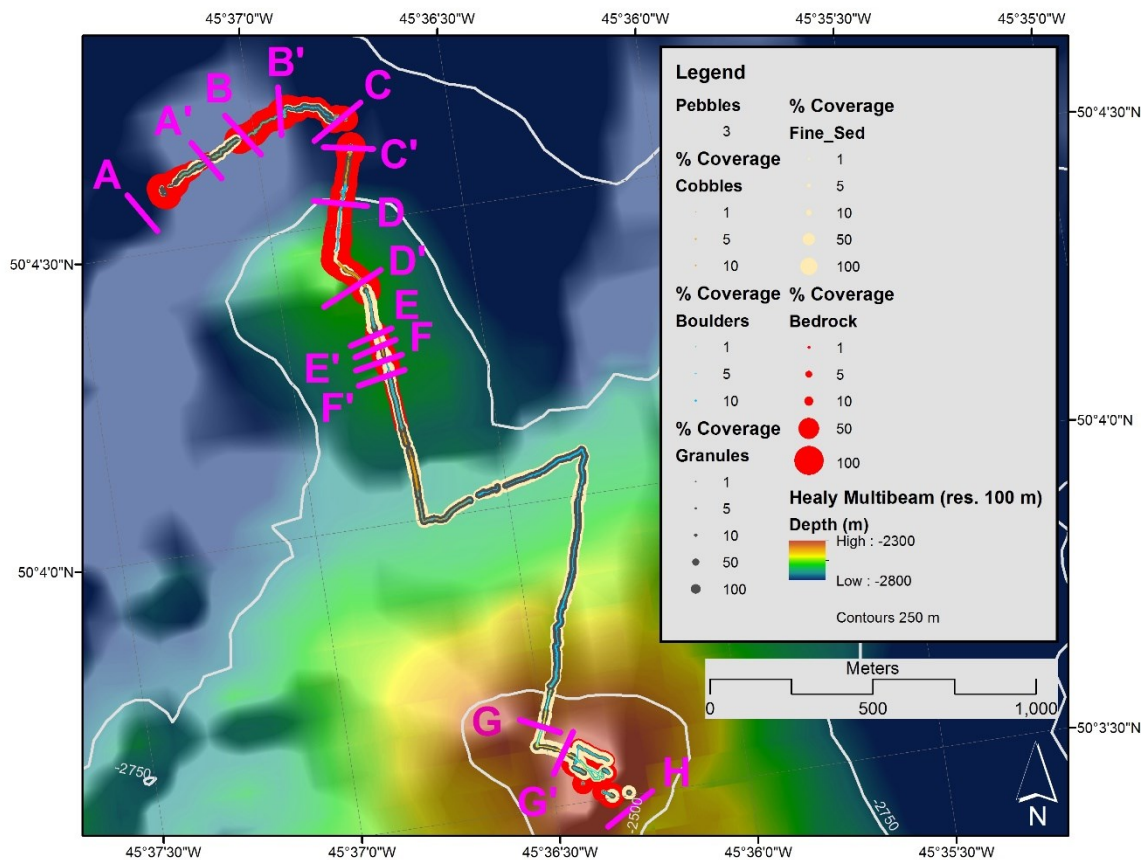


Figure 2-10. Dive 1341, SE Orphan Knoll Mounds Surficial Geology (% Coverage) separated into surficial geological units (pink features)

## 2.2.9 ROV Imagenex Multibeam Bathymetry Collection and Processing

An Imagenex model 837A “Delta T” multibeam unit using 120 beams (3°) at 260 kHz with 0.2% spatial range resolution (res.) (e.g. 2 mm res. at 1 m altitude to 30 mm res. at 15 m altitude) was forward mounted and calibrated by the Canadian Hydrographic Service (CHS) and the ROPOS engineering team. The Imagenex unit was monitored throughout each dive by an operator (research team) on-board the CCGS *Hudson*. The Imagenex multibeam data was preliminarily processed on-board and then extensively post-processed (beam and angle elimination were used to ‘clean-up’ the data; ~5% beam rejection) using CARIS HIPS & SIPS version 7 (service pack 3). The multibeam unit recorded backscatter data as well; however, due to the ROV flying close to the ground with a high output signal, there was too much acoustic energy (‘washed out’) to create a colour gradient. Additionally, the acoustic head physically accidentally changed orientation during dives due to mounting bracket limitations on the ROV. Therefore creating an accurate colour gradient backscatter image was not possible and thus not suitable for statistical analysis. CARIS image exports were created using 25 cm spatial resolution to smooth fine-scale artificial features within the data, to have the most accurate bathymetry capable. The raster exports, of the exposed enigmatic OK mounds, were exported from CARIS (ASCII format) and converted by ArcGIS 3D Analyst extension, into an ArcGIS raster grid.

### 2.2.9.1 *GIS Mapping Note*

The maps generated using the various bathymetric layers were labeled within the inset legend of the map. The depths of the various bathymetric layers are for the entire layer and not exclusively the visible layer. Therefore, the depths in the legends will not match each other. All bathymetric datasets were collected with high accuracy, no significant depth differences were noted between the vessel, and ROV mounted systems.

### 2.2.10 Measurements of Strikes and Dips

The position of ROPOS was plotted within GlobalMapper ver. 11 software by inputting the position data (decoded audio signal from the HD video) from a Geostamp® decoder. This method allows the post-processor to have the same experience as the *in-situ* user, with the added advantage of being able to pause, zoom, advance and reverse the video for questionable species and geological identifications. Strike measurements were made by observing the heading, pitch and roll of ROPOS, allowing the observer to identify the bedding strike (Fig. 2-11). Dip measurements were made by observing a feature in multiple directions (forward and downward camera perspectives) while being mindful of ROPOS's heading, pitch and roll (Fig. 2-11).

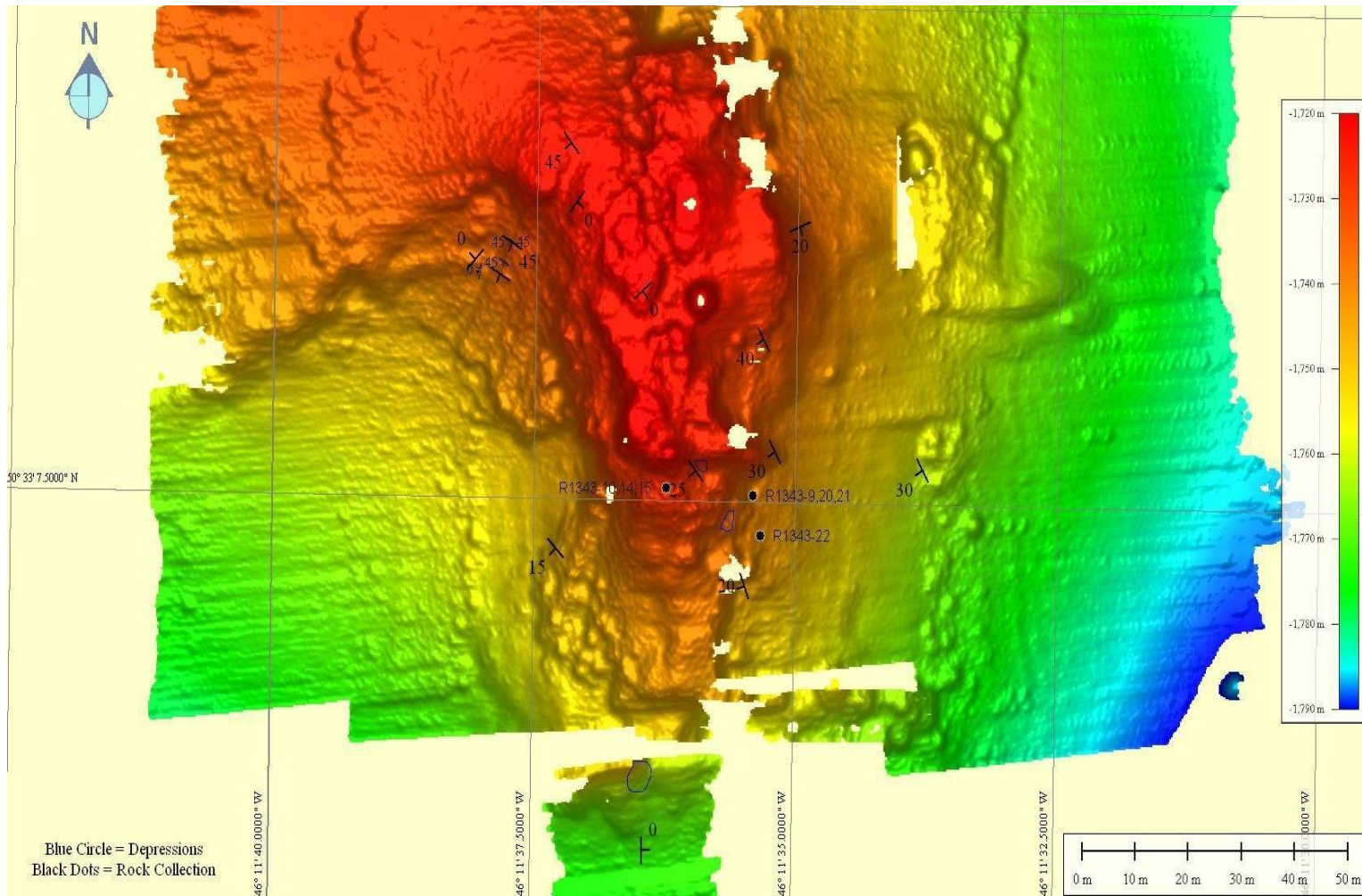
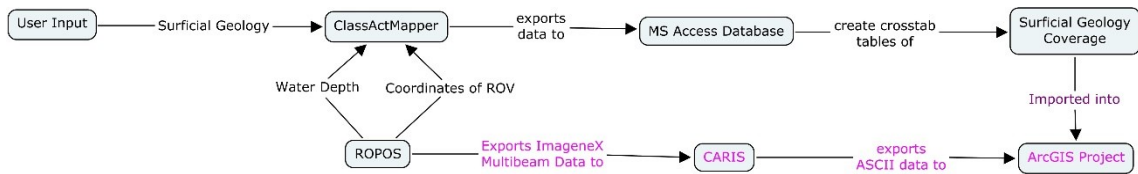


Figure 2-11. Strike and dip locations on Orphan Knoll bedrock outcrop (mound); including rock collection locations. Delta *T* multibeam data collected from ROPOS. Multibeam data was manually processed in CARIS's HIPS & SIPS.

## 2.2.11 Dataset Integration / Database Management

Data extraction from the MS Access<sup>®</sup> databases for Geographic Information Systems (GIS) mapping and statistical interrogation was done through exported tables via various MS Access<sup>®</sup> database queries. Figure 2-12 outlines the procedure used to combine and extract data from the various data tables through MS Access<sup>®</sup> and the eventual importation of the data into ArcGIS<sup>®</sup>.



*Figure 2-12. Geological Data Extraction and Processing Flow Diagram*

## 2.3 Results: Orphan Knoll (D1341- 46) Geological Survey

### 2.3.1 SE Orphan Knoll (Dive 1341)

This was the first dive on the Orphan Knoll and was expected, from *Healy* multibeam and historic seismic profiles, to contain three small enigmatic mounds. The dive (1341) plan was to start at the base of the mounds on the southeast ‘pan handle’ of OK (3000 m depth) and ‘fly’ up the slope of the enigmatic mounds following an orthogonal transect (Fig. 2-10).

#### 2.3.1.1 *Geological Sample Characteristics*

At the beginning of dive 1341 calcareous ooze (R1341-4) and Fe-Mn nodules (R1341-3 and 5) were recovered at the base of an ~7 m tall calcareous ooze outcrop (Fig. 2-13) on a 6° slope 541 m below the top of the southernmost SE OK mound (2345 m) (Fig. 2-14).

#### **Eocene Ooze**

The calcareous ooze sample R1341-4, contained nannofossils *Discoaster sublodoensis*, *Nannotetrina fulgens*, *Discoaster kuepperi* and *Discoaster lodoensis*. Nannofossil recovery was good but preservation was poor with extensive etching (central structure of most coccoliths were missing). Some hydrodynamic sorting was evident as only medium to large sized nannofossils were found, though smaller fossils could be absent due to dissolution. No definite recent nannofossils were identified; however,

evidence of reworking of early Eocene zones NP14a- NP12 nannofossils, *Discoaster kuepperi* and *Discoaster lodoensis*, was observed (Kevin Cooper, pers. comm. 2011) (Fig. 2-15).

Manual pattern matching analysis of the X-ray diffractogram of sample R1341-4 (ooze), using Jade®, identified Quartz, Calcite, Glauconite -1M, Kaolinite and Muscovite within the ooze (Fig. 2-16). Quantitative whole pattern fitting (WPF) in Jade identified that Quartz and Calcite were present in subequal amounts in the ooze. After accounting for the other clay minerals present, the percentage carbonate in the ooze is estimated at ~30%.

Cores 6 and 7, at DSDP site 111A , shows that all the Upper Pliocene to Quaternary sediments were indurated by carbonate-rich intervals, represented by glacial clays alternating with foraminiferal oozes, to a sub-seafloor depth (mbsf) of 147 m (Laughton et al. 1972). The DSDP site 111A core 6 and 7 also identified hard laminated nanoplankton marls and zeolitic clays (182-190 mbsf) containing 20-30% carbonate, calcareous nanoplankton without foraminifera, overlaying a friable chalk layer (Laughton et al. 1972).

The estimated carbonate fraction of the recovered ooze sample (R1341-4) resembles the 20-30% carbonate content of nanoplankton marls in the DSDP nanoplankton marls (cores 6 and 7); however, no evidence of zeolitic clays which are present in the Eocene in DSDP Hole 111A, were found in the ooze sample.

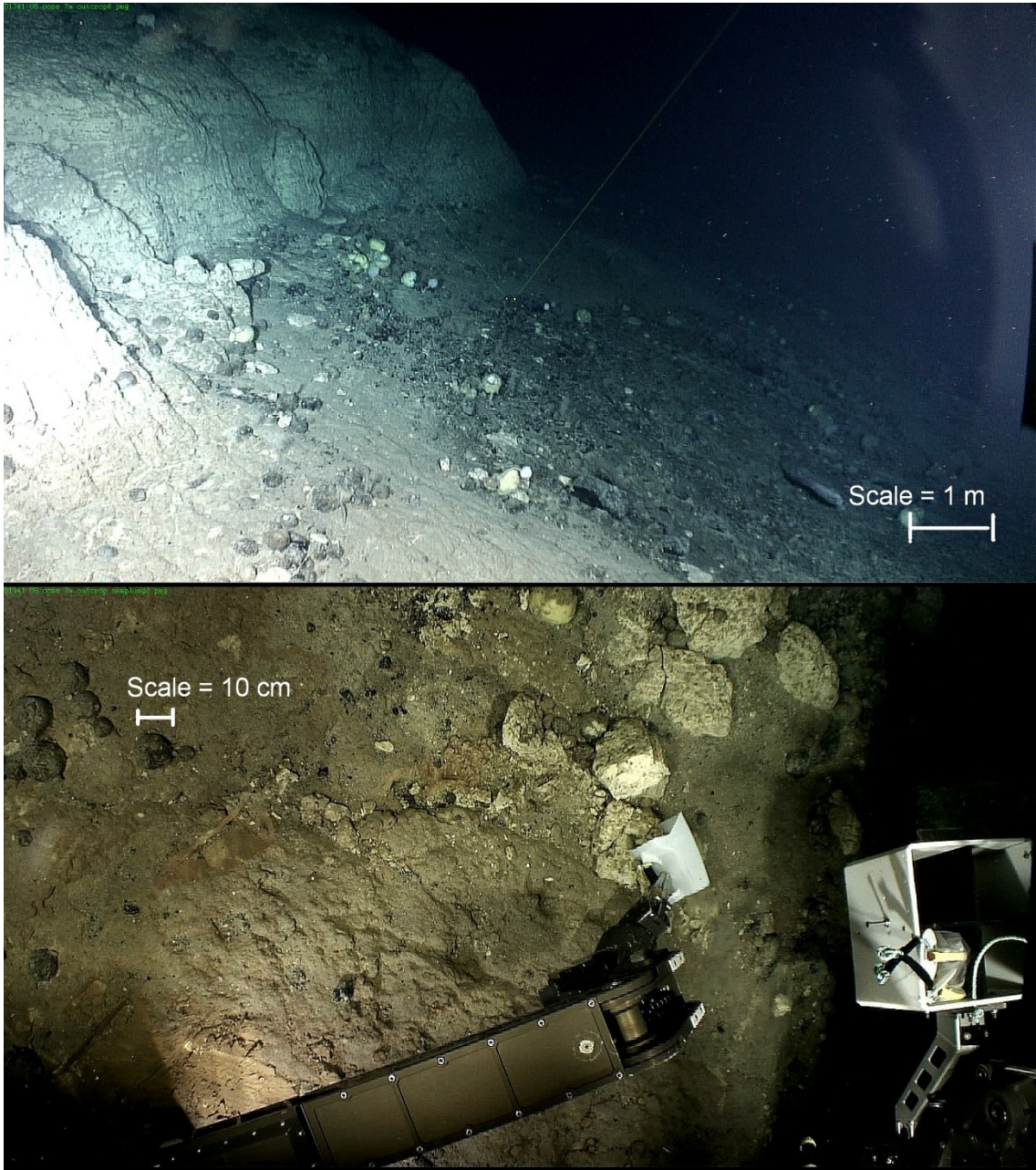


*Figure 2-13. ROPOS dive 1341, Calcareous ooze outcrop with Mn nodules on top of and at the base of the outcrop (Top) Scooping of calcareous ooze outcrop (bottom); green lasers are 10 cm apart; 2886 m depth*

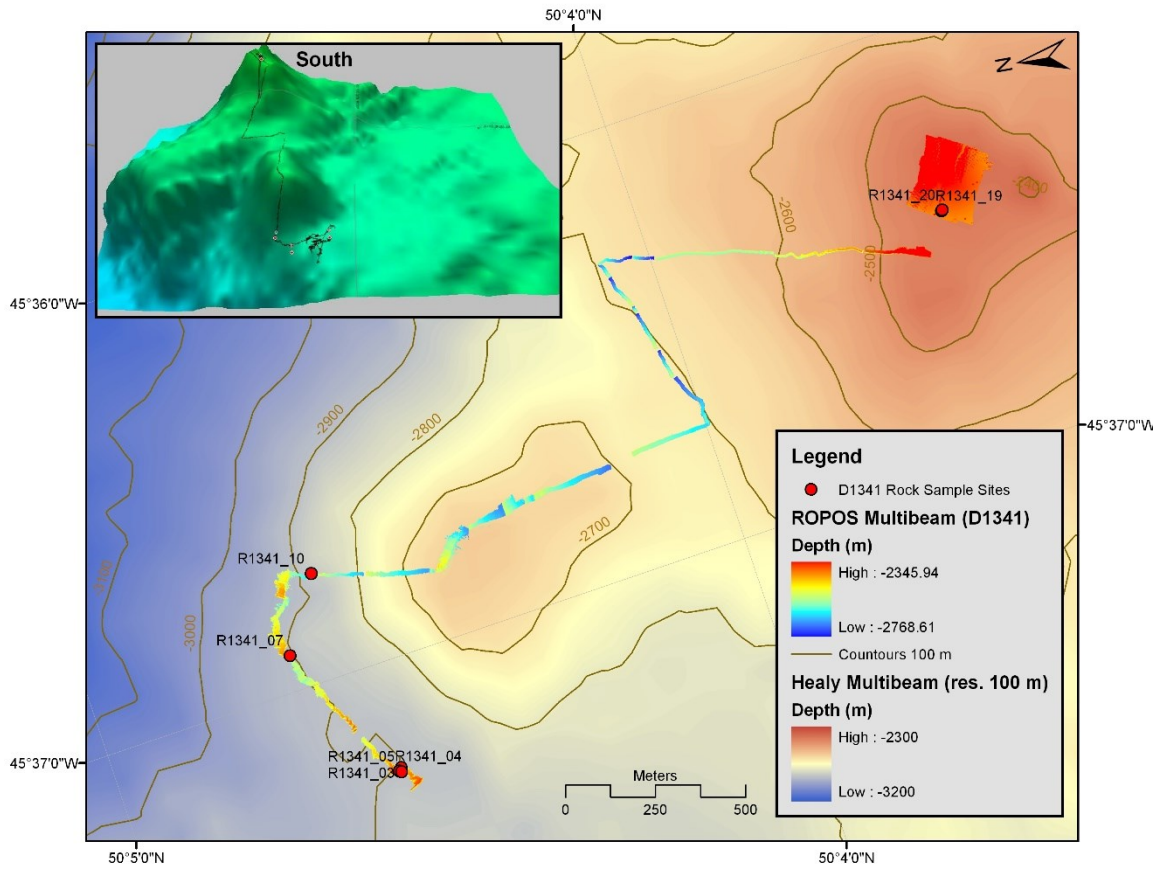
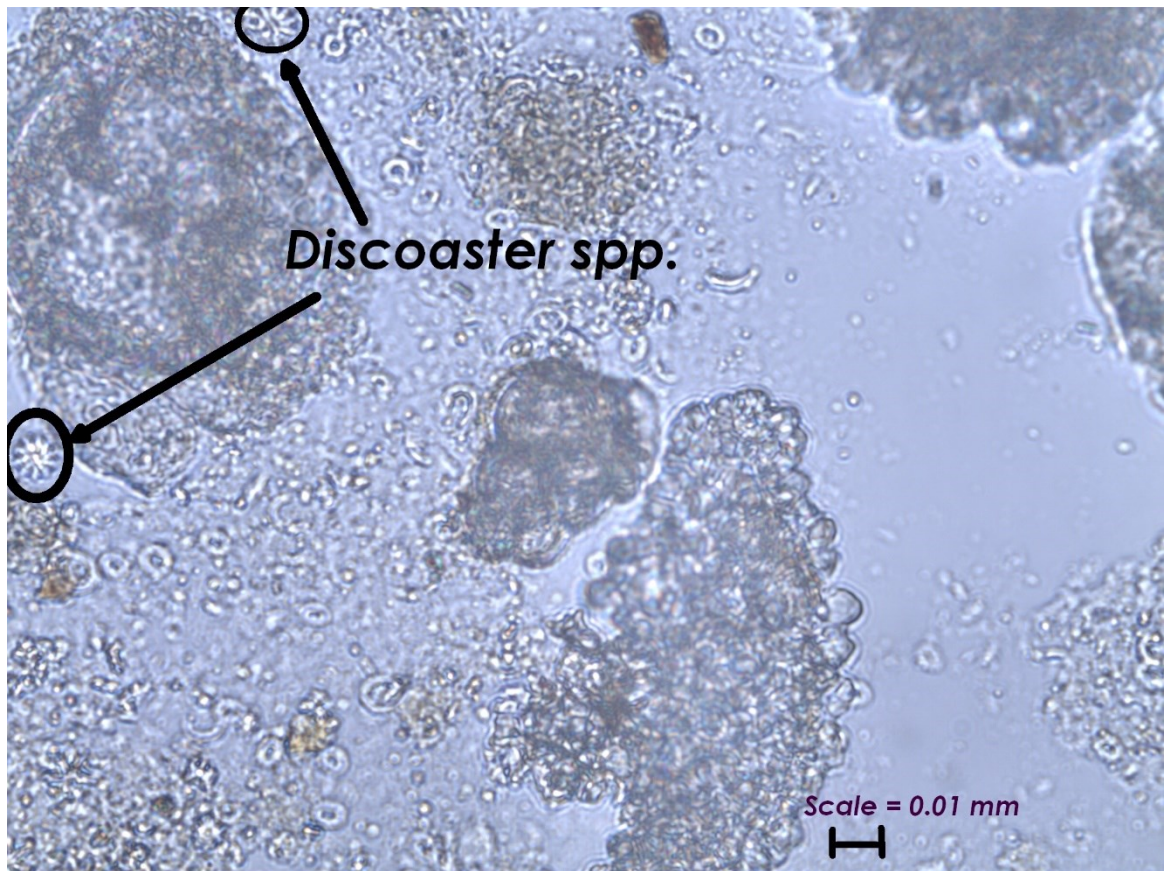


Figure 2-14. ROPOS Dive 1341 on SE Orphan Knoll mounds with inset 3D image of dive track relative to sampling locations



*Figure 2-15. Smear slide of Calcareous Ooze from SE Orphan Knoll showing nannofossil Discoaster spp. (early Eocene, viewed at 50x)*

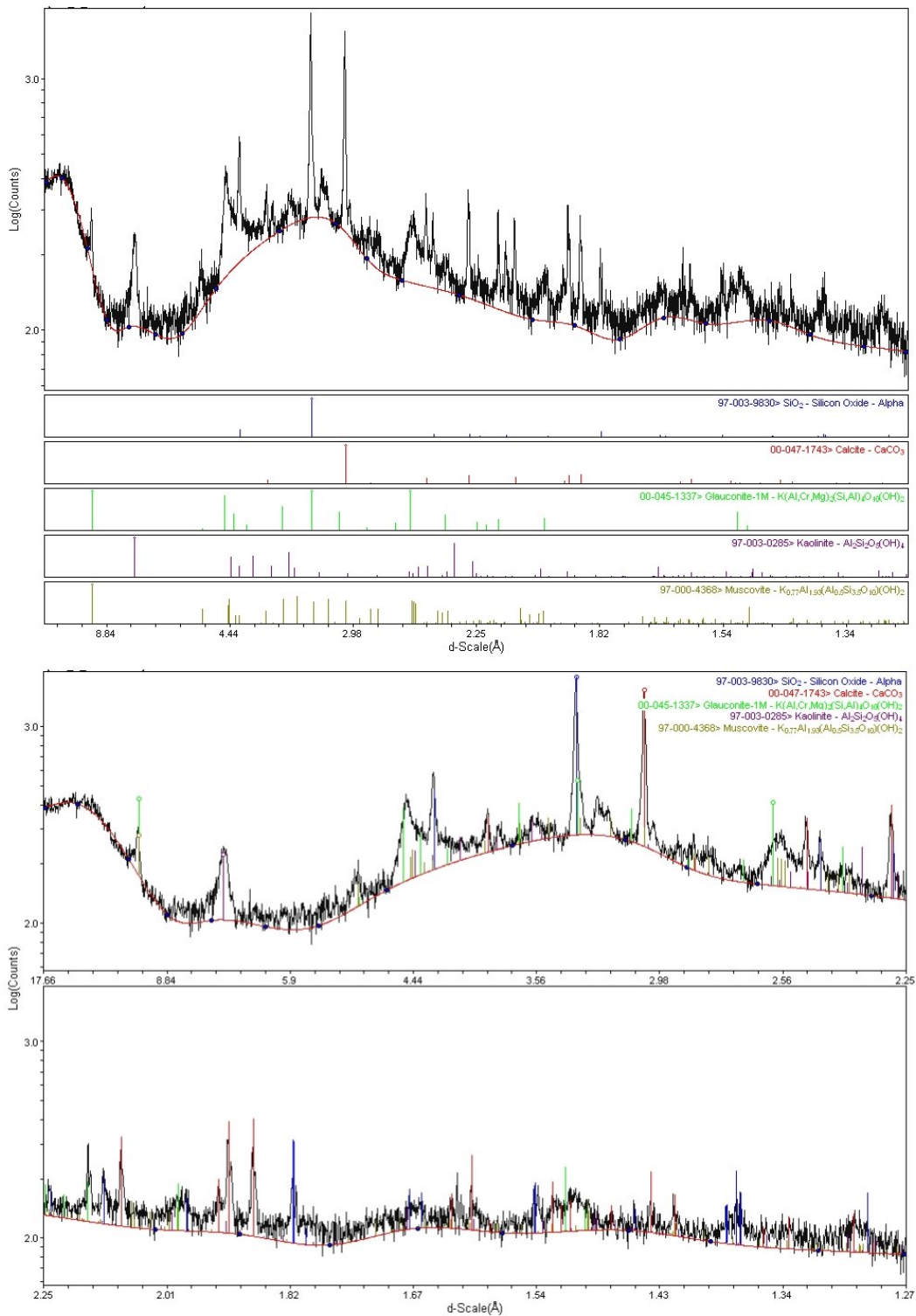


Figure 2-16. XRD results of Calcareous Ooze sample R1341-4 from SE Ok, identifying the top five matching minerals in two different viewable formats

### **2.3.1.2**     *Manganese Nodules and Crusts*

#### **Mn Nodules**

Mn nodules (R1341-3 and 5) were recovered from the base of the ooze outcrop (~7m tall) on SE OK on a 6° slope, 541 m below the top of the southernmost SE OK mound (2345 m) (Fig. 2-13). The Mn nodules were friable and averaged ~10 cm in diameter. Using Osmium isotope analysis the age of the Mn nodules was found to be Late Eocene in age (Poirier et al. 2011). This collection of Mn nodules was found in the same area as calcareous ooze, which appears to be analogous to the Early Eocene nanoplankton marl and zeolitic clay described in core 6 and 7 at DSDP site 111A. Glasby (1978) argued that the Mn oxidation in the form of nodules and /or crusts in the North Atlantic Ocean was Pleistocene in age and were correlated with the presence of pelagic clay, calcareous and siliceous sediments. Glasby (1978) observed that Mn nodules appear to accrete layers during periods of very low sedimentation and in a cooling global climate, probably due to increased bottom water circulation (Glasby 1978).

#### **Mn Crusts**

Covering absolutely every rock sample collected on Hudson 2010-029, was Mn oxidation (black). The Mn oxidation in the form of crust was found to be overlying bedrock (basalt and limestone). Mn oxide crust covering bedrock (R1341-19) was collected from a bedrock outcrop (2453 m) on a 12° slope 108 m below the peak of the SE OK mounds (2345 m) (Fig. 2-17).



*Figure 2-17. Mn-oxide crust (R1341-19) collected from a bedrock outcrop by ROPOS (green lasers are 10 cm apart)*

### **2.3.1.3 Limestone**

Limestone (R1341-7) was pulled out of a bedrock outcrop (2914 m) on a 14° slope 569 m below the peak of the SE OK mounds (-2345 m) (Fig. 2-18). Limestone (R1341-10) was collected from the top of a bedrock outcrop (2888 m) on a 30° slope 543 m below the peak of the SE OK mounds (2345 m) (Fig. 2-19). Microfossils *Globigerina* spp. and *Orbulina* spp. (Mid-Miocene to present) were found in both limestone samples (R1341-7 and R1341-10).

Ice-rafted argillaceous limestone (R1341-20) was collected from a bedrock outcrop (2453 m) on a 12° slope 108 m below the peak of the SE OK mounds (2345 m) (Fig. 2-20). R1341-20 was non-fossiliferous, sub-rounded and displayed 1-3 mm banding (dark grey to light grey in color) separated by a reddish-brown layer (Fig. 2-21). These non-fossiliferous and reddish-brown features are analogous to the Churchill River Formation (Late Ordovician) on Southampton Island in the sub-Arctic Foxe Basin (Heywood & Sanford 1976; King et al. 1985) and are likely correlative with strata in Akpatok Island within Ungava Bay (Workum et al. 2011), which suggests that it could have been ice-rafted from Foxe basin or Hudson Strait.



*Figure 2-18. Sample collection (R1341-7) pulled from bedrock outcrop on SE Orphan Knoll by ROPOS (green lasers are 10 cm apart)*



*Figure 2-19. Sample collection (R1341-10) from a bedrock outcrop on SE Orphan Knoll by ROPOS (green lasers are 10 cm apart)*

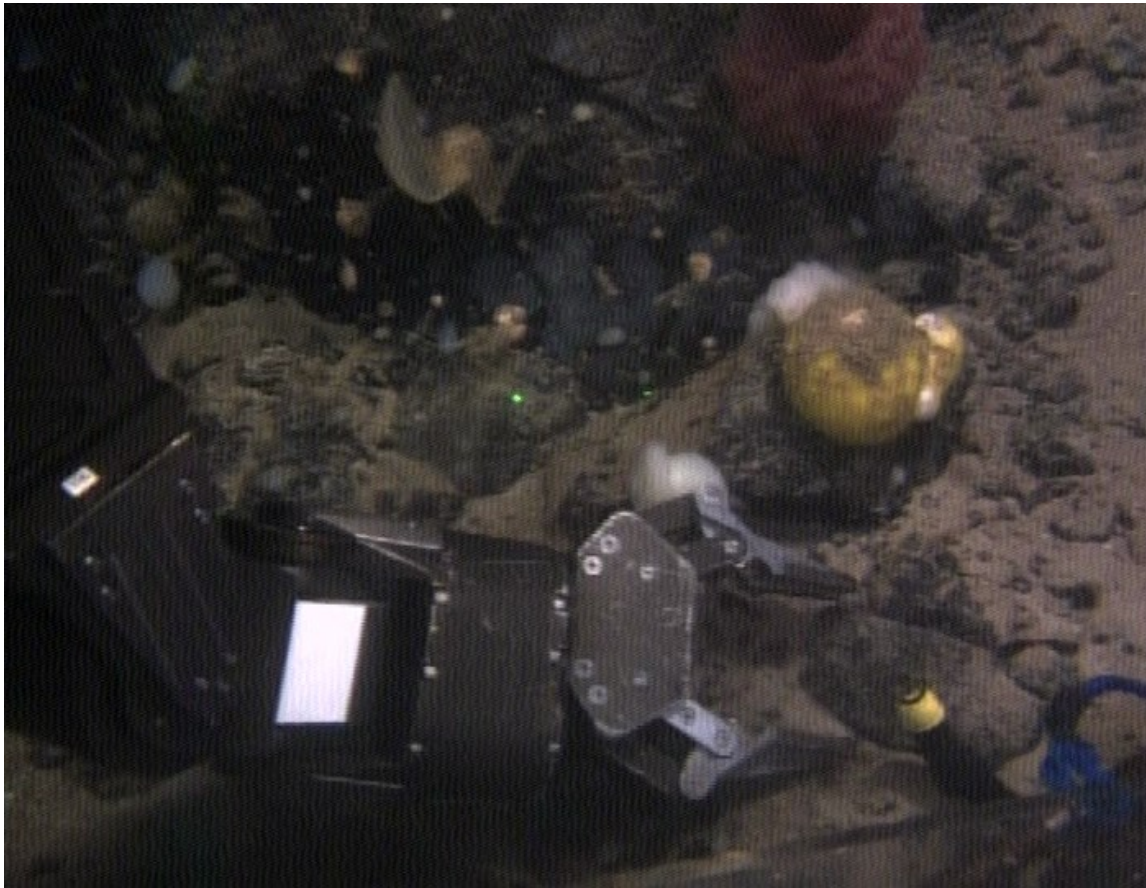


*Figure 2-20. Ice-Rafted Argillaceous Limestone (R1341-20) collected from a bedrock outcrop by ROPOS (green lasers are 10 cm)*

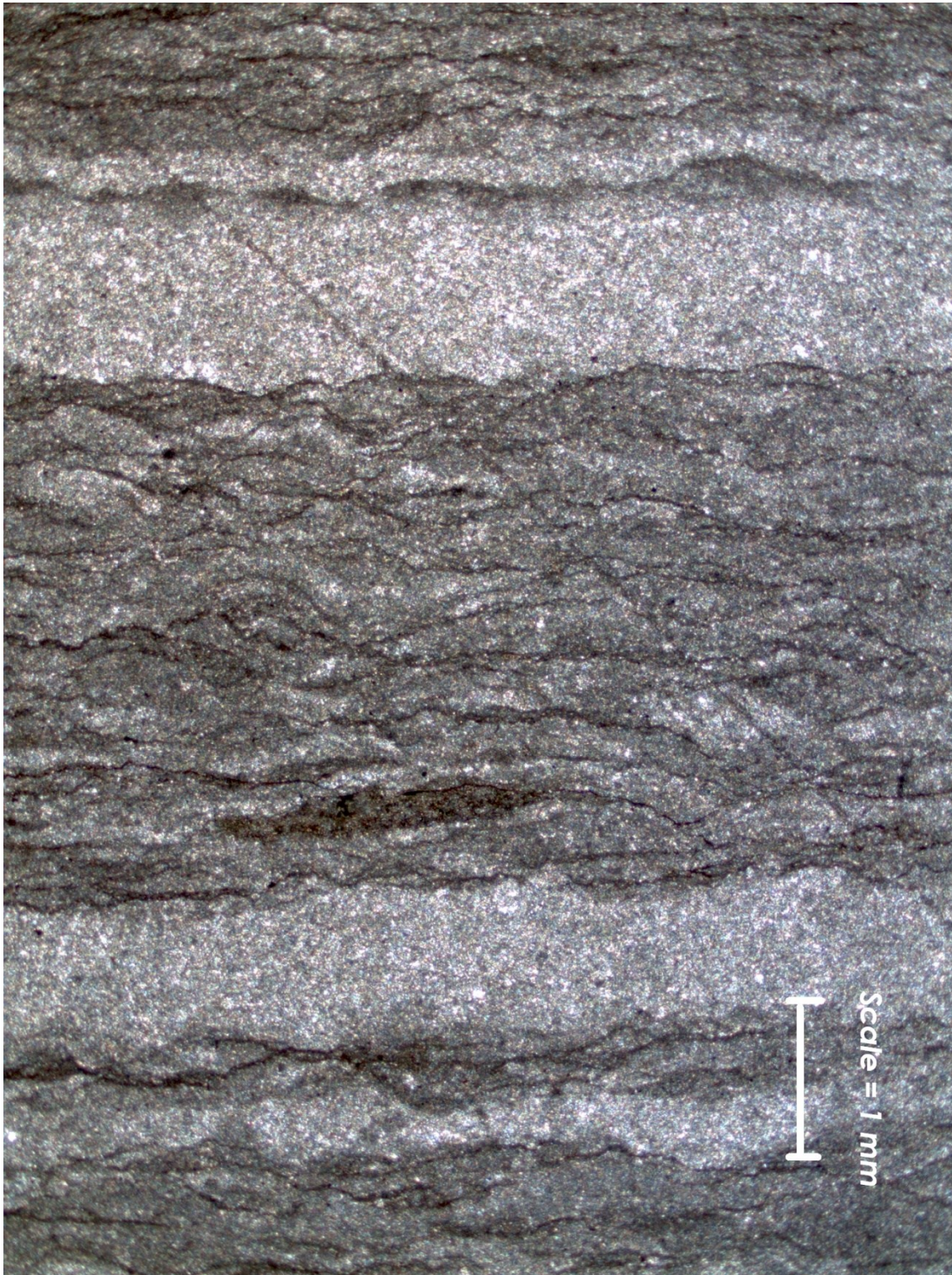


*Figure 2-21. R1341-20 Argillaceous Limestone collected from SE Orphan Knoll (Late Ordovician, IRD, viewed at 1.6x)*

### **2.3.1.4 *Characteristics of the Surficial Geological Units***

#### ***(SGU)***

Figure 2-10 delineates the surficial geology by substrate percent coverage throughout the dive survey. SGU 'A' consists of bedrock overlain by IRD (cobble and pebble sized) intermittently draped by fine-grained sediment. SGUs A'-B and D'-E both consist of extensive fine sediment accumulation at the base of the mounds.

Ascending the second mound on dive 1341, SGU F'-G consisted primarily of fine grained sediment sporadically covered with talus and IRD (boulder to granule sized). SGU G'-H consists of bedrock outcrops overlain by talus and IRD on the top of the second SE Orphan Knoll mound.

### **2.3.2 NE Orphan Knoll (Dive 1343)**

This was the third dive on the Orphan Knoll area and was expected (from previous Hunttec and GLORIA imagery) to contain one or more small enigmatic mounds. The dive (1343) site was northeast of the DSDP drill site on the flat crest of OK in ~1780 m water depth (Fig. 2-6 and 22).

#### **2.3.2.1 *Geological Sample Characteristics***

Fine grained limestone overlain by Fe-Mn crust (R1343-3) (Fig. 2-23) was recovered from an extensive bedrock outcrop on a 3° slope at 1786 m depth (Fig. 2-22).

Fe-Mn oxide crust (R1343-4) was collected from an extensive bedrock outcrop on a 3° slope at 1786 m depth (Fig. 2-24). Fe-Mn oxide crust samples (R1343-10, 14 and 15) were recovered from the SW flank of an extensive bedrock outcrop (OK mound) on a 6° slope at 7 m below the top of the OK mound (1720 m) (Fig. 2-25, 26 and 27).

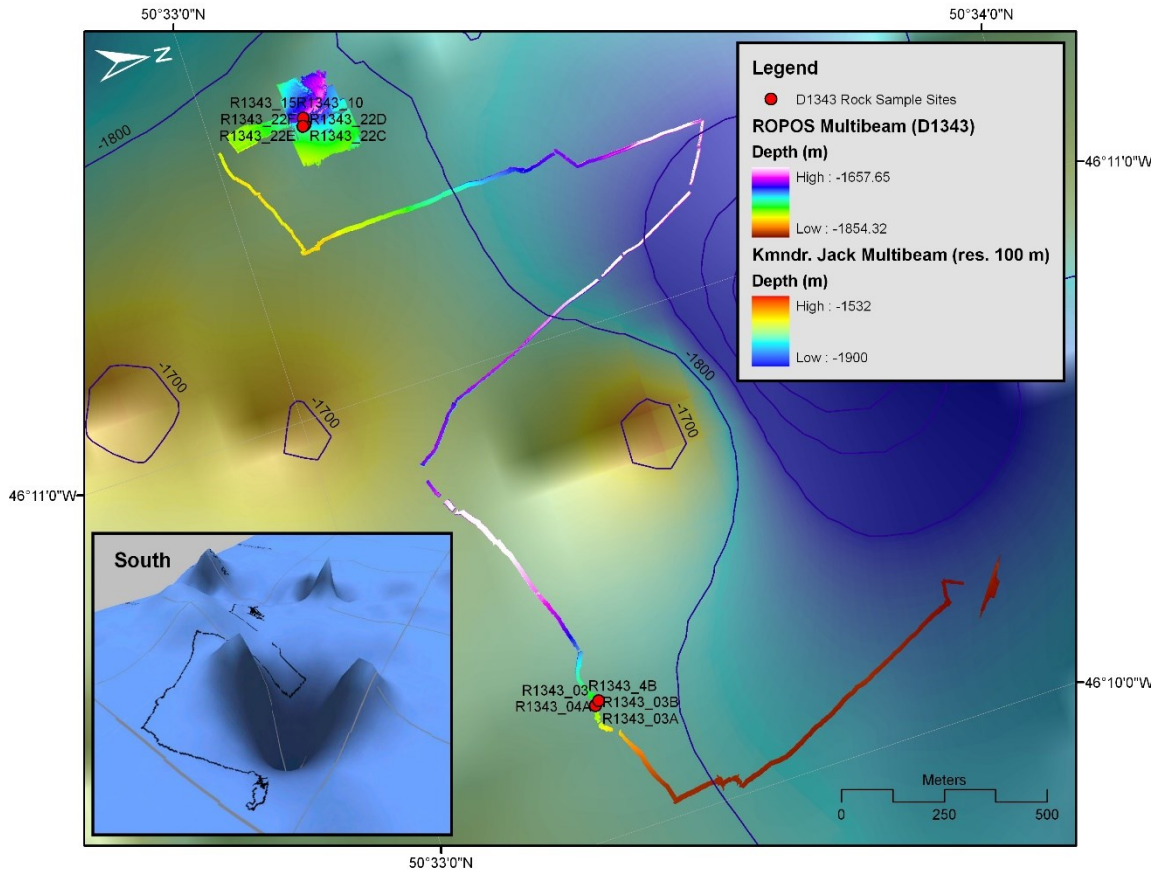


Figure 2-22. Rock sampling locations (red) for dive 1343 overlain with ROPOS collected multibeam data; inset 3D image of the latest multibeam imagery for the Orphan Knoll with the ROPOS dive track overlain.



*Figure 2-23. Pelagic Limestone (R1343-3) collected by ROPOS from a bedrock outcrop covered by extensive Mn oxidation*



*Figure 2-24. Fe-Mn Oxide crust (R1343-4) collected by ROPOS from a bedrock outcrop*



*Figure 2-25. Fe-Mn oxide crust (R1343-10) collected by ROPOS from a bedrock outcrop (green lasers are 10 cm apart)*

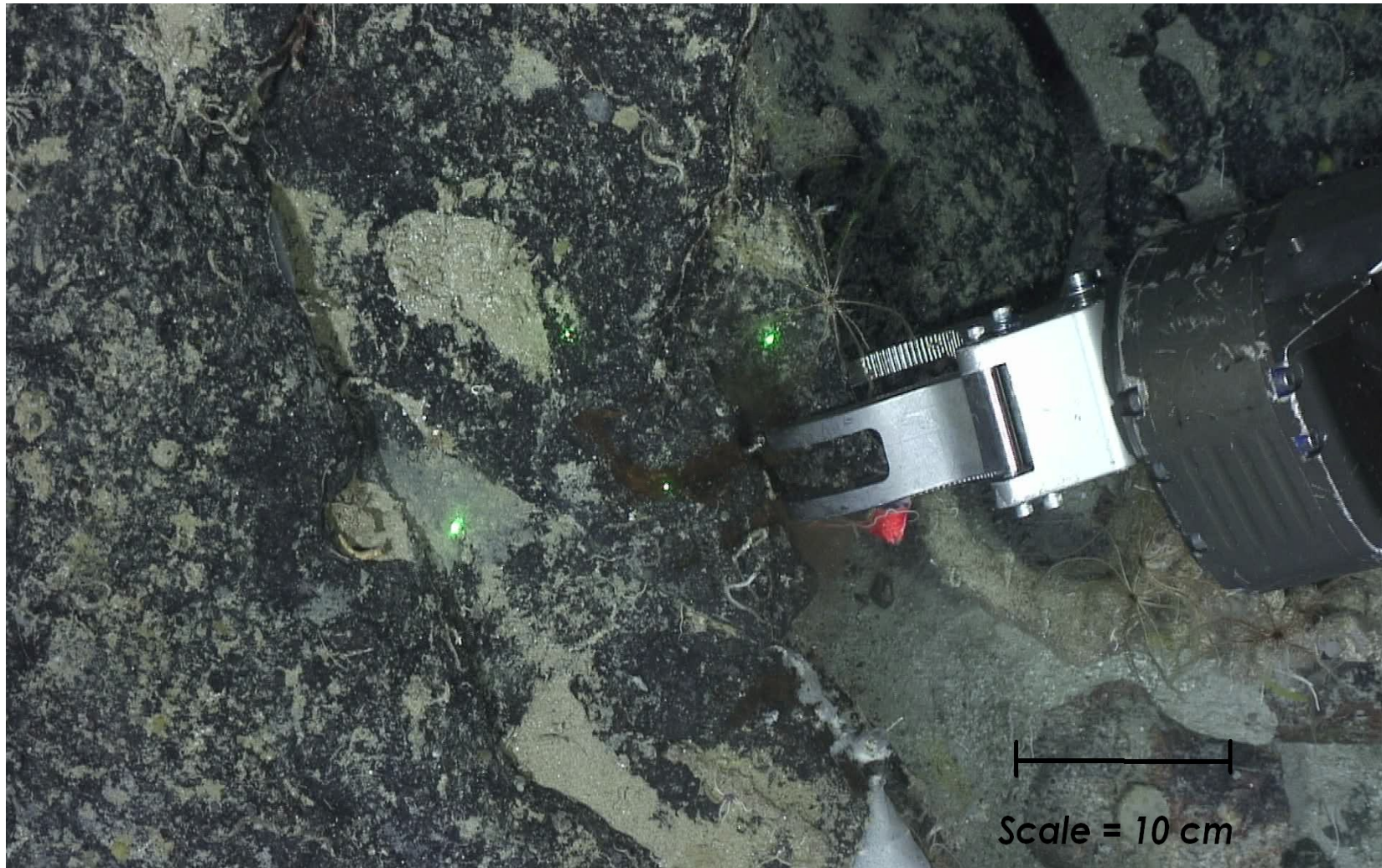


*Figure 2-26. Fe-Mn oxide crust (R1343-14) collected by ROPOS from a bedrock outcrop (green lasers are 10 cm apart)*



*Figure 2-27. Fe-Mn oxide crust (R1343-15) collected by ROPOS from a bedrock outcrop (green lasers are 10 cm apart)*

### 2.3.2.2 Characteristics of the Surficial Geological Segments

Figure 2-28 delineates the surficial geology by substrate percent coverage throughout the dive survey.

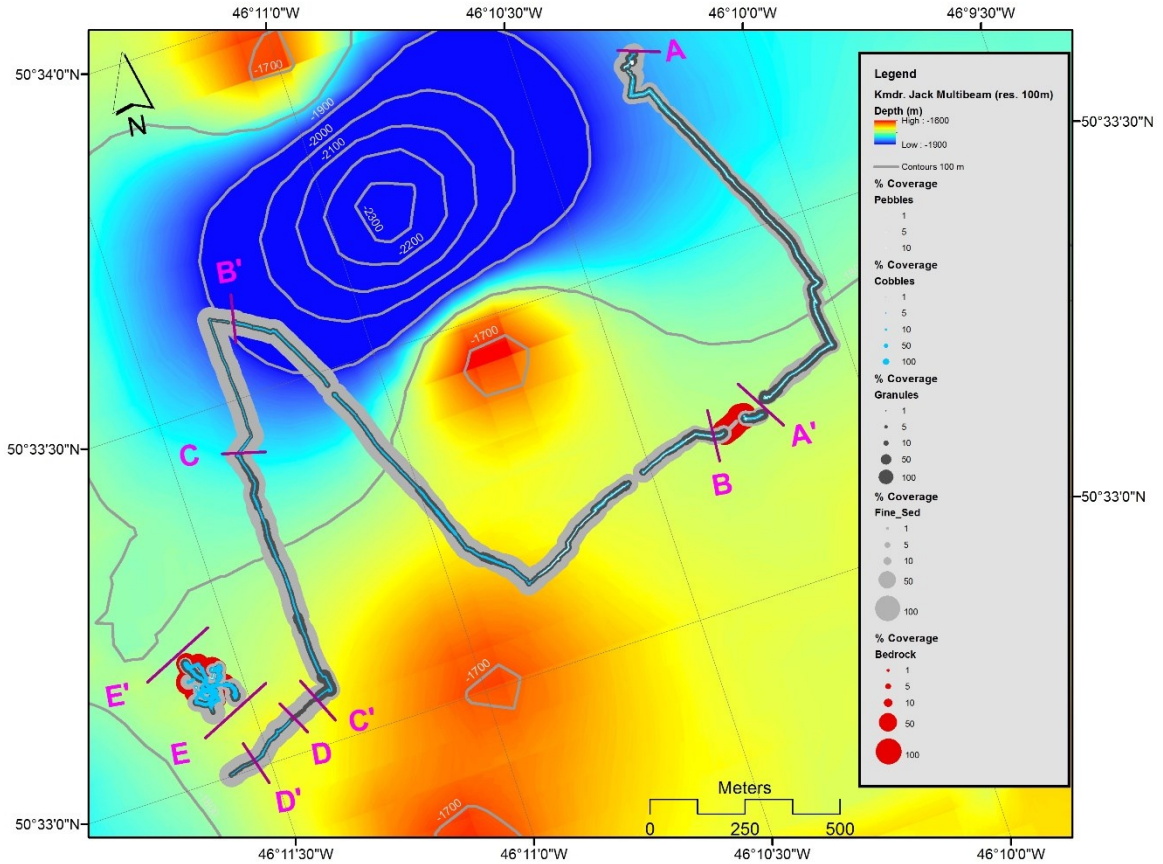


Figure 2-28. Surficial Geology (% Coverage) units from an Orphan Knoll NE Mound (D1343), divided into surficial Geological Segments (SGUs)

Dive 1343 was predominantly 90% fine grained sediment, 1% pebbles, 1% cobbles, 5% boulders and 3% granules; however, two extensive bedrock outcrops were discovered.

An extensive (250 m long) bedrock outcrop (SGU A'-B) along with another larger (500 m) bedrock outcrop (SGU E-E') were detected and thought to be two OK mound structures seen in legacy seismic-reflection and side scan imagery. An unconformity was seen in the larger bedrock outcrop (NE OK mound) between units 2 and 3 (Fig. 2-29). The upper limestone layers (layers 1 and 2) (Fig. 2-29 and 32) dipped  $25^{\circ}$ -  $45^{\circ}$  with a strike of  $135^{\circ}$  (SW-NE) (Fig. 2-11). Unit 1 had thinner bedding than unit 2, where unit 2 had thinner bedding than unit 3 (Fig. 2-29). Unit 3 had a different strike and dip than units 1 and 2, probably indicating an unconformity (Fig. 2-29 and 32); however, the horizon of the unconformity was covered by overlying IRD, talus and fine grained sediment (Fig. 2-29).

Video analysis from SGU E-E' identified exposed walls on the NW (Fig. 2-30) and SE sides (Fig. 2-33) of the exposed bedrock outcrop. The wall feature on the NW side was overlain by fine-grained sediment, while the SE side of the mound consisted primarily of bedrock and granules. The stepped nature of the bedrock (limestone) walls indicated etching or erosion by benthic currents (Fig. 2-33).

OK mound bedrock dips varied between  $0^{\circ}$  and  $45^{\circ}$ , accompanied by a general strike bearing of  $135^{\circ}$  (SW-NE) (Fig. 2-11 and 29). However, three strike and dip measurements at the NE OK mound indicated a general strike of  $225^{\circ}$  and a  $0$ - $20^{\circ}$  dip. This change in strike and dip possibly indicates an undetected unconformity above unit 3 (Fig. 2-11).

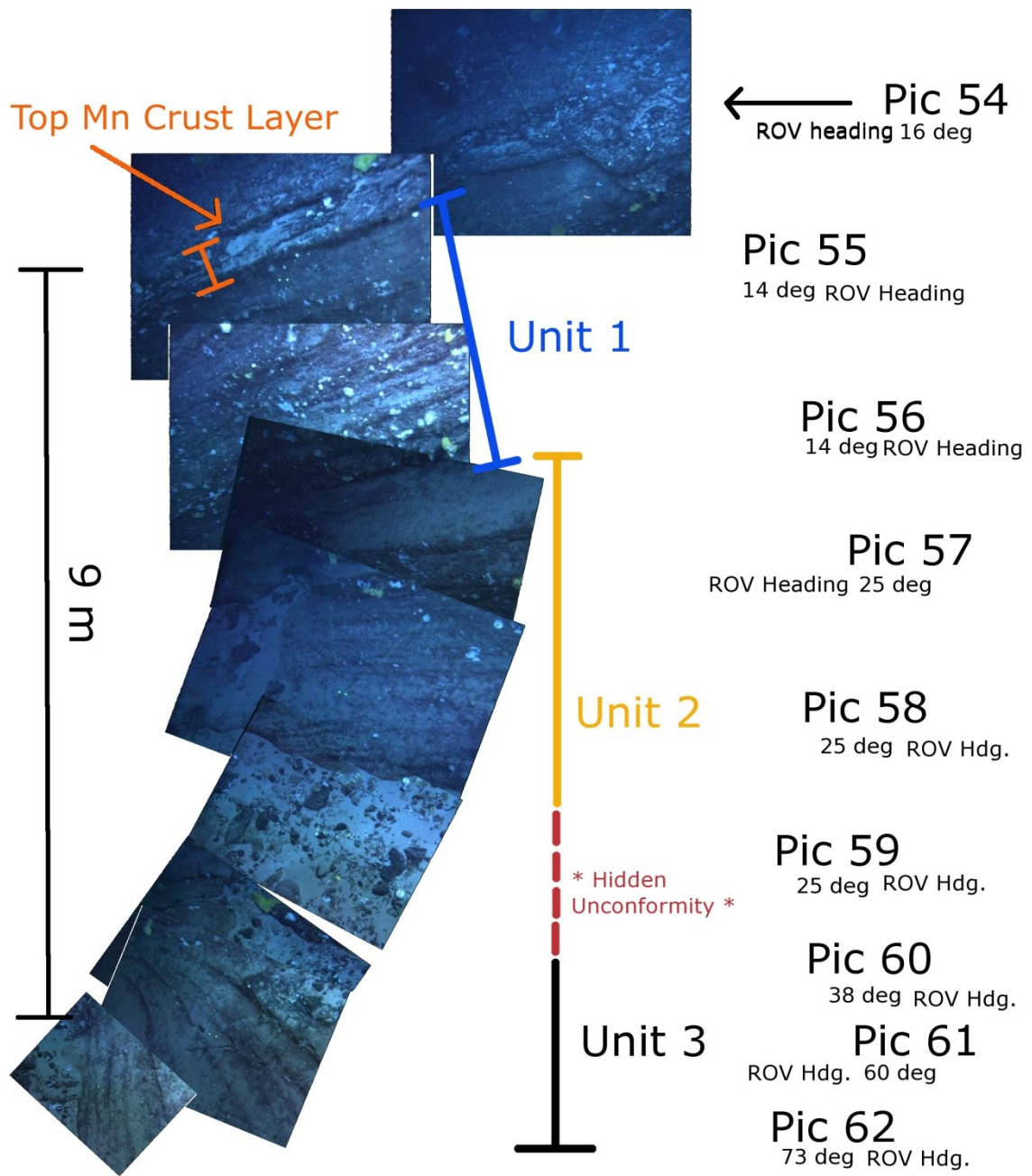
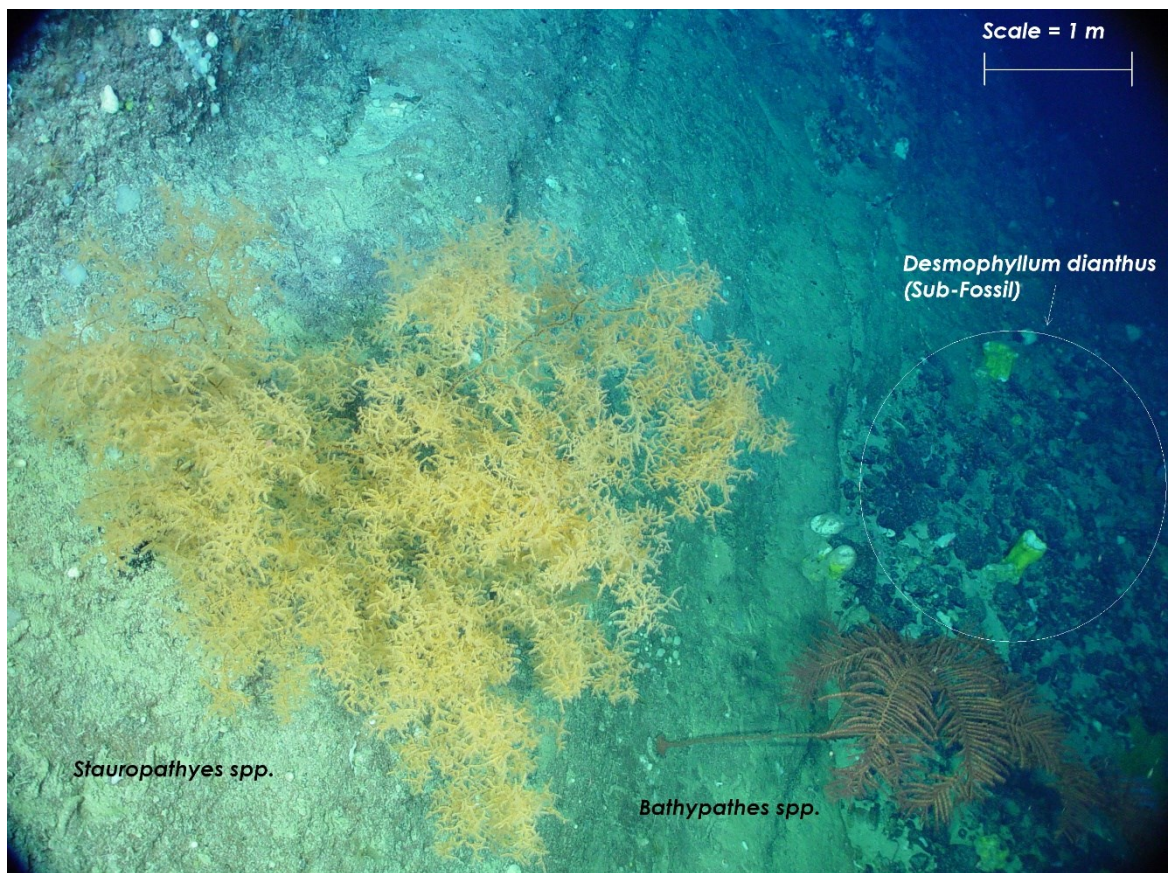


Figure 2-29. ROPOS HD video frame grabs as ROPOS travels down the exposed SW side of the NE OK mound. The picture ID is labeled 'Pic' and the heading of ROPOS is shown below the picture ID. Units 1 and 2 are of the same strike and dip; however Unit 2 has thicker bedded layers than Unit 1. Unit 3 is of a different strike, than Units 1 and 2, and has no apparent dip.



*Figure 2-30. SE wall of Orphan Knoll mound showing Antipatharian Cold-Water corals and a 'graveyard' of sub-fossil *Desmophyllum dianthus* (Scleractinian) found within a mixture of fine sediment and IRD at the base of the exposed bedded limestone bedrock outcrop*

### **2.3.2.3 Geomorphological Characteristics**

Depressions and erosionally accentuated limestone beds (Fig. 2-11) were observed within the ROPOS HD video, on and around the OK NE mound, and were also recorded within the ROPOS collected multibeam imagery (Fig. 2-31, 2-33).

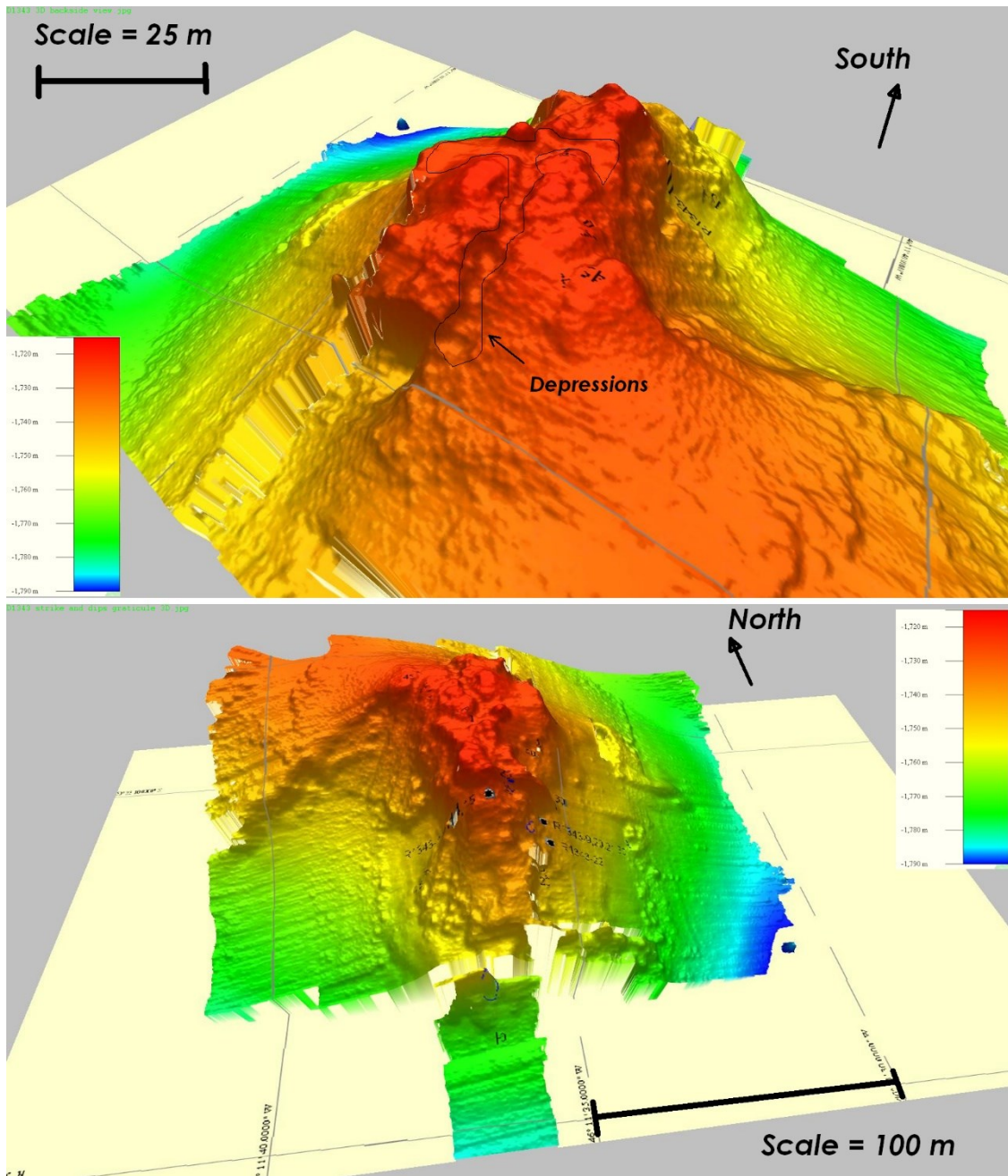


Figure 2-31. 2D rendering of 3D imagery from ROPOS Delta T multibeam survey on NE Orphan Knoll mound, dive (D1343), north and south faces.

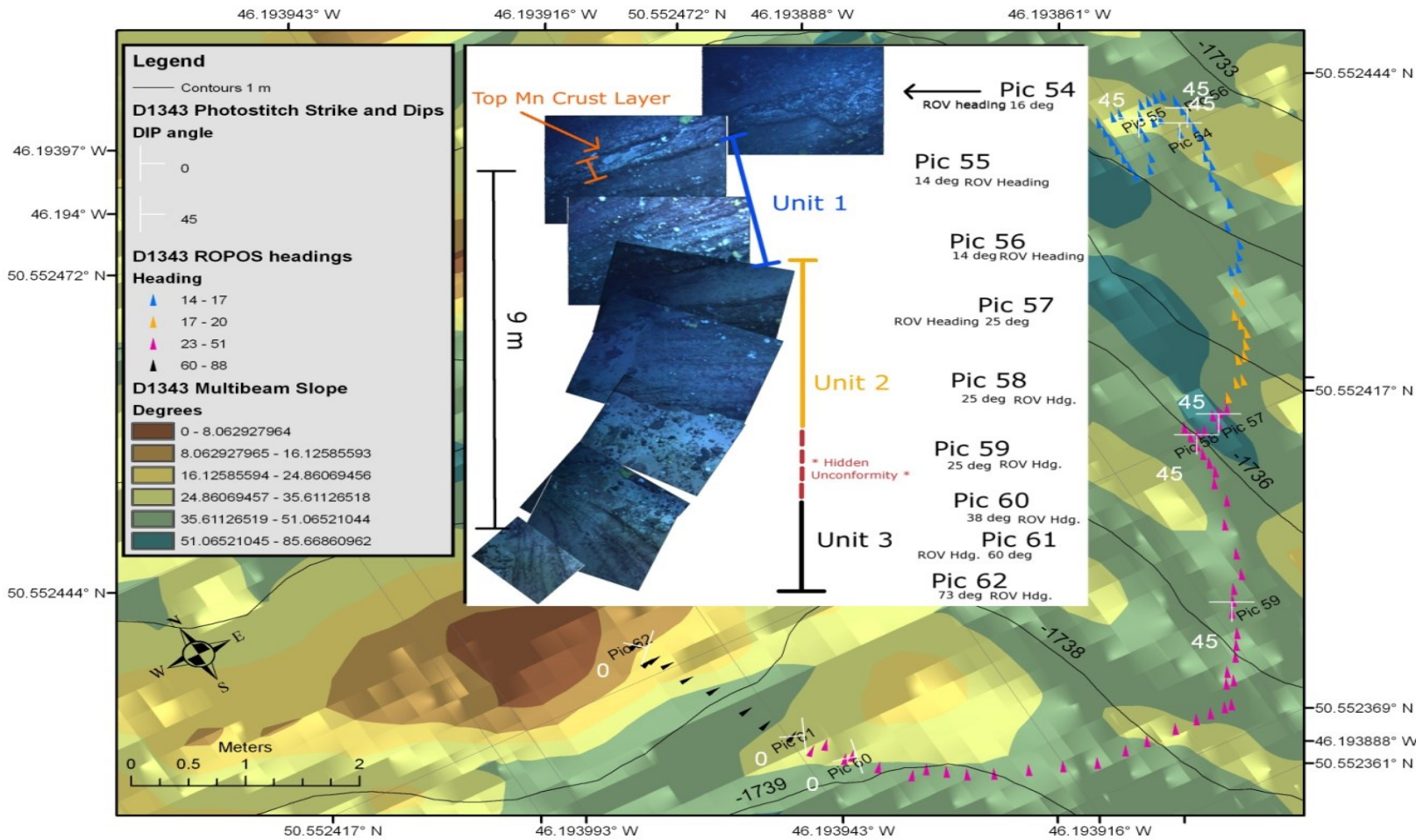
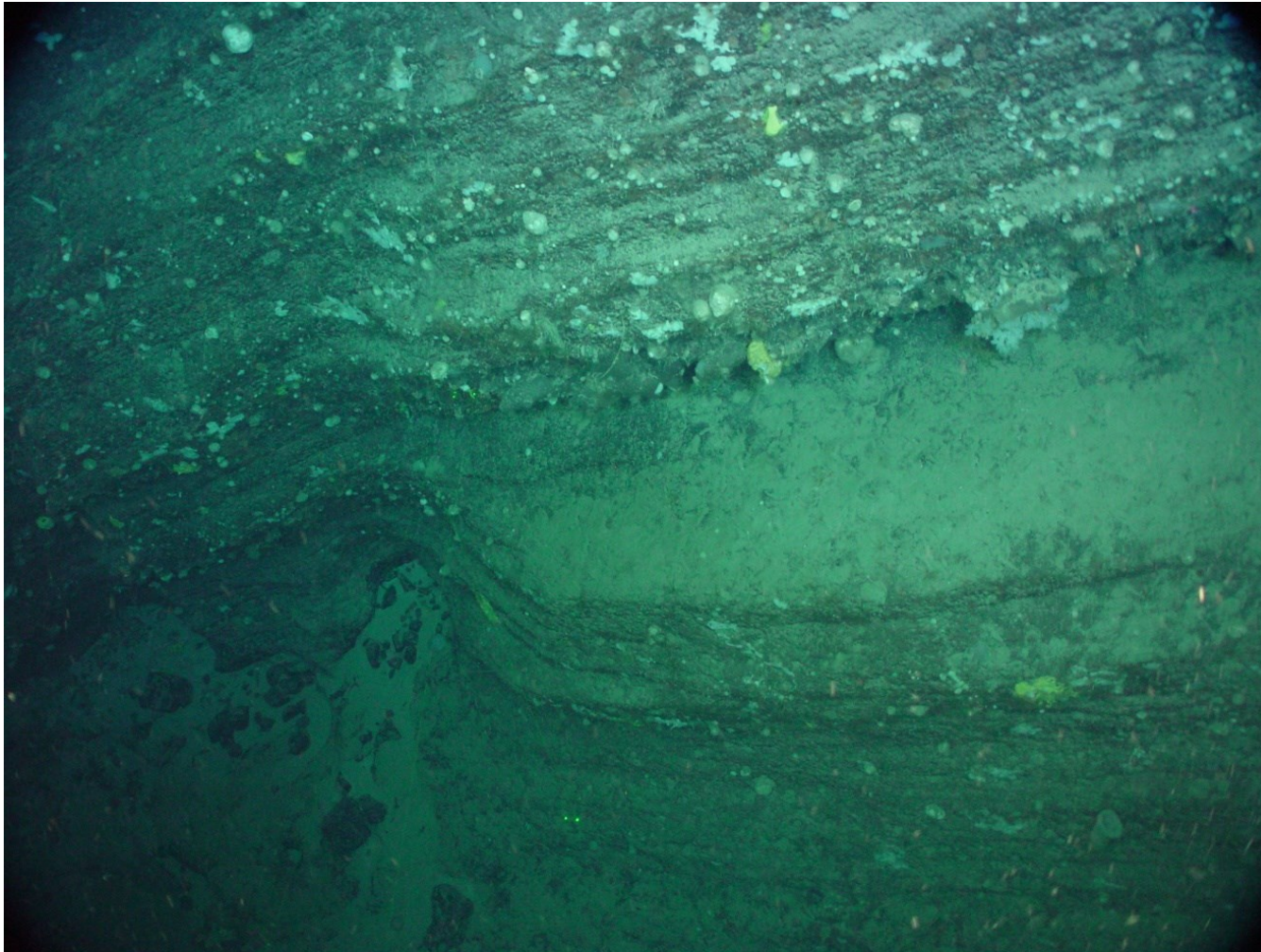


Figure 2-32. Dive 1343 (NE OK mound) ROPOS headings (colored arrows indicating heading) with strikes and dips (white); Fig. 2-28 inset, identifying the 'Pic' ID (black) relative to the stratigraphic Unit number.



*Figure 2-33. Orphan Knoll NE mound imagery of depression feature and eroded wall surface from dive 1343. Green dots are 10cm apart for scale reference (bottom center placement).*

## 2.4 Discussion

### 2.4.1 Were previous interpretations of “bedrock” based on IRD?

Rock sample R1341-20 (SE OK mound) was identified through petrographic analysis as being sub-rounded argillaceous limestone probably originating from the Churchill River Formation of Southampton Island (Late Ordovician) and likely correlative strata in Akpatok Island in Ungava Bay (Workum et al. 2011); thereby placing the origin of this rock as not being from the OK but rather having originated from the Foxe Basin or Hudson Strait, and clearly identifying it as IRD.

The Laurentide ice sheet exported a variety of sediment and rocks from the Foxe Basin via the Hudson Strait as IRD. Almost 50% of the ice-rafted debris consisted of Lower Paleozoic carbonates (Piper and deWolfe, 2003). It is therefore highly likely that Ordovician palynomorphs (Legault 1982), Ordovician acritarchs (Ruffman 1989) and Devonian ostracods (van Hinte et al. 1995) identified within the 1978 dredge samples were from IRD.

### 2.4.2 The role of faults in the formation of enigmatic mounds

The OK was not always at its present depth or location (Keen et al. 1987; Chian et al. 2001). Through complex (i.e. listric, normal, transform) extensional faulting (Enachescu 2009) within the Orphan Basin (failed rift event thinned the crust (Chian et al. 2001)) and then at the NW Atlantic Mid-Ocean Channel (NAMOC), the OK was displaced into its current location and sank to its Bathyal depth (Laughton et al. 1972;

Keen et al. 1987; Chian et al. 2001). Faults identified within the seismic profiles from the DSDP site 111 surveys (Laughton et al. 1972), FGP83-3C 2D seismic data (Fig. 2-3) extend down into the proposed crystalline basement horizon, underlying the locations of the OK mounds. The transparent sections (potential high porosity and / or fluid) within in the historical seismic profile (Fig. 2-3) were thought to be functions of normal faults that extended from the basement (Laughton et al. 1972). The TGS 2D seismic profile identifies a graben feature in the center of the OK, bounded by faults that trend NNW (Fig. 2-34). On the west and east regions of the graben feature are mounds buried and exposed (NE) (Fig. 2-34).

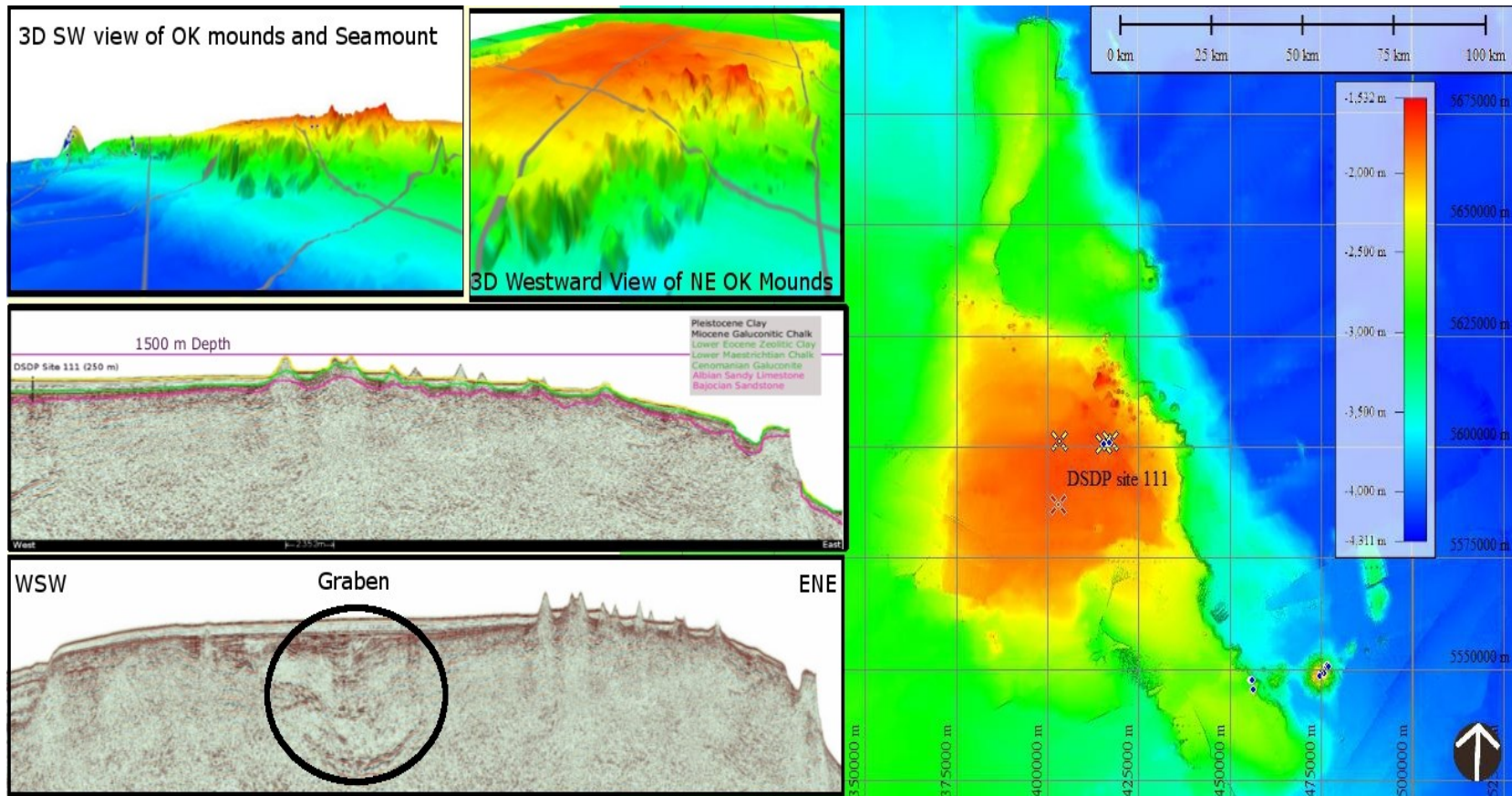


Figure 2-34. Inset TGS 2D seismic profile providing a cross sectional view WSW -ENE across the Orphan Knoll (right with 3x exaggeration), passing just north of the DSDP site 111 (red cross) and south of the historical dredge locations (yellow cross) and ROPOS 2010-029 rock sample sites (blue dot). Contact TGS for more information on seismic line placements.

Fault zones provide a pathway for fluid escape (e.g. oil, gas, etc.) (Immenhauser & Rameil 2011) to be potentially geothermally heated and rise to the surface, possibly creating hydrothermal vents (Curewitz & Karson 1997) or cold seeps (Pohlman et al. 2009). Hydrothermal vents and cold seeps are hotspots of biodiversity due to the unique living conditions (e.g. extreme heat, anoxic, lack of competition) for benthic marine life and can eventually form bioherms (Levin et al. 2009). Rock samples (R1341-7, 10 and R1343-3) from the NE and SE OK mounds identified the bedrock mounds as being mid-Miocene bedded limestone bedrock. There was no evidence of evaporitic diapirs or igneous diapirs (only bedded limestone was recovered) and no previous bioherm activity was observed in thin section or HD video.

#### ***2.4.2.1 Strike and Dip Evidence of Block Faulting***

The discovery of mid-Miocene bedded limestone within unit 1 (OK mounds) that dips SW-NE at  $\sim 45^\circ$  dip on a SE-NW strike ( $135^\circ$ ) varies from the lower unit 3, which is on a W-E strike ( $180\text{-}200^\circ$ ) with a  $0^\circ$  dip. These varying strikes and dips between the upper and lower units identify an unconformity (hidden) between unit 2 and 3 (Fig. 2-29 and 32). Unfortunately, mid-Miocene samples were not recovered from unit 2 and a finer time scale could not be identified between units 1, 2 and 3. Therefore, unit 3 is pre-mid-Miocene where unit 2 could possibly be mid-Miocene, though the lack of a representative unit 2 sample prevents further clarification and is by default pre-mid-Miocene. Taking some liberty and theorising the date of unit 3; deposition during the Ypresian (48 Myr), Maastrichtian (65.6 Myr) or mid-Albian ( $\sim 105$  Myr), when major pre-glacial

sedimentation events occurred on the OK (seen in DSDP cores 2-7) (Laughton et al. 1972), provide possible ages for unit 3.

### 2.4.3 Evidence for Sea-floor Dissolution of Carbonate

Depressions are seen in layers 1 and 2 on the top of the NE OK mound (Fig. 2-11, 29, and 32). The formation of the depressions could have been formed through subaerial dissolution similar to the dissolution of Cretaceous chinks of the Wyandot Formation on the Scotian Shelf (Wielens et al. 2002) or submarine fluid escape (Land, Paull, & Hobson 1995; Wielens *et al.* 2002) and / or a function of strong erosional bathyal currents (Miller & Fairbanks 1983; Via & Thomas 2006).

The dissolution theory relies on the assumption requiring the OK to be subaerial in the SW corner of the OB in the late Cretaceous (Hart 1977). The Late Cretaceous dissolution of OK limestone would have survived the OK extensional tectonic activity (Haworth & Keen 1979; Chian et al. 2001), subsequent burial by pre-glacial and glacial deposition (Laughton et al. 1972; Channell et al. 2006), and then was possibly exposed to its current position through reactivated faults in the Quaternary and Neogene (Toews & Piper 2002). Another variation on the dissolution hypothesis is that dissolution occurred sub-aerially at a slower rate with a shale cap overlying the Late Cretaceous limestone (Immenhauser & Rameil 2011); however, no shale was recovered from the enigmatic mounds so the presence of shale is speculative.

The submarine fluid escape theory is also a possibility, since the southeastern OB contains fine sediment with high organic content (Kimmeridgian aged Egret source rock)

(Enachescu 2005) and a variety of complex faulting (Burton-Ferguson et al. 2006), trapping hydrocarbon deposits that could have used the fault zones as conduits for fluid escape (Curewitz & Karson 1997). In this case, bioherms would be expected to be seen where the enigmatic mounds were located, this was not the case with either of the OK mound locations.

The possibility of strong erosional bottom currents forming these curved depressions as the Oligocene-Mid Miocene abyssal circulation changed in the western North Atlantic Ocean to produce strong erosional bottom water conditions (Miller & Fairbanks 1983), could also explain these curved depressions.

The depressions remain a mystery but the only speculative theory that seems plausible based on the evidence recovered so far, is the presence of strong erosional bottom currents creating these depressions.

#### 2.4.4 Evidence of Bedded Limestone

GSC donated Hunttec and air gun imagery (Fig. 2-4 and 2-35 respectively) identifies horizontally stratified sediment, acoustically similar to Upper Pleistocene to Holocene sediment collected at DSDP site 111, adjacent to the OK mounds (Laughton et al. 1972). The seismic imagery provides evidence that Miocene, or older, strata have been uplifted ~152 m, based on Miocene strata identified in DSDP core 6 sections 2 and 3 in hole 111A (Laughton et al. 1972), possibly along a reactivated (Quaternary - Neogene) fault zone. Sedimentary layers seen within seismic profiles adjacent to the mounds (Fig.

2-35) and on top of the mounds (Fig. 2-4), indicate that the exposed bedrock surface is a small portion of a large partially buried faulted block of bedded limestone.

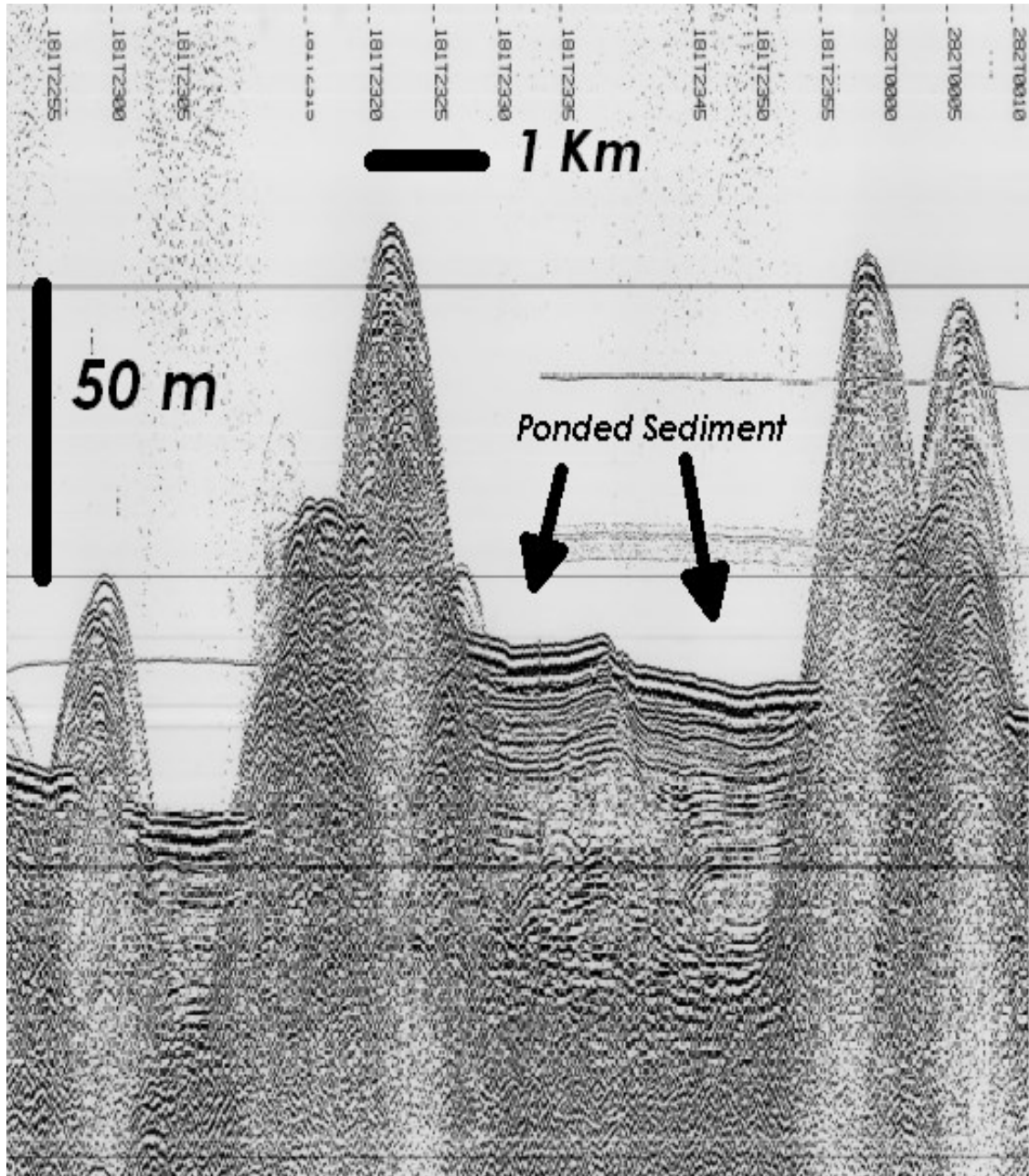
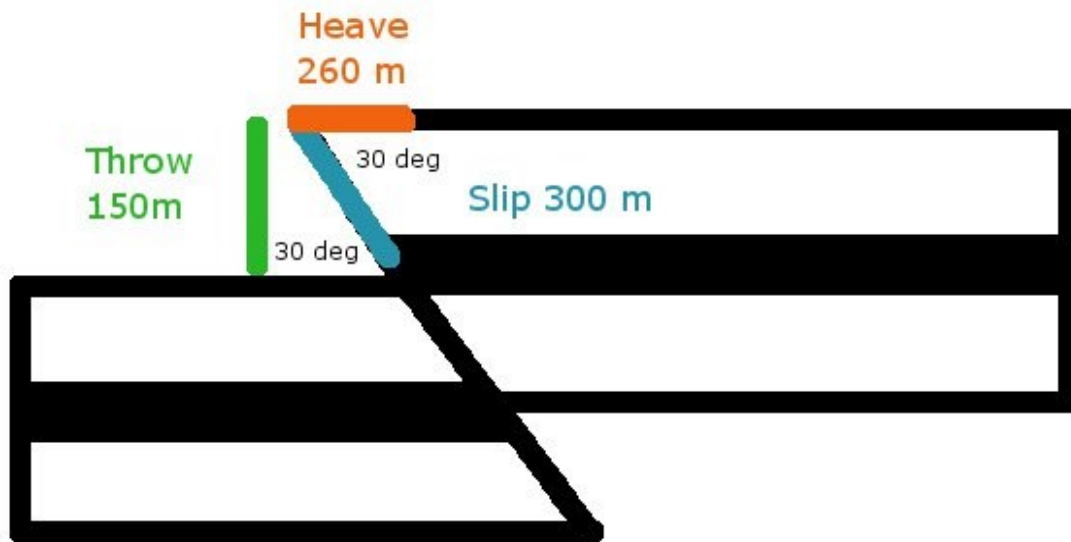


Figure 2-35. Gas injection (GI) air gun seismic profile from Hudson 2004-024 cruise, at the location of the 1978 dredge location, identifying ponded sediment between NE OK mounds (GSC-NRCAN)

The depressions flanking the mounds collected hemi-pelagic sediment during two major sediment pulses, Maastrichtian (65 Myr) until Late Eocene (35 Myr) and Early Miocene (22 Myr) until Late Miocene (5 Myr) (Laughton et al. 1972). In between the major sediment pulses, a 13 Myr hiatus (Oligocene-mid Miocene) of sedimentation was observed in DSDP site 111 cores (Laughton et al. 1972), likely due to stronger bottom currents (Miller & Fairbanks 1983; Via & Thomas 2006). Unit 3 was tilted prior to the Miocene, possibly during the Oligocene hiatus; therefore, some of the OK mounds could have resembled ridges of resistant bedded limestone, in their infancy, probably due to post-Miocene deformation caused by reactivated normal faults in the Quaternary – Neogene (Parson et al. 1984) and strong bottom currents.

Miocene faulting in the eastern Orphan Basin, possibly due to plate readjustments of the White Sail fault (Burton-Ferguson et al. 2006) and Quaternary faulting seen on the southern Labrador slope near the intersection with the Dover fault and Charlie Gibbs Fracture Zone (CGFZ), ~100 km north of the OK, and on the east side of the Flemish Pass (south of the OK.) (D. Piper, Pers. Comm.), could account for a fault throw of 150 m dipping at ~ 30°, in the north and eastern parts of OK (Fig. 2-36). The theoretical calculated fault throw resulted in a tilted block 260 m wide, which is consistent with the observed widths of OK mounds (Fig. 2-11) .



*Figure 2-36. Theoretical throw fault calculations (Pythagorean formula) for a 150 m throw dipping at 30 degrees resulting in a 260 m heave (i.e. NE OK mound)*

The combination of the theoretically calculated fault throw, evidence of Mass Transport Deposit (MTD) (Fig. 2-4) and seeing that not all of the mounds are fully exposed; the possibility that the OK mounds are a combination of fault throws and MTDs of faulted blocks of bedded limestone, possibly exposed as a function of reactivated faults during the Quaternary and Neogene, partially eroded by strong bottom currents, is now the standing theory on the composition, age and origins of the enigmatic mounds of OK.

## 2.5 Conclusions

### **Is the mystery of the enigmatic mounds solved?**

Previously collected rock dredges from OK were very likely IRD due to the discovery of Mid Miocene bedded limestone within the upper segment of the OK mound, a the recovered IRD argillaceous limestone sample (R1341-20), which appeared

analogous to the Churchill River Formation (Late Ordovician) on Southampton Island in the sub-Arctic Foxe Basin and are likely correlative with strata in Akpatok Island within Ungava Bay.

The OK surficial geology varied from a flat fine-grained sediment surface at non-mound locations (South, SW and East) to a high sloped surface with bedrock outcroppings, covered by talus and IRD at the mound locations (SE and NE).

Foraminiferal evidence (*Globigerina* spp. and *Orbulina* spp.) within the recovered limestone places the top bedrock layer (unit 1) of the OK mounds as being mid-Miocene or younger with depression features possibly formed through dissolution, fluid escape or strong bottom currents. The unconformity between units 2 and 3 indicated tilting, possibly from a fault throw at an activated fault zone, sometime between the Neogene and Quaternary periods.

The mounds of OK are exposed faulted blocks of bedded limestone that have an upper age of mid-Miocene and with a possibly lower age range of Late Eocene indicated by the recovered Late Eocene calcareous ooze sample at the base (3000 m depth) of the SE OK mounds. The OK mounds surveyed were buried and exposed but the base of the mounds was not sampled and has yet to be determined; therefore, the origins remain enigmatic and future endeavors to tackle mystery of the origins of the enigmatic mounds of OK, would benefit from sampling more mounds and from bedrock units 2 and 3 or deeper (OK eastern slope mounds could have potentially exposed mound strata worth investigating).

## 2.6 Bibliography

- Alt, J., 1988. Hydrothermal oxide and nontronite deposits on seamounts in the eastern Pacific. *Marine Geology*, 81(1–4), pp.227–239.
- Althaus, F. et al., 2009. Impacts of bottom trawling on deep-coral ecosystems of seamounts are long-lasting. *Marine Ecology Progress Series*, 397, pp.279–294. Available at: <http://www.int-res.com/abstracts/meps/v397/p279-294/>.
- Amos, C. & Judge, J., 1991. Sediment transport on the eastern Canadian continental shelf. *Continental Shelf Research*, 11(8–10), pp.1037–1068. Available at: <http://linkinghub.elsevier.com/retrieve/pii/027843439190090S>.
- Austin, M., 2002. Spatial prediction of species distribution: an interface between ecological theory and statistical modelling. *Ecological Modelling*, 157(2–3), pp.101–118. Available at: <http://linkinghub.elsevier.com/retrieve/pii/S0304380002002053>.
- Bailey, W. et al., 2003. The spatial distributions of fault and deep sea carbonate mounds in the Porcupine Basin, offshore Ireland. *Marine and Petroleum Geology*, 20, pp.509–522.
- Baillon, S., Hamel, J.-F. & Mercier, A., 2014. Diversity, distribution and nature of faunal associations with deep-sea pennatulacean corals in the northwest atlantic. *PloS one*, 9(11), p.16. Available at: <http://dx.plos.org/10.1371/journal.pone.0111519>.
- Baker, K. et al., 2012. Distributional patterns of deep-sea coral assemblages in three submarine canyons off Newfoundland, Canada. *Marine Ecology Progress Series*, 445, pp.235–249. Available at: <http://www.int-res.com/abstracts/meps/v445/p235-249/>.
- Barrett, T. et al., 1988. Geochemical aspects of hydrothermal sediments in the eastern Pacific Ocean; an update. *Canadian Mineralogist*, 26(3), p.841.
- Barrie, J. & Conway, K., 2008. Surficial geology: The third dimension in habitat mapping. In J. Reynolds & H. Greene, eds. *Marine Habitat Mapping Technology for Alaska*. Fairbanks, AK: University of Alaska Fairbanks, pp. 91–97.
- Beazley, L. et al., 2015. Drivers of epibenthic megafaunal composition in the sponge grounds of the Sackville Spur, northwest Atlantic. *Deep Sea Research Part I: Oceanographic Research Papers*, 98, pp.102–114.
- Bellier, J.-P., Mathieu, R. & Granier, B., 2010. Short Treatise on Foraminiferology (Essential on modern and fossil Foraminifera). In *Carnets de Geologie*. p. 106.
- Berggren, W. & Aubert, J., 1976. Eocene benthonic foraminiferal biostratigraphy and paleobathymetry of Orphan Knoll (Labrador Sea). *Micropaleontology*, 22(3), pp.327–346.
- Blow, W., 1956. Origin and Evolution of the Foraminiferal Genus *Orbulina* d'Orbigny. *Micropaleontology*, 2(1), pp.57–70. Available at: <http://www.jstor.org/stable/1484492>.
- Bluhm, B., Iken, K. & Hopcroft, R., 2010. Observations and exploration of the Arctic's Canada Basin and the Chukchi Sea: The Hidden Ocean and RUSALCA expeditions. *Deep Sea*

- Research Part II: Topical Studies in Oceanography*, 57(1–2), pp.1–4. Available at: <http://linkinghub.elsevier.com/retrieve/pii/S0967064509002446> [Accessed February 18, 2011].
- Bolton, B. et al., 1988. Geochemistry and mineralogy of seafloor hydrothermal and hydrogenetic Mn oxide deposits from the Manus Basin and Bismarck Archipelago region of the southwest Pacific Ocean. *Marine Geology*, 85(1), pp.65–87.
- Boutillier, J. et al., 2008. Status of Cold-Water Coral Communities of the World: A Brief Update. In T. Hourigan, ed. *Status of Coral Reefs of the World*. Australian Institute of Marine Science, pp. 58–66.
- Breeze, H. et al., 1997. Distribution and Status of Deep Sea Corals off Nova Scotia. *Ecology & Action*, (1), pp.1–40. Available at: [http://www.ecologyaction.ca/files/images/file/Marine/Distribution and Status of Deep Sea Coral off Nova Scotia Part 1.pdf](http://www.ecologyaction.ca/files/images/file/Marine/Distribution%20and%20Status%20of%20Deep%20Sea%20Coral%20off%20Nova%20Scotia%20Part%201.pdf).
- Bronner, A. et al., 2011. Magmatic breakup as an explanation for magnetic anomalies at magma-poor rifted margins. *Nature Geoscience Letters*, 4(8), pp.549–553. Available at: <http://dx.doi.org/10.1038/ngeo1201>.
- Brown, C. et al., 2011. Benthic habitat mapping: A review of progress towards improved understanding of the spatial ecology of the seafloor using acoustic techniques. *Estuarine, Coastal and Shelf Science*, 92(3), pp.502–520. Available at: <http://linkinghub.elsevier.com/retrieve/pii/S0272771411000485> [Accessed March 16, 2012].
- Bryan, T. & Metaxas, A., 2006. Distribution of deep-water corals along the North American continental margins: Relationships with environmental factors. *Deep Sea Research Part I: Oceanographic Research Papers*, 53(12), pp.1865–1879. Available at: <http://linkinghub.elsevier.com/retrieve/pii/S0967063706002378>.
- Bryan, T. & Metaxas, A., 2007. Predicting suitable habitat for deep-water gorgonian corals on the Atlantic and Pacific Continental Margins of North America. *Marine Ecology Progress Series*, 330, pp.113–126. Available at: <http://www.int-res.com/abstracts/meps/v330/p113-126/>.
- Buhl-Mortensen, L. et al., 2010. Biological structures as a source of habitat heterogeneity and biodiversity on the deep ocean margins. *Marine Ecology*, 31(1), pp.21–50. Available at: <http://blackwell-synergy.com/doi/abs/10.1111/j.1439-0485.2010.00359.x>.
- Buhl-Mortensen, L. et al., 2012. Habitat complexity and bottom fauna composition at different scales on the continental shelf and slope of northern Norway. *Hydrobiologia*, 685(1), pp.191–219.
- Buhl-Mortensen, P., Buhl-Mortensen, L., et al., 2009. Megafaunal diversity associated with marine landscapes of northern Norway: A preliminary assessment. *Norsk Geologisk Tidsskrift*, 89(1–2), pp.163–171.
- Buhl-Mortensen, P., Dolan, M. & Buhl-Mortensen, L., 2009. Prediction of benthic biotopes on a Norwegian offshore bank using a combination of multivariate analysis and GIS classification. *ICES Journal of Marine Science*, 66(9), pp.2026–2032. Available at:

- <http://icesjms.oxfordjournals.org/content/66/9/2026.short>.
- Burton-Ferguson, R., Enachescu, M. & Hiscott, R., 2006. Preliminary Seismic Interpretation and Maps for the Paleogene-Neogene (Tertiary) Succession, Orphan Basin. *Recorder*, 31(7), pp.28–32.
- Burton, E. & Lundsten, L., 2008. Davidson Seamount taxonomic guide. *Marine sanctuaries conservation series ; ONMS-08-08*, pp.1–160. Available at: <http://sanctuaries.noaa.gov/science/conservation/pdfs/taxonomic.pdf>.
- Carlson, A. et al., 2007. Geochemical proxies of North American freshwater routing during the Younger Dryas cold event. *Proceedings of the National Academy of Sciences*, 104(16), pp.6556–6561. Available at: <http://www.pubmedcentral.nih.gov/articlerender.fcgi?artid=1871824&tool=pmcentrez&rendertype=abstract>.
- Carmack, E. & Wassmann, P., 2006. Food webs and physical-biological coupling on pan-Arctic shelves: Unifying concepts and comprehensive perspectives. *Progress in Oceanography*, 71(2–4), pp.446–477.
- Carpenter, K. et al., 2008. One-Third of Reef-Building Corals Face Elevated Extinction Risk from Climate Change and Local Impacts. *Science*, 321(5888), pp.560–563. Available at: <http://www.sciencemag.org/content/321/5888/560.abstract>.
- Channell, J. et al., 2006. IODP Expeditions 303 and 306 Monitor Miocene-Quaternary Climate in the North Atlantic. *Scientific Drilling*, 2, pp.4–10.
- Chian, D., Reid, I. & Jackson, H., 2001. Crustal structure beneath Orphan Basin and implications for nonvolcanic continental rifting. *Journal Geophysical Research*, 106(B6), pp.10923–10940. Available at: <http://dx.doi.org/10.1029/2000JB900422>.
- Christiansen, B. & Wolff, G., 2009. The oceanography, biogeochemistry and ecology of two NE Atlantic seamounts: The OASIS project. *Deep Sea Research Part II: Topical Studies in Oceanography*, 56(25), pp.2579–2581. Available at: <http://linkinghub.elsevier.com/retrieve/pii/S0967064508004451> [Accessed September 2, 2010].
- Coles, G. et al., 1996. Foraminifera and Ostracoda from Quaternary carbonate mounds associated with gas seepage in the Porcupine Basin, offshore Western Ireland. *Revista Española de Micropaleontología*, XXVIII(2), pp.113–151.
- Colman, J. et al., 2005. Carbonate mounds off Mauritania, Northwest Africa: status of deep-water corals and implications for management of fishing and oil exploration activities. In A. Freiwald & J. M. Roberts, eds. Erlangen Earth Conference Series. Springer Berlin Heidelberg, pp. 417–441. Available at: [http://dx.doi.org/10.1007/3-540-27673-4\\_21](http://dx.doi.org/10.1007/3-540-27673-4_21).
- Compton, R., 1985. *Geology in the Field* 1st ed., John Wiley & Sons, Inc.
- Costello, M., 2009. Distinguishing marine habitat classification concepts for ecological data management. *Marine Ecology Progress Series*, 397, pp.253–268. Available at: <http://www.int-res.com/abstracts/meps/v397/p253-268/> [Accessed July 27, 2010].
- Cronan, D., Rothwell, G. & Croudace, I., 2010. An ITRAX Geochemical Study of

- Ferromanganiferous Sediments from the Penrhyn Basin, South Pacific Ocean. *Marine Georesources & Geotechnology*, 28(3), pp.207–221. Available at: <http://search.ebscohost.com/login.aspx?direct=true&db=aph&AN=53155598&site=ehost-live&scope=site>.
- Curewitz, D. & Karson, J., 1997. Structural settings of hydrothermal outflow: Fracture permeability maintained by fault propagation and interaction. *Journal of Volcanology and Geothermal Research*, 79(3–4), pp.149–168. Available at: <http://www.sciencedirect.com/science/article/pii/S0377027397000279>.
- Danovaro, R. et al., 2001. Deep-sea ecosystem response to climate changes: the eastern Mediterranean case study. *Trends in Ecology & Evolution*, 16(9), pp.505–510.
- Danovaro, R. et al., 2008. Exponential decline of deep-sea ecosystem functioning linked to benthic biodiversity loss. *Current Biology*, 18(1), pp.1–8. Available at: <http://www.sciencedirect.com/science/article/pii/S0960982207023421> [Accessed March 9, 2012].
- Davies, A. et al., 2009. Downwelling and deep-water bottom currents as food supply mechanisms to the cold-water coral *Lophelia pertusa* (Scleractinia) at the Mingulay Reef complex. *Limnology and Oceanography*, 54(2), pp.620–629. Available at: <http://hdl.handle.net/10242/44685>.
- Davies, A. et al., 2008. Predicting suitable habitat for the cold-water coral *Lophelia pertusa* (Scleractinia). *Deep Sea Research Part I: Oceanographic Research Papers*, 55(8), pp.1048–1062. Available at: <http://linkinghub.elsevier.com/retrieve/pii/S0967063708000836> [Accessed February 11, 2011].
- Davies, A., Roberts, M. & Hall-Spencer, J., 2007. Preserving deep-sea natural heritage: Emerging issues in offshore conservation and management. *Biological Conservation*, 138(3–4), pp.299–312. Available at: <http://www.sciencedirect.com/science/article/pii/S0006320707002285>.
- Davies, A.J. & Guinotte, J.M., 2011. Global habitat suitability for framework-forming cold-water corals. *PloS one*, 6(4), pp.1–15. Available at: <http://www.pubmedcentral.nih.gov/articlerender.fcgi?artid=3078123&tool=pmcentrez&rendertype=abstract> [Accessed March 18, 2012].
- Davies, J. et al., 2015. Benthic Assemblages of the Anton Dohrn Seamount (NE Atlantic): Defining Deep-Sea Biotopes to Support Habitat Mapping and Management Efforts with a Focus on Vulnerable Marine Ecosystems. *PloS one*, 10(5), p.33. Available at: <http://www.pubmedcentral.nih.gov/articlerender.fcgi?artid=4436255&tool=pmcentrez&rendertype=abstract>.
- Dowsett, H. & Robinson, M., 2007. Mid-Pliocene planktic foraminifera assemblage of the North Atlantic Ocean. *Micropaleontology*, 53(1–2), pp.105–126. Available at: <http://micropal.geoscienceworld.org/cgi/content/abstract/53/1-2/105>.
- Dronov, A., 1993. Middle paleozoic waulsortian-type mud mounds in Southern Fergana (Southern Tien-Shan, commonwealth of independent states): The shallow-water atoll model. *Facies*, 28(1), pp.169–180. Available at: <http://dx.doi.org/10.1007/BF02539735>.

- Durán Muñoz, P. & Sayago-Gil, M., 2011. An overview of cold-water coral protection on the high seas: The Hatton bank (NE Atlantic)—A case study. *Marine Policy*, 35(5), pp.615–622. Available at: <http://www.sciencedirect.com/science/article/pii/S0308597X11000248>.
- Edinger, E. et al., 2011. Geological features supporting deep-sea coral habitat in Atlantic Canada. *Continental Shelf Research*, 31(2, Supplement), pp.S69–S84. Available at: <http://www.sciencedirect.com/science/article/pii/S0278434310002220>.
- Elith, J. et al., 2010. A statistical explanation of MaxEnt for ecologists. *Diversity and Distributions*, 17(1), p.no-no. Available at: <http://doi.wiley.com/10.1111/j.1472-4642.2010.00725.x> [Accessed November 25, 2010].
- Ellis, N., Smith, S. & Pitcher, R., 2012. Gradient forests: calculating importance gradients on physical predictors. *Ecological Society of America*, 93(1), pp.156–168.
- Enachescu, M., 2004. Conspicuous deepwater submarine mounds in the northeastern Orphan Basin and on the Orphan Knoll, offshore Newfoundland. *The Leading Edge*, 23(12), pp.1290–1294. Available at: <http://link.aip.org/link/LEEDFF/v23/i12/p1290/s1&Agg=doi>.
- Enachescu, M., 2009. *Investigating basin architecture and evolution of the Orphan Basin by use of reflection, refraction, heatflow and potential filed transects*, St. John's, NL.
- Enachescu, M., 2005. Offshore Newfoundland and Labrador - An Emerging Energy Powerhouse. In *Offshore Technology Conference*. Houston, TX: Offshore Technology Conference, pp. 1–8. Available at: <http://www.onepetro.org/mslib/servlet/onepetropreview?id=OTC-17570-MS&soc=OTC>.
- Etnoyer, P., 2005. Seamount resolution in satellite-derived bathymetry. *Geochemistry Geophysics Geosystems*, 6(3), pp.311–312. Available at: <http://www.agu.org/pubs/crossref/2005/2004GC000833.shtml> [Accessed February 11, 2011].
- Farrand, W. & Lane, M., 2007. New observations of enigmatic landforms and surface terrains on the northern plains of Mars. In *Geological Society of America Annual Meeting*. Denver, CO: Geological Society of America. Available at: [https://gsa.confex.com/gsa/2007AM/finalprogram/abstract\\_129996.htm](https://gsa.confex.com/gsa/2007AM/finalprogram/abstract_129996.htm).
- Ferrier, S. et al., 2006. Novel methods improve prediction of species' distributions from occurrence data. *Ecography*, 29, pp.129–151.
- Ferrier, S. et al., 2007. Using generalized dissimilarity modelling to analyse and predict patterns of beta diversity in regional biodiversity assessment. *Diversity and Distributions*, 13(3), pp.252–264. Available at: <http://blackwell-synergy.com/doi/abs/10.1111/j.1472-4642.2007.00341.x>.
- Fischer, J. & Schott, F., 2002. Labrador Sea Water Tracked by Profiling Floats—From the Boundary Current into the Open North Atlantic. *Journal of Physical Oceanography*, 32(2), pp.573–584. Available at: [http://journals.ametsoc.org/doi/abs/10.1175/1520-0485\(2002\)032%3C0573:LSWTBP%3E2.0.CO;2](http://journals.ametsoc.org/doi/abs/10.1175/1520-0485(2002)032%3C0573:LSWTBP%3E2.0.CO;2).
- Fitzgerald, C. & Gillis, K., 2006. Hydrothermal manganese oxide deposits from Baby Bare seamount in the northeast Pacific Ocean. *Marine Geology*, 225(1–4), pp.145–156.

- Ford, D. & Williams, P., 1989. *Karst geomorphology and hydrology* 1st ed., London and Boston: Springer.
- Försterra, G. et al., 2005. Shallow-water *Desmophyllum dianthus* (Scleractinia) from Chile: characteristics of the biocoenoses, the bioeroding community, heterotrophic interactions and (paleo)-bathymetric implications. In A. Freiwald & J. M. Roberts, eds. *Cold-Water Corals and Ecosystems*. Erlangen Earth Conference Series. Berlin Heidelberg: Springer Berlin Heidelberg, pp. 937–977. Available at: [http://dx.doi.org/10.1007/3-540-27673-4\\_48](http://dx.doi.org/10.1007/3-540-27673-4_48).
- Fryer, P. & Fryer, G., 1987. Origins of Nonvolcanic Seamounts in a Forearc Environment. In *Seamounts, Islands, and Atolls*. American Geophysical Union, pp. 61–72.
- Genin, A. et al., 1986. Corals on seamount peaks provide evidence of current acceleration over deep-sea topography. *Nature*, 322(6074), pp.59–61. Available at: <http://dx.doi.org/10.1038/322059a0>.
- Gianni, M. et al., 2011. *Unfinished business: a review of the implementation of the provisions of UNGA resolutions 61/105 and 64/72 related to the management of bottom fisheries in areas beyond national jurisdiction*, Available at: [http://scholar.google.ca/scholar?hl=en&q=Unfinished+business:+a+review+of+the+implementation+of+the+provisions+of+UNGA+resolutions+61/105+and+64/72+related+to+the+management+of+bottom+fisheries+in+areas+beyond+national+jurisdiction&btnG=Search&as\\_sdt=1,5&](http://scholar.google.ca/scholar?hl=en&q=Unfinished+business:+a+review+of+the+implementation+of+the+provisions+of+UNGA+resolutions+61/105+and+64/72+related+to+the+management+of+bottom+fisheries+in+areas+beyond+national+jurisdiction&btnG=Search&as_sdt=1,5&).
- Gilkinson, K. & Edinger, E., 2009. *The Ecology of Deep-Sea Corals of Newfoundland and Labrador Waters : Biogeography, Life History, Biogeochemistry, and Role as Critical Habitat*, St.John's, NL.
- Glasby, G., 1978. Deep-sea manganese nodules in the stratigraphic record: Evidence from DSDP cores. *Marine Geology*, 28(1–2), pp.51–64. Available at: <http://www.sciencedirect.com/science/article/pii/0025322778900968>.
- Gonzalez-Mirelis, G. & Buhl-Mortensen, P., 2015. Modelling benthic habitats and biotopes off the coast of Norway to support spatial management. *Ecological Informatics*. Available at: <http://www.sciencedirect.com/science/article/pii/S1574954115000953>.
- Greenan, B. et al., 2010. *Serial No. N5774 NAFO SCR Doc. 10/19 SCIENTIFIC COUNCIL MEETING--JUNE 2010*,
- Guisan, A. et al., 2007. Sensitivity of predictive species distribution models to change in grain size. *Diversity and Distributions*, 13(3), pp.332–340. Available at: <http://dx.doi.org/10.1111/j.1472-4642.2007.00342.x>.
- Hall-spencer, J. et al., 2007. Deep-sea coral distribution on seamounts , oceanic islands , and continental slopes in the Northeast Atlantic. *Bulletin of Marine Science*, 81(1), pp.135–146. Available at: <http://www.ingentaconnect.com/contentone/umrsmas/bullmar/2007/00000081/A00103s1/art00013>.
- Han, G. et al., 2008. Seasonal variability of the Labrador Current and shelf circulation off Newfoundland. *Journal of Geophysical Research*, 113(C10013), pp.1–23. Available at: <http://www.agu.org/pubs/crossref/2008/2007JC004376.shtml> [Accessed February 18, 2011].

- Hart, B., 1977. The mid-Cretaceous succession of Orphan Knoll (northwest Atlantic): micropaleontology and palaeo-oceanographic implications. *Deep Sea Research*, 24(3–4), pp.272–272. Available at: <http://linkinghub.elsevier.com/retrieve/pii/0146629177902958>.
- Hart, M., 1976. The mid-Cretaceous succession of Orphan Knoll (northwest Atlantic): micropalaeontology and palaeo-oceanographic implications. *Canadian Journal of Earth Sciences*, 13(10), pp.1411–1421.
- Haworth, R. & Keen, C., 1979. The Canadian Atlantic Margin: A Passive Continental Margin Encompassing an Active Past. *Tectonophysics*, 59, pp.83–126.
- Heindel, K. et al., 2010. The sediment composition and predictive mapping of facies on the Propeller Mound—A cold-water coral mound (Porcupine Seabight, NE Atlantic). *Continental Shelf Research*, 30(17), pp.1814–1829. Available at: <http://linkinghub.elsevier.com/retrieve/pii/S0278434310002645> [Accessed March 18, 2012].
- Henriet, J.P. et al., 2010. Mounds and sediment drift in the Porcupine Basin, west of Ireland. In *European Margin Sediment Dynamics*. Springer Verlag. Available at: <http://eprints.soton.ac.uk/55535/>.
- Heywood, W. & Sanford, B., 1976. *Geology of Southampton, Coats and Mansel Islands, District of Keewatin, Northwest Territories*, Dartmouth, NS.
- van Hinte, J. et al., 1995. Palaeozoic microfossils from Orphan Knoll, NW Atlantic Ocean. *Scripta Geologica*, 109, pp.1–63. Available at: <http://www.narcis.nl/publication/RecordID/oai:naturalis.nl:317524> [Accessed October 26, 2011].
- Hoffmann, M. et al., 2010. The Impact of Conservation on the Status of the World's Vertebrates. *Science*, 330(6010), pp.1503–1509. Available at: <http://www.sciencemag.org/content/330/6010/1503.abstract>.
- Hovland, M., Croker, P. & Martin, M., 1994. Fault-associated seabed mounds(carbonate knolls?) off western Ireland and north-west Australia. *Marine and Petroleum Geology*, 11(2), pp.232–246.
- Howell, K., Davies, J. & Narayanaswamy, B., 2010. Identifying deep-sea megafaunal epibenthic assemblages for use in habitat mapping and marine protected area network design. *Journal of the Marine Biological Association of the United Kingdom*, 90, p.33. Available at: [http://www.journals.cambridge.org/abstract\\_S0025315409991299](http://www.journals.cambridge.org/abstract_S0025315409991299).
- Huuse, M. & Feary, D., 2005. Seismic inversion for acoustic impedance and porosity of Cenozoic cool-water carbonates on the upper continental slope of the Great Australian Bight. *Marine Geology*, 215(3–4), pp.123–134. Available at: <http://www.sciencedirect.com/science/article/pii/S002532270400355X>.
- Huvenne, V.A.I. et al., 2009. Sediment dynamics and palaeo-environmental context at key stages in the Challenger cold-water coral mound formation; clues from sediment deposits at the mound base. *Deep-Sea Research Part I: Oceanographic Research Papers*, 56(12), pp.2263–2280. Available at: <http://ezproxy.library.dal.ca/login?url=http://search.proquest.com/docview/877398895?acco>

untid=10406.

- ICES, 2007. *Report of the Working Group on Deep-eater Ecology (WGDEC)*,
- Immenhauser, A. & Rameil, N., 2011. Interpretation of ancient epikarst features in carbonate successions — A note of caution. *Sedimentary Geology*, 239(1–2), pp.1–9. Available at: <http://www.sciencedirect.com/science/article/pii/S0037073811001503> [Accessed March 10, 2012].
- Jauer, C. & Budkewitsch, P., 2010. Old marine seismic and new satellite radar data: Petroleum exploration of north west Labrador Sea, Canada. *Marine and Petroleum Geology*, 27(7), pp.1379–1394. Available at: <http://linkinghub.elsevier.com/retrieve/pii/S0264817210000620> [Accessed October 27, 2010].
- Keen, C. et al., 1987. Deep crustal structure and evolution of the rifted margin northeast of Newfoundland: results from LITHOPROBE East. *Canadian Journal of Earth Sciences*, 24(8), pp.1537–1549. Available at: <http://dx.doi.org/10.1139/e87-150>.
- King, L. et al., 1985. Occurrence and regional geological setting of Paleozoic rocks on the Grand Banks of Newfoundland. *Canadian Journal of Earth Sciences*, 23, pp.504–526.
- Land, L., Paull, C. & Hobson, B., 1995. Genesis of a submarine sinkhole without subaerial exposure: Straits of Florida. *Geology*, 23(10), pp.949–951. Available at: <http://geology.gsapubs.org/cgi/content/abstract/23/10/949>.
- Laughton, A. et al., 1972. Site 111. *International Deep Sea Drilling Project*, (12), pp.33–159.
- Leeper, R. et al., 2011. Predictions of beta diversity for reef macroalgae across southeastern Australia. *Ecosphere*, 2(7), p.art73. Available at: <http://dx.doi.org/10.1890/ES11-00089.1>.
- Legault, J., 1982. First report of Ordovician (Caradoc-Ashgill) palynomorphs from Orphan Knoll, Labrador Sea. *Canadian Journal of Earth Sciences*, 19(9), pp.1851–1856.
- Leverette, T. & Metaxas, A., 2004. Predicting habitat for two species of deep-water coral on the Canadian Atlantic continental shelf and slope. In A. Freiwald & M. Roberts, eds. *Cold-Water Corals and Ecosystems*. Berlin Heidelberg: Springer-Verlag, pp. 467–479. Available at: [http://link.springer.com/chapter/10.1007%2F3-540-27673-4\\_23](http://link.springer.com/chapter/10.1007%2F3-540-27673-4_23).
- Levin, L. et al., 2009. Macrobenthos community structure and trophic relationships within active and inactive Pacific hydrothermal sediments. *Deep Sea Research Part II: Topical Studies in Oceanography*, 56(19–20), pp.1632–1648. Available at: <http://linkinghub.elsevier.com/retrieve/pii/S0967064509001738> [Accessed November 19, 2010].
- Lodge, M., 2004. Improving International Governace in the Deep Sea. *The International Journal of Marine and Coastal Law*, 19(3), p.299.
- Logerwell, E., Rand, K. & Weingartner, T.J., 2011. Oceanographic characteristics of the habitat of benthic fish and invertebrates in the Beaufort Sea. *Polar Biology*, 34(11), pp.1783–1796.
- Long, D. et al., 2003. Mud mound / ?diapiric features in the Faroe - Shetland Channel. In *EGS - AGU - EUG Joint Assembly*. Nice: EGS- AGU - EUG Joint Assembly. Available at: <http://adsabs.harvard.edu/abs/2003EAEJA....11201L>.

- Lund, D., Adkins, J. & Ferrari, R., 2011. Abyssal Atlantic Circulation during the Last Glacial Maximum. *Paleoceanography*, 26(1), pp.1–18. Available at: [http://web.mit.edu/raffaele/www/Publications\\_files/LundAdkinsFerrariScience08.pdf](http://web.mit.edu/raffaele/www/Publications_files/LundAdkinsFerrariScience08.pdf) [Accessed January 11, 2017].
- Madi, A., Bourque, P.-A. & Mamet, B., 1996. Depth-related ecological zonation of a carboniferous carbonate ramp: Upper Viséan of Béchar Basin, Western Algeria. *Facies*, 35(1), pp.59–79. Available at: <http://dx.doi.org/10.1007/BF02536957>.
- Margles, S. et al., 2010. Conservation Without Borders: Building Communication and Action Across Disciplinary Boundaries for Effective Conservation. *Environmental Management*, 45(1), pp.1–4. Available at: <http://dx.doi.org/10.1007/s00267-009-9383-8>.
- Menabreaz, L., 2015. Neodymium isotopic composition of deep-sea corals from the Labrador Sea: implications for NW Atlantic deep-water masses circulation during the Holocene, MIS 5 and 7. In *AGU-GAC-MAC-CGU Joint Assembly*. Montreal, p. 146.
- Metaxas, A. & Bryan, T., 2007. Predictive habitat model for deep gorgonians needs better resolution: Reply to Etnoyer & Morgan. *Marine Ecology Progress Series*, 339(3), pp.313–314. Available at: <http://www.int-res.com/abstracts/meps/v339/p313-314/>.
- Miles, L., Edinger, E. & Piper, D., 2015. Investigating the relationship between cold-water corals distribution and surficial geology. In *14th Deep-Sea Biology Symposium*. Aveiro, Portugal: DSBS, p. 1.
- Miller, K. et al., 2011. Out of their depth? Isolated deep populations of the cosmopolitan coral *Desmophyllum dianthus* may be highly vulnerable to environmental change. *PLoS one*, 6(5), pp.1–10. Available at: [http://apps.webofknowledge.com.proxy-ub.rug.nl/full\\_record.do?product=UA&search\\_mode=GeneralSearch&qid=1&SID=T15EYVKBZuXIHfTAVsm&page=9&doc=87&cacheurlFromRightClick=no](http://apps.webofknowledge.com.proxy-ub.rug.nl/full_record.do?product=UA&search_mode=GeneralSearch&qid=1&SID=T15EYVKBZuXIHfTAVsm&page=9&doc=87&cacheurlFromRightClick=no).
- Miller, K. & Fairbanks, R., 1983. Evidence for Oligocene-Middle Miocene abyssal circulation changes in the western North Atlantic. *Nature*, 306(5940), pp.250–253. Available at: <http://dx.doi.org/10.1038/306250a0>.
- Monk, J. et al., 2010. Habitat suitability for marine fishes using presence-only modelling and multibeam sonar. *Marine Ecology Progress Series*, 420, pp.157–174. Available at: <http://www.int-res.com/abstracts/meps/v420/p157-174/> [Accessed March 18, 2012].
- Moore, J., Clague, D. & Normark, W., 1982. Diverse basalt types from Loihi seamount, Hawaii. *Geology*, 10(2), p.88.
- Mortensen, P. et al., 2006. *Deep-Water Corals In Atlantic Canada: A Summary Of ESRF-Funded Research (2001-2003)*, Report No. 143. Calgary, AB: Environmental Studies Research Funds.
- Moscardelli, L. et al., 2013. Seismic geomorphological analysis and hydrocarbon potential of the Lower Cretaceous Cromer Knoll Group, Heidrun field, Norway. *AAPG Bulletin*, 97(8), pp.1227–1248.
- Mullineau, L. & Mills, S., 1997. A test of the larval retention hypothesis in seamount-generated flows. *Deep Sea Research Part I: Oceanographic Research Papers*, 44(5), pp.745–770.

- Available at: [http://dx.doi.org/10.1016/S0967-0637\(96\)00130-6](http://dx.doi.org/10.1016/S0967-0637(96)00130-6) [Accessed March 9, 2011].
- NAFO, 2015. *NAFO Conservation and Enforcement Measures 2015*, Dartmouth, Nova Scotia, Canada B2Y 3Y9 Tel.: (902) 468-5590. Available at: [www.nafo.int](http://www.nafo.int).
- NAFO SCS, 2008. *Report of the NAFO Scientific Council Working Group on Ecosystem Approach to Fisheries Management (WGEAFM)*, Dartmouth, Canada.
- Neves, B., Du Preez, C. & Edinger, E., 2014. Mapping coral and sponge habitats on a shelf-depth environment using multibeam sonar and ROV video observations: Learmonth Bank, northern British Columbia, Canada. *Deep-Sea Research Part II: Topical Studies in Oceanography*, 99, pp.169–183. Available at: <http://dx.doi.org/10.1016/j.dsr2.2013.05.026>.
- O'Hara, T. et al., 2008. Cold-water coral habitats on seamounts: do they have a specialist fauna? *Global Ecology and Biogeography*, 14(6), pp.925–934. Available at: <http://blackwell-synergy.com/doi/abs/10.1111/j.1472-4642.2008.00495.x> [Accessed August 20, 2010].
- Paduan, J., Clague, D. & Davis, A., 2007. Erratic continental rocks on volcanic seamounts off the US west coast. *Marine Geology*, 246(1), pp.1–8.
- Parson, L. et al., 1984. Remnants of a submerged pre-Jurassic ( Devonian?) landscape on Orphan Knoll , offshore eastern Canada. *Canadian Journal of Earth Sciences*, 21(1), pp.61–66.
- Pautot, G., Auzende, J.-M. & Le Pichon, X., 1970. Continuous Deep Sea Salt Layer along North Atlantic Margins related to Early Phase of Rifting. *Nature*, 227(5256), pp.351–354. Available at: <http://dx.doi.org/10.1038/227351a0>.
- Pe-Piper, G. et al., 2013. Petrology and tectonic significance of seamounts within transitional crust east of Orphan Knoll, offshore eastern Canada. *Geo-Marine Letters*, 33(6), pp.433–447. Available at: <http://dx.doi.org/10.1007/s00367-013-0342-2>.
- Pettit, R., 2011. Culturability and Secondary Metabolite Diversity of Extreme Microbes: Expanding Contribution of Deep Sea and Deep-Sea Vent Microbes to Natural Product Discovery. *Marine Biotechnology*, 13(1), pp.1–11. Available at: <http://dx.doi.org/10.1007/s10126-010-9294-y>.
- Piper, D., 2005. *Hudson 2004-024 Cruise Report: Geohazards on the continental margin off Newfoundland*, Dartmouth, NS.
- Pitcher, C. et al., 2016. *Implications of current spatial management measures for AFMA ERAs for habitats - FRDC Project No 2014/204*, Brisbane.
- Pitcher, R. et al., 2012. Exploring the role of environmental variables in shaping patterns of seabed biodiversity composition in regional-scale ecosystems. *Journal of Applied Ecology*, 49(3), pp.670–679. Available at: <http://dx.doi.org/10.1111/j.1365-2664.2012.02148.x>.
- Pitcher, R., Ellis, N. & Smith, S., 2011. *Example analysis of biodiversity survey data with R package gradientForest*, Available at: <http://gradientforest.r-forge.r-project.org/biodiversity-survey.pdf>.
- Pohlman, J. et al., 2009. Methane sources in gas hydrate-bearing cold seeps: Evidence from radiocarbon and stable isotopes. *Marine Chemistry*, 115(1–2), pp.102–109. Available at: <http://linkinghub.elsevier.com/retrieve/pii/S0304420309000966> [Accessed November 19, 2010].

- Poirier, A. et al., 2011. Osmium isotopes in manganese nodules from the Labrador Sea. *Goldschmidt*, p.1. Available at: [www.minersoc.org](http://www.minersoc.org).
- Quilty, P., 1997. Eocene and younger biostratigraphy and lithofacies of the Cascade Seamount, East Tasman Plateau, southwest Pacific Ocean. *Australian Journal of Earth Sciences*, 44(5), pp.655–665.
- Reidenbach, M. et al., 2006. Boundary layer turbulence and flow structure over a fringing coral reef. *Limnology and Oceanography*, 51(5), pp.1956–1968. Available at: [http://www.aslo.org/lo/toc/vol\\_51/issue\\_5/1956.html](http://www.aslo.org/lo/toc/vol_51/issue_5/1956.html).
- Richer-de-Forges, B., Koslow, A. & Poore, G., 2000. Diversity and endemism of the benthic seamount fauna in the southwest Pacific. *Nature*, 405(6789), pp.944–947. Available at: <http://dx.doi.org/10.1038/35016066>.
- Roark, B. et al., 2009. Extreme longevity in proteinaceous deep-sea corals. *Proceedings of the National Academy of Sciences*, 106(13), pp.5204–5208. Available at: <http://www.pnas.org/content/106/13/5204.abstract>.
- Roberts, C., 2002. Deep impact: the rising toll of fishing in the deep sea. *Trends in Ecology & Evolution*, 17(5), pp.242–245. Available at: <http://www.sciencedirect.com/science/article/pii/S0169534702024928>.
- Roberts, M. et al., 2003. The cold-water coral *Lophelia pertusa* (Scleractinia) and enigmatic seabed mounds along the north-east Atlantic margin: are they related? *Marine Pollution Bulletin*, 46(1), pp.7–20. Available at: <http://www.sciencedirect.com/science/article/pii/S0025326X0200259X>.
- Roberts, M., Wheeler, A. & Freiwald, A., 2006. Reefs of the deep: the biology and geology of cold-water coral ecosystems. *Science*, 312(5773), pp.543–547. Available at: <http://www.ncbi.nlm.nih.gov/pubmed/16645087>.
- Roberts, S. & Nunn, J., 1995. Episodic fluid expulsion from geopressured sediments. *Marine and Petroleum Geology*, 12(2), pp.195–204. Available at: <http://www.sciencedirect.com/science/article/pii/0264817295928390>.
- Rodríguez-Martínez, M., 2011. Mud Mounds. In J. Reitner & V. Thiel, eds. *Encyclopedia of Geobiology*. Encyclopedia of Earth Sciences Series. Springer Netherlands, pp. 667–675. Available at: [http://dx.doi.org/10.1007/978-1-4020-9212-1\\_153](http://dx.doi.org/10.1007/978-1-4020-9212-1_153).
- Ruffman, A., 1989. First report of Ordovician (Caradoc-Ashgill) palynomorphs from Orphan Knoll, Labrador Sea: Discussion. *Canadian Journal of Earth Sciences*, 26(12), pp.2749–2751. Available at: [http://www.nrc.ca/cgi-bin/cisti/journals/rp/rp2\\_abst\\_e?cjes\\_e89-239\\_26\\_ns\\_nf\\_cjes26-89](http://www.nrc.ca/cgi-bin/cisti/journals/rp/rp2_abst_e?cjes_e89-239_26_ns_nf_cjes26-89).
- Ruffman, A., 2011. Orphan Knoll as a Window on the Palaeozoic : Seemingly ignored by the petroleum industry for 40 years. In *Recovery - CSPG CSEG CWLS Convention*. pp. 1–5.
- Ruffman, A. & van Hinte, J., 1973. Orphan Knoll—a“ chip” off the North American" plate. In *Earth Science Symposium on Offshore Eastern Canada*. Dartmouth, NS: Geological Survey of Canada (Atlantic), pp. 23–71.
- Rüggeberg, A. et al., 2005. Sedimentary patterns in the vicinity of a carbonate mound in the

- Hovland Mound Province, northern Porcupine Seabight. In A. Freiwald & J. M. Roberts, eds. Erlangen Earth Conference Series. Springer Berlin Heidelberg, pp. 87–112. Available at: [http://dx.doi.org/10.1007/3-540-27673-4\\_5](http://dx.doi.org/10.1007/3-540-27673-4_5).
- Santos, R.-S. et al., 2009. Toward the conservation and management of Sedlo Seamount: A case study. *Deep Sea Research Part II: Topical Studies in Oceanography*, 56(25), pp.2720–2730. Available at: <http://linkinghub.elsevier.com/retrieve/pii/S0967064508004578>.
- Shaw, J. et al., 2006. A conceptual model of the deglaciation of Atlantic Canada. *Quaternary Science Reviews*, 25(17–18), pp.2059–2081. Available at: <http://linkinghub.elsevier.com/retrieve/pii/S0277379106001326> [Accessed July 5, 2010].
- Sherwood, O. & Edinger, E., 2009. Ages and growth rates of some deep-sea gorgonian and antipatharian corals of Newfoundland and Labrador. *Canadian Journal of Fisheries Aquatic Science*, 66(1), pp.142–152. Available at: <http://dx.doi.org/10.1139/F08-195>.
- Shester, G. & Ayers, J., 2005. A cost effective approach to protecting deep-sea coral and sponge ecosystems with an application to Alaska’s Aleutian Islands region. In A. Freiwald & J. M. Roberts, eds. Erlangen Earth Conference Series. Springer Berlin Heidelberg, pp. 1151–1169. Available at: [http://dx.doi.org/10.1007/3-540-27673-4\\_59](http://dx.doi.org/10.1007/3-540-27673-4_59).
- Sibuet, J.-C., 1992. New constraints on the formation of the non-volcanic continental Galicia-Flemish Cap conjugate margins. *The Geological Society*, 149(5), pp.829–840. Available at: <http://jgs.lyellcollection.org/cgi/content/abstract/149/5/829>.
- Smee, J. et al., 2003. Orphan Basin , Offshore Newfoundland : New seismic data and hydrocarbon plays for a dormant Frontier Basin. In *Offshore Technology Conference*.
- Smith, J. et al., 1997. Rapid climate change in the North Atlantic during the Younger Dryas recorded by deep-sea corals. *Nature*, 386, pp.818–820. Available at: <http://www.nature.com/nature/journal/v386/n6627/abs/386818a0.html>.
- Srivastava, S. et al., 2000. Magnetic evidence for slow seafloor spreading during the formation of the Newfoundland and Iberian margins. *Earth and Planetary Science Letters*, 182(1), pp.61–76. Available at: <http://www.sciencedirect.com/science/article/pii/S0012821X00002314>.
- Stein, M., 2007. Oceanography of the Flemish Cap and Adjacent Waters. *Journal of Northwest Atlantic Fisheries Science*, 37(February), pp.135–146. Available at: <http://journal.nafo.int/37/stein/12-stein.pdf> [Accessed February 18, 2011].
- Tankard, A. & Balkwill, H., 1989. Extensional tectonics and stratigraphy of the North Atlantic margins. In *Extensional Tectonics and Stratigraphy of the North Atlantic Margins*. Calgary, AB: American Association of Petroleum Geologists, pp. 1–6.
- Thomson, R. et al., 2014. Congruence in demersal fish, macroinvertebrate, and macroalgal community turnover on shallow temperate reefs. *Ecological Applications*, 24(2), pp.287–299. Available at: <http://doi.wiley.com/10.1890/12-1549.1> [Accessed January 9, 2017].
- Thornburg, C., Zabriskie, M. & McPhail, K., 2010. Deep-Sea Hydrothermal Vents: Potential Hot Spots for Natural Products Discovery? *J. Nat. Prod.*, 73(3), pp.489–499. Available at: <http://dx.doi.org/10.1021/np900662k>.

- Toews, M. & Piper, D., 2002. *Recurrence interval of seismically triggered mass-transport deposition at Orphan Knoll , continental margin off Newfoundland and Labrador*, Dartmouth, NS.
- Tucholke, B., Sawyer, D. & Sibuet, J.-C., 2007. Breakup of the Newfoundland–Iberia rift. *Geological Society, London, Special Publications*, 282(1), pp.9–46. Available at: <http://sp.lyellcollection.org/content/282/1/9.abstract>.
- Via, R. & Thomas, D., 2006. Evolution of Atlantic thermohaline circulation: Early Oligocene onset of deep-water production in the North Atlantic. *Geology*, 34(6), pp.441–444. Available at: <http://geology.gsapubs.org/cgi/content/abstract/34/6/441>.
- Waller, R. et al., 2007. Anthropogenic impacts on the Corner Rise seamounts, north-west Atlantic Ocean. *Journal of the Marine Biological Association of the United Kingdom*, 87(5), pp.1075–1076. Available at: [http://www.journals.cambridge.org/abstract\\_S0025315407057785](http://www.journals.cambridge.org/abstract_S0025315407057785) [Accessed February 18, 2011].
- Wareham, V. & Edinger, E., 2007. Distribution of deep-sea corals in the Newfoundland and Labrador region , Northwest Atlantic Ocean. In R. Y. George & S. D. Cairns, eds. *Conservation and adaptive management of seamount and deep-sea coral ecosystems*. Miami: Rosentiel School of Marine and Atmosphere Science, University of Miami, pp. 289–313.
- Watanabe, S. et al., 2009. Patterns in abundance and size of two deep-water gorgonian octocorals, in relation to depth and substrate features off Nova Scotia. *Deep Sea Research Part I: Oceanographic Research Papers*, 56(12), pp.2235–2248. Available at: <http://linkinghub.elsevier.com/retrieve/pii/S0967063709001769> [Accessed February 18, 2011].
- Welford, K. et al., 2010. Structure across the northeastern margin of Flemish Cap, offshore Newfoundland from Erable multichannel seismic reflection profiles: evidence for a transtensional rifting environment. *Geophysical Journal International*, 183(2), pp.572–586. Available at: <http://dx.doi.org/10.1111/j.1365-246X.2010.04779.x>.
- Wendt, J. et al., 1997. The world’s most spectacular carbonate mud mounds (Middle Devonian, Algerian Sahara). *Journal of Sedimentary Research*, 67(Section A and B), pp.424–436.
- Wielens, H., MacRae, A. & Shimeld, J., 2002. Geochemistry and sequence stratigraphy of regional Upper Cretaceous limestone units, offshore eastern Canada. *Organic Geochemistry*, 33(12), pp.1559–1569. Available at: <http://www.sciencedirect.com/science/article/pii/S0146638002001031>.
- Wilson, M. et al., 2007. Multiscale Terrain Analysis of Multibeam Bathymetry Data for Habitat Mapping on the Continental Slope. *Marine Geodesy*, 30(1), pp.3–35. Available at: <http://www.informaworld.com/openurl?genre=article&doi=10.1080/01490410701295962&magic=crossref%7C%7CD404A21C5BB053405B1A640AFFD44AE3>.
- Workum, R., Bolton, T. & Barnes, C., 2011. Ordovician geology of Akpatok Island, Ungava Bay, District of Franklin. *Can. J. Earth Sci.*, 13(1), pp.157–178. Available at: <http://dx.doi.org/10.1139/e76-015>.

- Wright, D. & Goodchild, M., 1997. Data from the deep: implications for the GIS community. *International Journal of Geographical Information Science*, 11(6), pp.523–528. Available at: <http://www.ingentaconnect.com/content/tandf/tgis/1997/00000011/00000006/art00001>.
- Xu, Y., Eyles, N. & Simpson, M.J., 2009. Terrigenous organic matter sources in mid-pleistocene sediments from the orphan knoll, Northwest Atlantic Ocean. *Applied Geochemistry*, 24(10), pp.1934–1940. Available at: <http://www.sciencedirect.com/science/article/B6VDG-4WV77VG-1/2/7e4c6095d4f3c7f42008062fbd5e9664>.
- Yasuhara, M. et al., 2008. Abrupt climate change and collapse of deep-sea ecosystems. *Proceedings of the National Academy of Sciences*, 105, pp.1556–1560.
- Yesson, C. et al., 2011. The global distribution of seamounts based on 30 arc seconds bathymetry data. *Deep Sea Research Part I: Oceanographic Research Papers*, 58(4), pp.442–453. Available at: <http://www.sciencedirect.com/science/article/pii/S0967063711000392>.

## 2.7 Appendix

*Appendix 2-1. Rock collection Summary from CCGS Hudson 2010-029 cruise to Orphan Knoll and Orphan Seamount*

Calcareous Ooze	Limestone	Basalt	Mn Oxide Crust	Granitic (IRD)
R1341-4	R1340-14	R1340-26A (w/ limestone)	R1340-28	R1340-12
	R1340-19A	R1340-26B	R1341-19	R1340-13
	R1340-19B	R1343-4A	R1343-4A	R1343-22
	R1341-7	R1343-22B	R1343-4B	R1343-22C
	R1341-10		R1343-10	R1343-22E
	R1341-20		R1343-14A	
	R1343-3 (with Mn crust)		R1343-14B1	
	R1343-14B2 (with Mn crust)		R1343-15	

\*Grey Highlights indicate IRD rocks collected on the Orphan Seamount and Orphan Knoll.

Appendix 2-2. Rock Samples from Orphan Knoll and Orphan Seamount on Hudson 2010-029 Cruise

Rock Sample ID	JDayGMT	Area	Lat	Long	Depth(m)	Final Geological Assmt.	Assoc Biology / notes	Comments
R1340_06	2001200	Orphan Seamount	50.10876	-45.3303	-2833.76	Gneiss	Black Coral, Brittle Star	IRD, rounded, sample was not confirmed, only photo, granitic gneiss?
R1340_07	2001242	Orphan Seamount	50.10695	-45.3306	-2731.7	Granite	Sponge	IRD, rounded, sample was not confirmed, only photo
R1340_12	2001406	Orphan Seamount	50.10874	-45.3247	-2748.05	Diorite/ Granodiorite	encrusting sponge	
R1340_13	2001420	Orphan Seamount	50.10799	-45.3233	-2748.86	Greenstone	iron rust, sample taken from collapsed lava tube top	Greenstone Granite : plagioclase feldspar, polysynthetic, fu of zircons and amphibole
R1340_14	2001504	Orphan Seamount	50.10528	-45.3224	-2749.83	Limestone	Finger-like shape, from lava tube top	rounded, covered in Mn-oxide, found in rubble between two lava tubes
R1340_19A	2001853	Orphan Seamount	50.09344	-45.3354	-2262.81	Nodular Limestone, Breccia-Like	iron oxide	
R1340_19B	2001853	Orphan Seamount	50.09344	-45.3354	-2262.81	Nodular Limestone, Breccia-Like	iron oxide	
R1340_26A	2002225	Orphan Seamount	50.09202	-45.3493	-1994.06	Basalt and Limestone		Basalt is too weathered to radiometric dating. Fe and Mn evidence, pyroxenes altered the
R1340_26B	2002225	Orphan Seamount	50.09202	-45.3493	-1994.06	Basalt		Basalt is too weathered to radiometric dating. Fe and Mn evidence, pyroxenes altered the carbonate (expected of Deep-sea Basalt), silica inclusion. Two geopetal structures, vesicles with detrital / fine-grained carbonate ooze and Fe-oxides (bla
R1340_28	2002329	Orphan Seamount	50.08801	-45.3536	-1996.68	Mn-Crust	Swiftia? Soft coral, rock collected from 'float' / loose rocks; seamount	
R1341_03	2011654	SE Orphan Knoll	50.07654	-45.6209	-2873.12	Manganese Nodules	3 nodules (whole), 1 nodule (slightly crushed), Iron and Manganese Oxide	
R1341_04	2011708	SE Orphan Knoll	50.07662	-45.621	-2873.28	Calcareous Ooze	found near MN-nodules	Co-occurrence of the nanofossils Discoaster subloboensis and Nannotetrina fulgens.
R1341_05	2011733	SE Orphan Knoll	50.07656	-45.6211	-2873.5	Manganese Nodule	1 nodule, slightly broken, surface oxidation, Glass Tulip like Sponge on nodule	
R1341_07	2011815	SE Orphan Knoll	50.07826	-45.6155	-2874.77	Pelagic Limestone	Bedrock sample of the SE mound	Orbulina spp. forams; Mid-Miocene
R1341_10	2011901	SE Orphan Knoll	50.07712	-45.6128	-2848.07	Pelagic Limestone		Pelagic Forams, Orbulina spp. and Globigerina (atlantica?) Globigerinoides spp.?, Cenozoic (Mid Miocene)
R1341_19	2020033	SE Orphan Knoll	50.05945	-45.6075	-2398.83	Pelagic Limestone	Bedrock sample of the mound top	micritic, Fe staining, Globigerina spp.
R1341_20	2020037	SE Orphan Knoll	50.05943	-45.6074	-2378.93	Argillaceous Limestone	IRD, Styliolitic sample from mound top	subrounded, no fossils, stylolitic laminae (redish, algae), Paleozoic (Late Ordovician) limestone from Churchill River Group (Foxe Basin, Canada) brought through Hudson Stra
R1343_4B	2031745	NE Orphan Knoll	50.55423	-46.1716	-1777.52	Limestone and Mn-Crust	Mn-oxidation all over, bedded layers seen, encrusting sponge and encrusting worms in the Serpidulae family	Carbonate at edge is finer-grained, isotropic inclusion of unknown composition.
R1343_09,20,21,22	2032348	NE Orphan Knoll	50.55208	-46.1932	-1741.05	Mn-crusts, granite, Limestone, Gabbro, Basalt	Sludge samples, various types unidentified, 1/2 bag of collection from sample sites 9,20,21,22	
R1343_10	2040019	NE Orphan Knoll	50.55209	-46.1934	-1729.72	Limestone phenocryst in laminated Mn-crust	Mn-oxidation all over, bedded layers seen	
R1343_14A	2040119	NE Orphan Knoll	50.55209	-46.1934	-1729.72	Mn-Crusts	Mn-oxidation all over, bedded layers seen, encrusting sponge and encrusting worms in the Serpidulae family	
R1343_03A	2031727	NE Orphan Knoll	50.55414	-46.1715	-1779.72	Basalt	covered in sticky sponge and encrusting worms in the Serpidulae family	
R1343_03B	2031727	NE Orphan Knoll	50.55414	-46.1715	-1779.72	Limestone and Mn-crust	covered in sticky sponge and encrusting worms in the Serpidulae family	
R1343_03	2031727	NE Orphan Knoll	50.55414	-46.1715	-1779.72	Mn-Crust	covered in sticky sponge and encrusting worms in the Serpidulae family	
R1343_04A	2031745	NE Orphan Knoll	50.55423	-46.1716	-1777.52	Limestone and Mn-Crust	2 rocks, small, irregular, oxidized	
R1343_14B1	2040119	NE Orphan Knoll	50.55209	-46.1934	-1729.72	Mn-Crusts	Mn-oxidation all over, bedded layers seen, encrusting sponge and encrusting worms in the Serpidulae family	
R1343_14B2	2040119	NE Orphan Knoll	50.55209	-46.1934	-1729.72	Mn-Crust with Limestone	Mn-oxidation all over, bedded layers seen, encrusting sponge and encrusting worms in the Serpidulae family	
R1343_15	2040119	NE Orphan Knoll	50.55209	-46.1934	-1729.72	Mn-Crust		
R1343_22A	2040440	NE Orphan Knoll	50.55203	-46.1931	-1741.09	Granite	sludge samples, Quartzite Phenocryst	
R1343_22B	2040440	NE Orphan Knoll	50.55203	-46.1931	-1741.09	Basalt	sludge samples, Basalt, angular, in situ?	
R1343_22C	2040440	NE Orphan Knoll	50.55203	-46.1931	-1741.09	Granite	sludge samples, Granite, Quartz Phenocrysts	
R1343_22D	2040440	NE Orphan Knoll	50.55203	-46.1931	-1741.09	Quartzite	sludge samples, Quartzite	
R1343_22E	2040440	NE Orphan Knoll	50.55203	-46.1931	-1741.09	Granite	sludge samples, Granite	
R1343_22F	2040440	NE Orphan Knoll	50.55203	-46.1931	-1741.09	Gabbro	sludge samples, Gabbro	

Appendix 2-3. Surficial Geology in % Coverage separated by Surficial Geological Unit (SGU)

Dive	SGU	General Surficial Geology in % Coverage						
		Bedrock	Boulders	Cobbles	Fine_Sed	Granules	Pebbles	Mn-Nodules
D1340	A-A	55	20		5	20		
D1340	A'-B	30	5	10	15	30	5	
D1340	B-B'	1	3	3	42	41	5	
D1340	B'-C	5	3	10	32	50		
D1340	C-C'	86	3	10	1			
D1340	C'-D	17		3	10	70		
D1340	D-D'		1	3	56	40		
D1340	D'-E		1	1	49	46	3	
D1340	E-E'		3	10	55	29	3	
D1340	E'-F	67		10	20		3	
D1340	F-F'				40	57	3	
D1340	F'-G	9	10	20	37	21	3	
D1340	G-G'	23	1	35	30	10	1	
D1340	G'-H	40	1	6	25	25	3	
D1340	H-H'		1	1	93	5		
D1340	H'-I		1	10	64	25		
D1340	I-I'	94		5	1			
D1341	A-A'	34	1	10	20	35		
D1341	A'-B	1	1	5	38	45		10
D1341	B-B'	71	1	10	3	15		
D1341	B'-C	43	1		20	35		1
D1341	C-C'	69	1	10	5	15		
D1341	C'-D	55		5	10	30		
D1341	D-D'	95	1	3	1			
D1341	D'-E	17	3	20	50	10		
D1341	E-E'	53		5	42			
D1341	E'-F	26		5	44	25		
D1341	F-F'	70		5	25			
D1341	F'-G		5	10	35	50		
D1341	G-G'	15	10	35	29	8		
D1341	G'-H	57	10	20	10		3	
D1342			2	3	80	20		
D1343	A-A'			15	47	35	3	
D1343	A'-B	20	5	25	12	35	3	
D1343	B-B'		1	20	54	25		
D1343	B'-C			1	94	5		
D1343	C-C'		1	5	84	10		
D1343	C'-D					93	7	
D1343	D-D'		1	7	82	10		
D1343	D'-E			1	89	10		
D1343	E-E'	69	5	20	5	1		
D1345	A-A'		3	5	77	15		
D1345	A'-B			3	59	38		
D1345	B-B'		3	7	40	50		
D1345	B'-C				60	40		
D1345	C-C'		3	5	52	40		
D1345	C'-D				55	45		
D1345	D-D'			1	69	30		
D1345	D'-E				70	30		
D1346	A-A'			1	74	25		
D1346	A'-B				90	10		
D1346	B-B'			5	80	15		
D1346	B'-C				85	15		
D1346	C-C'			6	64	30		
D1346	C'-D				85	15		

### 3 Compositional Facies, Age and Origin of Orphan Seamount

*1. Preliminary geological data analysis, bathymetric and photographic datasets from this chapter were used in publishing (Pe-Piper et al. 2013), however text from this chapter is not the same as the publication.*

#### **Abstract**

A bathymetric high (“Orphan Seamount”) in the NW Atlantic Ocean, situated east of SE Orphan Knoll, might either be volcanic or a rifted continental fragment analogous to Orphan Knoll. Using the remotely operated vehicle, ROPOS, *in-situ* sampling of a variety of facies, along with collection of high-definition video, allowed for verification of samples and facies. Thin section analysis of the bedrock samples identified surface rocks from Orphan Seamount as basalt, occurring as pillow basalt with lava tubes. Talus and debris flow deposits of volcanic material and ice-rafted detritus are present. Granule-dominated sediment fills depressions between lava tubes, finer grained sediment overlies basaltic bedrock, and ferromanganese crusts have developed on basalt outcrops. The age of Orphan Seamount could not be constrained any further than saying that its origins are between mid-Miocene and Chron 34, with the possibility of its origins being pre-J anomaly (~112 Myr).

### 3.1 Introduction

Seamounts are unique underwater features that are known to be in most cases volcanic in nature with varying basalt types (Moore et al. 1982) and to contain high biodiversity of megafaunal inhabitants (Hall-spencer et al. 2007; O'Hara et al. 2008; Christiansen & Wolff 2009). The “Orphan Seamount” (OS) is located 9 km NE of the SE portion of Orphan Knoll (OK) and is 14 km wide at its base with a depth range between 1932 m to 3900 m (Fig. 3-1). Due to its deep setting, proximity to OK and the fact that it is largely unexplored by commercial fisheries, the seamount was an ideal opportunity near Canadian waters to investigate a unique geological feature with possibly unknown megafaunal inhabitants.

In 1969 the MV *Charcot* collected seismic reflection and magnetic anomaly profiles that identified mounds (buried and exposed) on the NW-SW side of OK, and detected a positive magnetic anomaly along the eastern edge of OK, indicating the presence of oceanic crust (Laughton et al. 1972), which suggested a basaltic composition for the OS (Laughton et al. 1972).

The OS is found on a passive non-volcanic rifted margin (NVRM), and the presence of volcanic activity was not expected (Keen et al. 1987; Tankard & Balkwill 1989; Srivastava et al. 2000), however, not improbable (Haworth & Keen 1979; Chian et al. 2001; Welford et al. 2010; Bronner et al. 2011). The close proximity (2.5 km) of OS to OK (continental crust), a lack of bottom photography and the fact that it is found on a passive NVRM, lead to the hypothesis that the OS could be a part of the same continental rifted fragment that the OK originated from. Or, that the OS resulted from magmatic pulses that formed the J-Anomaly Ridge and Newfoundland Seamounts (~130 and ~112 Ma) (Tucholke et al. 2007), which may have triggered continental

breakup before seafloor spreading of the North Atlantic Ocean occurred, which is seaward of Orphan Knoll and would have been at Chron 34 (84 Ma) ( Bronner *et al.* 2011).

### 3.1.1 Study Objectives

Using a remotely operated vehicle (ROV) equipped with high-definition (HD) video and high-resolution multibeam imagery, the collection of *in-situ* bedrock and detailed bathymetry were collected to verify the facies and petrology of these bedrock samples, in an effort to determine the seamount's composition, age and origin.

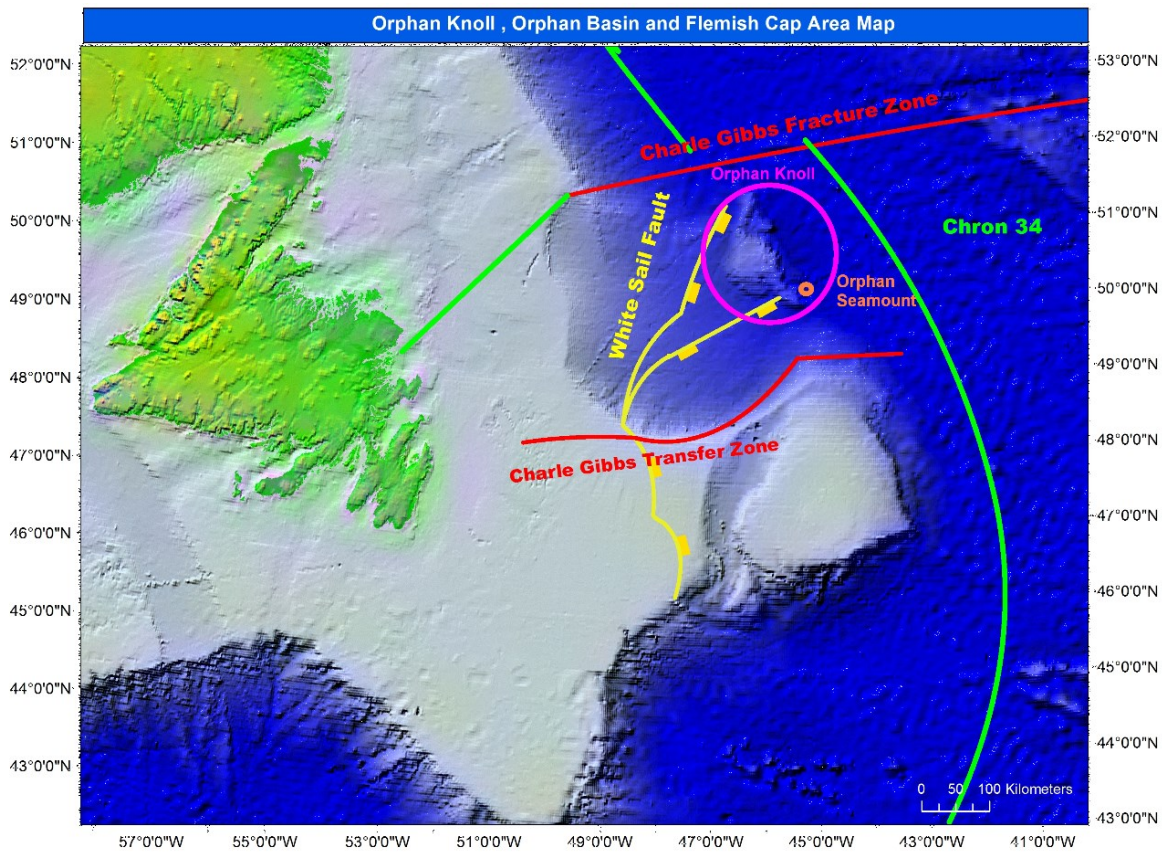


*Figure 3-1. Orphan Knoll (pink circle) and Orphan Seamount (orange) locations relative to Newfoundland and the Grand Banks of Newfoundland. Prominent faults near the Orphan Knoll area are also identified (Charlie Gibbs Fracture Zone (CBFZ) and Charlie Gibbs Transfer Zone (CBTZ) and White Sail fault). Chron 34 is ~100 Km eastward of Orphan Knoll.*

## 3.2 Methods

The field collection methods used in this chapter are the same as presented in chapter 2. For a detailed description of the various methods and datasets used in this study, please refer to section 2.2.

## 3.3 Results

### 3.3.1 Seismic Data Collection

The 3.5 kHz sub-bottom profiles consisted principally of diffraction hyperbolae and side echoes caused by rapid changes in seafloor elevation; therefore, they were not usable.

### 3.3.2 Geological Sample Characteristics

A variety of different rock types were recovered from the seamount and Appendix 2-2 summarizes the recovered rock sample characteristics.

#### 3.3.2.1 *Granites*

Granites (R1340-6, 7, 12, 13), interpreted as ice rafted, were collected from the western and eastern flanks of an extensive (2 km x 0.5 km) lava flow outcrop (2870 m), on a 30° slope 938 m below the peak of OS (1932 m) (Fig. 3-2). Samples R1340-6 and 7 were lost on recovery and were recorded through photographs, thus rock type could not be verified.

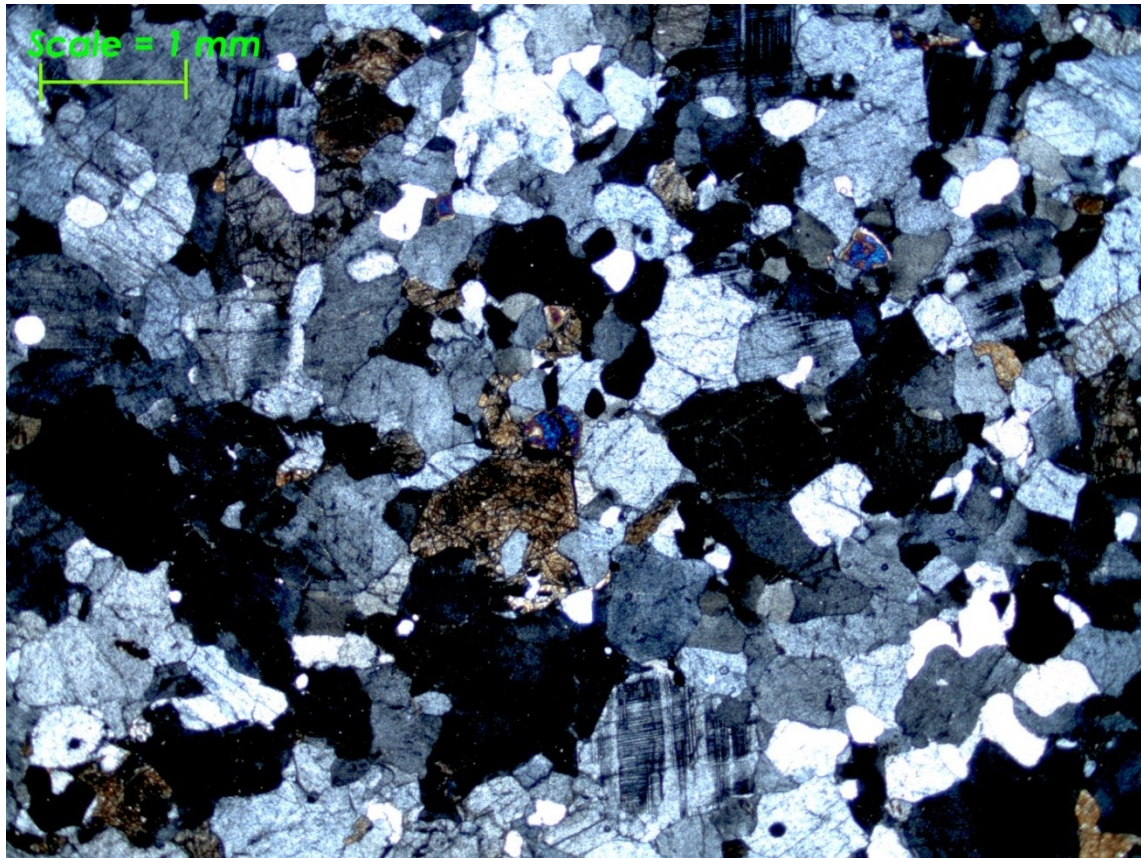


*Figure 3-2. Thin Section of Granodiorite sample (R1340-13) from Orphan Seamount talus and IRD facies (Cross Polarized View at 1.6x Mag.)*

### **3.3.2.2 Basalt**

Basalt (R1340-26(A,B)) was recovered from an extensive lava flow outcrop (2000 m) on a 22° slope 68 m below the peak of OS (1932 m) (Fig. 3-3). The amount of basalt recovered was relatively small, compared to the IRD recovered, due to thick (>10 cm) and ubiquitous Fe-Mn crust overlying the bedrock. Because of such crusts, many supposed bedrock samples commonly recovered only Fe-Mn crust. The only basalt sample, R1340-26, was highly weathered. Basalt Sample R1340-26 contained geopetal structures comprised of two layers of fine-grained

carbonate ooze containing silica patches, black oxide grains (possibly Fe-Mn, (Laughton et al. 1972)) and pyroxene; separated by a re-crystallized carbonate layer (Fig. 3-4).

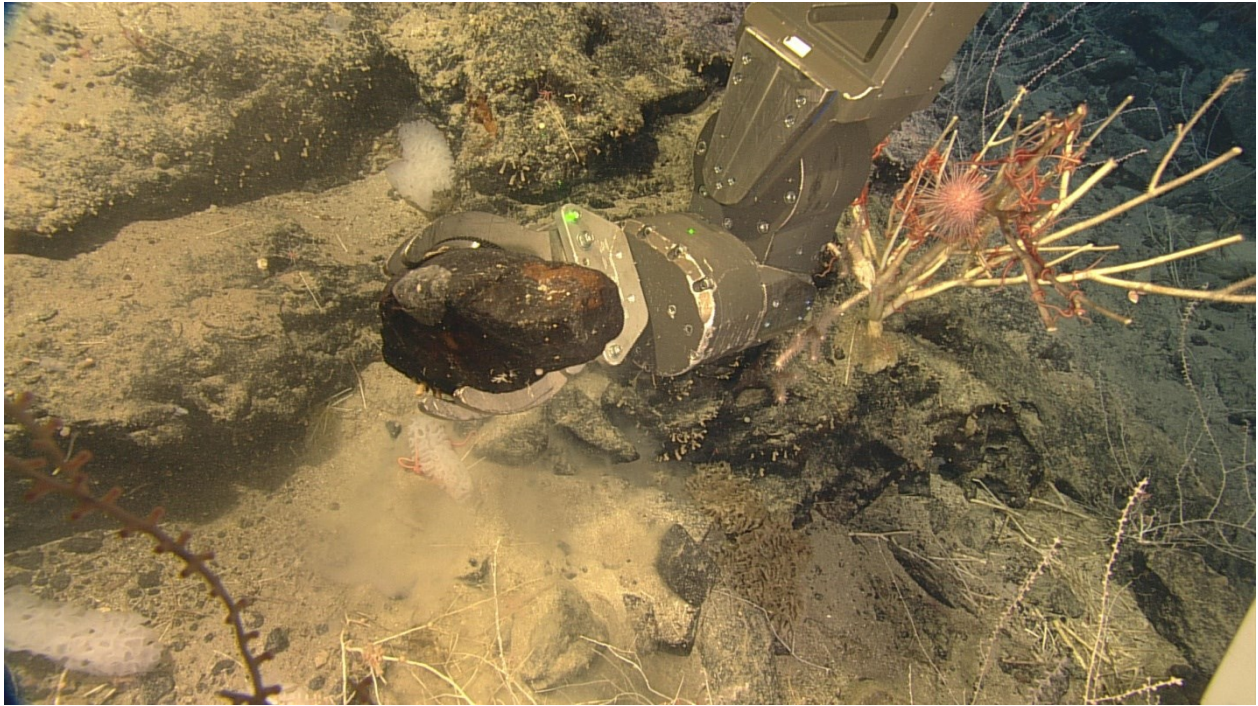


*Figure 3-3. Basalt sample R1340-26 extracted by ROPOS from a lava outcrop amongst Isididae coral (bamboo coral); green dots are 10 cm apart (visible on ROV armature).*

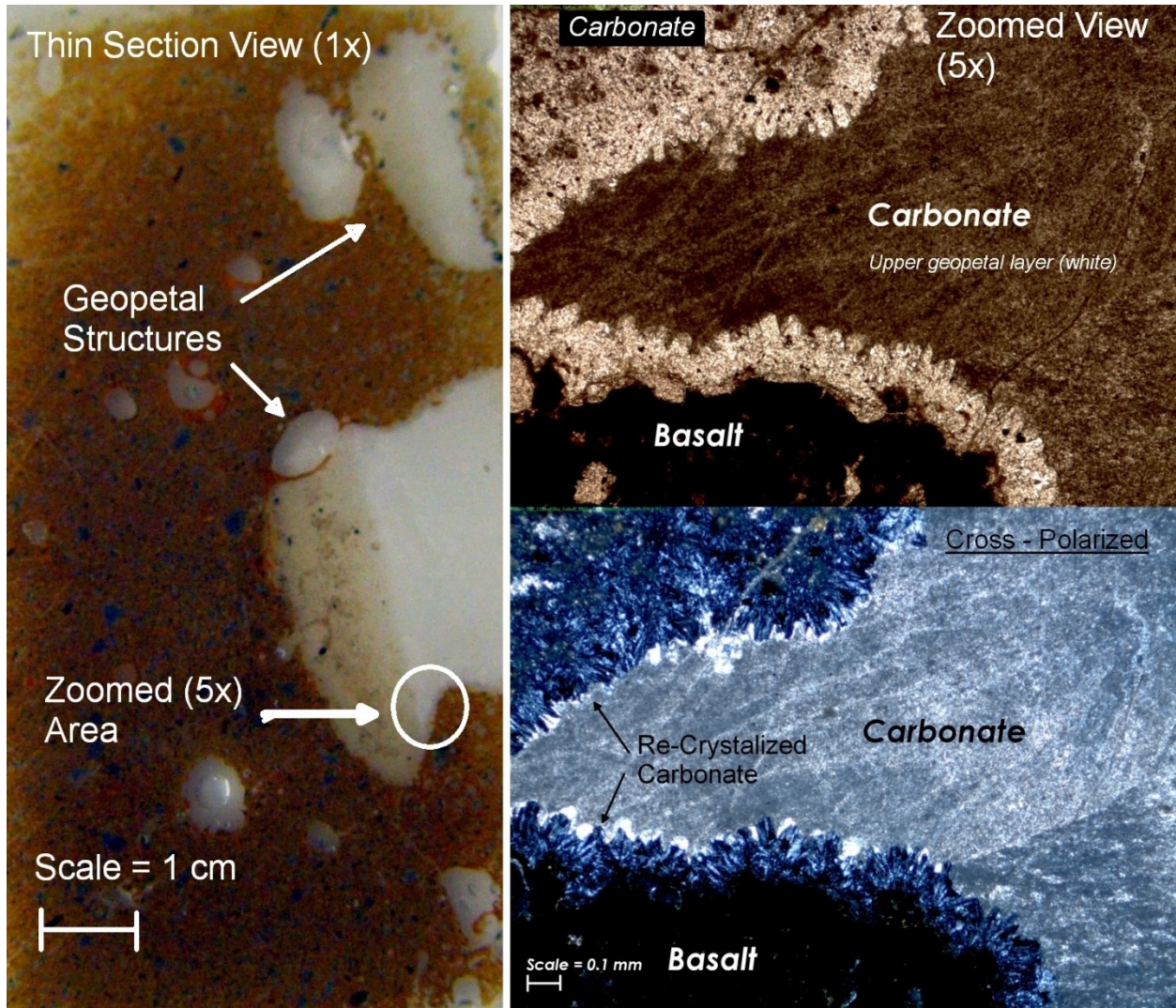


Figure 3-4. Thin Section of Orphan Seamount Basalt with geopetal structures (R1340-26B)(left) (1x); zoomed thin section views (right)(5x); carbonate fill within geopetal areas within weathered basalt; bottom right image is the cross polarized view of the above thin section (5x mag.)

### 3.3.2.3 Limestone

Limestone overlies basalt at Orphan Seamount, as seen in Fig. 3-4, by the presence of geopetal fill, indicating that vesicles were filled-in.

A limestone sample (R1340-14) was collected from an extensive lava flow outcrop (2720 m) draped by fine-grained sediment on a 40° slope 788 m below the crest of OS (1932 m) (Fig. 3-5). Limestone sample (R1340-19) was recovered from extensive lava outcropping on a 20° slope 341 m below the seamount crest (1932 m) (Fig. 3-6). Samples R1340-14 and 19 contained foraminifera from the genus *Globigerina* spp. and *Orbulina* spp. (Fig. 3-7). Previous biostratigraphic analysis done on the DSDP site 111 cores and through petrographic analysis of basalt sample R1340-26, verified by Dr. David Scott (Dalhousie University), the limestone within the OS basalt contained fossilized foraminifera, probably *Globigerina woodi*, *Globigerina atlantica* and *Orbulina universa*, that were found during the mid-Miocene (16 Myr) (Laughton et al. 1972; Dowsett & Robinson 2007; Bellier et al. 2010) (Fig. 3-7).

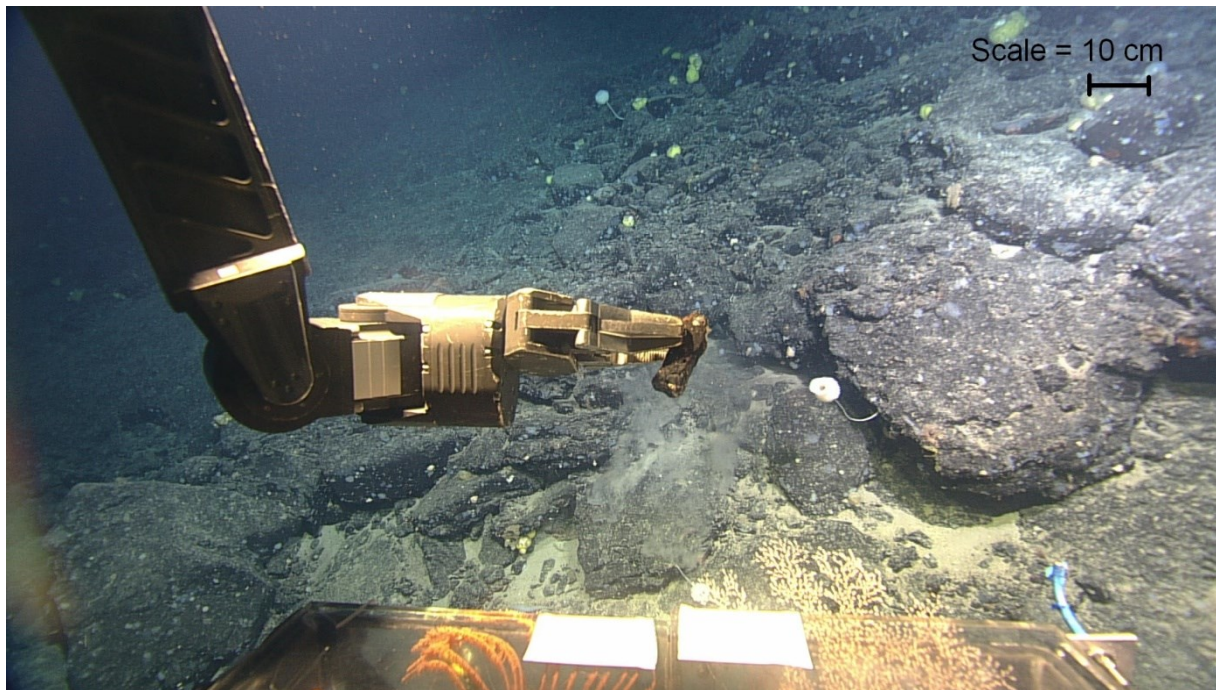


Figure 3-5. ROPOS extracting rock sample R1340-14 from lava outcrop on Orphan Seamount

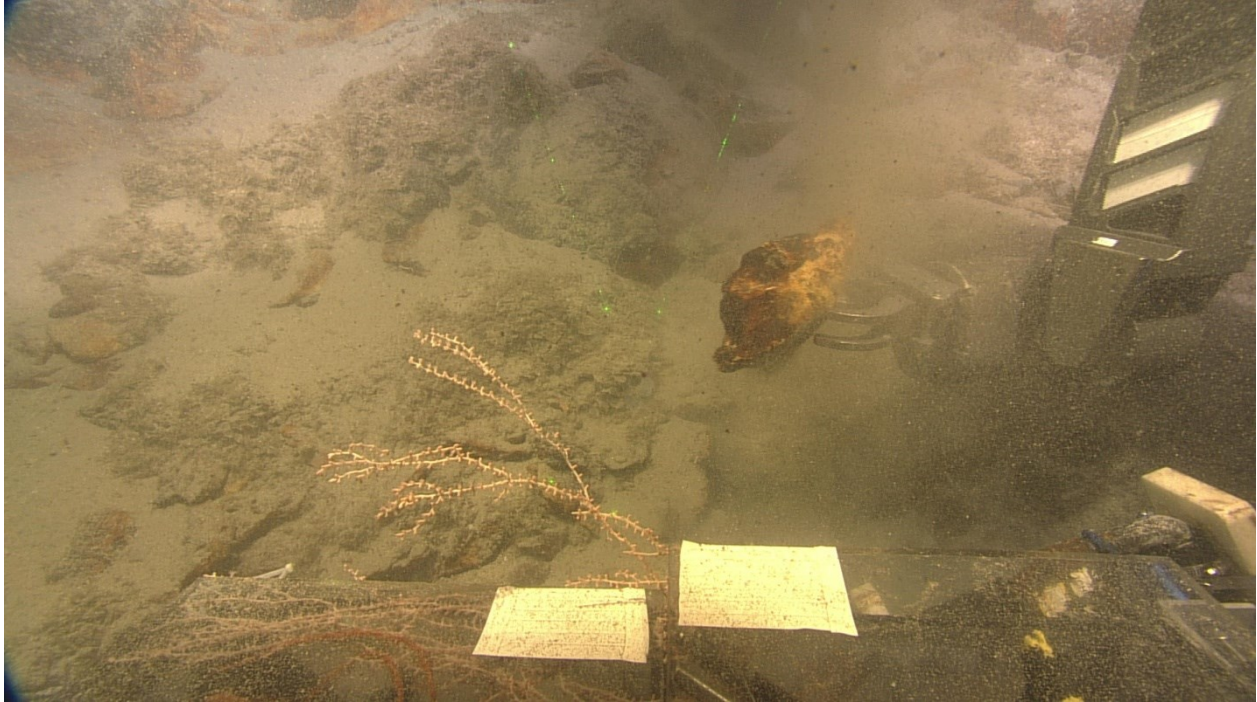


Figure 3-6. ROPOS extracting rock sample R1340-19 from lava outcrop from Orphan Seamount (green dots are 10 cm apart)

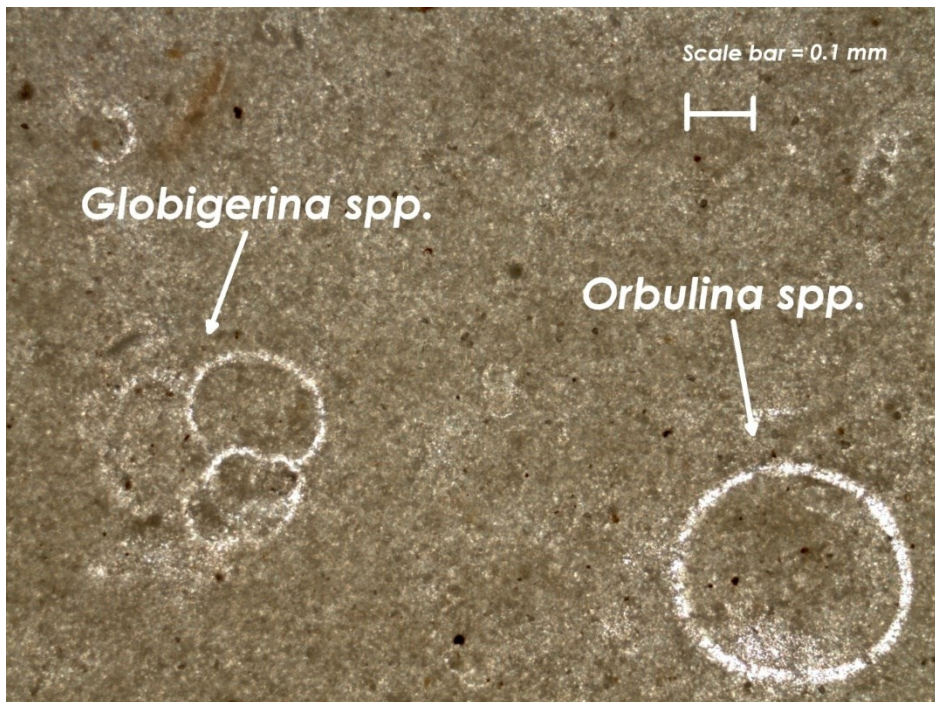


Figure 3-7. Thin Section (10x) of Pelagic Cenozoic limestone sample from Orphan Seamount (R1340-19), identifying foraminifera *Globigerina* spp. and *Orbulina* spp. foraminifera fossils.

### 3.3.3 Surficial Geological Segment Characteristics

Seven unique compositional facies were identified on OS and figure 3-5 delineates the surficial geology by percent coverage of a specific substrate type.

Lava tubes (Fig. 3-11), including collapsed lava tubes (Fig. 3-12), pillow lava (Fig. 3-15) were comprised of a basalt matrix seen in the recovered basalt sample (R1340-26).

The bedrock outcrops were overlain by talus and drape of IRD (boulders to fine sediment sizes) (Fig. 3-8). Slopes filled with talus (R1340-14, 19, and 26) and IRD (R1340-12 and 13) consisted of basalt, talus and IRD of many lithologies including granodiorite (Fig. 3-14).

Limestone facies (R1340-14 and 19) included the foraminiferal species *Globigerina* spp. and *Orbulina* spp (Fig. 3-7), whereby their presence indicates that the limestone found overlying the basaltic bedrock was derived from pelagic plankton sources formed in the mid-Miocene (Blow 1956; Coles et al. 1996; Dowsett & Robinson 2007; Bellier et al. 2010).

The Fe-Mn crust facies was found ubiquitously covering every available surface. Crust thickness varied amongst samples recovered (1 cm to >10 cm) and were not analyzed further than the thin section stage for this study.

Between bedrock outcrops, the surficial geology consisted primarily of granules overlying basaltic bedrock (Fig. 3-9), with the exception being near the top of the seamount (head of a south facing depression, (SGU H-I)) where fine-grained sediment covered basaltic bedrock (Fig. 3-10).

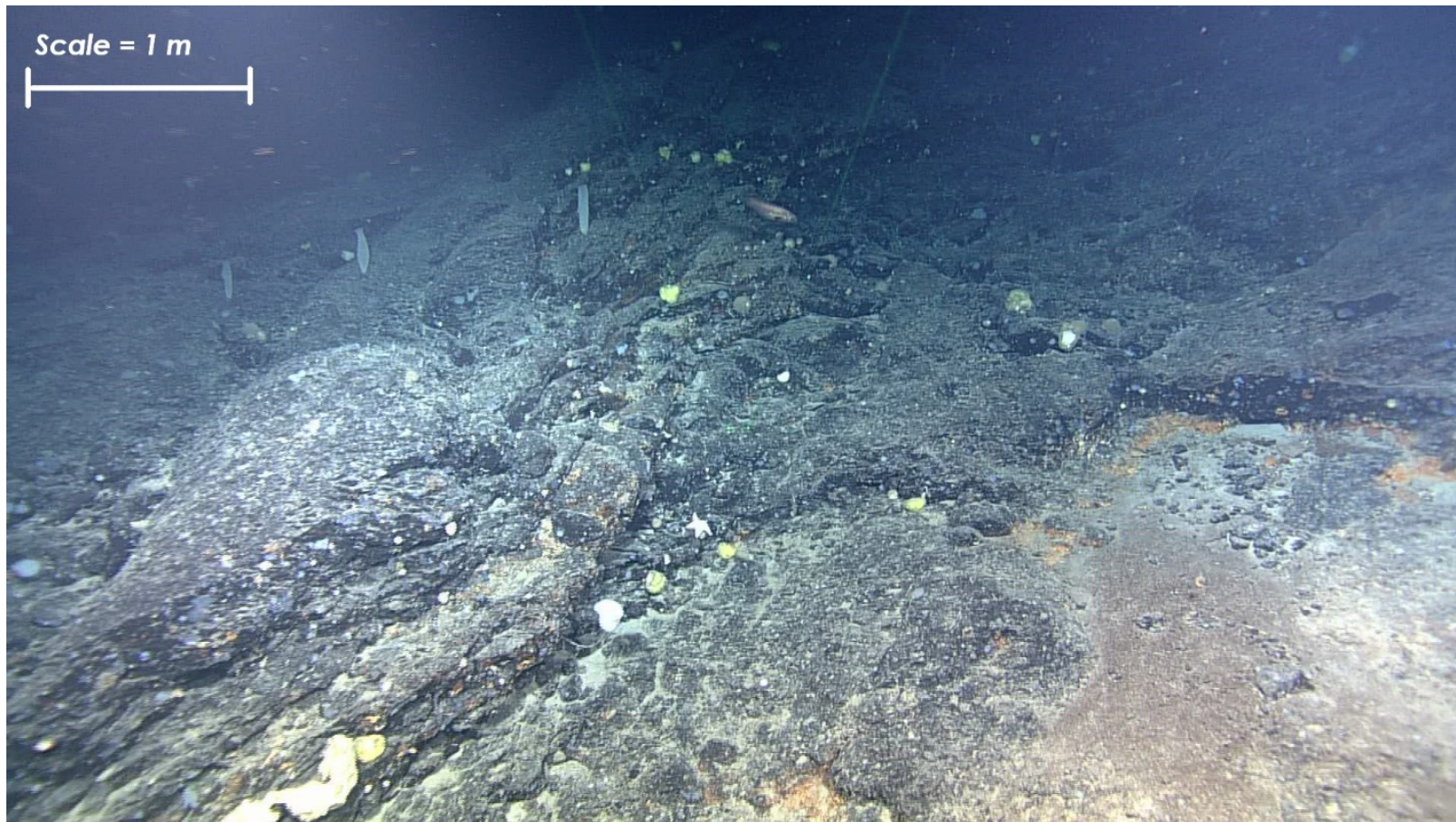


*Figure 3-8. Pillow Lava (bedrock), talus and IRD from the low-mid slope (3000 m) of Orphan Seamount (D1340).*



*Figure 3-9. Granule dominated facies on Orphan Seamount with Enteropneusta spp. (Acorn Worm); green dots are 10 cm apart*

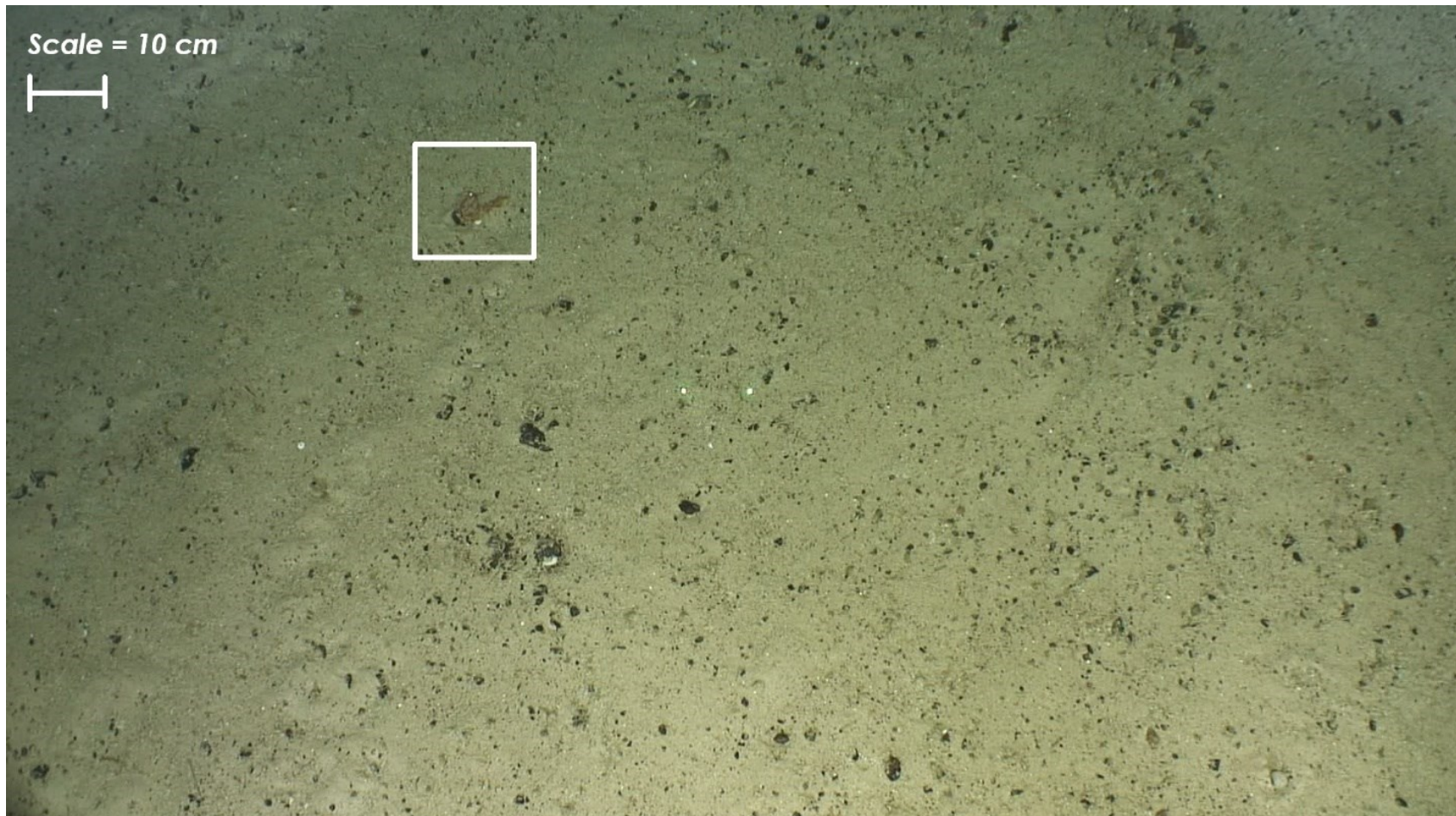


*Figure 3-10. Fine grained sediment dominated facies found near the top of Orphan Seamount; unknown Isididae spp. Cold-Water Coral(Gorgonian-white box); green dots are 10 cm apart (center of image)*

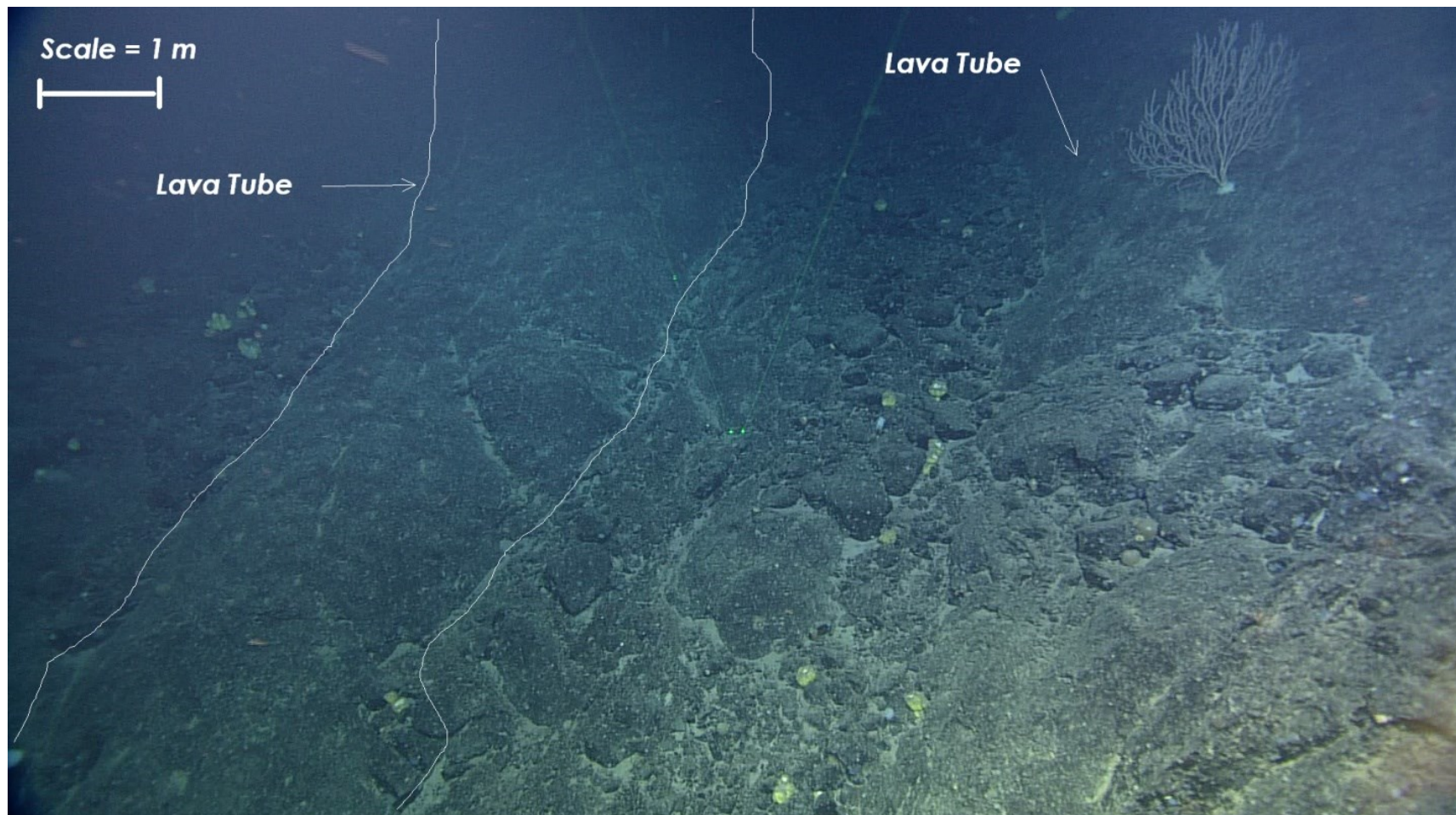
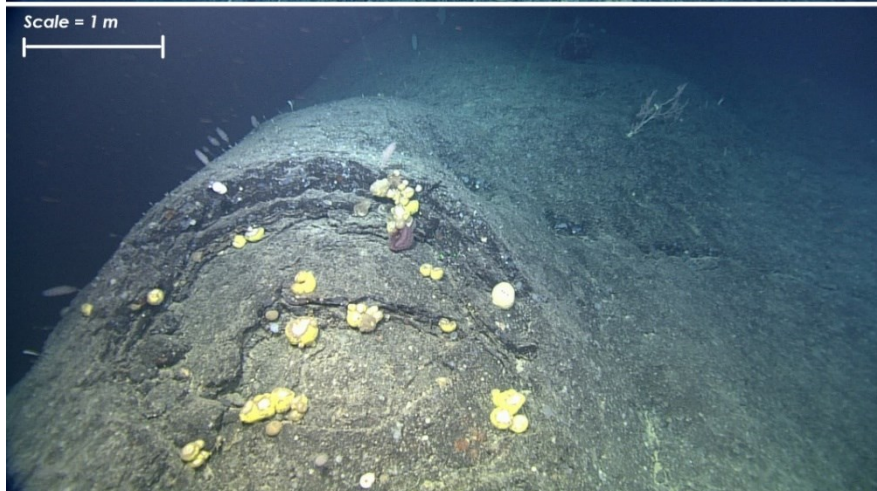
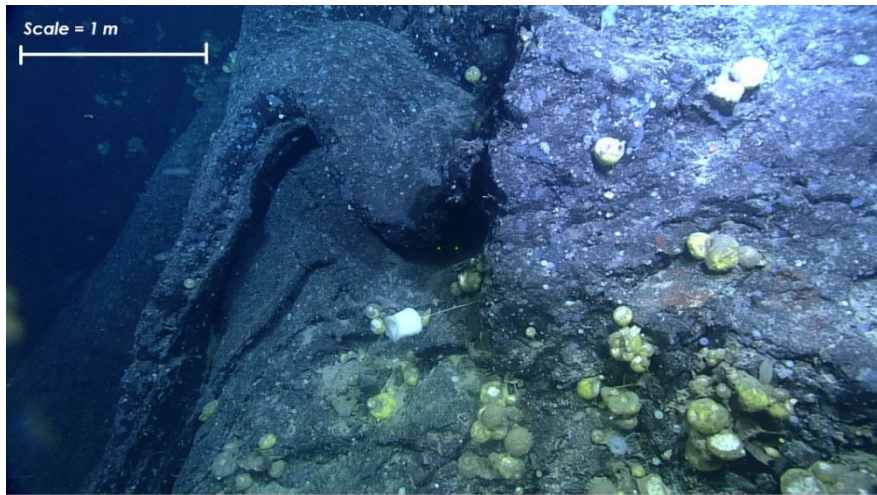
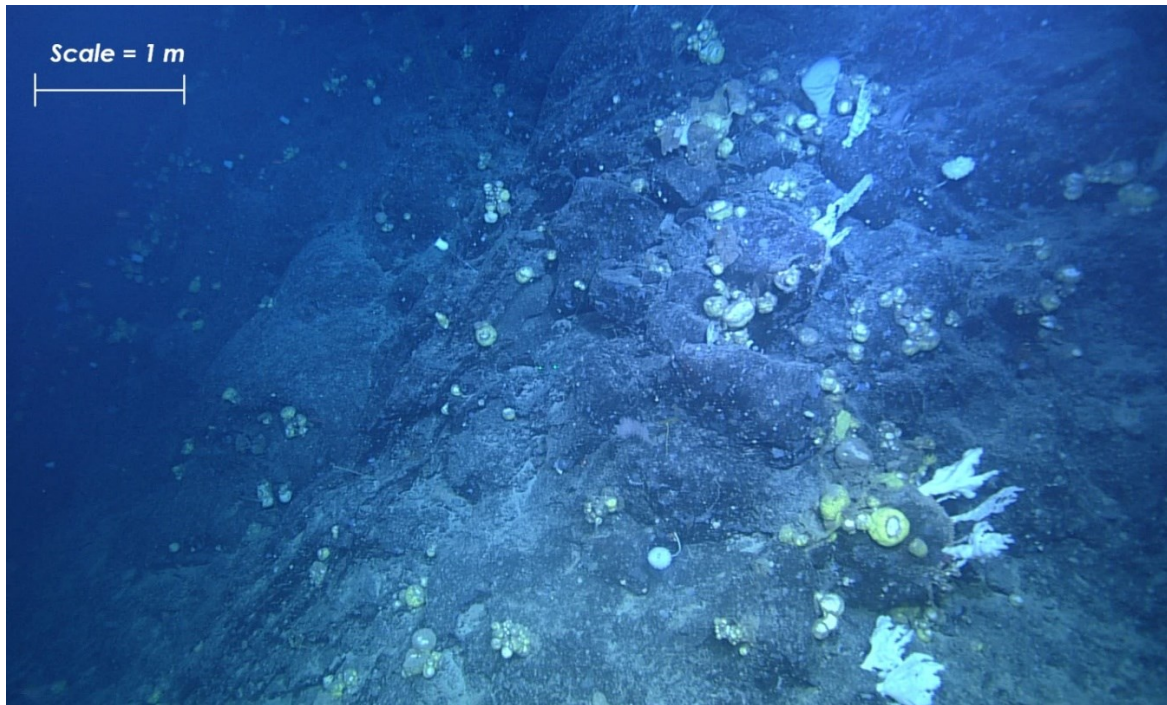


Figure 3-11. Lava tubes with talus and IRD filling the depressions in between the lava tubes; Cold-Water Coral *Paramuricea* spp. (Gorgonian) is seen growing on the lava tube on the right; green dots are 10 cm apart (center of image)



*Figure 3-12. Collapsed Lava Tubes from Orphan Seamount rather covered by Fe-Mn crust, talus, IRD, several unknown sponges (Hexactinellidae) and Chrysogorgia spp. and other unknown Isididae spp. coral (bottom).*



*Figure 3-13. Pillow Basalt from Orphan Knoll covered by several unknown species of Hexactinellidae sponges (glass sponges).*



*Figure 3-14. Talus, IRD and hemi-pelagic sediment from Orphan Seamount slopes in between lava tube outcrops*



*Figure 3-15. Pillow lava and Fe-Mn oxide crust from Orphan Seamount; covered in Crinoidea, Hexactinellidae, Isididae Zoantharia and Chrysogorgia spp. benthic megafauna.*

### 3.4 Discussion

Covering every rock sample collected on Hudson 2010-029 had a black oxidized Fe-Mn crust (Fig. 3-16). The age of the Fe-Mn crusts was not determined.

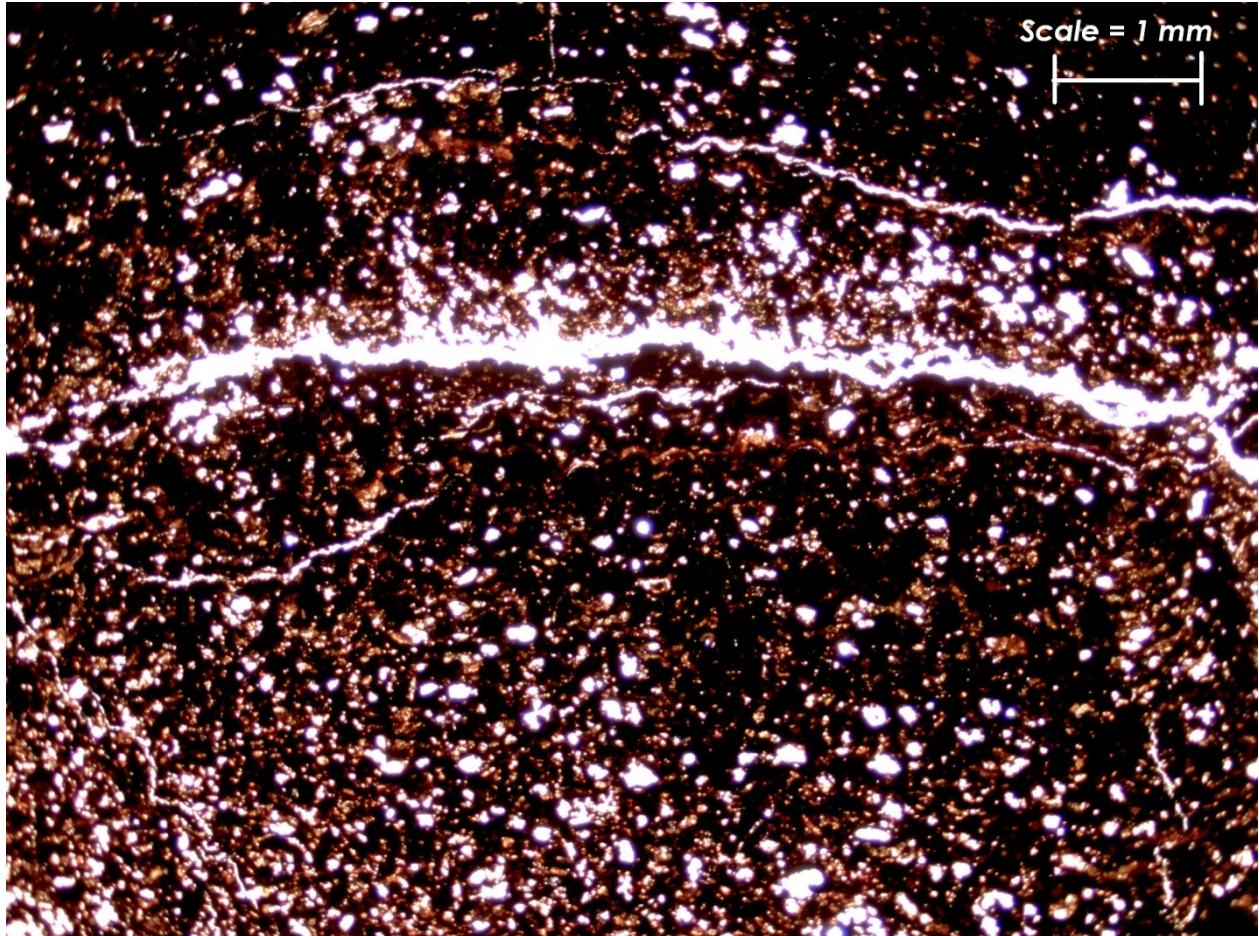


*Figure 3-16. Thin Section of Fe-Mn Crust from Orphan Seamount (1.6x)*

Petrographic analysis of rock sample R1340-26 identified that the bedrock was weathered basalt (Mn - Fe oxidation) containing pyroxene grains (Fig. 3-4). The HD video of lava tubes and pillow basalt, combined with the petrographic analysis of the basalt sample, confirmed that the OS is a volcanic seamount.

HD video data and the collected surficial geological data from dive 1340 indicated a general surficial geology of basaltic bedrock outcrop covered by limestone, overlaid by a thin fine sediment drape with patches of boulders and granules situated within depressions flanking the seamount. The presence of pelagic foraminifera fossils, *Globigerina* spp. and *Orbulina* spp., within the limestone sample R1340-14 allows for a probable youngest age limit for the basalt, since the limestone formed after the basalt. Unfortunately, the geopetal structures within the limestone-filled vesicles of basalt sample (R1340-26) could not be verified (by SEM) for foraminiferal fossils. However, it is probable that the limestone (probable pelagic source) formed in the basalt vesicles at the same time (mid-Miocene) as limestone sample R1340-14. Therefore, the basalt is older than the mid-Miocene but younger than the Late Cretaceous age (K anomaly ~105 Myr) (Chian et al. 2001) or possibly earlier to the pre-Mid-Atlantic rift J Anomaly event (~112 to ~140 Myr) (Bronner et al. 2011).

Seamounts experience a down-welling water current movement (Mullineau & Mills 1997) that encourages sediment deposition on the seamount summit and reduces deposition on the seamount slopes (Genin et al. 1986; Reidenbach et al. 2006). Combined with present day North Atlantic bottom currents (Fischer & Schott 2002; Carlson et al. 2007; Huvenne et al. 2009; Lund et al. 2011) and the steep slopes of OS, limited sedimentation was seen as unusual along the slopes of OS and presumably throughout its history.

### 3.5 Conclusion

The Orphan Seamount is a basaltic submarine volcano covered by IRD, talus, Fe-Mn oxidation (crust) and pelagic mid-Miocene limestone (identified by foraminifera *Globigerina* spp. and *Orbulina* spp.). Limestone-filled vesicles within the basalt, which are theorized in being from the same time and source (pelagic) to the mid-Miocene limestone samples. Therefore, the age of the seamount lies somewhere before the mid-Miocene up to the late Cretaceous (K anomaly ~105 Ma). Seven compositional facies were identified; lava tubes, talus and IRD, Fe-Mn crust, granule dominated and fine grained sediment, the latter five types overlying basaltic bedrock. Bottom currents and the sloping nature of the seamount, between the mid-Miocene until present, have largely kept the steep slopes of the seamount free of sediment, though limestone presence in vesicles found in bedrock basalt identify that this sedimentation rate was presumably more active prior to the mid-Miocene.

### 3.6 Bibliography

- Alt, J., 1988. Hydrothermal oxide and nontronite deposits on seamounts in the eastern Pacific. *Marine Geology*, 81(1–4), pp.227–239.
- Althaus, F. et al., 2009. Impacts of bottom trawling on deep-coral ecosystems of seamounts are long-lasting. *Marine Ecology Progress Series*, 397, pp.279–294. Available at: <http://www.int-res.com/abstracts/meps/v397/p279-294/>.
- Amos, C. & Judge, J., 1991. Sediment transport on the eastern Canadian continental shelf. *Continental Shelf Research*, 11(8–10), pp.1037–1068. Available at: <http://linkinghub.elsevier.com/retrieve/pii/027843439190090S>.
- Austin, M., 2002. Spatial prediction of species distribution: an interface between ecological theory and statistical modelling. *Ecological Modelling*, 157(2–3), pp.101–118. Available at: <http://linkinghub.elsevier.com/retrieve/pii/S0304380002002053>.
- Bailey, W. et al., 2003. The spatial distributions of fault and deep sea carbonate mounds in the Porcupine Basin, offshore Ireland. *Marine and Petroleum Geology*, 20, pp.509–522.
- Baillon, S., Hamel, J.-F. & Mercier, A., 2014. Diversity, distribution and nature of faunal associations with deep-sea pennatulacean corals in the northwest atlantic. *PloS one*, 9(11), p.16. Available at: <http://dx.plos.org/10.1371/journal.pone.0111519>.
- Baker, K. et al., 2012. Distributional patterns of deep-sea coral assemblages in three submarine canyons off Newfoundland, Canada. *Marine Ecology Progress Series*, 445, pp.235–249. Available at: <http://www.int-res.com/abstracts/meps/v445/p235-249/>.
- Barrett, T. et al., 1988. Geochemical aspects of hydrothermal sediments in the eastern Pacific Ocean; an update. *Canadian Mineralogist*, 26(3), p.841.
- Barrie, J. & Conway, K., 2008. Surficial geology: The third dimension in habitat mapping. In J. Reynolds & H. Greene, eds. *Marine Habitat Mapping Technology for Alaska*. Fairbanks, AK: University of Alaska Fairbanks, pp. 91–97.
- Beazley, L. et al., 2015. Drivers of epibenthic megafaunal composition in the sponge grounds of the Sackville Spur, northwest Atlantic. *Deep Sea Research Part I: Oceanographic Research Papers*, 98, pp.102–114.
- Bellier, J.-P., Mathieu, R. & Granier, B., 2010. Short Treatise on Foraminiferology (Essential on modern and fossil Foraminifera). In *Carnets de Geologie*. p. 106.
- Berggren, W. & Aubert, J., 1976. Eocene benthonic foraminiferal biostratigraphy and paleobathymetry of Orphan Knoll (Labrador Sea). *Micropaleontology*, 22(3), pp.327–346.
- Blow, W., 1956. Origin and Evolution of the Foraminiferal Genus *Orbulina* d’Orbigny. *Micropaleontology*, 2(1), pp.57–70. Available at: <http://www.jstor.org/stable/1484492>.
- Bluhm, B., Iken, K. & Hopcroft, R., 2010. Observations and exploration of the Arctic’s Canada Basin and the Chukchi Sea: The Hidden Ocean and RUSALCA expeditions. *Deep Sea Research Part II: Topical Studies in Oceanography*, 57(1–2), pp.1–4. Available at: <http://linkinghub.elsevier.com/retrieve/pii/S0967064509002446> [Accessed February 18,

- 2011].
- Bolton, B. et al., 1988. Geochemistry and mineralogy of seafloor hydrothermal and hydrogenetic Mn oxide deposits from the Manus Basin and Bismarck Archipelago region of the southwest Pacific Ocean. *Marine Geology*, 85(1), pp.65–87.
- Boutillier, J. et al., 2008. Status of Cold-Water Coral Communities of the World: A Brief Update. In T. Hourigan, ed. *Status of Coral Reefs of the World*. Australian Institute of Marine Science, pp. 58–66.
- Breeze, H. et al., 1997. Distribution and Status of Deep Sea Corals off Nova Scotia. *Ecology & Action*, (1), pp.1–40. Available at: [http://www.ecologyaction.ca/files/images/file/Marine/Distribution and Status of Deep Sea Coral off Nova Scotia Part 1.pdf](http://www.ecologyaction.ca/files/images/file/Marine/Distribution%20and%20Status%20of%20Deep%20Sea%20Coral%20off%20Nova%20Scotia%20Part%201.pdf).
- Bronner, A. et al., 2011. Magmatic breakup as an explanation for magnetic anomalies at magma-poor rifted margins. *Nature Geoscience Letters*, 4(8), pp.549–553. Available at: <http://dx.doi.org/10.1038/ngeo1201>.
- Brown, C. et al., 2011. Benthic habitat mapping: A review of progress towards improved understanding of the spatial ecology of the seafloor using acoustic techniques. *Estuarine, Coastal and Shelf Science*, 92(3), pp.502–520. Available at: <http://linkinghub.elsevier.com/retrieve/pii/S0272771411000485> [Accessed March 16, 2012].
- Bryan, T. & Metaxas, A., 2006. Distribution of deep-water corals along the North American continental margins: Relationships with environmental factors. *Deep Sea Research Part I: Oceanographic Research Papers*, 53(12), pp.1865–1879. Available at: <http://linkinghub.elsevier.com/retrieve/pii/S0967063706002378>.
- Bryan, T. & Metaxas, A., 2007. Predicting suitable habitat for deep-water gorgonian corals on the Atlantic and Pacific Continental Margins of North America. *Marine Ecology Progress Series*, 330, pp.113–126. Available at: <http://www.int-res.com/abstracts/meps/v330/p113-126/>.
- Buhl-Mortensen, L. et al., 2010. Biological structures as a source of habitat heterogeneity and biodiversity on the deep ocean margins. *Marine Ecology*, 31(1), pp.21–50. Available at: <http://blackwell-synergy.com/doi/abs/10.1111/j.1439-0485.2010.00359.x>.
- Buhl-Mortensen, L. et al., 2012. Habitat complexity and bottom fauna composition at different scales on the continental shelf and slope of northern Norway. *Hydrobiologia*, 685(1), pp.191–219.
- Buhl-Mortensen, P., Buhl-Mortensen, L., et al., 2009. Megafaunal diversity associated with marine landscapes of northern Norway: A preliminary assessment. *Norsk Geologisk Tidsskrift*, 89(1–2), pp.163–171.
- Buhl-Mortensen, P., Dolan, M. & Buhl-Mortensen, L., 2009. Prediction of benthic biotopes on a Norwegian offshore bank using a combination of multivariate analysis and GIS classification. *ICES Journal of Marine Science*, 66(9), pp.2026–2032. Available at: <http://icesjms.oxfordjournals.org/content/66/9/2026.short>.
- Burton-Ferguson, R., Enachescu, M. & Hiscott, R., 2006. Preliminary Seismic Interpretation and

- Maps for the Paleogene-Neogene (Tertiary) Succession, Orphan Basin. *Recorder*, 31(7), pp.28–32.
- Burton, E. & Lundsten, L., 2008. Davidson Seamount taxonomic guide. *Marine sanctuaries conservation series ; ONMS-08-08*, pp.1–160. Available at: <http://sanctuaries.noaa.gov/science/conservation/pdfs/taxonomic.pdf>.
- Carlson, A. et al., 2007. Geochemical proxies of North American freshwater routing during the Younger Dryas cold event. *Proceedings of the National Academy of Sciences*, 104(16), pp.6556–6561. Available at: <http://www.pubmedcentral.nih.gov/articlerender.fcgi?artid=1871824&tool=pmcentrez&rendertype=abstract>.
- Carmack, E. & Wassmann, P., 2006. Food webs and physical-biological coupling on pan-Arctic shelves: Unifying concepts and comprehensive perspectives. *Progress in Oceanography*, 71(2–4), pp.446–477.
- Carpenter, K. et al., 2008. One-Third of Reef-Building Corals Face Elevated Extinction Risk from Climate Change and Local Impacts. *Science*, 321(5888), pp.560–563. Available at: <http://www.sciencemag.org/content/321/5888/560.abstract>.
- Channell, J. et al., 2006. IODP Expeditions 303 and 306 Monitor Miocene-Quaternary Climate in the North Atlantic. *Scientific Drilling*, 2, pp.4–10.
- Chian, D., Reid, I. & Jackson, H., 2001. Crustal structure beneath Orphan Basin and implications for nonvolcanic continental rifting. *Journal Geophysical Research*, 106(B6), pp.10923–10940. Available at: <http://dx.doi.org/10.1029/2000JB900422>.
- Christiansen, B. & Wolff, G., 2009. The oceanography, biogeochemistry and ecology of two NE Atlantic seamounts: The OASIS project. *Deep Sea Research Part II: Topical Studies in Oceanography*, 56(25), pp.2579–2581. Available at: <http://linkinghub.elsevier.com/retrieve/pii/S0967064508004451> [Accessed September 2, 2010].
- Coles, G. et al., 1996. Foraminifera and Ostracoda from Quaternary carbonate mounds associated with gas seepage in the Porcupine Basin, offshore Western Ireland. *Revista Española de Micropaleontología*, XXVIII(2), pp.113–151.
- Colman, J. et al., 2005. Carbonate mounds off Mauritania, Northwest Africa: status of deep-water corals and implications for management of fishing and oil exploration activities. In A. Freiwald & J. M. Roberts, eds. Erlangen Earth Conference Series. Springer Berlin Heidelberg, pp. 417–441. Available at: [http://dx.doi.org/10.1007/3-540-27673-4\\_21](http://dx.doi.org/10.1007/3-540-27673-4_21).
- Compton, R., 1985. *Geology in the Field* 1st ed., John Wiley & Sons, Inc.
- Costello, M., 2009. Distinguishing marine habitat classification concepts for ecological data management. *Marine Ecology Progress Series*, 397, pp.253–268. Available at: <http://www.int-res.com/abstracts/meps/v397/p253-268/> [Accessed July 27, 2010].
- Cronan, D., Rothwell, G. & Croudace, I., 2010. An ITRAX Geochemical Study of Ferromanganiferous Sediments from the Penrhyn Basin, South Pacific Ocean. *Marine Georesources & Geotechnology*, 28(3), pp.207–221. Available at: <http://search.ebscohost.com/login.aspx?direct=true&db=aph&AN=53155598&site=ehost->

live&scope=site.

- Curewitz, D. & Karson, J., 1997. Structural settings of hydrothermal outflow: Fracture permeability maintained by fault propagation and interaction. *Journal of Volcanology and Geothermal Research*, 79(3–4), pp.149–168. Available at: <http://www.sciencedirect.com/science/article/pii/S0377027397000279>.
- Danovaro, R. et al., 2001. Deep-sea ecosystem response to climate changes: the eastern Mediterranean case study. *Trends in Ecology & Evolution*, 16(9), pp.505–510.
- Danovaro, R. et al., 2008. Exponential decline of deep-sea ecosystem functioning linked to benthic biodiversity loss. *Current Biology*, 18(1), pp.1–8. Available at: <http://www.sciencedirect.com/science/article/pii/S0960982207023421> [Accessed March 9, 2012].
- Davies, A. et al., 2009. Downwelling and deep-water bottom currents as food supply mechanisms to the cold-water coral *Lophelia pertusa* (Scleractinia) at the Mingulay Reef complex. *Limnology and Oceanography*, 54(2), pp.620–629. Available at: <http://hdl.handle.net/10242/44685>.
- Davies, A. et al., 2008. Predicting suitable habitat for the cold-water coral *Lophelia pertusa* (Scleractinia). *Deep Sea Research Part I: Oceanographic Research Papers*, 55(8), pp.1048–1062. Available at: <http://linkinghub.elsevier.com/retrieve/pii/S0967063708000836> [Accessed February 11, 2011].
- Davies, A., Roberts, M. & Hall-Spencer, J., 2007. Preserving deep-sea natural heritage: Emerging issues in offshore conservation and management. *Biological Conservation*, 138(3–4), pp.299–312. Available at: <http://www.sciencedirect.com/science/article/pii/S0006320707002285>.
- Davies, A.J. & Guinotte, J.M., 2011. Global habitat suitability for framework-forming cold-water corals. *PloS one*, 6(4), pp.1–15. Available at: <http://www.pubmedcentral.nih.gov/articlerender.fcgi?artid=3078123&tool=pmcentrez&rendertype=abstract> [Accessed March 18, 2012].
- Davies, J. et al., 2015. Benthic Assemblages of the Anton Dohrn Seamount (NE Atlantic): Defining Deep-Sea Biotopes to Support Habitat Mapping and Management Efforts with a Focus on Vulnerable Marine Ecosystems. *PloS one*, 10(5), p.33. Available at: <http://www.pubmedcentral.nih.gov/articlerender.fcgi?artid=4436255&tool=pmcentrez&rendertype=abstract>.
- Dowsett, H. & Robinson, M., 2007. Mid-Pliocene planktic foraminifera assemblage of the North Atlantic Ocean. *Micropaleontology*, 53(1–2), pp.105–126. Available at: <http://micropal.geoscienceworld.org/cgi/content/abstract/53/1-2/105>.
- Dronov, A., 1993. Middle paleozoic waulsortian-type mud mounds in Southern Fergana (Southern Tien-Shan, commonwealth of independent states): The shallow-water atoll model. *Facies*, 28(1), pp.169–180. Available at: <http://dx.doi.org/10.1007/BF02539735>.
- Durán Muñoz, P. & Sayago-Gil, M., 2011. An overview of cold-water coral protection on the high seas: The Hatton bank (NE Atlantic)—A case study. *Marine Policy*, 35(5), pp.615–622. Available at: <http://www.sciencedirect.com/science/article/pii/S0308597X11000248>.

- Edinger, E. et al., 2011. Geological features supporting deep-sea coral habitat in Atlantic Canada. *Continental Shelf Research*, 31(2, Supplement), pp.S69–S84. Available at: <http://www.sciencedirect.com/science/article/pii/S0278434310002220>.
- Elith, J. et al., 2010. A statistical explanation of MaxEnt for ecologists. *Diversity and Distributions*, 17(1), p.no-no. Available at: <http://doi.wiley.com/10.1111/j.1472-4642.2010.00725.x> [Accessed November 25, 2010].
- Ellis, N., Smith, S. & Pitcher, R., 2012. Gradient forests: calculating importance gradients on physical predictors. *Ecological Society of America*, 93(1), pp.156–168.
- Enachescu, M., 2004. Conspicuous deepwater submarine mounds in the northeastern Orphan Basin and on the Orphan Knoll, offshore Newfoundland. *The Leading Edge*, 23(12), pp.1290–1294. Available at: <http://link.aip.org/link/LEEDFF/v23/i12/p1290/s1&Agg=doi>.
- Enachescu, M., 2009. *Investigating basin architecture and evolution of the Orphan Basin by use of reflection, refraction, heatflow and potential filed transects*, St. John's, NL.
- Enachescu, M., 2005. Offshore Newfoundland and Labrador - An Emerging Energy Powerhouse. In *Offshore Technology Conference*. Houston, TX: Offshore Technology Conference, pp. 1–8. Available at: <http://www.onepetro.org/mslib/servlet/onepetropreview?id=OTC-17570-MS&soc=OTC>.
- Etnoyer, P., 2005. Seamount resolution in satellite-derived bathymetry. *Geochemistry Geophysics Geosystems*, 6(3), pp.311–312. Available at: <http://www.agu.org/pubs/crossref/2005/2004GC000833.shtml> [Accessed February 11, 2011].
- Farrand, W. & Lane, M., 2007. New observations of enigmatic landforms and surface terrains on the northern plains of Mars. In *Geological Society of America Annual Meeting*. Denver, CO: Geological Society of America. Available at: [https://gsa.confex.com/gsa/2007AM/finalprogram/abstract\\_129996.htm](https://gsa.confex.com/gsa/2007AM/finalprogram/abstract_129996.htm).
- Ferrier, S. et al., 2006. Novel methods improve prediction of species' distributions from occurrence data. *Ecography*, 29, pp.129–151.
- Ferrier, S. et al., 2007. Using generalized dissimilarity modelling to analyse and predict patterns of beta diversity in regional biodiversity assessment. *Diversity and Distributions*, 13(3), pp.252–264. Available at: <http://blackwell-synergy.com/doi/abs/10.1111/j.1472-4642.2007.00341.x>.
- Fischer, J. & Schott, F., 2002. Labrador Sea Water Tracked by Profiling Floats—From the Boundary Current into the Open North Atlantic. *Journal of Physical Oceanography*, 32(2), pp.573–584. Available at: [http://journals.ametsoc.org/doi/abs/10.1175/1520-0485\(2002\)032%3C0573:LSWTBP%3E2.0.CO;2](http://journals.ametsoc.org/doi/abs/10.1175/1520-0485(2002)032%3C0573:LSWTBP%3E2.0.CO;2).
- Fitzgerald, C. & Gillis, K., 2006. Hydrothermal manganese oxide deposits from Baby Bare seamount in the northeast Pacific Ocean. *Marine Geology*, 225(1–4), pp.145–156.
- Ford, D. & Williams, P., 1989. *Karst geomorphology and hydrology* 1st ed., London and Boston: Springer.
- Försterra, G. et al., 2005. Shallow-water *Desmophyllum dianthus* (Scleractinia) from Chile:

- characteristics of the biocoenoses, the bioeroding community, heterotrophic interactions and (paleo)-bathymetric implications. In A. Freiwald & J. M. Roberts, eds. *Cold-Water Corals and Ecosystems*. Erlangen Earth Conference Series. Berlin Heidelberg: Springer Berlin Heidelberg, pp. 937–977. Available at: [http://dx.doi.org/10.1007/3-540-27673-4\\_48](http://dx.doi.org/10.1007/3-540-27673-4_48).
- Fryer, P. & Fryer, G., 1987. Origins of Nonvolcanic Seamounts in a Forearc Environment. In *Seamounts, Islands, and Atolls*. American Geophysical Union, pp. 61–72.
- Genin, A. et al., 1986. Corals on seamount peaks provide evidence of current acceleration over deep-sea topography. *Nature*, 322(6074), pp.59–61. Available at: <http://dx.doi.org/10.1038/322059a0>.
- Gianni, M. et al., 2011. *Unfinished business: a review of the implementation of the provisions of UNGA resolutions 61/105 and 64/72 related to the management of bottom fisheries in areas beyond national jurisdiction*, Available at: [http://scholar.google.ca/scholar?hl=en&q=Unfinished+business:+a+review+of+the+implementation+of+the+provisions+of+UNGA+resolutions+61/105+and+64/72+related+to+the+management+of+bottom+fisheries+in+areas+beyond+national+jurisdiction&btnG=Search&as\\_sdt=1,5&](http://scholar.google.ca/scholar?hl=en&q=Unfinished+business:+a+review+of+the+implementation+of+the+provisions+of+UNGA+resolutions+61/105+and+64/72+related+to+the+management+of+bottom+fisheries+in+areas+beyond+national+jurisdiction&btnG=Search&as_sdt=1,5&).
- Gilkinson, K. & Edinger, E., 2009. *The Ecology of Deep-Sea Corals of Newfoundland and Labrador Waters : Biogeography, Life History, Biogeochemistry, and Role as Critical Habitat*, St.John's, NL.
- Glasby, G., 1978. Deep-sea manganese nodules in the stratigraphic record: Evidence from DSDP cores. *Marine Geology*, 28(1–2), pp.51–64. Available at: <http://www.sciencedirect.com/science/article/pii/0025322778900968>.
- Gonzalez-Mirelis, G. & Buhl-Mortensen, P., 2015. Modelling benthic habitats and biotopes off the coast of Norway to support spatial management. *Ecological Informatics*. Available at: <http://www.sciencedirect.com/science/article/pii/S1574954115000953>.
- Greenan, B. et al., 2010. *Serial No. N5774 NAFO SCR Doc. 10/19 SCIENTIFIC COUNCIL MEETING--JUNE 2010*,
- Guisan, A. et al., 2007. Sensitivity of predictive species distribution models to change in grain size. *Diversity and Distributions*, 13(3), pp.332–340. Available at: <http://dx.doi.org/10.1111/j.1472-4642.2007.00342.x>.
- Hall-spencer, J. et al., 2007. Deep-sea coral distribution on seamounts , oceanic islands , and continental slopes in the Northeast Atlantic. *Bulletin of Marine Science*, 81(1), pp.135–146. Available at: <http://www.ingentaconnect.com/contentone/umrsmas/bullmar/2007/00000081/A00103s1/art00013>.
- Han, G. et al., 2008. Seasonal variability of the Labrador Current and shelf circulation off Newfoundland. *Journal of Geophysical Research*, 113(C10013), pp.1–23. Available at: <http://www.agu.org/pubs/crossref/2008/2007JC004376.shtml> [Accessed February 18, 2011].
- Hart, B., 1977. The mid-Cretaceous succession of Orphan Knoll (northwest Atlantic): micropaleontology and palaeo-oceanographic implications. *Deep Sea Research*, 24(3–4), pp.272–272. Available at: <http://linkinghub.elsevier.com/retrieve/pii/0146629177902958>.

- Hart, M., 1976. The mid-Cretaceous succession of Orphan Knoll (northwest Atlantic): micropalaeontology and palaeo-oceanographic implications. *Canadian Journal of Earth Sciences*, 13(10), pp.1411–1421.
- Haworth, R. & Keen, C., 1979. The Canadian Atlantic Margin: A Passive Continental Margin Encompassing an Active Past. *Tectonophysics*, 59, pp.83–126.
- Heindel, K. et al., 2010. The sediment composition and predictive mapping of facies on the Propeller Mound—A cold-water coral mound (Porcupine Seabight, NE Atlantic). *Continental Shelf Research*, 30(17), pp.1814–1829. Available at: <http://linkinghub.elsevier.com/retrieve/pii/S0278434310002645> [Accessed March 18, 2012].
- Henriet, J.P. et al., 2010. Mounds and sediment drift in the Porcupine Basin, west of Ireland. In *European Margin Sediment Dynamics*. Springer Verlag. Available at: <http://eprints.soton.ac.uk/55535/>.
- Heywood, W. & Sanford, B., 1976. *Geology of Southampton, Coats and Mansel Islands, District of Keewatin, Northwest Territories*, Dartmouth, NS.
- van Hinte, J. et al., 1995. Palaeozoic microfossils from Orphan Knoll, NW Atlantic Ocean. *Scripta Geologica*, 109, pp.1–63. Available at: <http://www.narcis.nl/publication/RecordID/oai:naturalis.nl:317524> [Accessed October 26, 2011].
- Hoffmann, M. et al., 2010. The Impact of Conservation on the Status of the World's Vertebrates. *Science*, 330(6010), pp.1503–1509. Available at: <http://www.sciencemag.org/content/330/6010/1503.abstract>.
- Hovland, M., Croker, P. & Martin, M., 1994. Fault-associated seabed mounds(carbonate knolls?) off western Ireland and north-west Australia. *Marine and Petroleum Geology*, 11(2), pp.232–246.
- Howell, K., Davies, J. & Narayanaswamy, B., 2010. Identifying deep-sea megafaunal epibenthic assemblages for use in habitat mapping and marine protected area network design. *Journal of the Marine Biological Association of the United Kingdom*, 90, p.33. Available at: [http://www.journals.cambridge.org/abstract\\_S0025315409991299](http://www.journals.cambridge.org/abstract_S0025315409991299).
- Huuse, M. & Feary, D., 2005. Seismic inversion for acoustic impedance and porosity of Cenozoic cool-water carbonates on the upper continental slope of the Great Australian Bight. *Marine Geology*, 215(3–4), pp.123–134. Available at: <http://www.sciencedirect.com/science/article/pii/S002532270400355X>.
- Huvenne, V.A.I. et al., 2009. Sediment dynamics and palaeo-environmental context at key stages in the Challenger cold-water coral mound formation; clues from sediment deposits at the mound base. *Deep-Sea Research Part I: Oceanographic Research Papers*, 56(12), pp.2263–2280. Available at: <http://ezproxy.library.dal.ca/login?url=http://search.proquest.com/docview/877398895?accountid=10406>.
- ICES, 2007. *Report of the Working Group on Deep-eater Ecology (WGDEC)*,
- Immenhauser, A. & Rameil, N., 2011. Interpretation of ancient epikarst features in carbonate

- successions — A note of caution. *Sedimentary Geology*, 239(1–2), pp.1–9. Available at: <http://www.sciencedirect.com/science/article/pii/S0037073811001503> [Accessed March 10, 2012].
- Jauer, C. & Budkewitsch, P., 2010. Old marine seismic and new satellite radar data: Petroleum exploration of north west Labrador Sea, Canada. *Marine and Petroleum Geology*, 27(7), pp.1379–1394. Available at: <http://linkinghub.elsevier.com/retrieve/pii/S0264817210000620> [Accessed October 27, 2010].
- Keen, C. et al., 1987. Deep crustal structure and evolution of the rifted margin northeast of Newfoundland: results from LITHOPROBE East. *Canadian Journal of Earth Sciences*, 24(8), pp.1537–1549. Available at: <http://dx.doi.org/10.1139/e87-150>.
- King, L. et al., 1985. Occurrence and regional geological setting of Paleozoic rocks on the Grand Banks of Newfoundland. *Canadian Journal of Earth Sciences*, 23, pp.504–526.
- Land, L., Paull, C. & Hobson, B., 1995. Genesis of a submarine sinkhole without subaerial exposure: Straits of Florida. *Geology*, 23(10), pp.949–951. Available at: <http://geology.gsapubs.org/cgi/content/abstract/23/10/949>.
- Laughton, A. et al., 1972. Site 111. *International Deep Sea Drilling Project*, (12), pp.33–159.
- Leaper, R. et al., 2011. Predictions of beta diversity for reef macroalgae across southeastern Australia. *Ecosphere*, 2(7), p.art73. Available at: <http://dx.doi.org/10.1890/ES11-00089.1>.
- Legault, J., 1982. First report of Ordovician (Caradoc-Ashgill) palynomorphs from Orphan Knoll, Labrador Sea. *Canadian Journal of Earth Sciences*, 19(9), pp.1851–1856.
- Leverette, T. & Metaxas, A., 2004. Predicting habitat for two species of deep-water coral on the Canadian Atlantic continental shelf and slope. In A. Freiwald & M. Roberts, eds. *Cold-Water Corals and Ecosystems*. Berlin Heidelberg: Springer-Verlag, pp. 467–479. Available at: [http://link.springer.com/chapter/10.1007%2F3-540-27673-4\\_23](http://link.springer.com/chapter/10.1007%2F3-540-27673-4_23).
- Levin, L. et al., 2009. Macrobenthos community structure and trophic relationships within active and inactive Pacific hydrothermal sediments. *Deep Sea Research Part II: Topical Studies in Oceanography*, 56(19–20), pp.1632–1648. Available at: <http://linkinghub.elsevier.com/retrieve/pii/S0967064509001738> [Accessed November 19, 2010].
- Lodge, M., 2004. Improving International Governace in the Deep Sea. *The International Journal of Marine and Coastal Law*, 19(3), p.299.
- Logerwell, E., Rand, K. & Weingartner, T.J., 2011. Oceanographic characteristics of the habitat of benthic fish and invertebrates in the Beaufort Sea. *Polar Biology*, 34(11), pp.1783–1796.
- Long, D. et al., 2003. Mud mound / ?diapiric features in the Faroe - Shetland Channel. In *EGS - AGU - EUG Joint Assembly*. Nice: EGS- AGU - EUG Joint Assembly. Available at: <http://adsabs.harvard.edu/abs/2003EAEJA....11201L>.
- Lund, D., Adkins, J. & Ferrari, R., 2011. Abyssal Atlantic Circulation during the Last Glacial Maximum. *Paleoceanography*, 26(1), pp.1–18. Available at: [http://web.mit.edu/raffaele/www/Publications\\_files/LundAdkinsFerrariScience08.pdf](http://web.mit.edu/raffaele/www/Publications_files/LundAdkinsFerrariScience08.pdf)

[Accessed January 11, 2017].

- Madi, A., Bourque, P.-A. & Mamet, B., 1996. Depth-related ecological zonation of a carboniferous carbonate ramp: Upper Viséan of Béchar Basin, Western Algeria. *Facies*, 35(1), pp.59–79. Available at: <http://dx.doi.org/10.1007/BF02536957>.
- Margles, S. et al., 2010. Conservation Without Borders: Building Communication and Action Across Disciplinary Boundaries for Effective Conservation. *Environmental Management*, 45(1), pp.1–4. Available at: <http://dx.doi.org/10.1007/s00267-009-9383-8>.
- Menabreaz, L., 2015. Neodymium isotopic composition of deep-sea corals from the Labrador Sea: implications for NW Atlantic deep-water masses circulation during the Holocene, MIS 5 and 7. In *AGU-GAC-MAC-CGU Joint Assembly*. Montreal, p. 146.
- Metaxas, A. & Bryan, T., 2007. Predictive habitat model for deep gorgonians needs better resolution: Reply to Etnoyer & Morgan. *Marine Ecology Progress Series*, 339(3), pp.313–314. Available at: <http://www.int-res.com/abstracts/meps/v339/p313-314/>.
- Miles, L., Edinger, E. & Piper, D., 2015. Investigating the relationship between cold-water corals distribution and surficial geology. In *14th Deep-Sea Biology Symposium*. Aveiro, Portugal: DSBS, p. 1.
- Miller, K. et al., 2011. Out of their depth? Isolated deep populations of the cosmopolitan coral *Desmophyllum dianthus* may be highly vulnerable to environmental change. *PloS one*, 6(5), pp.1–10. Available at: [http://apps.webofknowledge.com.proxy-ub.rug.nl/full\\_record.do?product=UA&search\\_mode=GeneralSearch&qid=1&SID=T15EYVKBZuXIHfTAVsm&page=9&doc=87&cacheurlFromRightClick=no](http://apps.webofknowledge.com.proxy-ub.rug.nl/full_record.do?product=UA&search_mode=GeneralSearch&qid=1&SID=T15EYVKBZuXIHfTAVsm&page=9&doc=87&cacheurlFromRightClick=no).
- Miller, K. & Fairbanks, R., 1983. Evidence for Oligocene-Middle Miocene abyssal circulation changes in the western North Atlantic. *Nature*, 306(5940), pp.250–253. Available at: <http://dx.doi.org/10.1038/306250a0>.
- Monk, J. et al., 2010. Habitat suitability for marine fishes using presence-only modelling and multibeam sonar. *Marine Ecology Progress Series*, 420, pp.157–174. Available at: <http://www.int-res.com/abstracts/meps/v420/p157-174/> [Accessed March 18, 2012].
- Moore, J., Clague, D. & Normark, W., 1982. Diverse basalt types from Loihi seamount, Hawaii. *Geology*, 10(2), p.88.
- Mortensen, P. et al., 2006. *Deep-Water Corals In Atlantic Canada: A Summary Of ESRF-Funded Research (2001-2003)*, Report No. 143. Calgary, AB: Environmental Studies Research Funds.
- Moscardelli, L. et al., 2013. Seismic geomorphological analysis and hydrocarbon potential of the Lower Cretaceous Cromer Knoll Group, Heidrun field, Norway. *AAPG Bulletin*, 97(8), pp.1227–1248.
- Mullineau, L. & Mills, S., 1997. A test of the larval retention hypothesis in seamount-generated flows. *Deep Sea Research Part I: Oceanographic Research Papers*, 44(5), pp.745–770. Available at: [http://dx.doi.org/10.1016/S0967-0637\(96\)00130-6](http://dx.doi.org/10.1016/S0967-0637(96)00130-6) [Accessed March 9, 2011].
- NAFO, 2015. *NAFO Conservation and Enforcement Measures 2015*, Dartmouth, Nova Scotia,

- Canada B2Y 3Y9 Tel.: (902) 468-5590. Available at: [www.nafo.int](http://www.nafo.int).
- NAFO SCS, 2008. *Report of the NAFO Scientific Council Working Group on Ecosystem Approach to Fisheries Management (WGEAFM)*, Dartmouth, Canada.
- Neves, B., Du Preez, C. & Edinger, E., 2014. Mapping coral and sponge habitats on a shelf-depth environment using multibeam sonar and ROV video observations: Learmonth Bank, northern British Columbia, Canada. *Deep-Sea Research Part II: Topical Studies in Oceanography*, 99, pp.169–183. Available at: <http://dx.doi.org/10.1016/j.dsr2.2013.05.026>.
- O'Hara, T. et al., 2008. Cold-water coral habitats on seamounts: do they have a specialist fauna? *Global Ecology and Biogeography*, 14(6), pp.925–934. Available at: <http://blackwell-synergy.com/doi/abs/10.1111/j.1472-4642.2008.00495.x> [Accessed August 20, 2010].
- Paduan, J., Clague, D. & Davis, A., 2007. Erratic continental rocks on volcanic seamounts off the US west coast. *Marine Geology*, 246(1), pp.1–8.
- Parson, L. et al., 1984. Remnants of a submerged pre-Jurassic ( Devonian?) landscape on Orphan Knoll , offshore eastern Canada. *Canadian Journal of Earth Sciences*, 21(1), pp.61–66.
- Pautot, G., Auzende, J.-M. & Le Pichon, X., 1970. Continuous Deep Sea Salt Layer along North Atlantic Margins related to Early Phase of Rifting. *Nature*, 227(5256), pp.351–354. Available at: <http://dx.doi.org/10.1038/227351a0>.
- Pe-Piper, G. et al., 2013. Petrology and tectonic significance of seamounts within transitional crust east of Orphan Knoll, offshore eastern Canada. *Geo-Marine Letters*, 33(6), pp.433–447. Available at: <http://dx.doi.org/10.1007/s00367-013-0342-2>.
- Pettit, R., 2011. Culturability and Secondary Metabolite Diversity of Extreme Microbes: Expanding Contribution of Deep Sea and Deep-Sea Vent Microbes to Natural Product Discovery. *Marine Biotechnology*, 13(1), pp.1–11. Available at: <http://dx.doi.org/10.1007/s10126-010-9294-y>.
- Piper, D., 2005. *Hudson 2004-024 Cruise Report: Geohazards on the continental margin off Newfoundland*, Dartmouth, NS.
- Pitcher, C. et al., 2016. *Implications of current spatial management measures for AFMA ERAs for habitats - FRDC Project No 2014/204*, Brisbane.
- Pitcher, R. et al., 2012. Exploring the role of environmental variables in shaping patterns of seabed biodiversity composition in regional-scale ecosystems. *Journal of Applied Ecology*, 49(3), pp.670–679. Available at: <http://dx.doi.org/10.1111/j.1365-2664.2012.02148.x>.
- Pitcher, R., Ellis, N. & Smith, S., 2011. *Example analysis of biodiversity survey data with R package gradientForest*, Available at: <http://gradientforest.r-forge.r-project.org/biodiversity-survey.pdf>.
- Pohlman, J. et al., 2009. Methane sources in gas hydrate-bearing cold seeps: Evidence from radiocarbon and stable isotopes. *Marine Chemistry*, 115(1–2), pp.102–109. Available at: <http://linkinghub.elsevier.com/retrieve/pii/S0304420309000966> [Accessed November 19, 2010].
- Poirier, A. et al., 2011. Osmium isotopes in manganese nodules from the Labrador Sea. *Goldschmidt*, p.1. Available at: [www.minersoc.org](http://www.minersoc.org).

- Quilty, P., 1997. Eocene and younger biostratigraphy and lithofacies of the Cascade Seamount, East Tasman Plateau, southwest Pacific Ocean. *Australian Journal of Earth Sciences*, 44(5), pp.655–665.
- Reidenbach, M. et al., 2006. Boundary layer turbulence and flow structure over a fringing coral reef. *Limnology and Oceanography*, 51(5), pp.1956–1968. Available at: [http://www.aslo.org/lo/toc/vol\\_51/issue\\_5/1956.html](http://www.aslo.org/lo/toc/vol_51/issue_5/1956.html).
- Richer-de-Forges, B., Koslow, A. & Poore, G., 2000. Diversity and endemism of the benthic seamount fauna in the southwest Pacific. *Nature*, 405(6789), pp.944–947. Available at: <http://dx.doi.org/10.1038/35016066>.
- Roark, B. et al., 2009. Extreme longevity in proteinaceous deep-sea corals. *Proceedings of the National Academy of Sciences*, 106(13), pp.5204–5208. Available at: <http://www.pnas.org/content/106/13/5204.abstract>.
- Roberts, C., 2002. Deep impact: the rising toll of fishing in the deep sea. *Trends in Ecology & Evolution*, 17(5), pp.242–245. Available at: <http://www.sciencedirect.com/science/article/pii/S0169534702024928>.
- Roberts, M. et al., 2003. The cold-water coral *Lophelia pertusa* (Scleractinia) and enigmatic seabed mounds along the north-east Atlantic margin: are they related? *Marine Pollution Bulletin*, 46(1), pp.7–20. Available at: <http://www.sciencedirect.com/science/article/pii/S0025326X0200259X>.
- Roberts, M., Wheeler, A. & Freiwald, A., 2006. Reefs of the deep: the biology and geology of cold-water coral ecosystems. *Science*, 312(5773), pp.543–547. Available at: <http://www.ncbi.nlm.nih.gov/pubmed/16645087>.
- Roberts, S. & Nunn, J., 1995. Episodic fluid expulsion from geopressured sediments. *Marine and Petroleum Geology*, 12(2), pp.195–204. Available at: <http://www.sciencedirect.com/science/article/pii/0264817295928390>.
- Rodríguez-Martínez, M., 2011. Mud Mounds. In J. Reitner & V. Thiel, eds. *Encyclopedia of Geobiology*. Encyclopedia of Earth Sciences Series. Springer Netherlands, pp. 667–675. Available at: [http://dx.doi.org/10.1007/978-1-4020-9212-1\\_153](http://dx.doi.org/10.1007/978-1-4020-9212-1_153).
- Ruffman, A., 1989. First report of Ordovician (Caradoc-Ashgill) palynomorphs from Orphan Knoll, Labrador Sea: Discussion. *Canadian Journal of Earth Sciences*, 26(12), pp.2749–2751. Available at: [http://www.nrc.ca/cgi-bin/cisti/journals/rp/rp2\\_abst\\_e?cjes\\_e89-239\\_26\\_ns\\_nf\\_cjes26-89](http://www.nrc.ca/cgi-bin/cisti/journals/rp/rp2_abst_e?cjes_e89-239_26_ns_nf_cjes26-89).
- Ruffman, A., 2011. Orphan Knoll as a Window on the Palaeozoic : Seemingly ignored by the petroleum industry for 40 years. In *Recovery - CSPG CSEG CWLS Convention*. pp. 1–5.
- Ruffman, A. & van Hinte, J., 1973. Orphan Knoll—a“ chip” off the North American" plate. In *Earth Science Symposium on Offshore Eastern Canada*. Dartmouth, NS: Geological Survey of Canada (Atlantic), pp. 23–71.
- Rüggeberg, A. et al., 2005. Sedimentary patterns in the vicinity of a carbonate mound in the Hovland Mound Province, northern Porcupine Seabight. In A. Freiwald & J. M. Roberts, eds. Erlangen Earth Conference Series. Springer Berlin Heidelberg, pp. 87–112. Available at: [http://dx.doi.org/10.1007/3-540-27673-4\\_5](http://dx.doi.org/10.1007/3-540-27673-4_5).

- Santos, R.-S. et al., 2009. Toward the conservation and management of Sedlo Seamount: A case study. *Deep Sea Research Part II: Topical Studies in Oceanography*, 56(25), pp.2720–2730. Available at: <http://linkinghub.elsevier.com/retrieve/pii/S0967064508004578>.
- Shaw, J. et al., 2006. A conceptual model of the deglaciation of Atlantic Canada. *Quaternary Science Reviews*, 25(17–18), pp.2059–2081. Available at: <http://linkinghub.elsevier.com/retrieve/pii/S0277379106001326> [Accessed July 5, 2010].
- Sherwood, O. & Edinger, E., 2009. Ages and growth rates of some deep-sea gorgonian and antipatharian corals of Newfoundland and Labrador. *Canadian Journal of Fisheries Aquatic Science*, 66(1), pp.142–152. Available at: <http://dx.doi.org/10.1139/F08-195>.
- Shester, G. & Ayers, J., 2005. A cost effective approach to protecting deep-sea coral and sponge ecosystems with an application to Alaska's Aleutian Islands region. In A. Freiwald & J. M. Roberts, eds. Erlangen Earth Conference Series. Springer Berlin Heidelberg, pp. 1151–1169. Available at: [http://dx.doi.org/10.1007/3-540-27673-4\\_59](http://dx.doi.org/10.1007/3-540-27673-4_59).
- Sibuet, J.-C., 1992. New constraints on the formation of the non-volcanic continental Galicia-Flemish Cap conjugate margins. *The Geological Society*, 149(5), pp.829–840. Available at: <http://jgs.lyellcollection.org/cgi/content/abstract/149/5/829>.
- Smee, J. et al., 2003. Orphan Basin , Offshore Newfoundland : New seismic data and hydrocarbon plays for a dormant Frontier Basin. In *Offshore Technology Conference*.
- Smith, J. et al., 1997. Rapid climate change in the North Atlantic during the Younger Dryas recorded by deep-sea corals. *Nature*, 386, pp.818–820. Available at: <http://www.nature.com/nature/journal/v386/n6627/abs/386818a0.html>.
- Srivastava, S. et al., 2000. Magnetic evidence for slow seafloor spreading during the formation of the Newfoundland and Iberian margins. *Earth and Planetary Science Letters*, 182(1), pp.61–76. Available at: <http://www.sciencedirect.com/science/article/pii/S0012821X00002314>.
- Stein, M., 2007. Oceanography of the Flemish Cap and Adjacent Waters. *Journal of Northwest Atlantic Fisheries Science*, 37(February), pp.135–146. Available at: <http://journal.nafo.int/37/stein/12-stein.pdf> [Accessed February 18, 2011].
- Tankard, A. & Balkwill, H., 1989. Extensional tectonics and stratigraphy of the North Atlantic margins. In *Extensional Tectonics and Stratigraphy of the North Atlantic Margins*. Calgary, AB: American Association of Petroleum Geologists, pp. 1–6.
- Thomson, R. et al., 2014. Congruence in demersal fish, macroinvertebrate, and macroalgal community turnover on shallow temperate reefs. *Ecological Applications*, 24(2), pp.287–299. Available at: <http://doi.wiley.com/10.1890/12-1549.1> [Accessed January 9, 2017].
- Thornburg, C., Zabriskie, M. & McPhail, K., 2010. Deep-Sea Hydrothermal Vents: Potential Hot Spots for Natural Products Discovery? *J. Nat. Prod.*, 73(3), pp.489–499. Available at: <http://dx.doi.org/10.1021/np900662k>.
- Toews, M. & Piper, D., 2002. *Recurrence interval of seismically triggered mass-transport deposition at Orphan Knoll , continental margin off Newfoundland and Labrador*, Dartmouth, NS.

- Tucholke, B., Sawyer, D. & Sibuet, J.-C., 2007. Breakup of the Newfoundland–Iberia rift. *Geological Society, London, Special Publications*, 282(1), pp.9–46. Available at: <http://sp.lyellcollection.org/content/282/1/9.abstract>.
- Via, R. & Thomas, D., 2006. Evolution of Atlantic thermohaline circulation: Early Oligocene onset of deep-water production in the North Atlantic. *Geology*, 34(6), pp.441–444. Available at: <http://geology.gsapubs.org/cgi/content/abstract/34/6/441>.
- Waller, R. et al., 2007. Anthropogenic impacts on the Corner Rise seamounts, north-west Atlantic Ocean. *Journal of the Marine Biological Association of the United Kingdom*, 87(5), pp.1075–1076. Available at: [http://www.journals.cambridge.org/abstract\\_S0025315407057785](http://www.journals.cambridge.org/abstract_S0025315407057785) [Accessed February 18, 2011].
- Wareham, V. & Edinger, E., 2007. Distribution of deep-sea corals in the Newfoundland and Labrador region, Northwest Atlantic Ocean. In R. Y. George & S. D. Cairns, eds. *Conservation and adaptive management of seamount and deep-sea coral ecosystems*. Miami: Rosentiel School of Marine and Atmosphere Science, University of Miami, pp. 289–313.
- Watanabe, S. et al., 2009. Patterns in abundance and size of two deep-water gorgonian octocorals, in relation to depth and substrate features off Nova Scotia. *Deep Sea Research Part I: Oceanographic Research Papers*, 56(12), pp.2235–2248. Available at: <http://linkinghub.elsevier.com/retrieve/pii/S0967063709001769> [Accessed February 18, 2011].
- Welford, K. et al., 2010. Structure across the northeastern margin of Flemish Cap, offshore Newfoundland from Erable multichannel seismic reflection profiles: evidence for a transtensional rifting environment. *Geophysical Journal International*, 183(2), pp.572–586. Available at: <http://dx.doi.org/10.1111/j.1365-246X.2010.04779.x>.
- Wendt, J. et al., 1997. The world's most spectacular carbonate mud mounds (Middle Devonian, Algerian Sahara). *Journal of Sedimentary Research*, 67(Section A and B), pp.424–436.
- Wielens, H., MacRae, A. & Shimeld, J., 2002. Geochemistry and sequence stratigraphy of regional Upper Cretaceous limestone units, offshore eastern Canada. *Organic Geochemistry*, 33(12), pp.1559–1569. Available at: <http://www.sciencedirect.com/science/article/pii/S0146638002001031>.
- Wilson, M. et al., 2007. Multiscale Terrain Analysis of Multibeam Bathymetry Data for Habitat Mapping on the Continental Slope. *Marine Geodesy*, 30(1), pp.3–35. Available at: <http://www.informaworld.com/openurl?genre=article&doi=10.1080/01490410701295962&magic=crossref%7C%7CD404A21C5BB053405B1A640AFFD44AE3>.
- Workum, R., Bolton, T. & Barnes, C., 2011. Ordovician geology of Akpatok Island, Ungava Bay, District of Franklin. *Can. J. Earth Sci.*, 13(1), pp.157–178. Available at: <http://dx.doi.org/10.1139/e76-015>.
- Wright, D. & Goodchild, M., 1997. Data from the deep: implications for the GIS community. *International Journal of Geographical Information Science*, 11(6), pp.523–528. Available at: <http://www.ingentaconnect.com/content/tandf/tgis/1997/00000011/00000006/art00001>.

- Xu, Y., Eyles, N. & Simpson, M.J., 2009. Terrigenous organic matter sources in mid-pleistocene sediments from the orphan knoll, Northwest Atlantic Ocean. *Applied Geochemistry*, 24(10), pp.1934–1940. Available at: <http://www.sciencedirect.com/science/article/B6VDG-4WV77VG-1/2/7e4c6095d4f3c7f42008062fbd5e9664>.
- Yasuhara, M. et al., 2008. Abrupt climate change and collapse of deep-sea ecosystems. *Proceedings of the National Academy of Sciences*, 105, pp.1556–1560.
- Yesson, C. et al., 2011. The global distribution of seamounts based on 30 arc seconds bathymetry data. *Deep Sea Research Part I: Oceanographic Research Papers*, 58(4), pp.442–453. Available at: <http://www.sciencedirect.com/science/article/pii/S0967063711000392>.

## **4 Environmental Drivers of Community Composition, Abundance and Distribution of Deep-Sea Megafauna from the Orphan Knoll and Orphan Seamount**

Meredyk, S., Edinger, E., Piper, D.J.W.

1. *Eventually to be submitted to the journals Deep Research I and / or Community Ecology*

### **Abstract**

Deep-sea megafaunal ecosystems are hotspots of biodiversity and are relatively unexplored due to the high costs of vessel assisted oceanographic research. Therefore, efficient and effective time and sampling strategies are essential while at sea. This study used the remotely operated vehicle ROPOS to collect deep-sea megafaunal species occurrence data, oceanographic data, multibeam data and surficial geological samples which were used to examine variable gradients driving deep-sea megafaunal distribution and community turnover. gradientForest, a relatively novel non-parametric model, was used to examine the gradients of multiple variables in an effort to better understand which predicting variables are most important to identify benthic megafauna presence, distribution and community ecology. Bathymetric variables depth, slope, aspect and water density were identified as being the most important drivers of megafaunal community composition for the Orphan Knoll and Orphan Seamount.

## 4.1 Introduction

The deep sea is the largest biome on earth, representing the largest reservoir of biomass on the planet and contains large proportions of undiscovered biodiversity and unknown species (Danovaro et al. 2008). The deep sea is a marine resource that has only been one millionth biologically explored (Roberts 2002). Areas of the deep-sea are not only biodiverse but contain several economically important oil, gas and minerals reserves (Colman et al. 2005; Bluhm et al. 2010; Jauer & Budkewitsch 2010; Cronan et al. 2010), benthic fisheries (Roberts 2002), and have also produced various bioactive molecules for commercial sale (Thornburg et al. 2010; Pettit 2011). Through advances in marine technology, the deep-sea is continually becoming more accessible to deep-sea exploration (Colman et al. 2005; Bluhm et al. 2010) and natural resources exploitation (Roberts 2002; Danovaro et al. 2008; Althaus et al. 2009).

The majority of the global oceans are a 'commons' resource that falls under varying levels of national and international conservation, preservation and management of benthic ecosystems and habitat (Lodge 2004; Margles et al. 2010). Therefore, it is becoming a conservation and preservation priority on a global scale (Gianni et al. 2011).

Predictive habitat and species models are not new methods in the realm of ecological modelling and conservation processes (Austin 2002; Ferrier et al. 2007; Monk et al. 2010). But these models have traditionally examined individual variables through univariate and/or multivariate statistics and not necessarily the gradient of the predicting variables, which could provide information on changes in community turnover (Ferrier et al. 2007; Leaper et al. 2011). Examining the multiple variables and how they change

along their gradient can provide another layer of insight in deep sea benthic megafaunal community analysis (Leaper et al. 2011; Pitcher et al. 2012; Ellis et al. 2012).

The deep sea ecosystems and habitats have been subjects of study with the purpose of describing the dynamics of deep sea megafauna and their environment mainly with the intent of understanding more about the needs and restrictions of megafaunal species in the deep-sea (Metaxas & Bryan 2007; Gilkinson & Edinger 2009; Buhl-Mortensen et al. 2010; Brown et al. 2011). But, before these deep-sea habitats and associated species are to be protected they need to be identified, delineated and examined for drivers of community ecology (Leverette & Metaxas 2004; Bryan & Metaxas 2007; Wilson et al. 2007; NAFO SCS 2008; Davies et al. 2008; Costello 2009; Durán Muñoz & Sayago-Gil 2011; Leaper et al. 2011).

The benthic ecology of deep-sea environments has been described as being a function of habitat suitability, influenced by surrounding geological and environmental factors (Bryan & Metaxas 2006). General habitat characteristics (oceanographic, geological) have been described and associated for a select few families of deep-sea coral, such as, hard substrates foster hard coral colonization and soft sediments are areas of sponge and soft coral abundance; but, these previous studies were able to glean patterns at a large scale (Roberts et al. 2003; Bryan & Metaxas 2006; Wareham & Edinger 2007; Gilkinson & Edinger 2009; Davies & Guinotte 2011). Understanding the weighted importance of which variables have the most effect on benthic ecology concerning coral and sponge distribution on a fine scale was the primary objective in this study.

Habitat distribution modeling (HDM) and species distribution modeling (SDM) are relatively new (1990) (Ellis et al. 2012) processes that have become essential tools in biodiversity conservation planning and management efforts (Ellis et al. 2012). HDMs and SDMs are numerical modeling tools that combine occurrence or abundance of sampled species data with environmental variable estimates. The ability to understand the drivers of community turnover, distribution and abundance of deep-sea megafauna within unexplored portions of the deep-sea can potentially save these unknown ecosystems from being destroyed. Habitat and species distribution models also have the potential to save time and money in conservation planning and ecosystem management decisions.

The purpose of this study was to identify the distribution and abundance of the megafauna of Orphan Knoll and Orphan Seamount and to examine the effects of bathymetry, oceanography and geology on deep-sea community turnover.

#### 4.1.1 Study Area

##### ***4.1.1.1 Orphan Knoll***

In international waters, 550 km East of St. John's, NL, Canada, a rifted fragment of continental crust, the Orphan Knoll (OK) measures 190 km long (NW-SE), 90 Km wide (SW-NE) with a depth range between ~1500 m to ~ 4000 m (Fig.4-1).

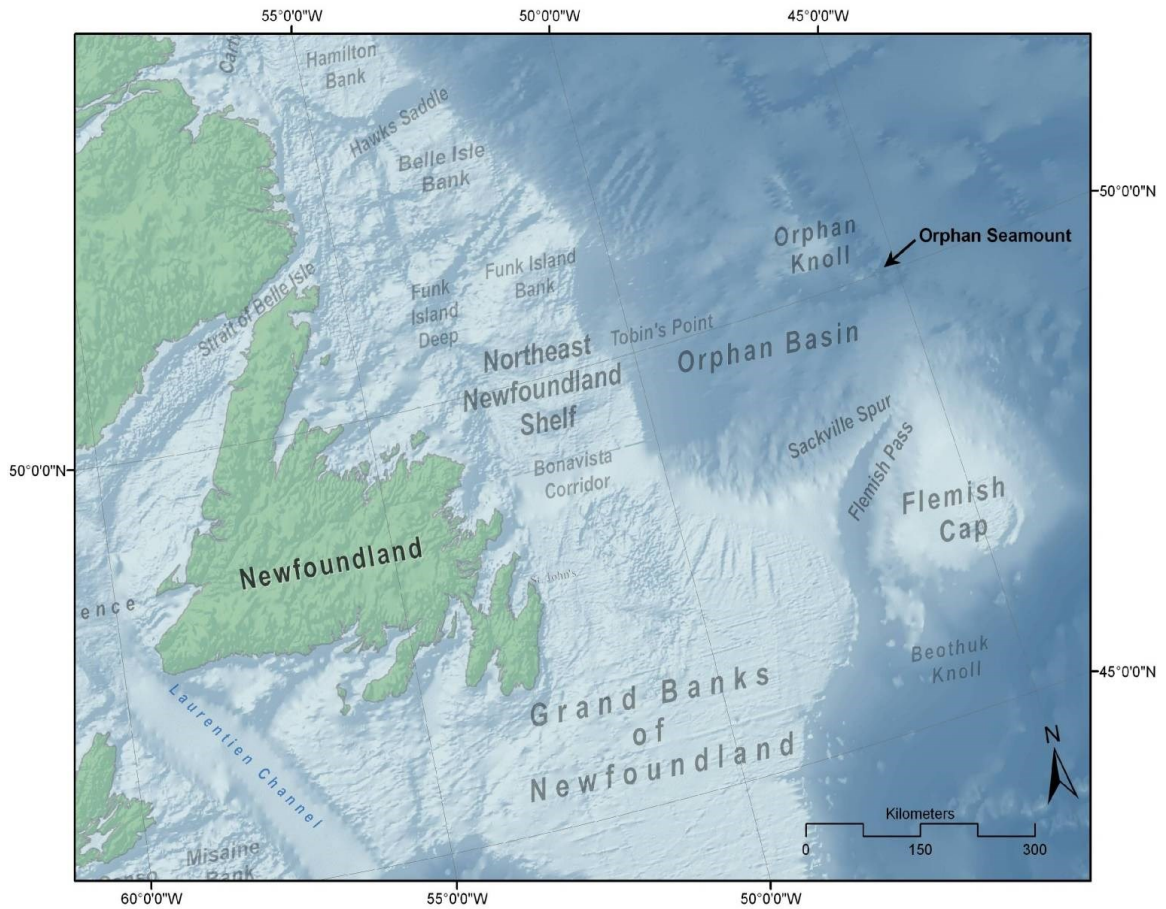


Figure 4-1. Orphan Knoll and Orphan Seamount locations relative to Newfoundland, Canada

#### 4.1.1.2 Orphan Seamount

The Orphan Seamount OS is submarine volcano located 9 Km NE of the SE portion of Orphan Knoll and is 14 Km wide at its base with a depth range between 1879 m to 3900 m (Fig. 4-1). Seamounts are hotspots of biodiversity (O'Hara et al. 2008) and the possibility of discovering unique or rare species of coral and sponge on OS was expected.

### ***4.1.1.3 Oceanographic Characteristics of Orphan Knoll and Orphan Seamount***

The flow of surface and bottom currents in and around the Orphan Knoll (OK) varies by depth and relative proximity to the Knoll's cap. The top of OK showed little movement of oceanographic CTD drifters (ARGO floats) in a recent study by Blair Greenan (Pers. Comms; DFO, 2010)(Fig. 4-2); however, the water does circulate in an anti-cyclonic motion, otherwise known as a Taylor Column. Greenan's water current data identifies swifter currents (mean  $0.085 \text{ m}\cdot\text{s}^{-1}$ , std.  $0.047 \text{ m}\cdot\text{s}^{-1}$ , max  $0.32 \text{ m}\cdot\text{s}^{-1}$ ) along the eastern side of Orphan Knoll (Greenan et al. 2010), which is also where the enigmatic OK mounds are found (Fig. 4-2) . The increased current speed, higher elevation (relative to the deepest part of the knoll) and exposed hard substrate identified on the eastern side / slope of Orphan Knoll make for potentially favorable habitats for coral and sponge megafauna.

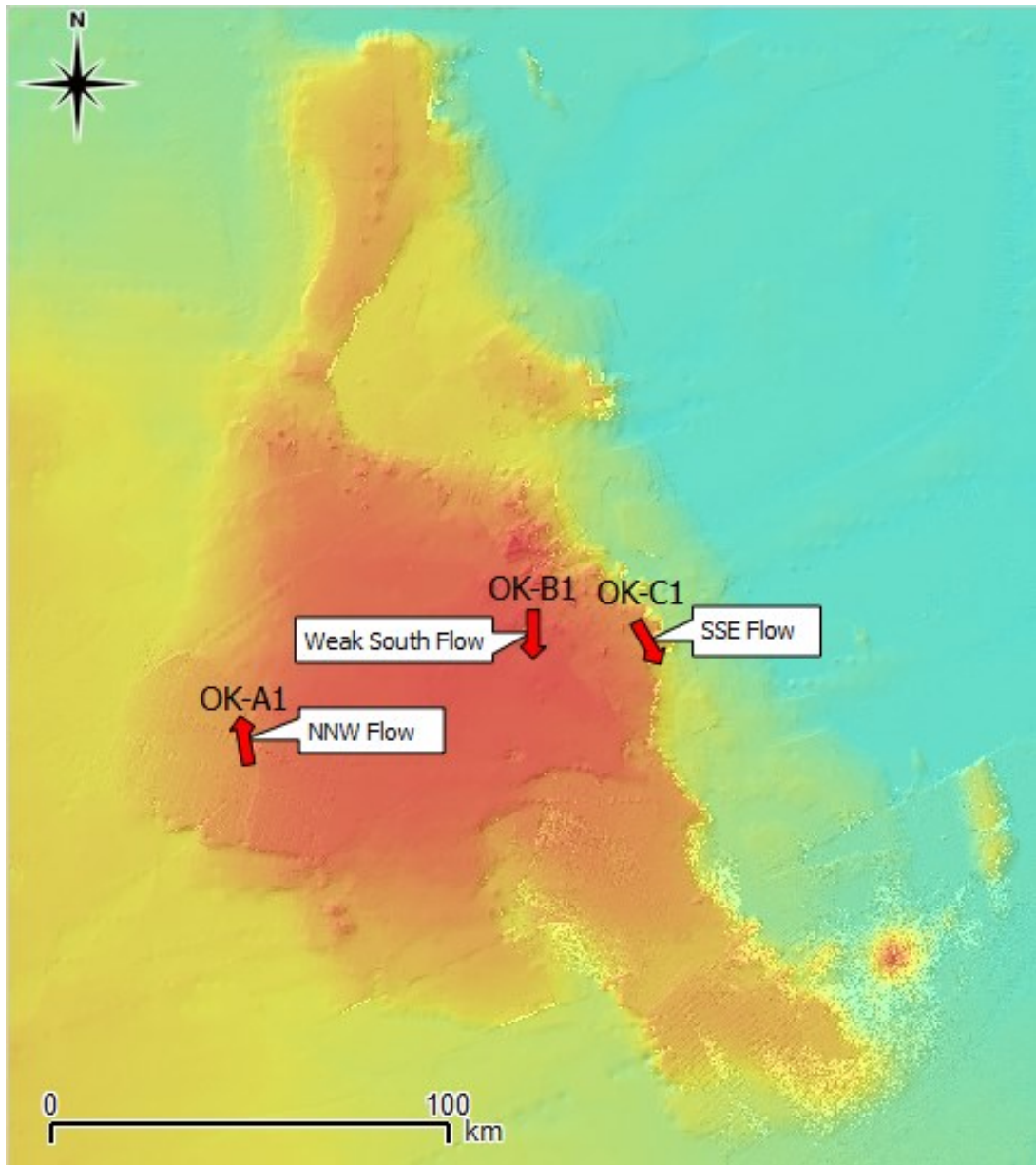


Figure 4-2. Patterns of benthic current flow above Orphan Knoll. Arrows indicate direction of flow (Greenan et al. 2010).

#### **4.1.1.4     *Anthropogenic Activities on Orphan Knoll and Orphan Seamount***

The Orphan Knoll (OK) and Orphan Seamount (OS) are not commercially fished at this present time due to the deep depth (1532m minimum depth), high potential for gear loss (ice-rafted debris (IRD) and pinnacle mounds) and international conservation efforts.

#### **4.1.1.5     *Conservation- Preservation Measures for Orphan Knoll***

Orphan Knoll was designated a protected vulnerable marine ecosystem (VME) area and given interim protection from 2007 - 2020 by the international Northwest Atlantic Fisheries Organization (NAFO) (NAFO 2015). It was protected for its high potential for unique corals and sponges and associated megafauna found within the Convention on International Trade in Endangered Species (CITES) Appendix II list; while possibly being part of network of genetically connected coral and sponge species with the Flemish Cap and Sackville Spur areas (NAFO SCS 2008).

#### **4.1.1.6     *Deep Sea Habitats***

Some stony coral colonies (e.g. *Lophelia pertusa*) can form complex reef-like structures, which provide habitat for a variety of associated megafauna (Roberts et al. 2006; Althaus et al. 2009). Reefs, seamounts and steep bathymetry have been found to be hotspots of biodiversity (Hall-spencer et al. 2007; Levin et al. 2009; Buhl-Mortensen et

al. 2010) and are worth discovering and protecting these unique habitats (Waller et al. 2007; Hall-spencer et al. 2007; Santos et al. 2009; Althaus et al. 2009).

#### 4.1.2 Study Summary

This study used the Canadian Remotely-Operated Vehicle (ROV) ROPOS to collect distribution data (video) of coral and sponge and other megafaunal species on the OK and OS. The video observations were accompanied by biological species collection of never-before observed species. The datasets were collated and raster point-sampling techniques extracted joined datasets that were then used to investigate bathymetric, oceanographic and geological gradient drivers within and across a variety of benthic invertebrate communities / habitats (i.e. flats, slopes and mounds at various depths) using the gradientForest algorithm in R, thereby examining which variables and at which point along gradients of these variables (oceanographic, geologic and bathymetric) are the most accurate in describing changes in distribution and community composition of deep-sea benthic megafauna.

## 4.2 Methods

The field collection methods used in this chapter are the same as presented in chapter 2. For a detailed description of the various methods and datasets used in this study, please refer to section 2.2. In addition to the methods detailed in chapter 2, additional datasets were used in the data analysis of this chapter and are presented below.

### 4.2.1 ROV Oceanographic Data Collection

A Seabird 19<sup>plus</sup> v2 unit measured conductivity, temperature and density (CTD) and was mounted on ROPOS. The ROPOS mounted Seabird unit recorded data for the entirety of each dive. The ASCII data was extracted using Seabird's SBE Data Processing software. The file was then imported into MS Access<sup>®</sup> to be combined with the existing geological and biological data that was collected through the CAM program. The time on the Seabird unit was not accurately set before being deployed and a linking JDayGMT field could not be created to link the CTD data to the CAM data tables; therefore, the Seabird depth measurements needed to be rounded to 10 cm intervals. The CAM depth data received from the ROPOS navigation table were then linked to the 10 cm interval Seabird depths. To prevent multiple instances of similar depths for any one JDayGMT time period, a 10 second moving average was used.

Due to the nature of ROV operations (use of 6-8 high-torque propellers) and the need for high-powered lights, cameras, etc. slight changes (Max.  $\pm 0.30$  °C) in temperature were observed within the CTD plots during the dives due to water mixing from the propellers and the heat of the equipment. A 200-second moving average could

have been applied to ‘smooth’ the temperature and salinity data; however, this was not used due to the potential risk of over-generalizing the temperature and salinity data during the dives.

#### 4.2.2 Benthic Terrain Characterization

Four Benthic Position Index (BPI) raster layers (standardized broad scale (500m res.) bathymetry, standardized finer scale (300m res.) bathymetry, finer scale structures (potential micro-habitats), broad scale zones (potential macro-habitats) (Appendix 4-1)) and a rugosity raster layer were created using ArcGIS® and NOAA’s Benthic Terrain Modeler plug-in, based-on a 3x3 cell grid neighbourhood analysis function using an annulus shape (BTM 2005). The BTM algorithms were applied to three separate bathymetric data sources of different two different spatial resolutions (Healy multibeam (year 2000: 100m res.), Kommander Jack multibeam (year 2007: 100m res.) and ROPOS ImogeneX multibeam (year 2010: 0.25m res.).

### 4.2.3 Dataset Integration / Database Management

See chapter 2 sections 2.1.11 for a general description of the various data and how it was collected for this study. However, this chapter incorporates more oceanographic and biological datasets into the database and Appendix 4-4 outlines the complete process of integrating the various datasets and the process of extracting data from MS Access ® and importing it into ArcGIS® and gradientForest.

### 4.2.4 Species Distribution

Megafaunal species' distribution and abundance were plotted in maps created by GIS. Maps delineate the various abundance and geological data identifying the spatial distribution of the various megafaunal species with relation to the surficial geology.

As noted in chapter 2 section 2.1.9, the maps generated using the various bathymetric layers were labeled within the inset legend of the map. The depths of the bathymetric layer are for the entire layer and not exclusively the visible layer. The bathymetric depths did not significantly vary in accuracy between the vessel and ROV mounted systems.

### 4.2.5 Community Analysis

Generalized dissimilarity modeling (GDM) has been used to study ecological community turnover and recent studies identify that GDM and gradientforst (gF) are similar in their community analysis capabilities, with gF being more 'biologically

informed' than GDM (Leaper et al. 2011). The gF technique allows for predictions of biodiversity through identification of influential changes in surficial and environmental drivers, relative to changes in species abundance and distribution (Pitcher et al. 2012; Ellis et al. 2012; Beazley et al. 2015).

The gradientForest package, in the statistical software R, was used to visually determine the most important environmental variable along their gradients, which identify thresholds within community composition. gradientForest is a non-parametric tree-based method based on random and extended forest models, which fits an ensemble of bootstrapped regression tree models between individual species abundance and environmental drivers (Pitcher et al. 2016). However, gradientForest incorporates whole assemblages instead of only single species, which allows the simultaneous modeling of multiple taxa and environmental covariates ('drivers').

The gradientForest package determines the compositional turnover based on a 50% weight and 50% turnover threshold ('splits') of each predicting (environmental) variable along its gradient, relative to each individual species. The overall importance of predictors is derived from computational permutation of the out-of-bag sample (OOB), where the OOB sample refers to the observations that were not selected in the bootstrap (in-bag) sample for a given tree, where using a 'forest' of 500 classification trees provides a cross-validated estimate of the expected variance of the residuals for new observations. This variance is compared with the variance of the observations to create a measure of biodiversity (Ellis et al. 2012).

## **Community Analysis Plotting**

Four plots were generated with the gradientForest results. Plot one shows the overall importance of the predicting variables using the mean accuracy importance and the mean importance by species  $R^2$ . Plot two shows the splits density plot, which indicate important changes in the abundance of several species along a variables' gradient (composition change). The third plot is the species cumulative plot, which show cumulative change in abundance of individual species along the variables' gradient. Plot 3 identifies in the legend of each variable plot, the top 5 most responsive species for each variable. Plot 4 is the predictor cumulative plot, which shows cumulative change in overall composition of the community along a variables' gradient. Plot 4 as in plot 3, plots the 5 most responsive species for each variable.

## **gradientForest Predictions**

The data collected for this study was all spatially referenced and as such, able to be used to transform environmental drivers to a scale of biological importance. This transformation involved converting multi-dimensional environmental data to a geo-referenced position, associating community composition with the predicting environmental variables. The conversion was analogous to ordination, but with the added benefit of using the non-parametric nature of the data along the variables' gradients (Pitcher et al. 2011; Thomson et al. 2014).

The predictors were first transformed and gridded (spatial relevance by dive sites) along with all of the predicting environmental variables. Then to capture the majority of variation amongst all the environmental gradients, reducing the dimensions of

environmental variables by principal component analysis (PCA) was applied using CLARA (clustering large applications R algorithm), which is based on the PAM (partitioning around medoids) algorithm (Pitcher et al. 2011). Based on the four megafauna groups recorded during the sampling dives (i.e. coral, sponge, other inverts, faunal concentrations) and in an effort to capture all the possible clusters throughout the various survey sites (large spatial area over variable terrain and depths), eight clusters was conservatively chosen. Other methods to determine the number of clusters could have been applied (e.g. multivariate regression trees), though due to time constraints, eight clusters were selected and plotted as such. With that being said, it was seen that no more than 4 clusters were actually needed in this study.

The first few dimensions capture most variation in composition patterns and thus, the higher dimensions were not plotted. The visualisation of the PCA results were also plotted as a biplot (fifth plot) using the first two dimensions and the most important predictors as vectors relative to the 8 colour coded clusters. Additionally, the biplot and clusters were visualised geographically to examine spatial compositional patterns (sixth and final community analysis plot). This geospatial PCA plot provides the ‘biological’ context to the gF analysis whereby, the weight mean location of species (blue rings) and the most responsive species could be manually selected (black crosses turn red when selected) (Pitcher et al. 2011).

R scripts created by (Pitcher et al. 2011) were modified for this community analysis and an example can be seen in Appendix 4-3.

## **4.3 Results**

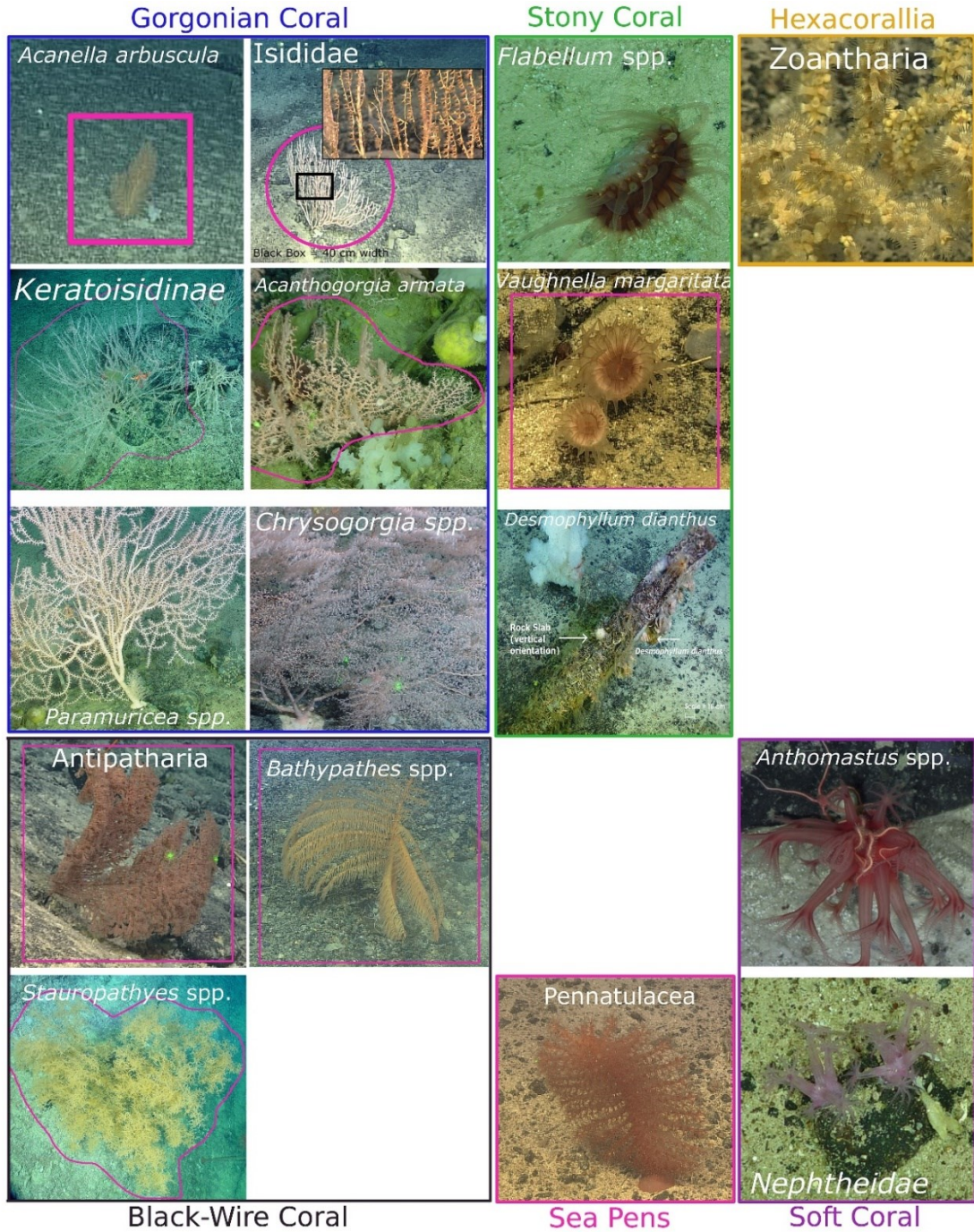
### **4.3.1 Distribution and Abundance of Deep-Sea Megafauna on Three Deep-Sea Habitat Types (Seamount, Mounds, Flats)**

#### **4.3.1.1 *Identified Megafauna***

The following three figures are organized into photo plates of coral, sponge and other invertebrates, identified during the exploration of OK and OS. A list of coral, sponge, other invertebrates and grouped concentrations of megafauna recorded during all six dives on the Orphan Knoll and Orphan Seamount (D1340) are documented in Appendices 4-4, 4-5, 4-6 and 4-7.

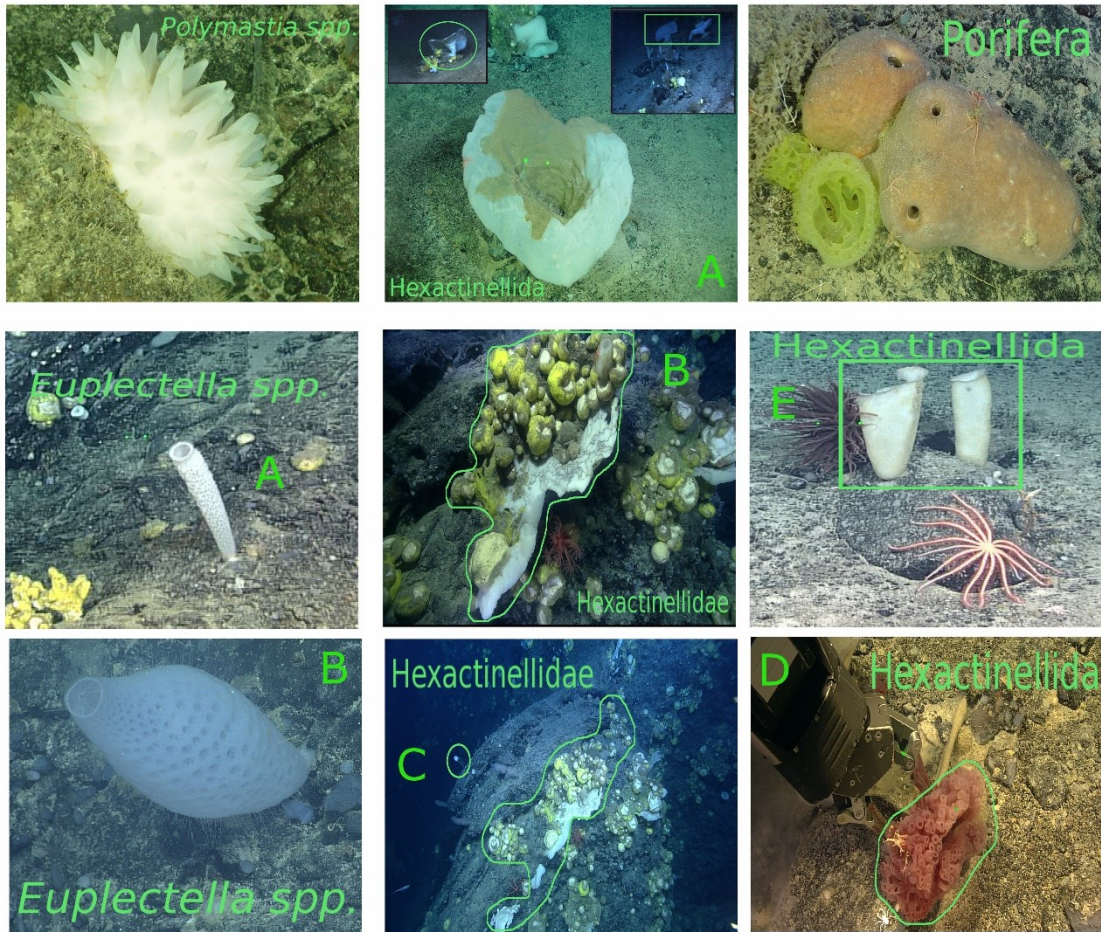
### 4.3.1.2 Coral Species Identified

Photo Plate 4-1. Coral fauna from Orphan Seamount and Orphan Knoll; Gorgonian corals (top left), Black-wire coral (bottom-left), Stony coral (green box), Sea Pen (pink box), Soft coral (bottom-right) and Hexacorallia (top-right).



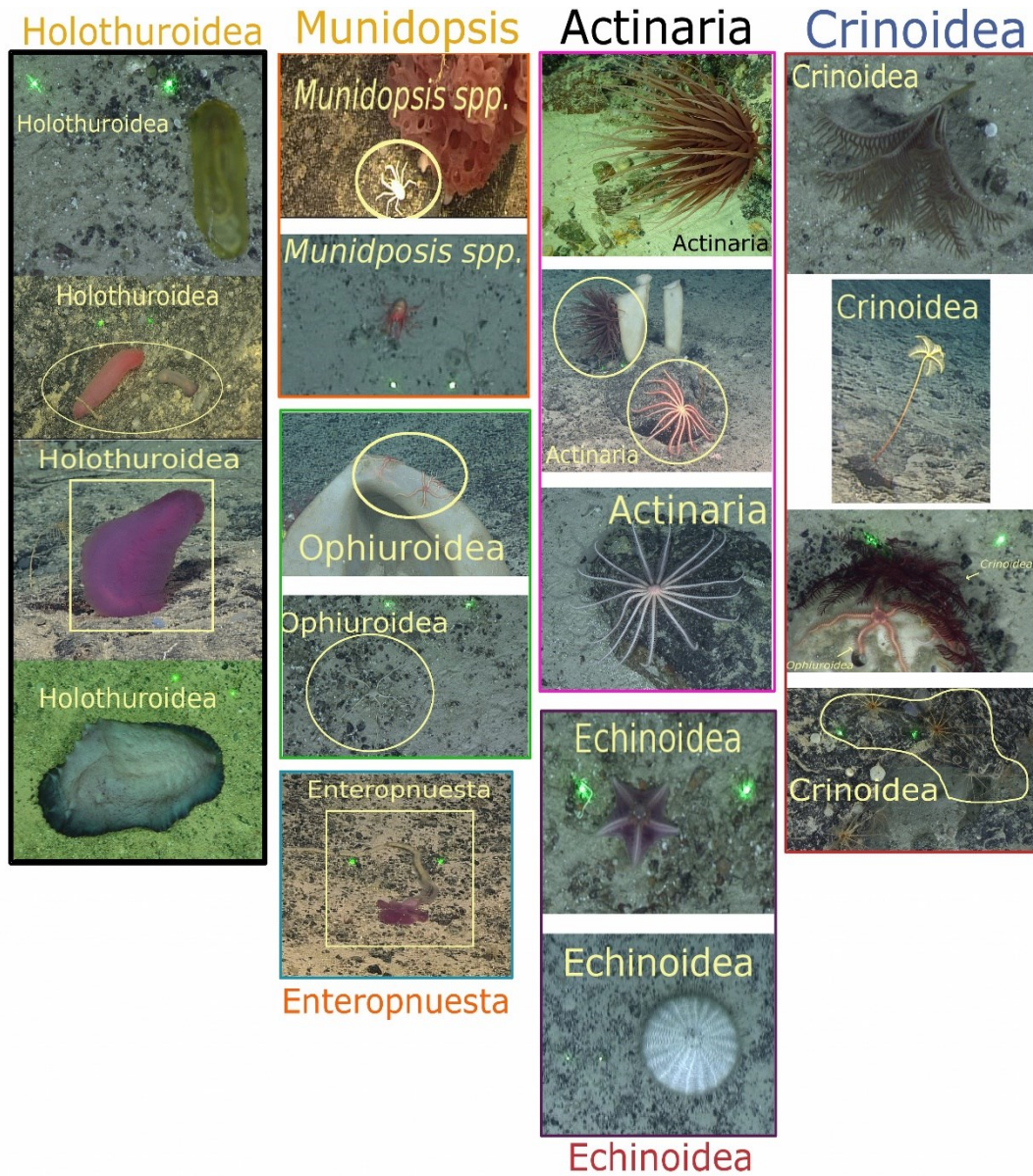
### 4.3.1.3 *Sponge Species Identified*

Photo Plate 4-2. *Sponge fauna from Orphan Seamount and Orphan Knoll; Polymastia spp (top left), Euplectella spp. (A and B), Hexactinellidae (Mid and right columns: A-E) except an unknown sponge (top right).*



### 4.3.1.4 *Non-Coral and Non-Sponge Species Identified*

Photo Plate 4-3. *Non-Coral and non-Sponge Megafaunal from Orphan Seamount and Orphan Knoll (green dots = 10cm scale); black box (Holothuroidea), red box (Munidopsis spp.), green box (Ophiuroidea), teal blue box (Enteropneusta), pink box (Actinaria), purple box (Echinoidea), magenta box (Crinoidea: stalked (top two images) and unstalked (bottom two images)).*



## 4.3.2 Habitat 1 - Orphan Seamount (D1340)

### 4.3.2.1 *Coral*

The distribution and abundance of 18 identifiable coral groups by Phylum, Family, Order, Genus or Species was collected from OS (Fig. 4-3b) (Appendix 4-4). From these identified coral groups the observed trends were: Sea pen distribution was limited to depths greater than 2700m (Fig. 4-3b) and not found on bedrock (Fig. 4-3a); A high abundance of *Isididae* (Family) (Fig. 4-3b) was found on bedrock on a 22° slope 110 m below the crest of OS (Fig. 4-3a); *Acathagorgia armata* was found on bedrock (Fig. 4-3b); *Zoantharia* (Order) was found throughout the dive but was found to be most abundant in the depth range between 2750 and 3000 m (Fig. 4-3b).

### 4.3.2.2 *Sponge*

*Polymastia* spp. was found between the crest of OS down to 2500 m (Fig. 4-3c) and was most abundant on bedrock and boulders (Fig. 4-3a). An absence of sponge was observed on the north side of a large bedrock outcrop between 2850 m and 2750 m (Fig. 4-3a and Fig. 4-3c). Euplectellidae (*glass sponge*) was not found below 2750 m (Fig. 4-3c) and was most abundant on bedrock and boulders (Fig. 4-3a) (Appendix 4-5).

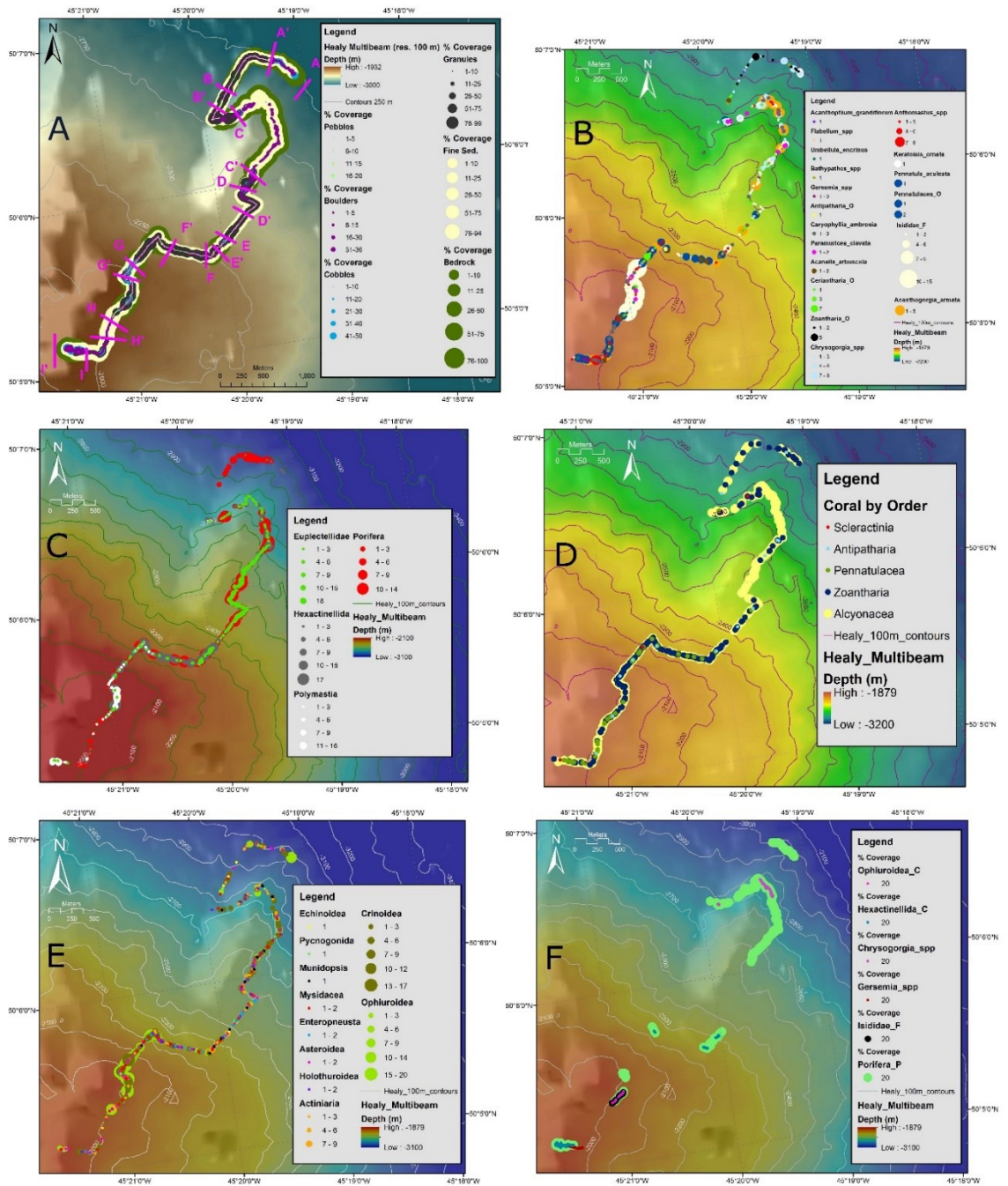


Figure 4-3. Orphan Seamount Surficial Geology and Megafauna Abundance and Distributions Maps (colour gradients in maps have been individually optimized for ease of viewing): Surficial Geology (A), Coral Species Distribution (B), Sponge Distribution (C), Coral Group Distribution by Taxonomic Order (D), Non-Coral or Sponge Invertebrates Distribution (E), Concentrations (>20% surficial coverage) of Megafaunal Groups Distributions (F).

#### **4.3.2.3 Other Invertebrates**

Ophiuroidea (brittle star) was found in largest abundance at 3000 m and at 2000 m depths. Crinoidea abundance was highest between 2250 m and 2000 m. *Munidopsis* spp. (squat lobster) was sporadically found below 2200 m, primarily on bedrock (Fig. 4-3a). Mysidacea (shrimp) were ubiquitous throughout the dive; however, in relatively low abundance compared to Ophiuroidea. Holothuroidea (sea cucumber) were most abundant on fine sediment (Fig. 4-3a) and sporadically found throughout the dive. Echinoidea (sea urchin) were sporadically found on fine sediment (Fig. 4-3a) (Appendix 4-6).

#### **4.3.2.4 Concentrations of Megafauna**

All megafaunal concentrations (surface area coverage greater than 20%) were found on bedrock outcrops (Fig. 4-3a). *Gersemia* spp. concentrations were found only at the crest of the OS, within 70 m from the top of OS (-1879 m) on an 11° slope. *Chrysogorgia* spp. concentrations were found on the outer edge of a large bedrock outcrop (Fig. 4-3a) on a 22° slope along the 2750 m contour. Concentrations of Isididae (bamboo coral), Ophiuroidea (brittle stars), Hexactinellida (unidentified glass sponges) and Porifera (unidentified sponges) were found at 2000 m on a 16° slope 120m from the crest of OS (Appendix 4-7).

### 4.3.3 Habitat 2 - Orphan Knoll Enigmatic Mounds (D1341 and D1343)

#### 4.3.3.1 *SE Mounds (D1341)*

##### **Coral**

*Chrysogorgia* spp. was found on the north side of the mounds on a 9° slope at 2645 m depth, while Isididae was found throughout the dive. The most biodiverse species composition was found below the 2<sup>nd</sup> mound (southerly mound), running up-slope from 12-17° slope, starting at 2690 m (Fig. 4-4b) (Appendix 4-4).

##### **Sponges**

Unidentified Porifera (sponges) and Hexactinellida (glass sponges) were found on fine sediment overlain primarily by granules (Fig. 4-4e). Euplectellidae (glass vase sponge) were found throughout the dive and were most abundant on the mound crests (Fig. 4-4e) (Appendix 4-5).

##### **Other Invertebrates**

Enteropneusta (acorn worm) was found on granules overlain by fine sediment. Ophiuroidea was found throughout the 2700 m to 2400 m depth range and was not found on mound 1. The 2700 m to 2400 m depth range varied from 12-17° slopes, respectively and contained the largest amount of other invertebrate biodiversity (Fig. 4-4d) (Appendix 4-6).

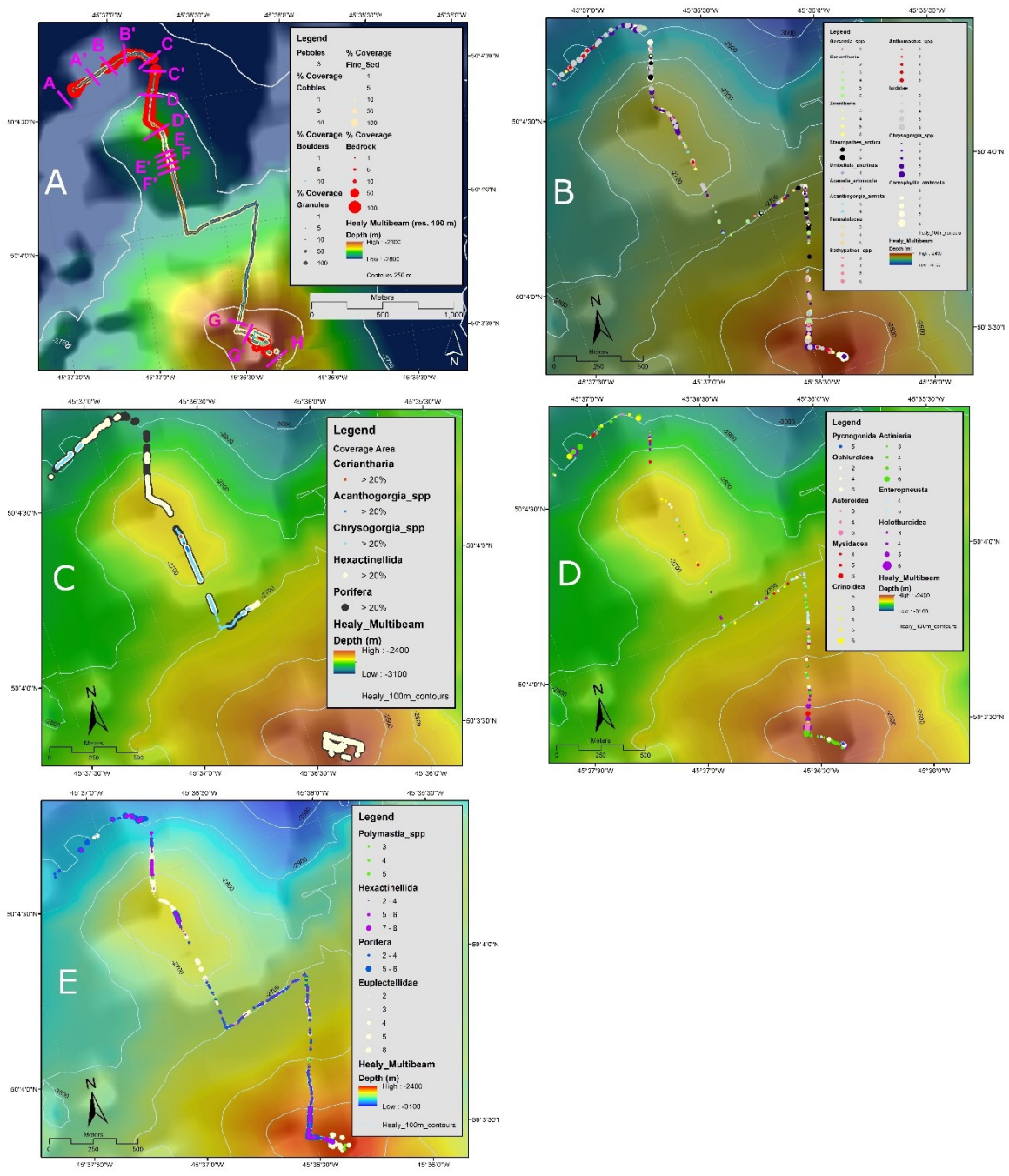


Figure 4-4. SE Orphan Knoll Mounds' Surficial Geology, Megafauna Abundance and Distributions Maps (colour gradients in maps have been individually optimized for ease of viewing): Surficial Geology (A), Coral Species Distribution (B), Concentrations (>30% surficial coverage) of Megafaunal Groups Distributions (C), Non-Coral or Sponge Invertebrates Distribution (D), Sponge Distribution (E).

## **Concentrations of Megafauna**

Unknown Porifera (sponge) and Hexactinellidae (glass sponge) concentrations dominated the 2<sup>nd</sup> mound crest. Ceriantharia and *Acanthogorgia armata* were found together on the crest of the deeper / 1<sup>st</sup> explored mound (Fig. 4-4c) (Appendix 4-7).

### **4.3.3.2 NE Mounds (D1343)**

#### **Coral**

There were 11 recorded coral types identified on the NE Orphan Knoll mounds (Photo Plate 1) (Appendix 4-4). *Bathypathes* spp. and *Flabellum* spp. were the most commonly found species throughout the dive and occurred on fine-grained sediment overlain by granules and cobbles (Fig. 4-5a). The most abundance species were Isididae coral (Fig. 4-5b). The highest abundance for Isididae, *Flabellum* spp. and *Bathypathes* spp. coral was found to be on a 25° slope at 1914 m (Fig. 4-5b). Sub-fossil (dead) coral, *Desmophyllum dianthus* was found within a depression on the north side of a large exposed limestone bedrock outcrop (NE OK mound) (Fig. 4-5a).

#### **Sponge**

The unknown Hexactinellidae (glass sponge) sponges were found to be most abundant on bedrock, especially on the large bedrock outcrop at the end of the dive (NE OK mound) (Fig. 4-5a,b). The NE OK mound contained a greater diversity in sponges, when compared to the flat sections within the dive (Fig. 4-5b) (Appendix 4-5).

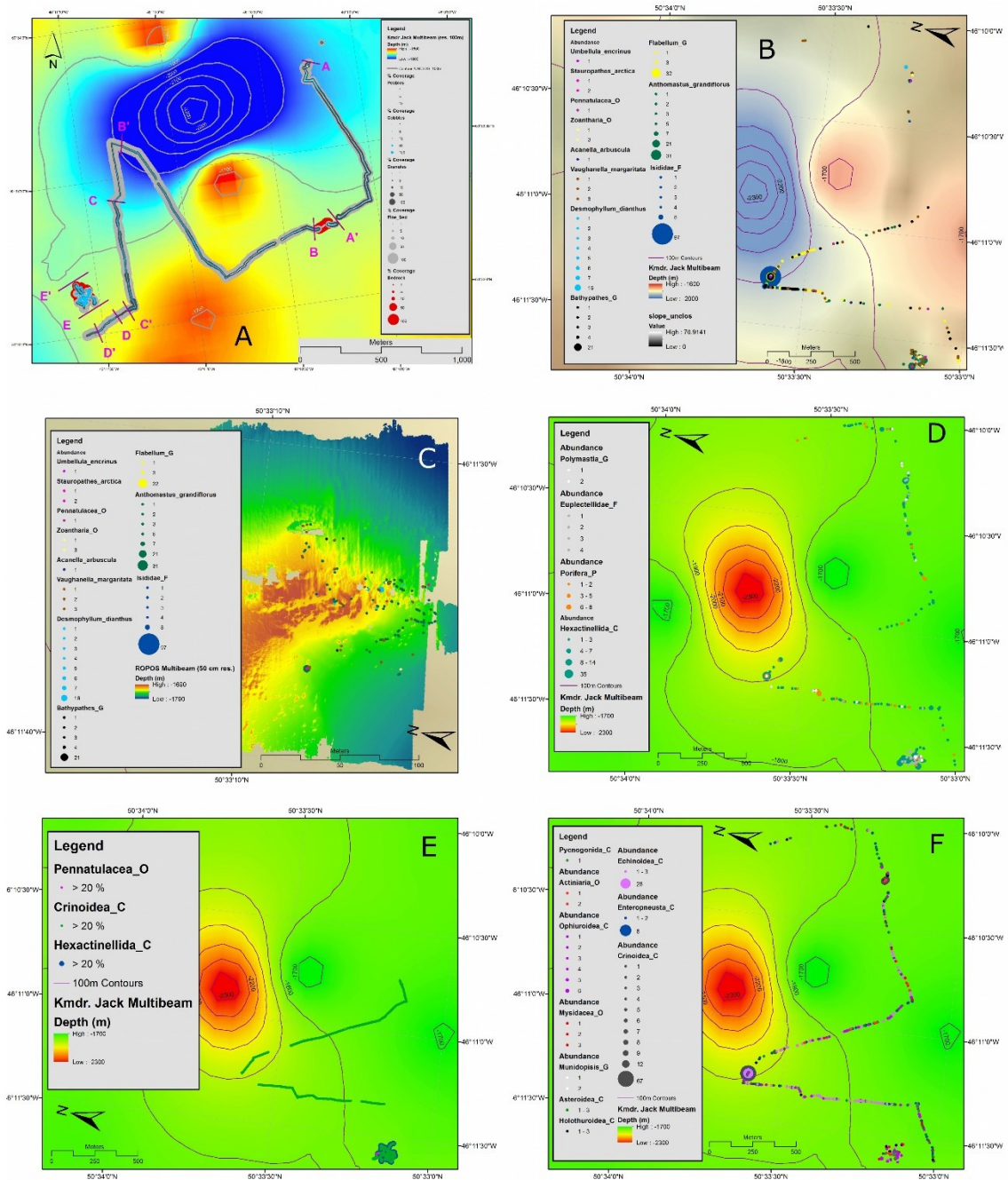


Figure 4-5. NE Orphan Knoll Mound Surficial Geology, Megafauna Abundance and Distributions Maps (colour gradients in maps have been individually optimized for ease of viewing): Surficial Geology (A), Coral Species Distribution (B), Coral Species Distribution just on the mound top (C), Sponge Distribution (D), Non-Coral or Sponge Invertebrates Distribution (E), Concentrations (>30% surficial coverage) of Megafaunal Groups Distributions (F).

### **Other Invertebrates**

Throughout dive 1343, biodiversity of non-coral or non-sponge invertebrates was highest on the NE OK mound and not the flat sections leading up to the mound (Appendix 4-6). The highest abundance of all recorded species was from the Crinoidea (e.g. Sea Lillies and / or feather stars), Echinoidea (sea urchin) and Enterpneusta (acorn worm) animal classes and was found on a 25° slope at 1914 m, 1 km NE of the large bedrock outcrop (NE OK mound). Echinoidea was found throughout the dive on variable substrates, most notably on 80% fine-grained sediment, 10% cobbles and 10% granules (Fig. 4-5e).

### **Concentrations of Megafauna**

Crinoidea concentration was observed throughout the dive, primarily on 80% fine-grained sediment, 10% cobbles and 10% granules (Fig. 4-5a). On the large bedrock outcrop (NE OK mound), Crinoidea and Hexactinellidae were found to cover the entire mound (Fig. 4-5f); while Pennatulacea was only found to be concentrated in a small area, on the north side of the mound (Fig. 4-5f) (Appendix 4-7).

#### 4.3.4 Habitat 3 – Orphan Knoll Deep-Sea Flats (D1342, 1345, 1346)

##### 4.3.4.1 *South OK (D1342)*

###### **Coral**

Of the 5 species of coral recorded on the South Orphan Knoll flat, each species was found on 80% fine-grained sediment and 20% granules (Fig. 4-6a,b) (Appendix 4-4). There were no discernible bathymetric or surficial geological features correlated to the presence of coral throughout the dive (Fig. 4-6a,b).

###### **Sponge**

Low abundance of unknown Hexactinellidae (glass sponge) on 80% fine-grained sediment and 20% granules was the only sponge type recorded during the dive (Fig. 4-6b,c) (Appendix 4-5).

###### **Other Invertebrates**

Enteropneusta (acorn worm) was found, in low abundance, intermittently throughout the dive (Appendix 4-6). Holothuroidea (sea cucumber) was found in a single location on 80% fine-grained sediment and 20% granules (Fig. 4-6b,d).

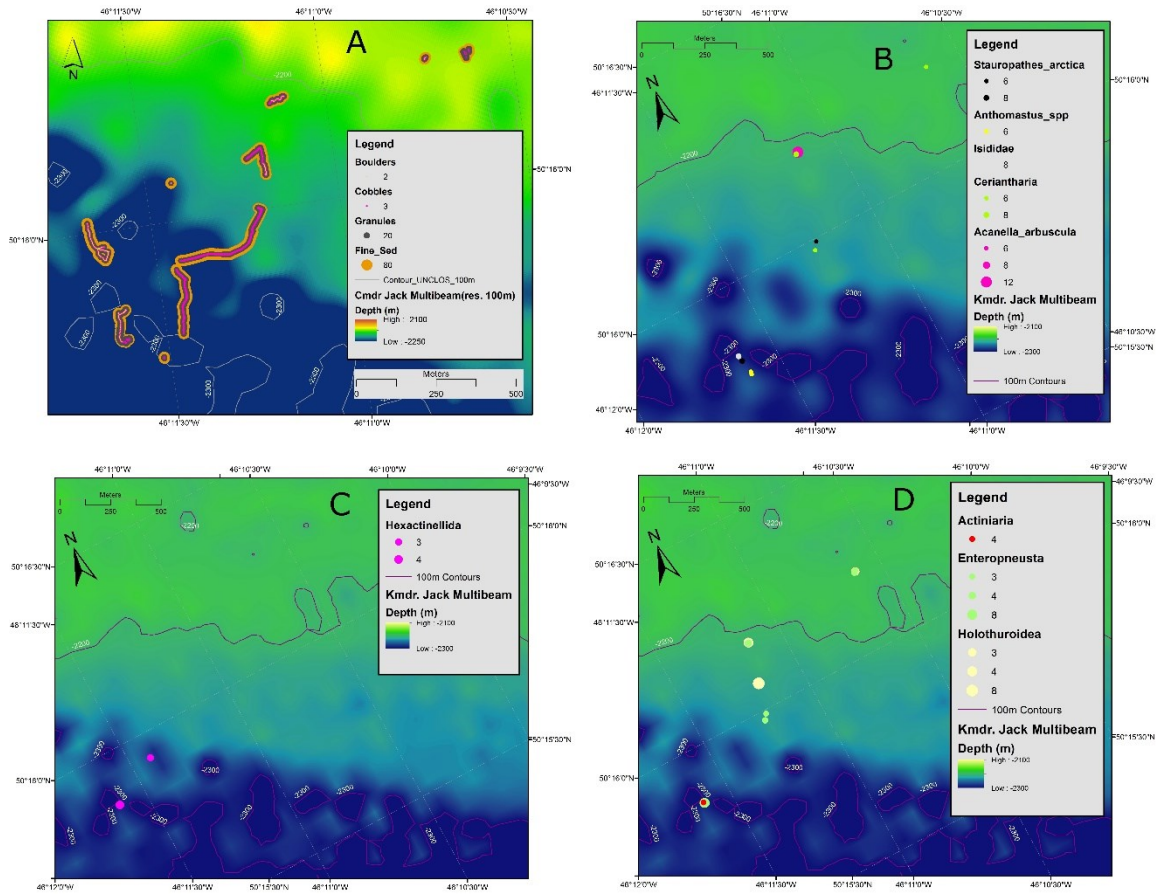


Figure 4-6. Southern Orphan Knoll Flats Surficial Geology , Megafauna Abundance and Distributions Maps (colour gradients in maps have been individually optimized for ease of viewing): Surficial Geology (A), Coral Species Distribution (B), Sponge Distribution (C), Non-Coral or Sponge Invertebrates Distribution (D).

#### **4.3.4.2 Eastern OK (D1345)**

##### **Coral**

*Chrysogorgia* spp. was found between 2280 m and 2285 m with a slope range between 2° - 7° respectively. *Vaughnella margarita* and *Bathypathes* spp. was found throughout the dive, while *Acanella arbuscula* and *Umbellula ecrinus* only occurred in a single location (Fig. 4-7b) (Appendix 4-4).

##### **Sponge**

All three recorded sponge species types were found throughout the dive on 50% fine-grained sediment and 50% granules; however, without an apparent association to depth or surficial geology (Fig. 4-7a,c) (Appendix 4-5).

##### **Other Invertebrates**

All 11 recorded invertebrate types were found throughout the dive on 50% fine-grained sediment and 50% granules (Fig. 4-7a,d); however, without an apparent association to depth or surficial geology (Appendix 4-6).

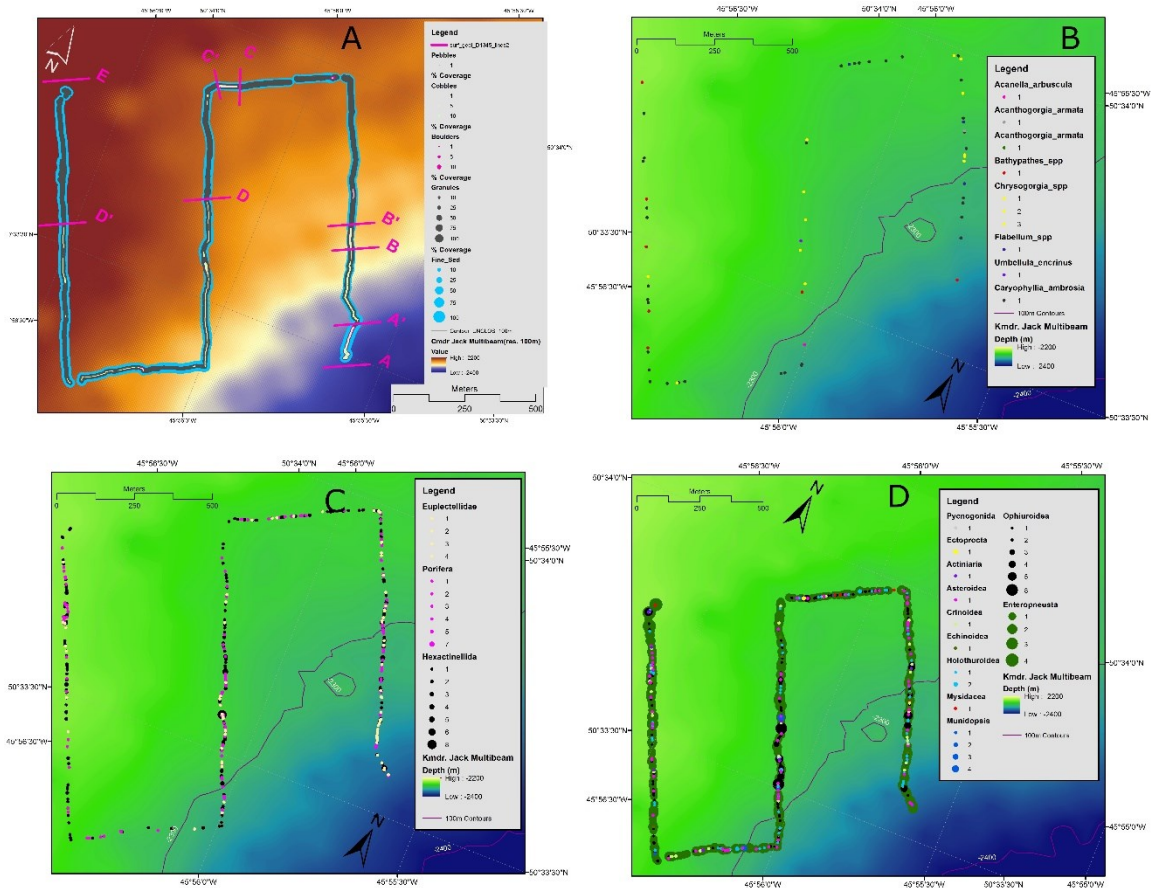


Figure 4-7. Eastern Orphan Knoll Flats Surficial Geology , Megafauna Abundance and Distributions Maps (colour gradients in maps have been individually optimized for ease of viewing): Surficial Geology (A), Coral Species Distribution (B), Sponge Distribution (C), Non-Coral or Sponge Invertebrates Distribution (D).

#### **4.3.4.3 Western OK (D1346)**

##### **Coral**

Intermittent presence of all coral types throughout the dive had no apparent affinity with surficial geology (Fig. 4-8a,b) (Appendix 4-4). *Anthomastus grandiflorum* was found primarily along the 2300 m depth contour on an 11° slope (Fig. 4-8b).

##### **Sponge**

Hexactinellidae and Porifera were found together throughout the dive, except for within an area SE of the raised bathymetric feature, where no sponges were recorded (Appendix 4-5). None of the sponge types had shown an affinity for bathymetric or surficial geological features (Fig. 4-8a,c).

##### **Other Invertebrates**

Crinoidea and Enteropneusta were the predominant species found together and throughout the dive (Appendix 4-6). Asteroidea and Holothuroidea were recorded throughout the dive (Fig. 4-8d). All other invertebrate types were found intermittently during the dive and since the surficial geology was the same throughout the dive (Fig. 4-8a,d), there was no apparent species-surficial geology affinity.

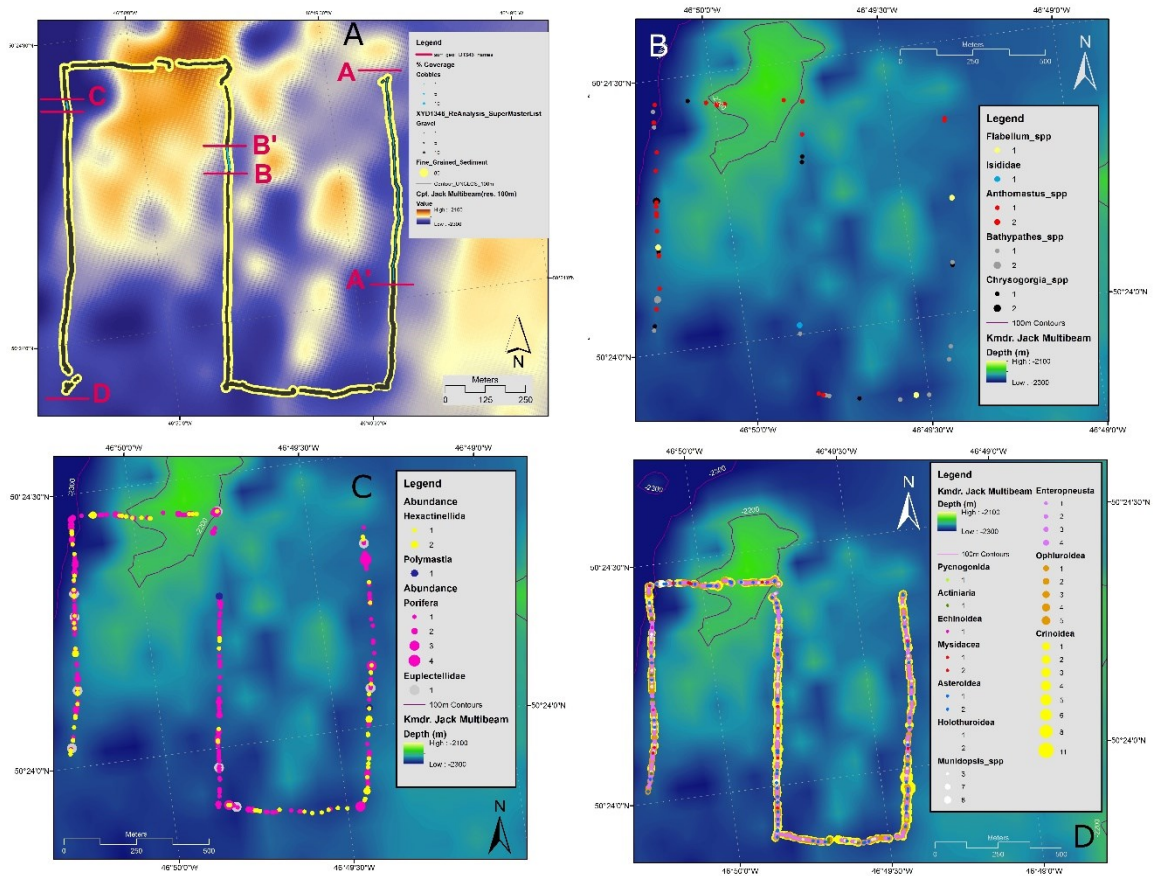


Figure 4-8. Western Orphan Knoll Flats Surficial Geology, Megafauna Abundance and Distributions Maps (colour gradients in maps have been individually optimized for ease of viewing): Surficial Geology (A), Coral Species Distribution (B), Sponge Distribution (C), Non-Coral or Sponge Invertebrates Distribution (D).

## **4.4 Community Composition Results**

### **4.4.1 Deep-Sea Benthic Coral Community**

#### ***4.4.1.1 Coral Predictor Importance***

A forest of 500 regression trees for each of 11 of the 18 recorded coral fauna (Appendix 4-4), from 2351 'sites' (individual observations), resulted in identifying: Depth, Aspect, Slope, B500s and Conductivity as the most important variables in predicting coral presence in the OK and OS area, between depths of 1720 m to 3000 m (Fig. 4-9).

#### ***4.4.1.2 Coral Predictor Importance Gradients***

An increase in biodiversity was indicated by increases in the abundance of multiple species occurring along the same gradient at: 2000 m depth; 50°, 105°, 300° aspect bearings; 5° and 15°-25° slope; on intermediate scale similar sloping areas (e.g. flats) and intermediate scale mild slopes B500s value of 400; conductivity values at 3.235 and 3.29 PSU; density values at 1035.5 and 1038.5 kg/m<sup>3</sup>; 8% and 75% fine grained sediment (Fine\_Sed); mid-scale low-mild slopes F300s value of 250; 2.9°C and 3.35°C temperatures; 0.25 curvature; 1.07 rugosity (low surficial complexity); 5%, 35% and 51% granules; 6% and 8% boulders; 2% and 28% cobbles, 1.8% pebbles; 58% bedrock; 'structures' 3 (mid-slope depression), 7 (shelf), 10 (crest on a flat), 13 (near vertical wall); no 'zonal' differentiation (Fig. 4-10).

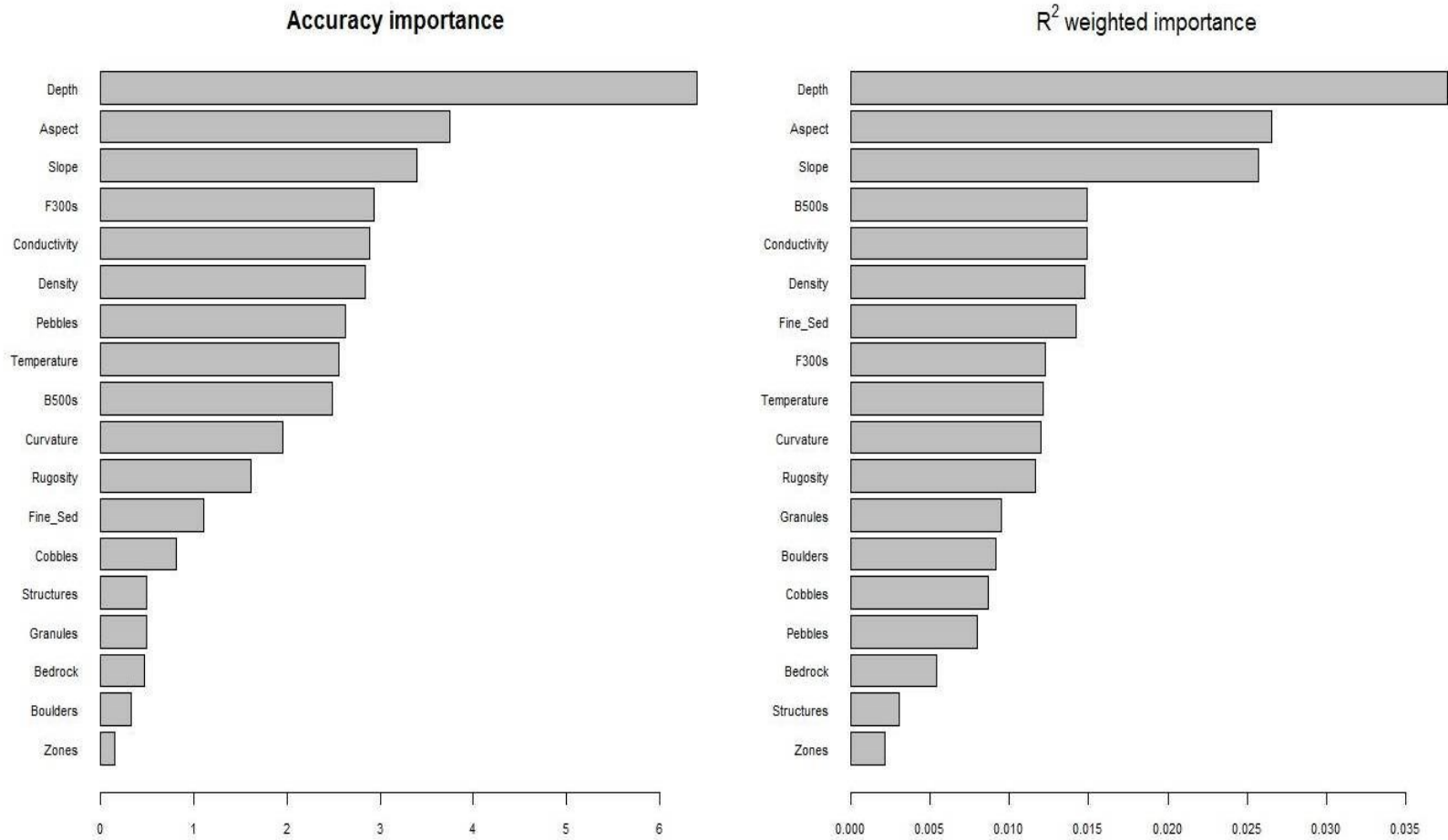


Figure 4-9. *gradientForest* overall accuracy of community turnover predictors for all coral species (left); species-weighted importance analysis of predictors for coral species (right) from Orphan Seamount and Orphan Knoll.

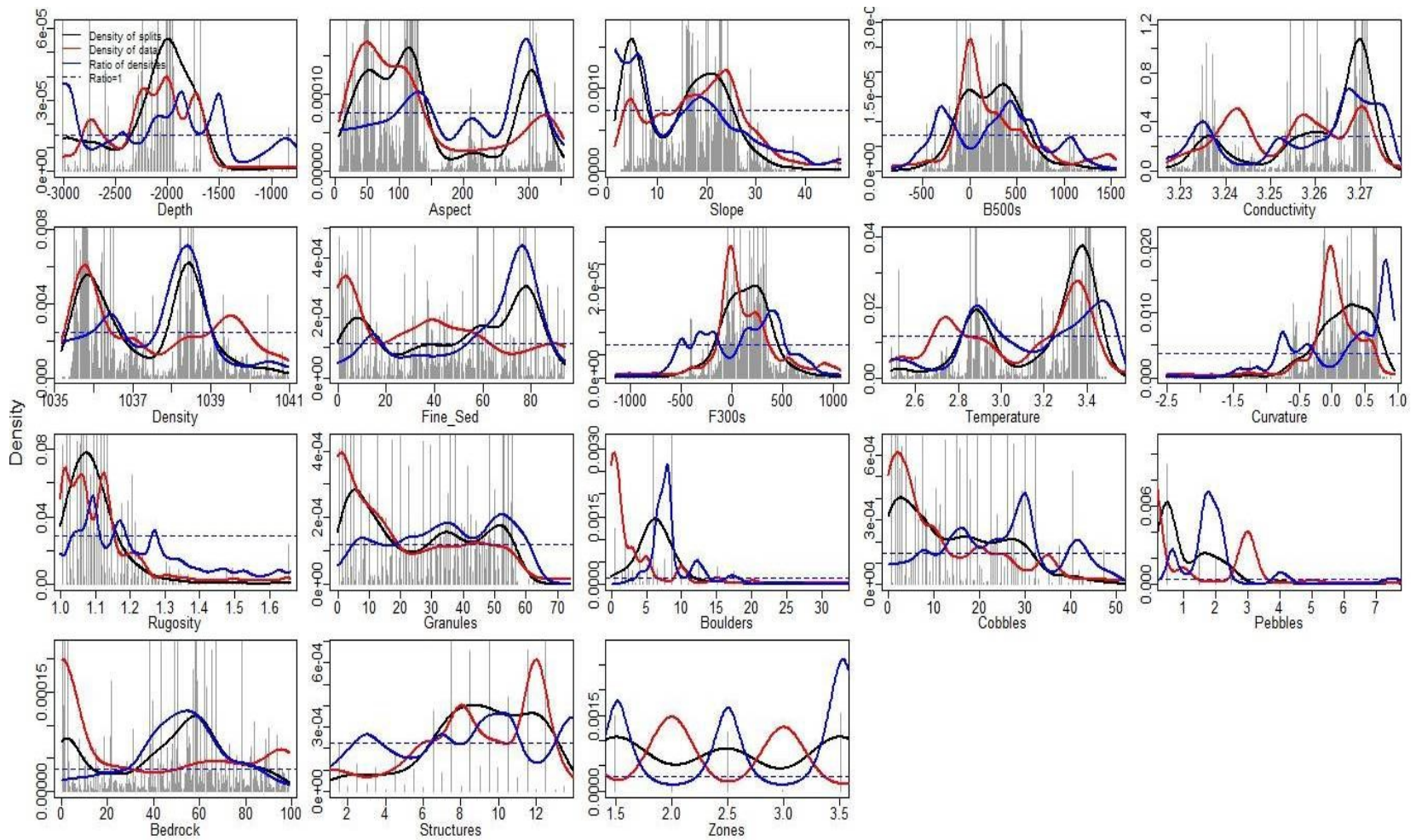


Figure 4-10. Kernel density plots of surrogate gradient changes affecting coral presence from Orphan Seamount and Orphan Knoll

### **Coral Species Cumulative Importance (SPI)**

*Chrysogorgia* spp. rapidly increased in cumulative importance (CI) (abundance) between 2750 m to 2500 m; where *Flabellum* spp., *Anthomastus grandiflorus*, Isididae (Family), Zoantharia (Order) increased in CI between 2400 m to 1750 m (Fig. 4-11). *Desmophyllum dianthus* rapidly increased in cumulative importance (abundance) at - 1750 m (Fig. 4-11). All other species did not indicate noticeable changes in CI.

Zoantharia, Isididae increased in CI between aspect headings of 50°- 60° and between 90° - 110° (Fig. 4-11). *Anthomastus grandiflorus* increased in CI between aspect headings of 125° (Fig. 4-11). *Acanella arbuscula* increased in CI on aspect heading 225° (Fig. 4-11). *Desmophyllum dianthus* rapidly increased in CI on aspect heading 300° (Fig. 4-11). All other species didn't indicate noticeable changes in CI.

*Desmophyllum dianthus* rapidly increased in CI on a 5° slope (Fig. 4-11). *Acanella arbuscula* increased in CI on an 8° slope (Fig. 4-11). *Anthomastus grandiflorus* increased in CI on a 15° - 18° slope (Fig. 4-11). Isididae increased in CI at a 18° slope and Isididae and Zoantharia increased in CI between 20°-25° slope (Fig. 4-11). All other species didn't indicate noticeable changes in CI.

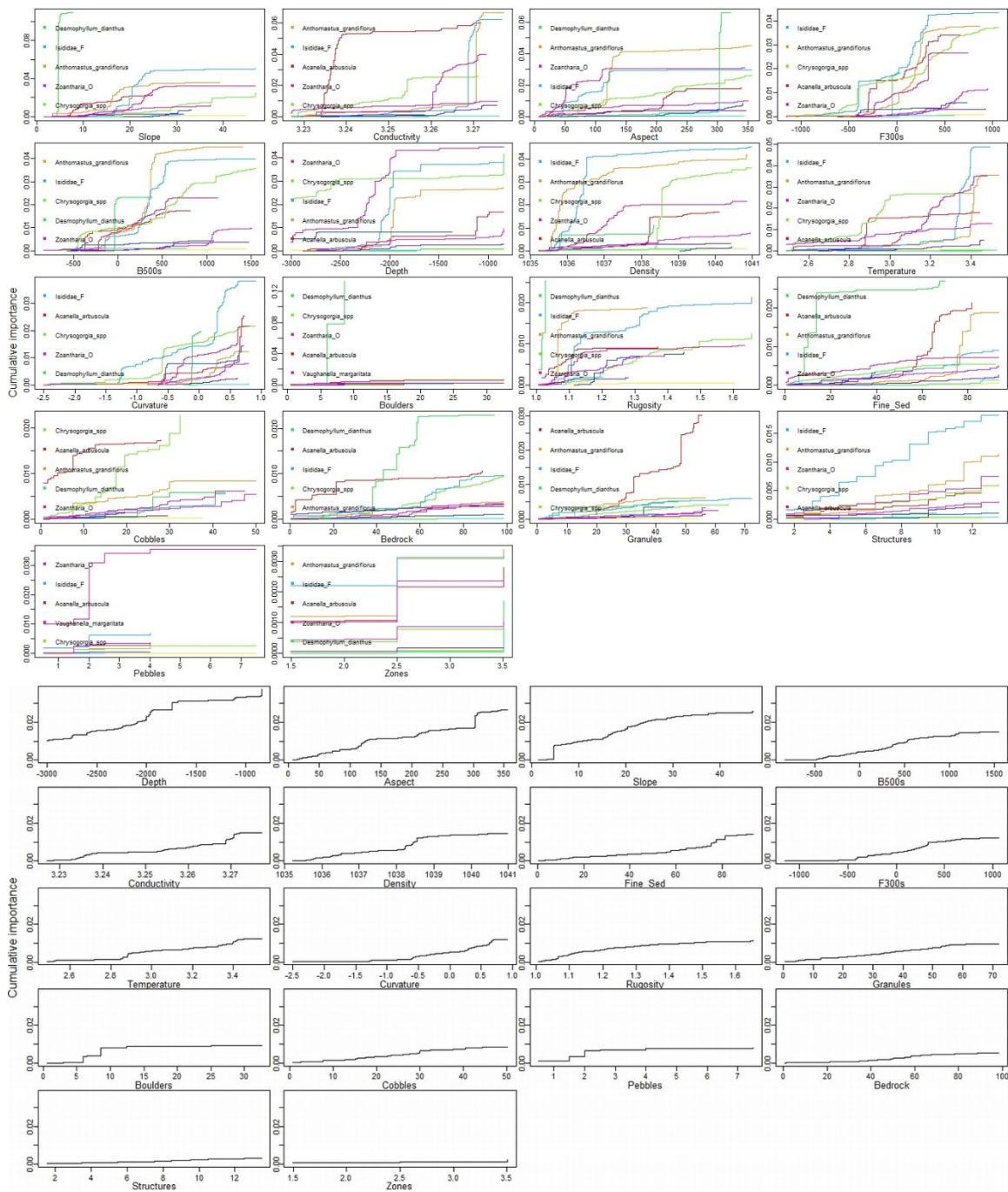


Figure 4-11. Cumulative importance (CI)(top) and Overall CI (bottom) plots for coral types for the OK and OS areas; showing change in abundance of individual species, where changes occur on the gradient and the species changing most on each gradient. The top 5 (from 11) species responses are noted within the individual plots.

The B500s SPI plot (Fig. 4-11) indicated that *D. dianthus* increased in CI at a low negative value (~ -75) indicating a change in abundance in small depressions that are on flats (or of constant slope, e.g. vertical wall). Within the B500s plot (Fig. 4-11), Isididae, *A. grandiflorus*, Zoantharia and *A. arbuscula* ranged from a low of -450 (dipping low-mid slope) to a high of 600 (elevated mid-slope). *Chrysogorgia* spp. and *V. margarita* indicated a CI increase, in B500s plot, to 1100 (Fig. 4-11). All other species didn't indicate noticeable changes in CI.

*Acanella arbuscula* increased in CI in the conductivity plot between 3.235 (S /cm) and 3.24 (S /cm) (Fig. 4-11). *Chrysogorgia* spp. increased in CI in the conductivity plot at 3.255 (S /cm) (Fig. 4-11). Zoantharia increased in CI in the conductivity plot at 3.26 (S /cm) (Fig. 4-11). Isididae and *A. grandiflorus* increased in CI in the conductivity plot at 3.27 (S /cm) (Fig. 4-11). All other species didn't indicate noticeable changes in CI.

The density SPI plot indicated an increase in CI between 1035.5 (kg /m<sup>3</sup>) to 1036.5 (kg /m<sup>3</sup>) for Isididae, *A. grandiflorus* and *D. dianthus* (Fig. 4-11). The density SPI plot indicated an increase in CI between 1036.5 (kg /m<sup>3</sup>) to 1037.5 (kg /m<sup>3</sup>) for Zoantharia (Fig. 4-11). The density SPI plot indicated an increase in CI at 1038.25 (kg /m<sup>3</sup>) for *Chrysogorgia* spp., *D. dianthus*, *A. arbuscula* (Fig. 4-11).

The fine sediment SPI plot indicated an increase in CI for *Chrysogorgia* spp. at 9% and 15% surficial area coverage (Fig. 4-11). *A. arbuscula* increased in CI at 32%, 56%, 65% and 81% surficial area coverage (Fig. 4-11). *A. grandiflorus* increased in CI at

32%, 56%, 65% and 81% surficial area coverage (Fig. 4-11). All other species didn't indicate noticeable changes in CI.

The F300s SPI plot identified that *Zoantharia*, Isididae, *Chrysogorgia* spp. and *A. arbuscula* increased in CI between -400 (low falling slopes) to 300 (low rising slopes) (Fig. 4-11). The F300s SPI plot indicated that *A. grandiflorus* increased in CI between 0 (flat or constant slope) and 300 (low rising slopes) (Fig. 4-11). The F300s SPI plot (Fig. 4-11) indicated that *D. dianthus* increased in CI at a low negative value (~ -75) indicating a change in abundance in small depressions that are flats (or of constant slope, e.g. vertical wall). All other species did not indicate noticeable changes in CI.

The temperature SPI plot identifies an increase in CI for *Chrysogorgia* spp. and *A. arbuscula* at 2.85 °C and again for *Chrysogorgia* spp. at 2.95 °C, while CI increased for *Zoantharia* between 3.15°C to 3.4°C (Fig. 4-11). The temperature SPI plot identifies an increase in CI for Isididae at 3.3°C and at 3.4°C for *A. grandiflorus* (Fig. 4-11). All other species didn't indicate noticeable changes in CI.

The curvature SPI plot identifies an increase in CI for Isididae at -1.25 and 0.3 (Fig. 4-11). The curvature SPI plot identifies an increase in CI for *D. dianthus* at -0.2, where *Chrysogorgia* spp. increased in CI at -0.6 and 0.2 (Fig. 4-11). The curvature SPI plot identifies an increase in CI for *Zoantharia* and *A. arbuscula* at -0.5 and 0.6 (Fig. 4-11). The curvature SPI plot identifies an increase in CI for *V. margarita* at 0.45 (Fig. 4-11). All other species didn't indicate noticeable changes in CI.

The rugosity SPI plot identifies a rapid increase in CI for *D. dianthus* at 1.0, where *A. grandiflorus* increased in CI at 1.05 and *Chrysogorgia* spp. at 1.1 (Fig. 4-11). All other species didn't indicate noticeable changes in CI.

Not many species responded to surficial geological cues; however, *A. arbuscula* was the only species to respond to granule area coverage at 20%, 33%, 49%, 53% and 55% (Fig. 4-11). *D. dianthus* showed an increased CI at 6% and 8% boulder surficial coverage, while *Chrysogorgia* spp. showed slight increases in CI at 12.5% and 17.5% boulder surficial coverage (Fig. 4-11). *Chrysogorgia* spp. showed increased CI in cobble surficial coverage between 18% - 20% and again between 30% - 33% (Fig. 4-11). *A. grandiflorus*, *D. dianthus* and Zoantharia showed increased CI in cobble surficial coverage at 30% (Fig. 4-11). Isididae showed increased CI in cobble surficial coverage at 40% and *V. margarita* increased at 48% (Fig. 4-11). Zoantharia, Isididae and *V. margarita* increased in CI at 1.5% and 2% of pebble surficial geological coverage (Fig. 4-11). *A. arbuscula* increased in CI at 1%, 21%, 40% - 50% and 82% bedrock surficial geological coverage (Fig. 4-11). *D. dianthus* increased in CI at 42%, 50%, 60% bedrock surficial coverage (Fig. 4-11). *Chrysogorgia* spp. increased in CI at 65% - 67%, along with Isididae and *V. margarita*; where Isididae increased in CI again at 80% bedrock surficial coverage (Fig. 4-11).

The structures SPI plot identifies a rapid increase in CI for *D. dianthus* at 7.8 (shelf-escarpment). Isididae, *Chrysogorgia* spp. , and Zoantharia increase in CI at 3 (mid-slope depression), 4.5 (depression on crest – open depression), 8.5 (escarpment – crest in depression) and between 11.5 (midslope crest – narrow crest) and 12.5 (narrow crest –

near vertical wall) (Fig. 4-11). *A. grandiflorus*, *A. arbuscula* and *Pennatulacea* (Order) increased in CI at 9.5 (crest in depression – crest n flat) (Fig. 4-11).

The zones SPI plot identifies a rapid increase in CI for *D. dianthus* at 3.5 (flat-slope); where a slight increase in CI was observed for all other species at zone 2.5 (depression – flat) (Fig. 4-11).

### **Geographic clustering of important predictors relative to species abundance**

Dive 1340 contained the most clusters (1,2,3); dive 1431 contained clusters 5,6; dive 1343 contained clusters 4,7; dived 1345, 1342 and 1346 shared the cluster 8 class . The slope predictor was most accurate on OS, depth at SE OK, aspect at NE OK and conductivity at E OK (Fig. 4-12). Abundant species on OS (D1340) that are best predicted by slope were *Anthoptilium grandiflorum* and *Zoantharia* . Abundant species on SE OK (D1341) that are best predicted by depth were *Ceriantharia* and *Vaughnella margarita* (Fig. 4-12). Abundant species on NE OK (D1343) that are best predicted by aspect were *Desmophyllum dianthus* and *Bathypathes* spp. . Abundant species on E OK (D1345) that are best predicted by conductivity were *Anthomastus grandiflorus* and *Pennatulacea* (Order).

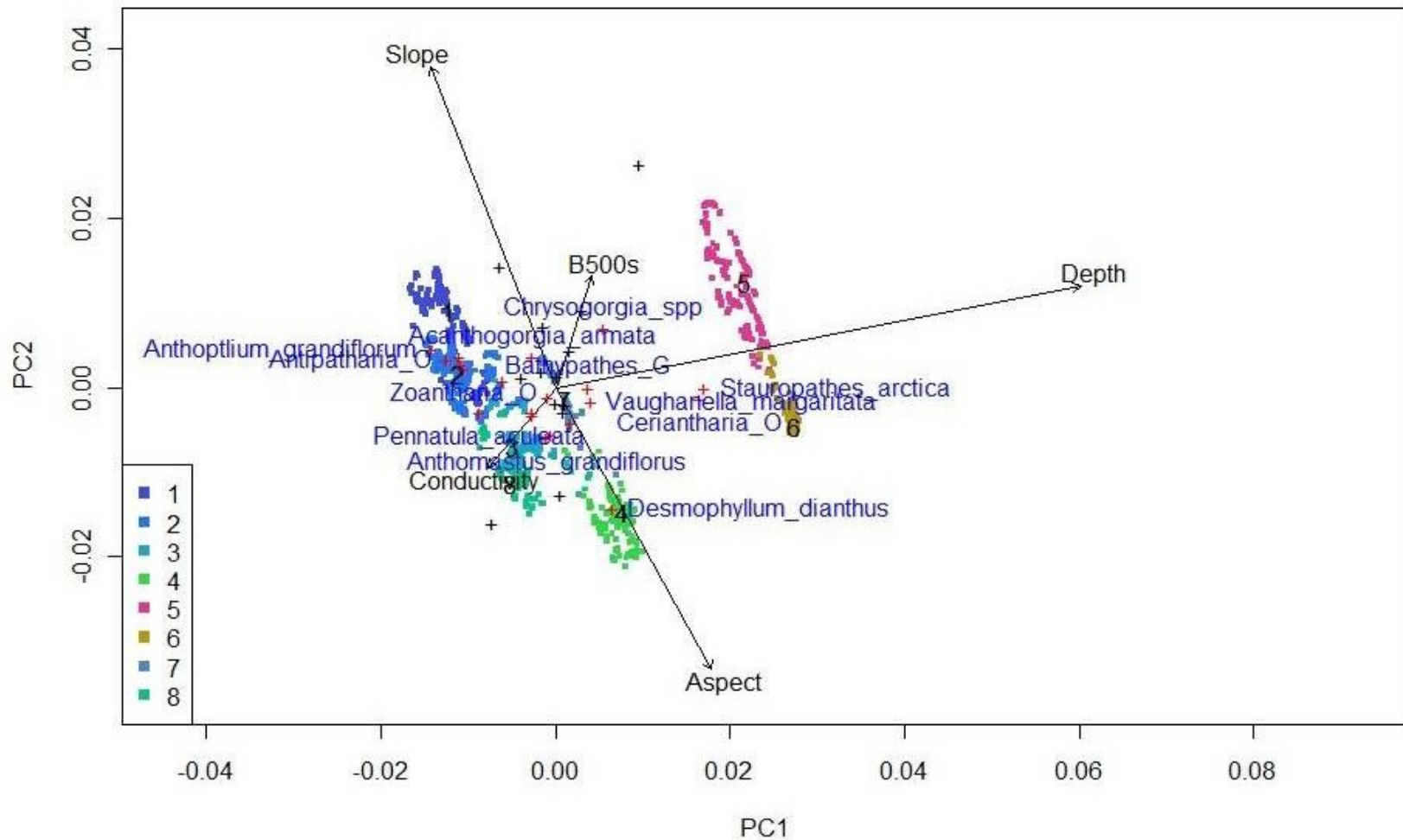


Figure 4-12. Principal Components Analysis of the first two dimensions and the most important predictors as vectors; red crosses identify the most responsive coral fauna; colored and numbered clusters represent inferred assemblages, rather than a continuous representation of coral biodiversity at Orphan Seamount and Orphan Knoll.

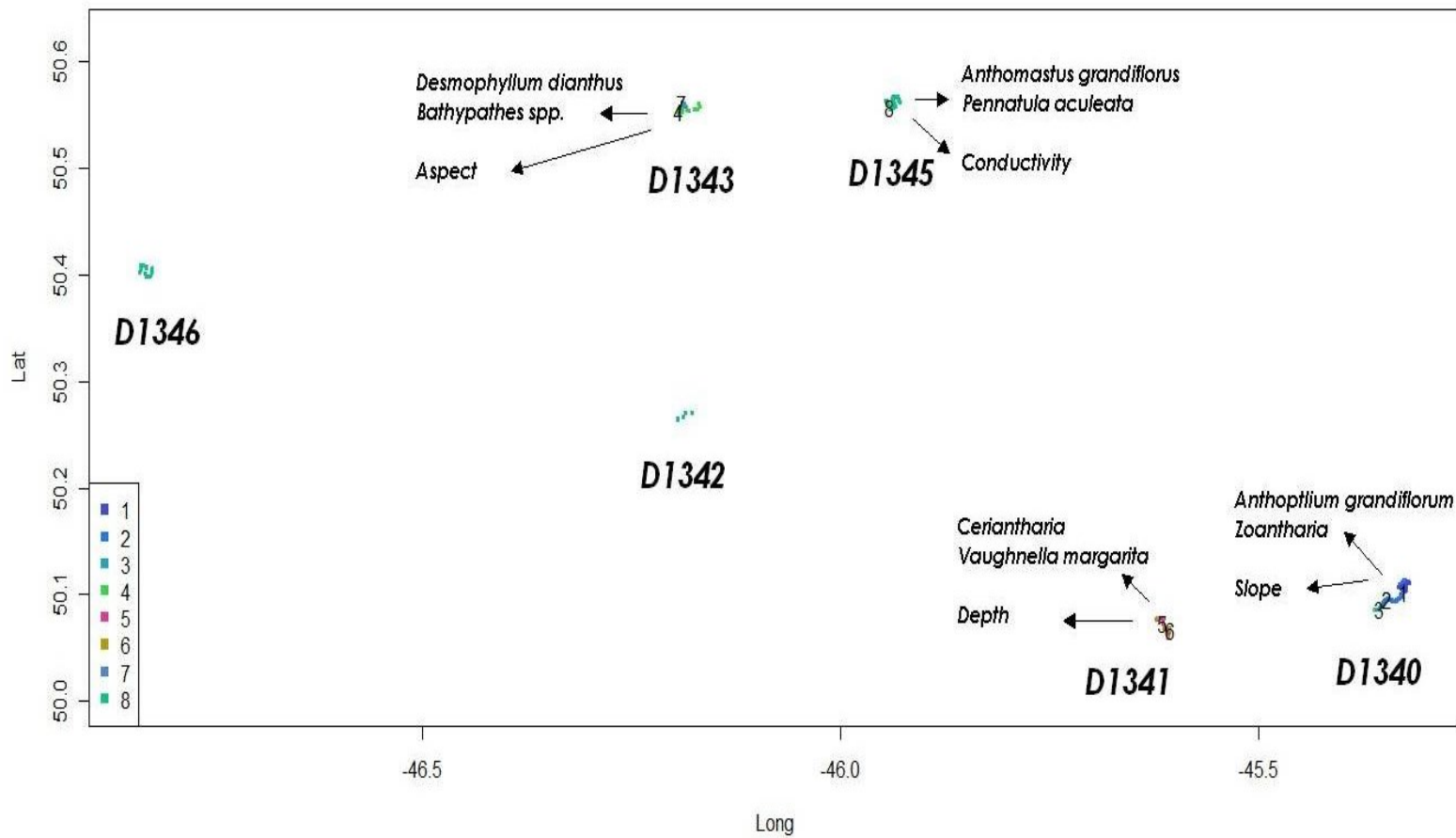


Figure 4-13. Geospatial cluster occurrences of PCA scores. Dive ID (e.g. D1340) is shown below the actual dive location; Arrows are not vectors, but rather labeling arrows for the most responsive coral fauna and the most important environmental drivers relative to a specific dive site.

#### **4.4.1.3 *Sponge Predictor Importance***

A forest of 500 regression trees for each of 4 of the 4 recorded sponge fauna, from 5167 'sites' (individual observations), resulted in identifying: Depth, Aspect, Slope, Density, and B500s as the most important variables in predicting sponge presence in the OK and OS area, between depths of 1720 m to 3000 m (Fig. 4-14) (Appendix 4-5).

#### **4.4.1.4 *Sponge Predictor Importance Gradients***

A significant change in community composition was indicated by increases in the abundance of multiple species occurring along the same gradient at: 2500 m depth; 25°, 90-100°, 330° aspect bearings; 12°, 22° and 25° slopes; density values at 1035.9 and 1038.75 kg/m<sup>3</sup>; on intermediate scale similar sloping areas (e.g. flats) (B500s value of 0); mid-scale low-mild slopes (F300s value of 250); 0 - 0.25 curvature; 2.9°C and 3.35 °C temperatures; 4% and 15% cobbles; 5-10% and 35-40% granules; 5%, 30% and 55% fine grained sediment (Fine\_Sed); 1.09 rugosity (low surficial complexity); 'structures' 3 (mid-slope depression), 11 (mid-slope crest); 6% and 8% boulders; slight bedrock signal at 60%; lack of data density identified low-to-none conductivity, pebbles or 'zonal' predictive accuracy (Fig. 4-15).

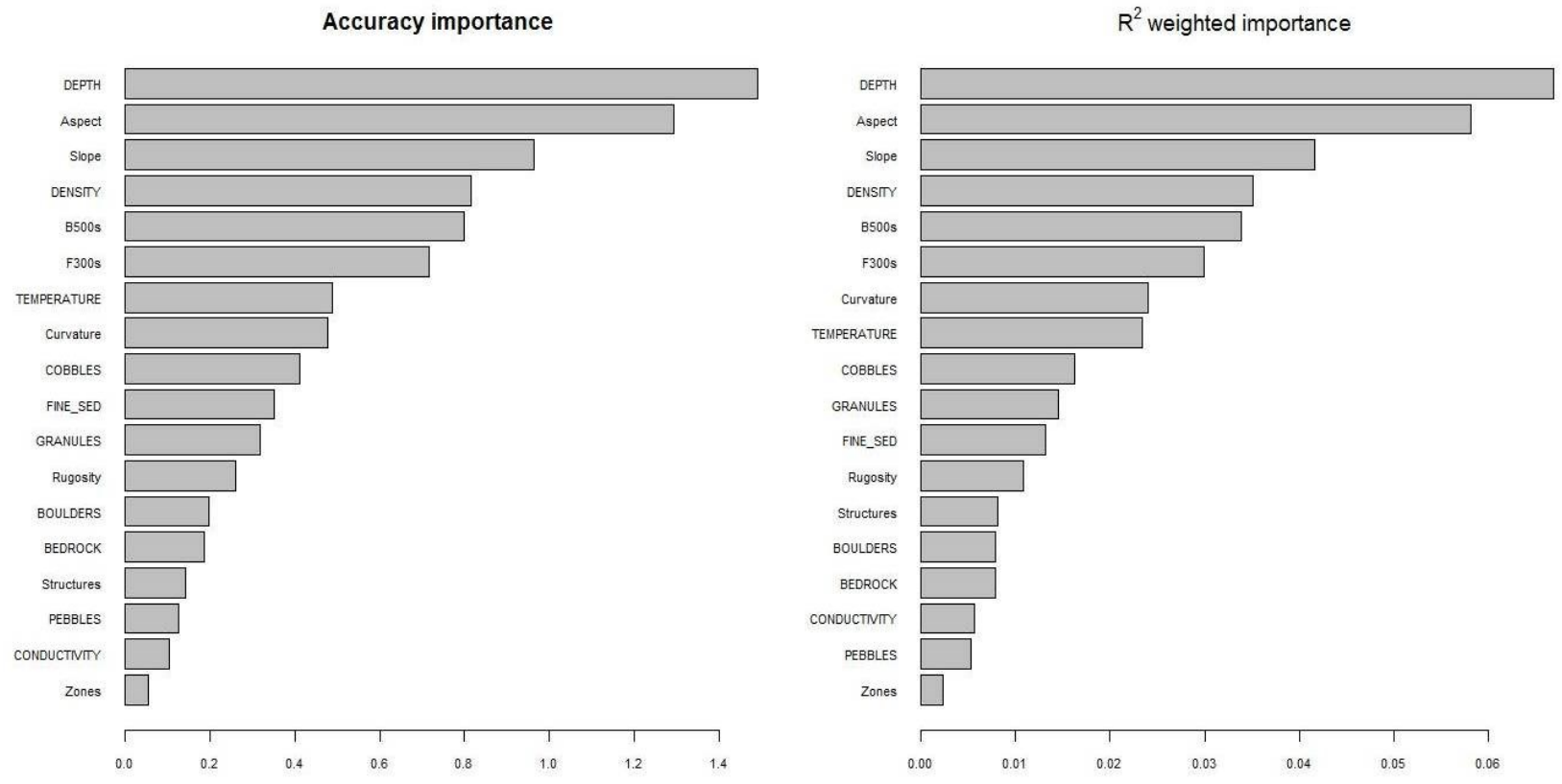


Figure 4-14. gradientForest overall importance analysis of predictors for all sponge species (left); species-weighted importance analysis of predictors for coral species (right) from Orphan Seamount and Orphan Knoll

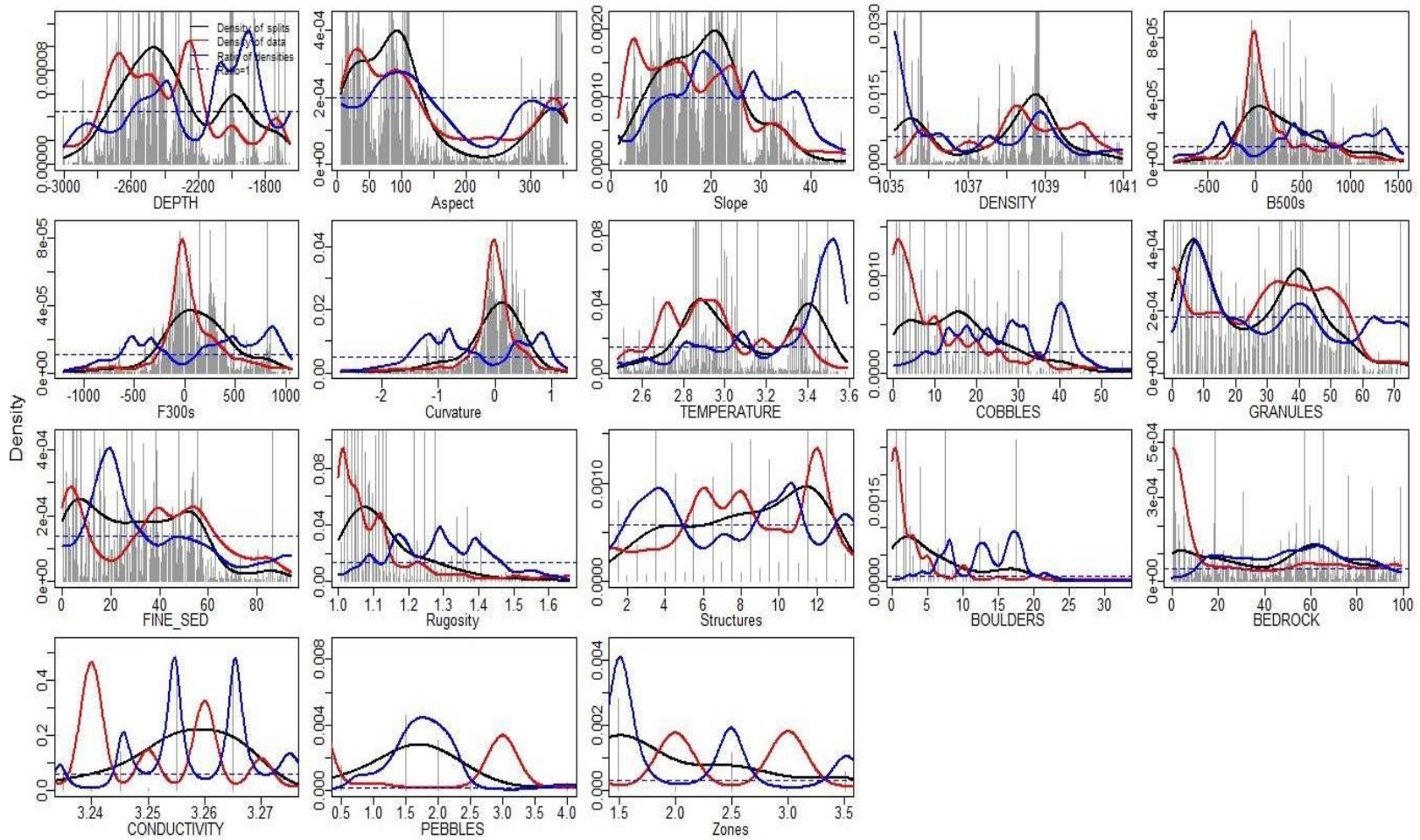


Figure 4-15. Kernel density analysis plots of surrogate gradient change for sponge presence from Orphan Seamount and Orphan Knoll (blue peaks are standardised by observation density).

### **Sponge Species Cumulative Importance (SPI)**

*Porifera* rapidly increased in cumulative importance (CI) 2400 m; where, *Euplectella* abruptly increased at 2300m and Hexactinellidae rapidly increased in CI at 2200 m (Fig. 4-16). *Polymastia* gradually increased in cumulative importance, as the depth gets shallower at 1900 m (Fig. 4-16).

All four sponge species gradually increased in CI, though aspect headings of 90°, 110° and 165° identified increases in accuracy at these headings (Fig. 4-16). Hexactinellidae responded to the same aspect headings at the rest of the sponges but the increase in change was less rapid.

All four sponge species gradually increased in CI as slope increases; however, Hexactinellidae and *Polymastia* rapidly increased at 20° and *Polymastia* and *Euplectella* showed an increase in CI at 33°.

The density plot indicated a rapid increase in CI at 1035.2 (kg /m<sup>3</sup>) for Hexactinellidae only; however, all sponge species rapidly increased CI at 1038.75 (kg /m<sup>3</sup>).

The B500s SPI plot indicated that all sponge species gradually increased in CI but that *Euplectella* was the only species to show a rapid increase at 1250 (highly sloped).

The F300s SPI plot identified that all sponge species gradually increased in CI as the slope rises but that *Euplectella* showed a rapid increase in CI at 750 (mid-high rising slope) and *Porifera* increased at -600 (mid falling slopes) and 400 (low-mid rising slopes) (Fig. 4-16).

The curvature SPI plot identifies a gradually increasing CI for all sponge species, though Hexactinellidae showed a slight increase at -1 (slightly rounded dipping surface) and 0.25 (slightly rounded).

The temperature SPI plot identifies a gradual increase in CI for all sponge species, however, increases in CI at 2.85°C for all species was identified along with two increases in CI at 3.4°C and 3.5°C for Polymastia (Fig. 4-16).

The conductivity SPI plot identifies a low gradual increase in CI for all sponge species, however, Euplectella and Porifera increases in CI at 3.25, with albeit, a narrow range for all species (3.23 – 3.28), hence the low CI (Fig. 4-16).

Not all species responded to surficial geological cues; however, Hexactinellidae and Euplectella were the only species to show an increase CI for cobble area coverage at 40% (Fig. 4-16). Euplectella and Porifera slightly increased CI at 7% and 40% respectively concerning granules area coverage. All of the other surficial geology variables displayed a low gradual increase in CI with increasing unit values, though their overall CI importance / predictive accuracy was very low. With that being said Euplectella showed slight increases in CI with respect to boulders (17%) and Porifera showed an increase in CI at 57% bedrock. Pebbles importance slightly increased when the signal went from 0 to 1.5-2% area coverage for all sponge species.

The rugosity, structures and zones SPI plots identify a low gradual increase in CI for all sponge species with Polymastia showing a slight increase on a midslope crest – narrow crest (class 11 structure), Hexactinellidae slightly increase the CI concerning

rugosity at 1.11 (slightly rugose) and all sponge species identified the zones between 2- 3 (depression-flat) and 3-4 (flat-slope) as slightly increasing the CI.

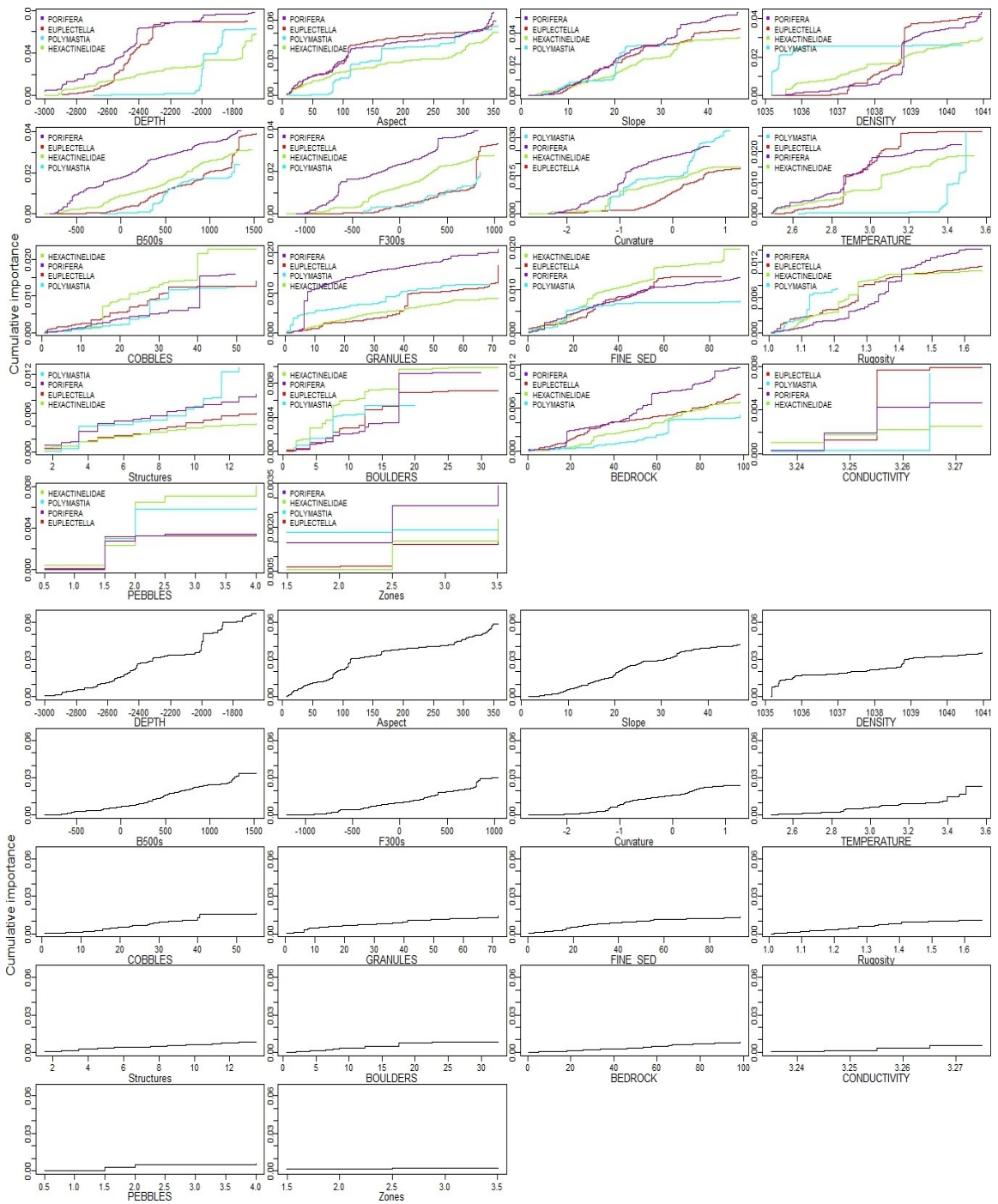
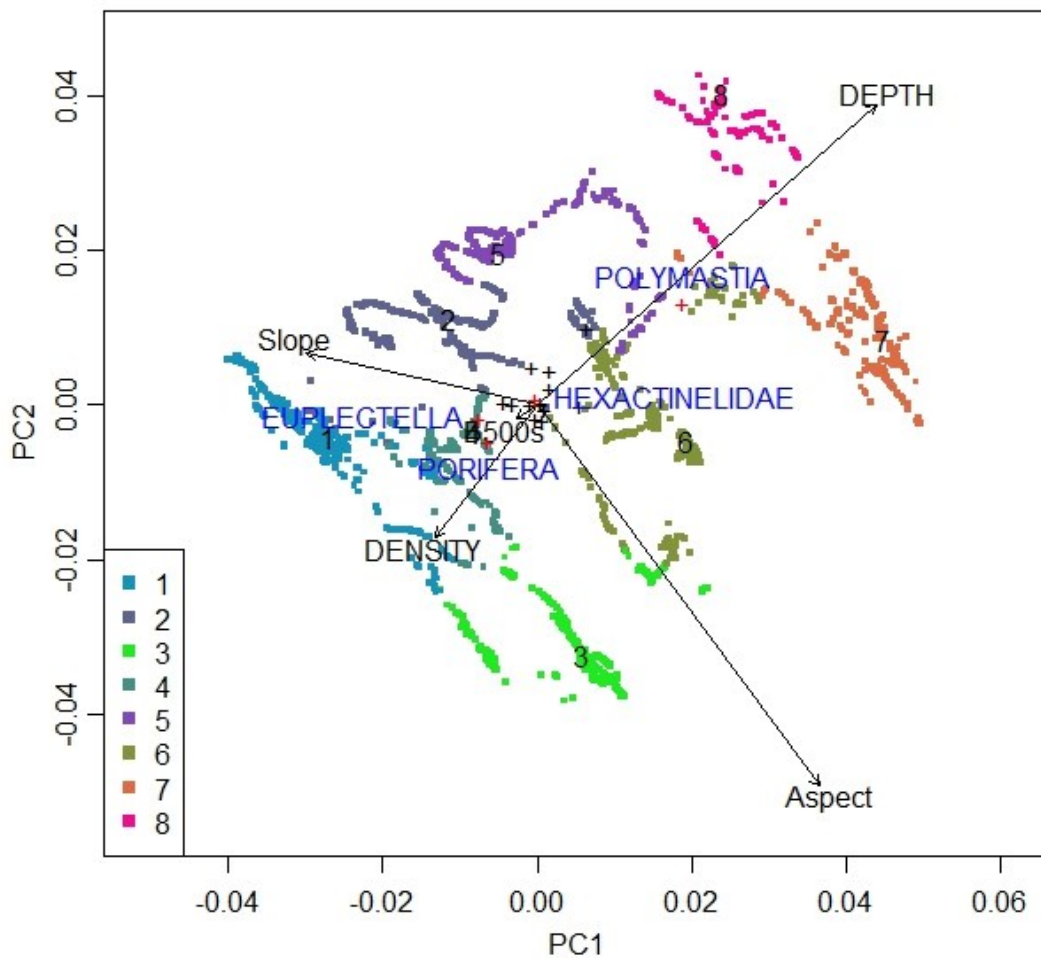


Figure 4-16. Cumulative importance (CI)(top) and Overall CI (bottom) plots for sponge types for the OK and OS areas; showing change in abundance of individual species, where changes occur on the gradient and the species changing most on each gradient.

### **Geographic clustering of important predictors relative to species abundance**

Dive 1340 contained the most clusters (1, 2, 4, and 5); dive 1431 contained cluster 3; dive 1343 contained clusters 7, 8; dive 1345 and 1342 contained no significant clustered variables (Fig. 4-17).

Slope and density predictors were most accurate on OS, density at SE OK, depth at NE OK and depth and aspect at Eastern OK (Fig. 4-18). Abundant species on OS (D1340) that are best predicted by slope and density were Euplectella and Porifera. Abundant species on SE OK (D1341) that are best predicted by density were Porifera. Abundant species on NE OK (D1343) that are best predicted by depth was Polymastia. Abundant species on Eastern OK (D1345) that are best predicted by depth was Hexactinellidae (Fig. 4-18).



*Figure 4-17. Principal Components Analysis of the first two dimensions and the most important predictors as vectors; red crosses identify the most responsive sponge fauna; colored and numbered clusters represent inferred assemblages, rather than a continuous representation of coral biodiversity at Orphan Seamount and Orphan Knoll.*

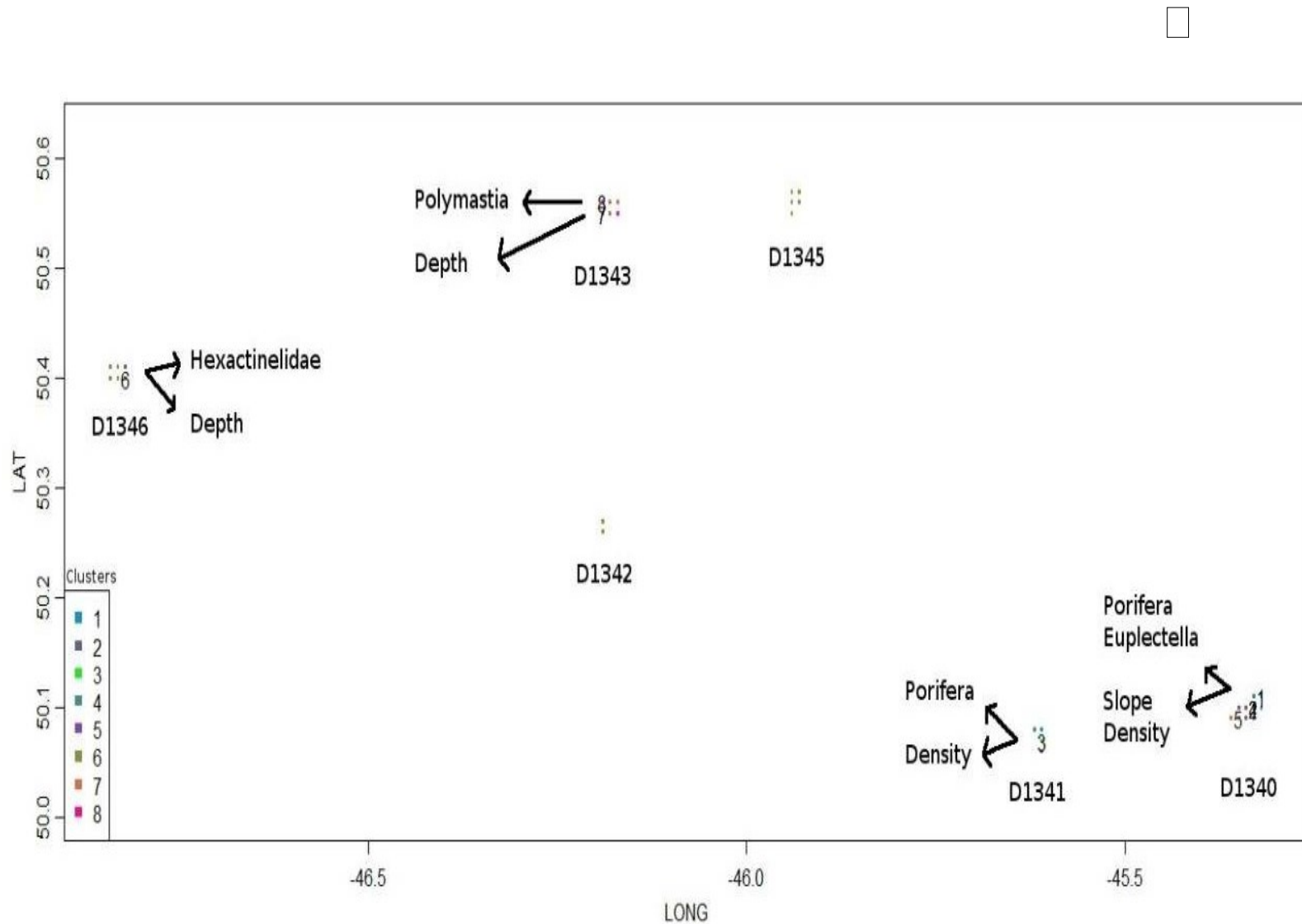


Figure 4-18. Geospatial cluster occurrences of PCA scores. Dive ID (e.g. D1340) is shown below the actual dive location; Arrows are not vectors, but rather labeling arrows for the most responsive sponge fauna and the most important environmental drivers relative to a specific dive site.

#### ***4.4.1.5 Non-Coral and Non-Sponge Megafaunal Predictor***

##### ***Importance***

A forest of 500 regression trees for each of 5 of the 10 recorded faunal types, from 4831 'sites' (individual observations), resulted in identifying: Depth, Aspect, B500s, Slope, and Density as the most important variables in predicting coral presence in the OK and OS area, between depths of 1720 m to 3000 m (Fig. 4-19) (Appendix 4-6).

#### ***4.4.1.6 Non-Coral and Non-Sponge Megafaunal Predictor***

##### ***Importance Gradients***

A significant change in community composition was indicated by increases in the abundance of multiple species and kernel density analysis occurring along the various data gradients: between 2300 and 2250 m depth; at between 40-60° and 330° aspect bearings; on intermediate scale similar sloping areas (e.g. flats) and intermediate scale mild slopes B500s value of 0 and 750 respectively; 5°, 10° and 20°-22° slopes; density values at 1036, 1037 and 1040 kg /m<sup>3</sup>; flats and low-mild slopes F300s values of 0 and 400 respectively; between 2.8-3°C and 3.35°C temperatures; 0 (flat) to 0.4 (very slight curve) curvatures; between 40% and 60% fine grained sediment (Fine\_Sed); 1.08 rugosity (low surficial complexity - flat); between 5% and 60% granules; pebbles, conductivity, boulders, zones had poor data density and no notable affects to model accuracy; 'structures' also had low data density but there was a mild response for areas 6 (broad

flat) ,7 (shelf), 8 (escarpment), bedrock and cobbles had adequate data density but showed no predictive affects (Fig. 4-20).

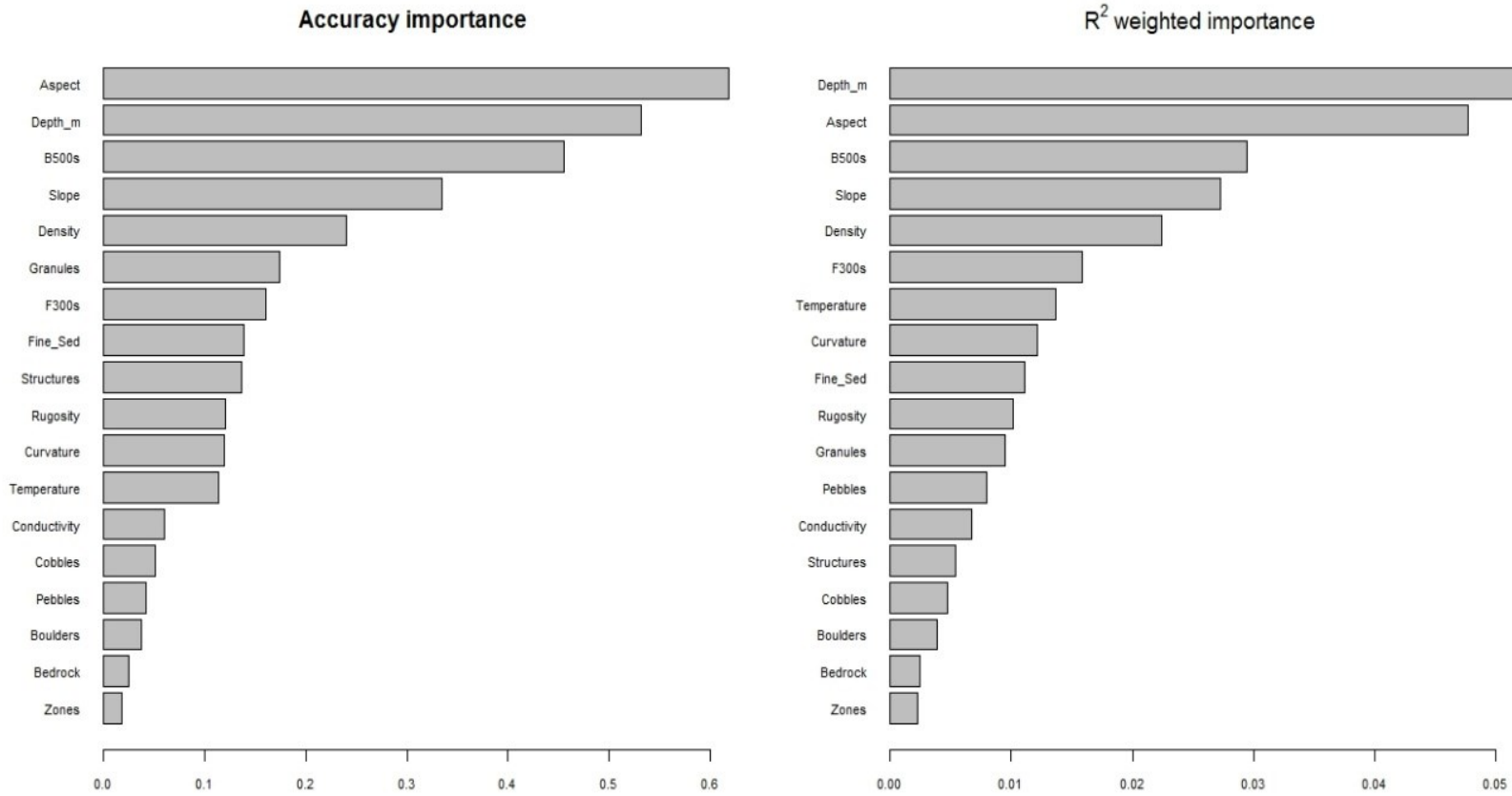


Figure 4-19. *gradientForest* overall importance analysis of predictors for all non-coral and non-sponge megafaunal species (left); species-weighted importance analysis of predictors for coral species (right) from Orphan Seamount and Orphan Knoll

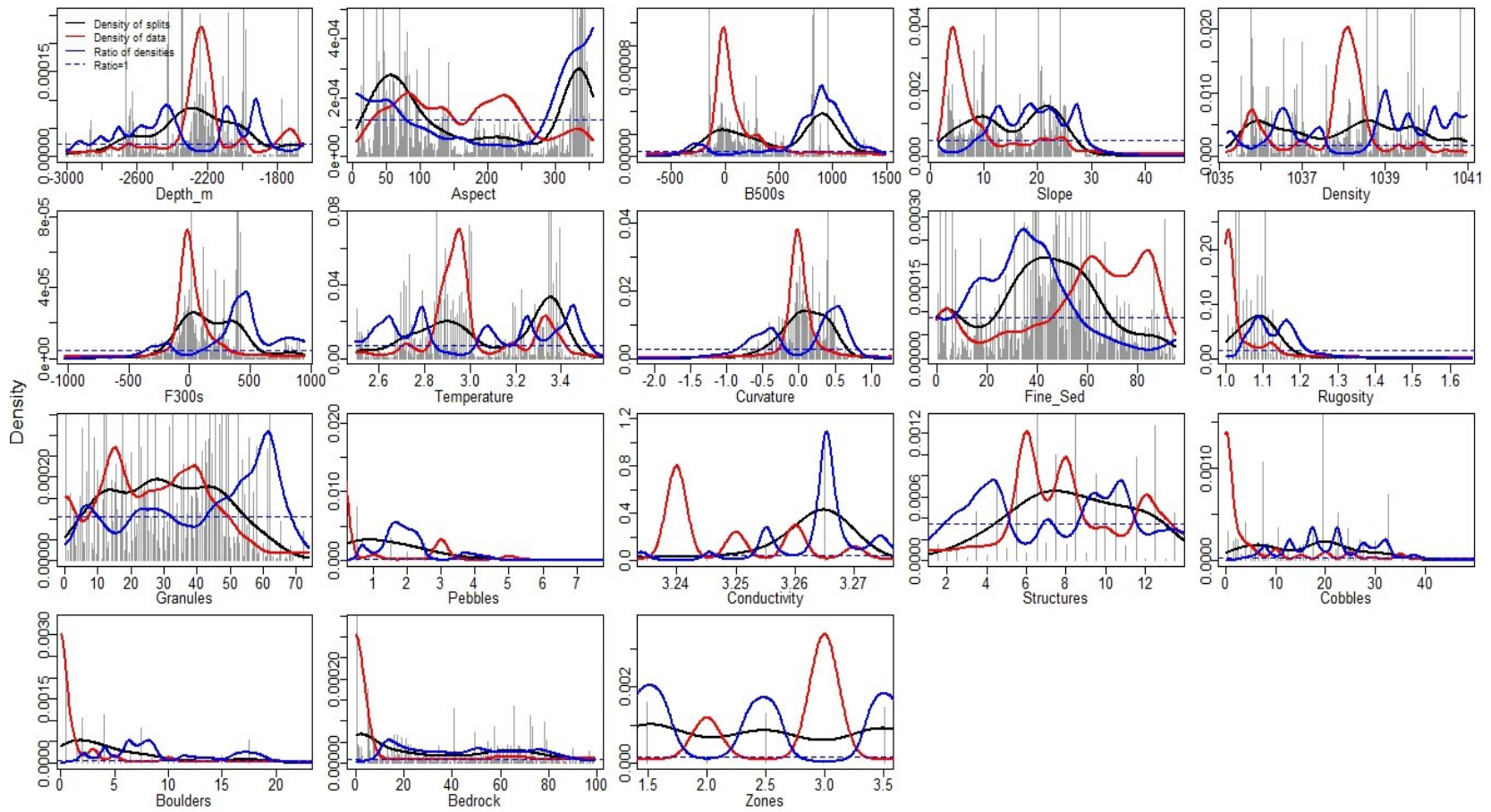


Figure 4-20. Kernel density plots of surrogate gradient changes affecting non-coral and non-sponge presence from Orphan Seamount and Orphan Knoll

### **Non-Coral and Non-Sponge Megafaunal Species Cumulative Importance (SPI)**

A gradual increase in cumulative importance (CI) (abundance) was seen for all species except Actinaria, Enteropneusta and Ophiuroidea with decreasing depths.

Actinaria showed a gradual increase in CI between 2900 m to 2450 m, at which point its CI rapidly increased until 2350m depth; where, Enteropneusta exhibited a slight increase in CI at 2700m and then levels-out; where, Ophiuroidea very gradually increased in CI until 2120m to 2000 m (Fig. 4-21).

A gradual increase in cumulative importance (CI) (abundance) was seen for all species except Actinaria, Enteropneusta and Ophiuroidea with increasing aspect.

Actinaria rapidly increased in CI at 40° then gradually increased in CI between 40° and 325°, at which point its CI rapidly increased until 350°, whereby Enteropneusta's CI rapidly increases. Ophiuroidea rapidly increased in CI at 50°, where it quickly increases in CI until 100°, where it then levels-out. Crinoidea shows a slight rapid increase in CI at 75° and then remains level (Fig. 4-21).

The B500s gradient response plot indicated that Holothuroidea and Enteropneusta gradually increased in CI as variability in slope increased, while Crinoidea, Ophiuroidea and Actinaria indicated increases. Crinoidea increased in CI in flat depressions (-200), whereby, it remains relatively level as slope increases and depth decreases (upwards). Ophiuroidea quickly increases in CI between 200 (low relief) to 600 (elevated mid-slope). Actinaria didn't show a response until 750 (large mid-slope) and 1000 (high-slope), where its CI rapidly increased (Fig. 4-21).

All species show an overall gradual increase in CI as slope increases. However, Actinaria and Ophiuroidea rapidly increase in CI at 12° and 20° slope respectively (Fig. 4-21); whereby, all species seem to level-out concerning their CI above 25° slope (Fig. 4-21).

All species show a gradual increase in CI between 1035.5 (kg /m<sup>3</sup>) to 1041 (kg /m<sup>3</sup>), though Ophiuroidea CI rapidly increases between 1305.8 and 1037 (kg /m<sup>3</sup>). Enteropneusta's CI rapidly increases between 1039.5 and 1040 (kg /m<sup>3</sup>), where Actinaria's CI gradually increases until 1040.8 (kg /m<sup>3</sup>), whereby, it rapidly increased in CI (Fig. 4-21).

The F300s SPI plot indentified that Actinaria increased CI at 400 (low rising slopes) and 750 (large mid-slope). The F300s SPI plot indicated an increase in CI between 200 (low rising slope) and 300 (low rising slope) for Ophiuroidea (Fig. 4-21).

The temperature SPI plot identifies a general increase in CI as temperature increases from 2.5 to 3.5°C. A rapid increase in CI for Ophiuroidea was seen at 3.35°C, though the gradient plots shows a quick increase in Ophiuroidea CI from 3.2 to 3.4°C.

The curvature SPI plot identifies a gradual increase in CI at either -0.5 and 0.5 curvature. Actinaria and Ophiuroidea have a more pronounced increase than the other invertebrates (Fig. 4-21).

The fine sediment SPI plot indicates a gradual increase in CI for all species with the exception of Enteropneusta indicating an increase in CI at 30% area coverage. The gradient plot also shows no change in CI above 60% fine sediment area coverage (Fig. 4-21).

The rugosity SPI plot identifies a rapid increase in CI for Actinaria at 1.025 and Ophiuroidea at 1.1, though the other species do not respond to increasing rugosity (Fig. 4-21).

Not many species responded to surficial geological cues; however, Actinaria increased in CI between 1.5 to 2.5% pebble cover, 62% granule coverage and 32% cobble coverage, while Ophiuroidea increased in CI at 27% granules and between 18-22% cobble coverage. The rest of the species with respect to surficial geology, structures and zones showed an overall gradual increase in CI, but the overall importance indicates reduced predictive importance (Fig. 4-21).

The conductivity SPI plot showed that Holothuroidea increased rapidly in CI at 3.265 (S/cm), where the other species gradually increased in CI between 3.24 and 3.27 (S/cm) (Fig. 4-21).

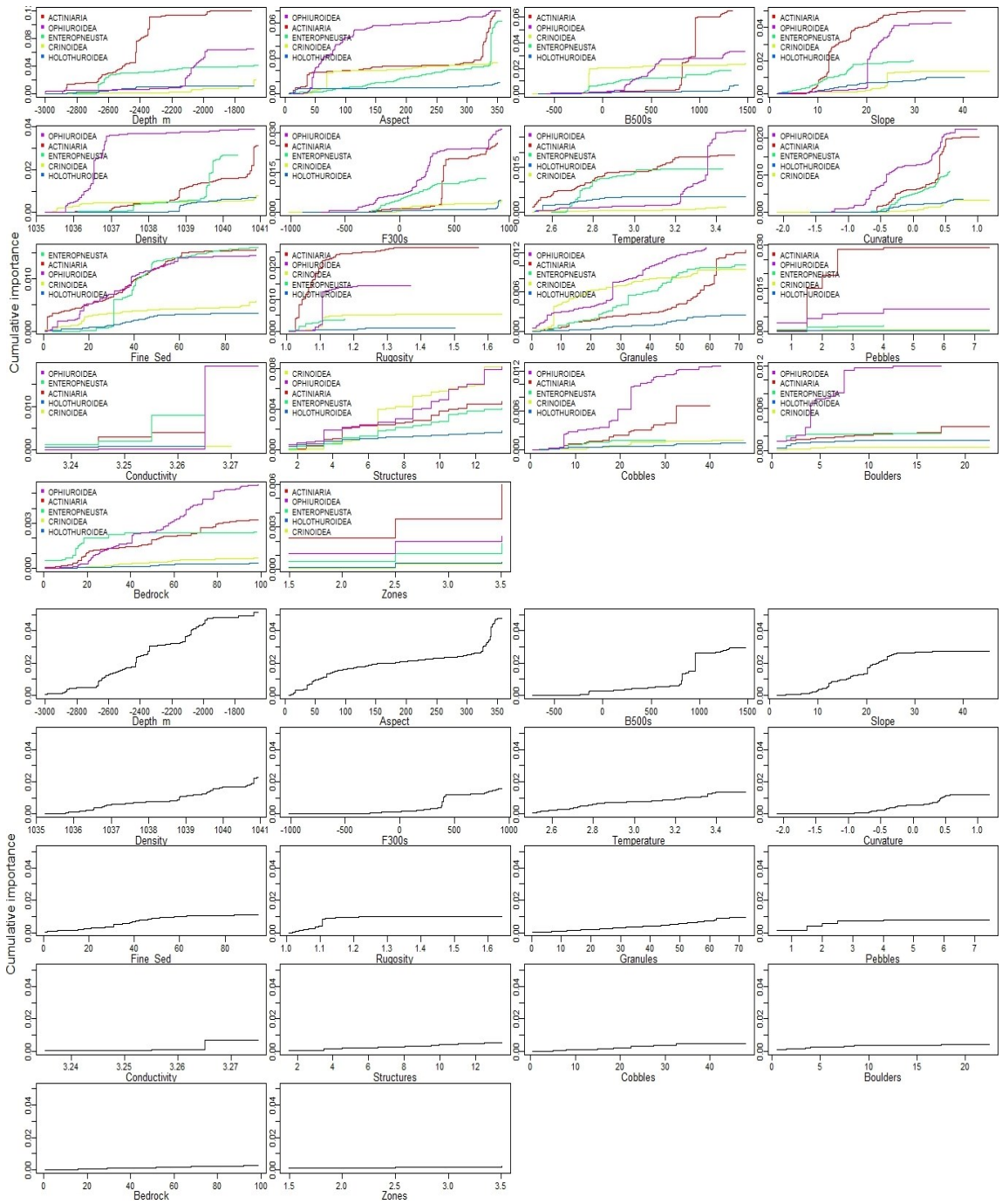


Figure 4-21. Cumulative importance plot (top) and Overall CI for non-coral and non-sponge megafaunal species for the OK and OS areas; showing change in abundance of individual species, where changes occur on the gradient and the species changing most on each gradient.

### **Geographic clustering of important predictors relative to species abundance**

Dive 1340 contained the most clusters (1,2,5); dive 1431 contained clusters 3,7; dive 1343 contained cluster 6; dive 1345 contained cluster 4; dive 1346 contained cluster 8 and dive 1342 didn't contain any clusters (Fig. 4-22).

The slope predictor was most accurate on OS and NE OK, density at SE OK and aspect at Eastern and Western OK (Fig. 4-23).

Abundant species on OS (D1340) that are best predicted by slope were Asteroidea, Mysidacea and Ophiuroidea (Fig. 4-23). Abundant species on SE OK (D1341) that are best predicted by density were Actinaria, Halothuroidea and Enteropneusta (Fig. 4-23). Abundant species on NE OK (D1343) that are best predicted by depth were Echinodermata and Pycnogonidae (Fig. 4-23). Abundant species on East and west OK (D1345, D1346) that are best predicted by aspect was Enteropneusta (Fig. 4-23).

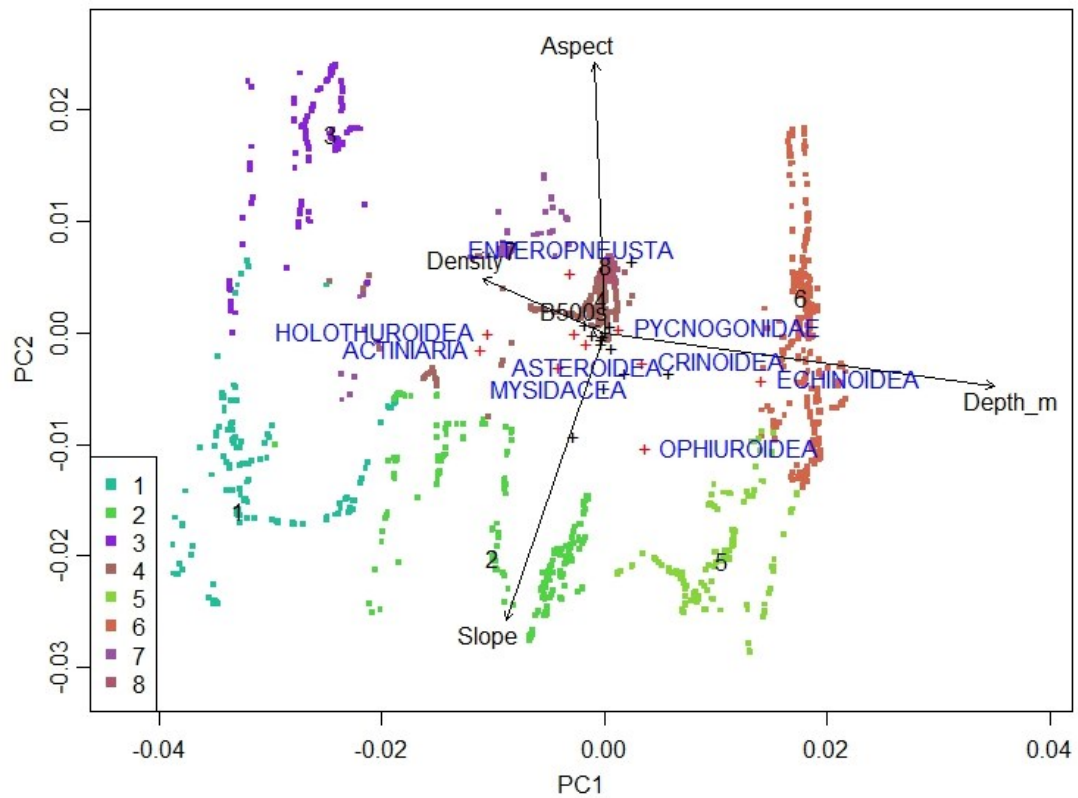


*Figure 4-22. Principal Components Analysis of the first two dimensions and the most important predictors as vectors; red crosses identify the most responsive coral fauna; colored and numbered clusters represent inferred assemblages, rather than a continuous representation of non-coral and non-sponge biodiversity at Orphan Seamount and Orphan Knoll.*

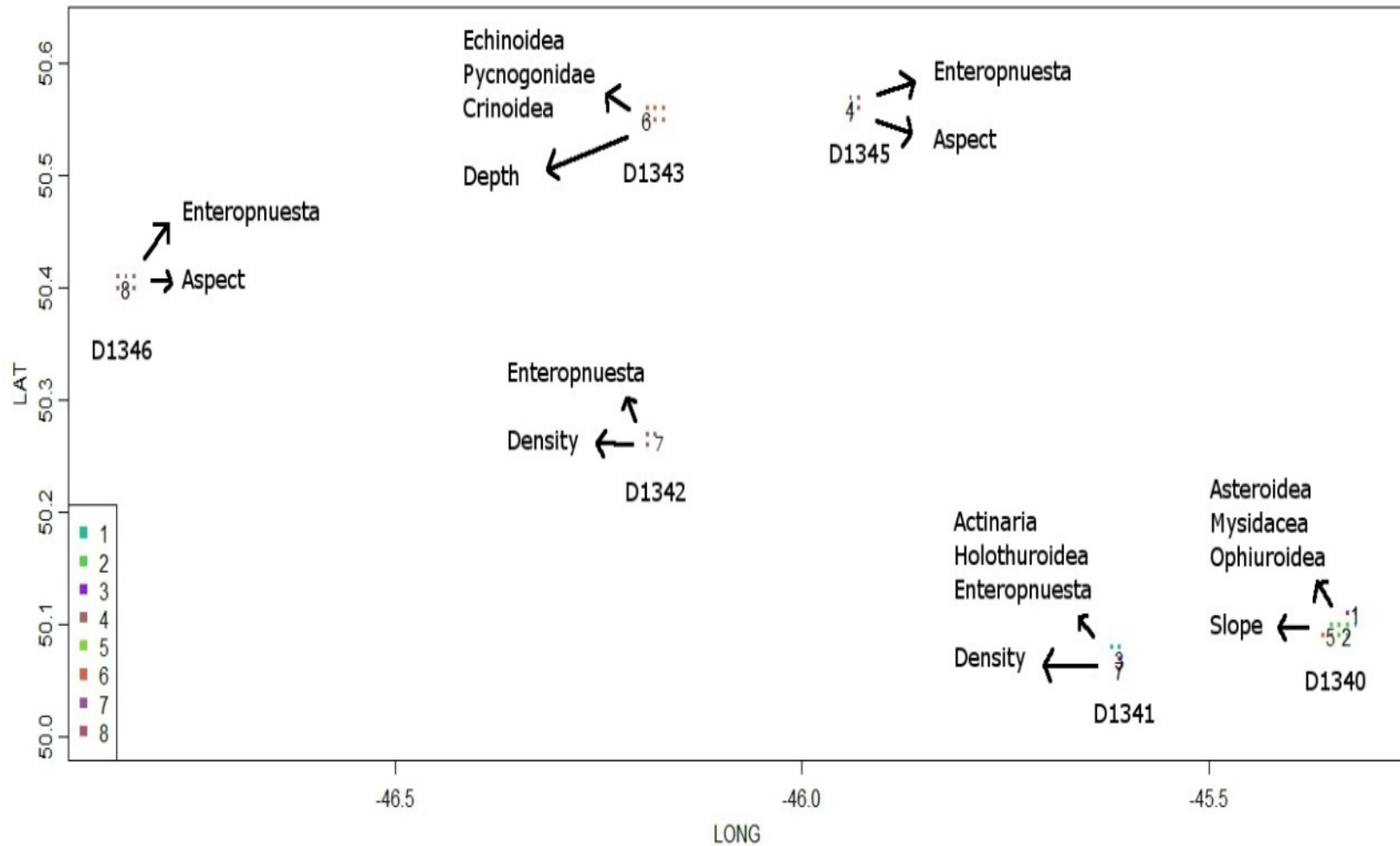


Figure 4-23. Geospatial cluster occurrences of PCA scores. Dive ID (e.g. D1340) is shown below the actual dive location; Arrows are not vectors, but rather labeling arrows for the most responsive non-coral and non-sponge megafauna and the most important environmental drivers relative to a specific dive site.

#### **4.4.1.7 Concentrated Megafaunal Predictor Importance**

A forest of 500 regression trees for each of 10 of the 10 recorded concentrations (>20\*% area coverage) of benthic megafauna, from 19219 ‘sites’ (individual observations), resulted in identifying: Depth, Fine\_Sed, B500s, Slope, and F300s as the most important variables in predicting coral presence in the OK and OS area, between depths of 1720 m to 3000 m (Fig. 4-24) (Appendix 4-7).

#### **4.4.1.8 Concentrated Megafaunal Predictor Importance**

##### ***Gradients***

An increase in biodiversity was indicated by increases in the magnitude of change affecting abundance of multiple species, visualized as kernel density plots occurring along the various data gradients: at 2600 and 1850 m depth; at 5%, 10% and 45% fine grained sediment (Fine\_Sed); on low mid-slopes and low-mid mid-slopes B500s value of 400 and 800 respectively; 11° and 20° slopes; flats and low-mild slopes F300s values of 0 and 400 respectively; 1 – 1.1 rugosity (low surficial complexity - flat), between 5% and 10% and again at 35% granules, between 100-150° and 210° aspect bearings; density values at 1035.8 and 1039.8 kg /m<sup>3</sup>; at 2.75 and 3.4°C temperatures; -0..25 (slight curve) to 0.25 (slight curve) curvatures; pebbles had very poor data density (no notable affects), at 5% and 30% cobbles, conductivity had very poor data density but showed a weak signal at 3.26, at 5% boulders, at 0% , 39% and 65%area coverage of bedrock, ‘structures’

also had low data density but there was a weak response for structure class 12 (wall), zones had poor data density and no notable affects to model accuracy (Fig. 4-25).

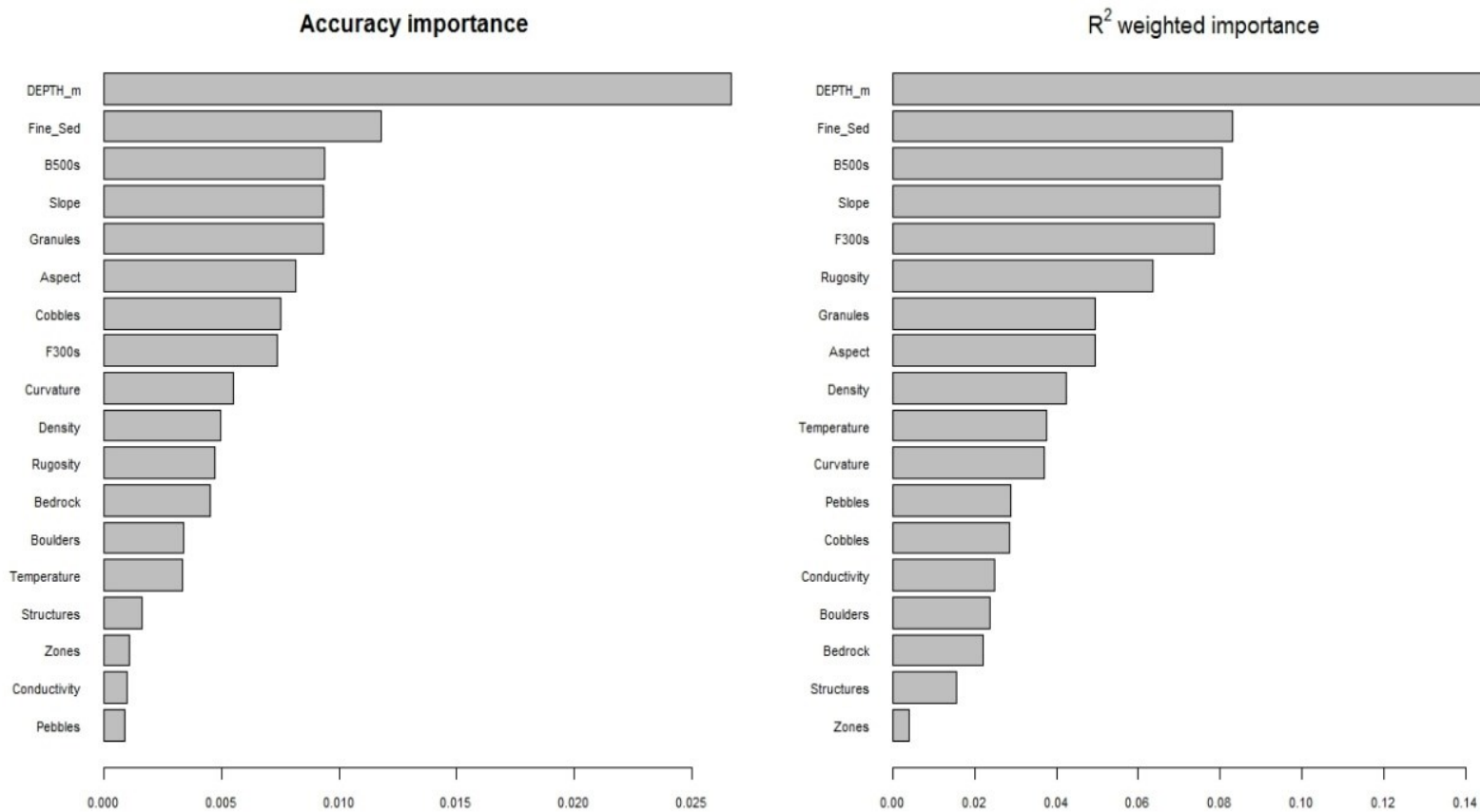


Figure 4-24. gradientForest overall importance analysis of predictors for all concentrations (>20% area coverage) of megafaunal species (left); species-weighted importance analysis of predictors for coral species (right) from Orphan Seamount and Orphan Knoll

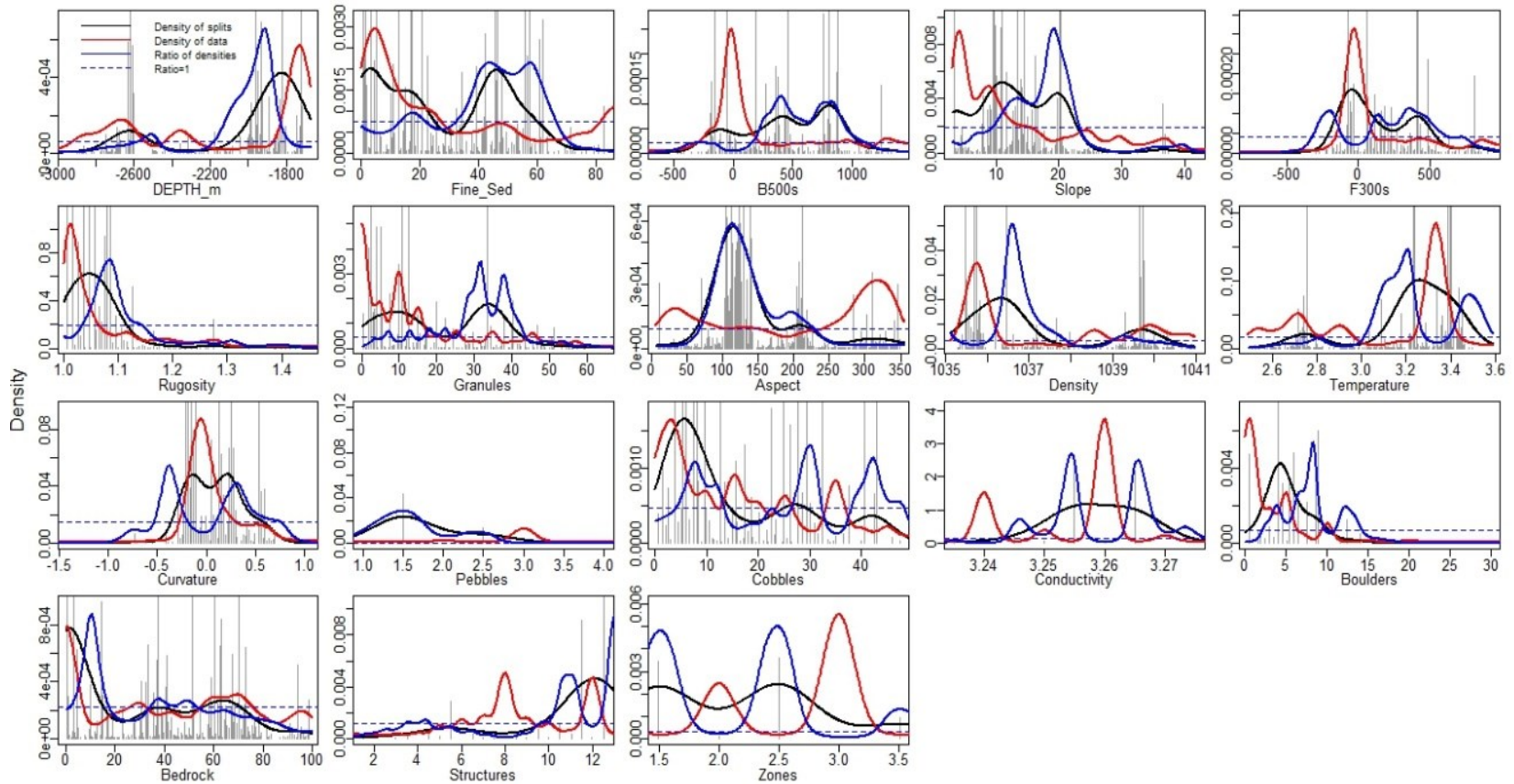


Figure 4-25. Kernel density analysis plots of surrogate gradient change for concentrations (>20% area coverage) of megafaunal species presence from Orphan Seamount and Orphan Knoll

### **Concentrated Megafaunal Species Cumulative Importance (SPI)**

A very gradual increase in cumulative importance (CI) (abundance) was seen for all species with decreasing depths until -2000m whereby a rapid increase in CI was seen for Porifera, *Gersemia* spp. and Isididae until 1900m, and an additional rapid increase in CI for Crinoidea was seen at 1850m (Fig. 4-26).

The fine sediment SPI plots indicate a gradual overall increase in CI with turnovers (rapid increases in CI) between 16-24% (*Chrysogorgia* spp.), 45% (Hexactinellidae/ Porifera/*Acanthogorgia* spp.) and 62% (Pennatulacea)(Fig. 4-26).

The B500s gradient response plots indicated a community turnover for *Chrysogorgia* spp. at -200 (flat depressions), Ophiuroidea and Isididae at 400 (low mid-slope) and *Acanthogorgia* between 750-800 (upper slope)(Fig. 4-26).

The gradient response plots for slope indicated an increase in CI (community turnover) for *Acanthogorgia* and Ceriantharia at 9°, *Chrysogorgia* spp. at 14° and Hexactinellidae / Isididae and Ophiuroidea at 20°(Fig. 4-26).

The F300s SPI plots identified that *Chrysogorgia* spp. and *Gersemia* spp. showed an increased CI at 100 (low slope) and Ceriantharia and *Acanthogorgia* at 400 (large mid-slope)(Fig. 4-26).

The rugosity SPI plots identify a rapid increase in CI for Actinaria, Ophiuroidea and Porifera at 1.05, though the gradual increase in CI for the other species is spread throughout the 1.0 - 1.09 range (Fig. 4-26).

The gradient response plots for granules indicated an increase in CI (community turnover) for *Chrysogorgia* spp. at 34% and Porifera at 40% (Fig. 4-26).

Beginning at 100° aspect a rapid increase in cumulative importance (CI) (abundance) followed by a gradual increase in CI until 140° aspect was seen for all species with Hexactinellidae exhibiting the largest CI increase at 110°.

The gradient response plots for density indicated an increase in CI (community turnover) for *Gersemia* spp. and Crinoidea at 1035.5 kg /m<sup>3</sup>, Pennatulacea and Porifera at 1036.5 kg /m<sup>3</sup> and *Chrysogorgia* spp., Ceriantharia and *Acanthogorgia* spp. at 1039.6 kg /m<sup>3</sup> (Fig. 4-26).

The temperature SPI plots identify three increases in CI as temperature increases from 2.5 to 3.6°C. A rapid increase in CI for *Acanthogorgia* spp., Crinoidea and *Chrysogorgia* spp. at 2.75°C, Pennatulacea and Porifera increased in CI at 3.25°C (greatest overall important turnover), and Ophiuroidea, Isididae and *Gersemia* spp. was seen at 3.4°C (Fig. 4-26).

The curvature SPI plot identifies a gradual increase in CI from -0.25 to 0.6 curvature for all species, however, -0.25 and 0.25 were the two main turnover points (slight curve)(Fig. 4-26).

Not many species responded to surficial geological cues; however, Ophiuroidea and Isididae had a turnover at 1.5% and 2.5% pebbles, *Chrysogorgia* spp. between 5-10% cobbles and Hexactinellidae indicated a turnover at 42% cobbles. Turnover of Isididae occurred at 4% and 9% boulder coverage and *Gersemia* spp. showed turnover at 12% (Fig. 4-26).

The conductivity SPI plot showed that Isididae increased rapidly in CI at 3.265 (S /cm), where the other species gradually increased in CI between 3.24 and 3.27 (S /cm) (Fig. 4-26).

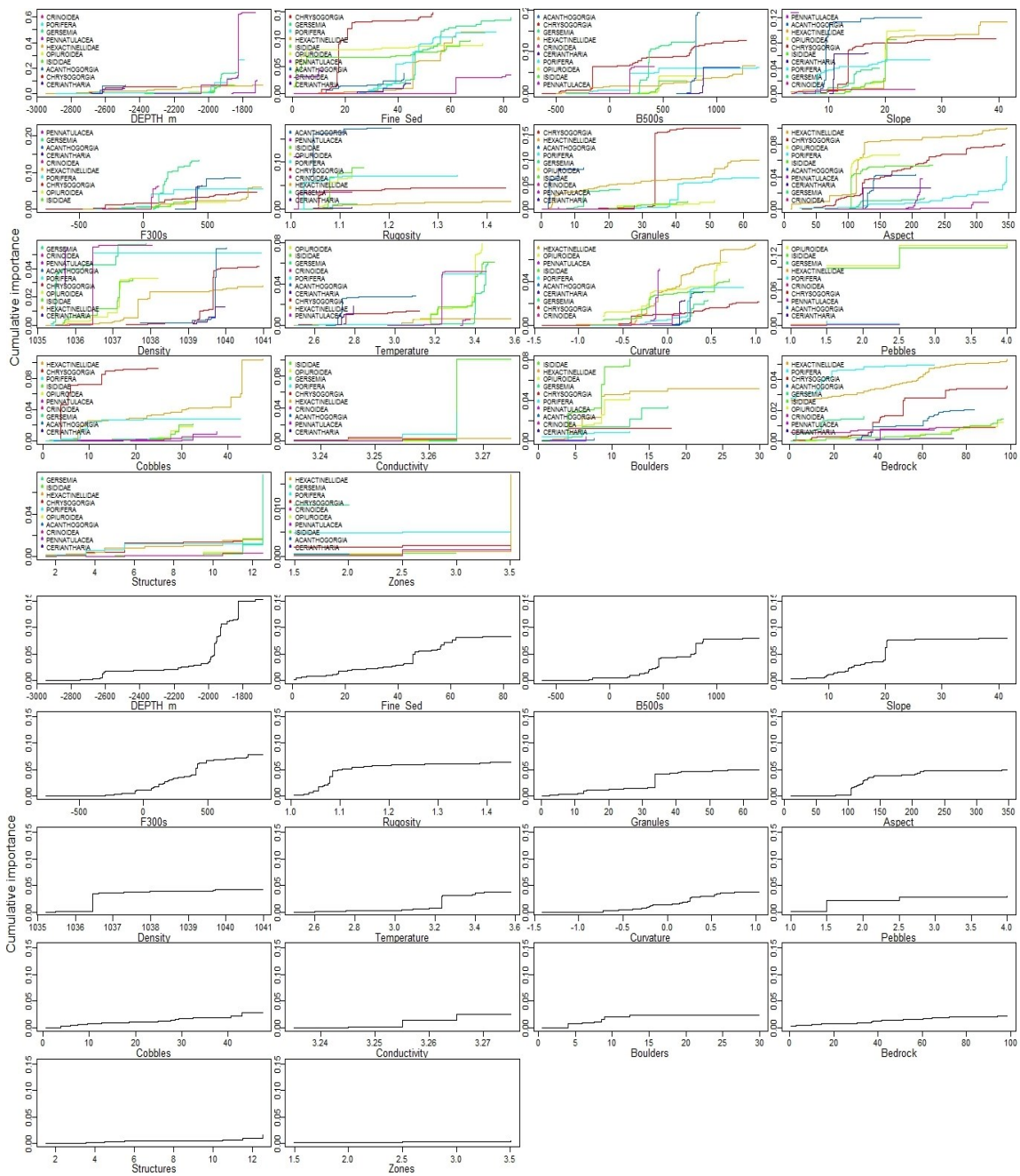


Figure 4-26. Cumulative importance (CI)(top) and Overall CI plots for concentrations (>20% area coverage) of megafaunal species for the OK and OS areas; showing change in abundance of individual species, where changes occur on the gradient and the species changing most on each gradient.

### **Geographic clustering of important predictors relative to species abundance**

Dive 1340 and 1341 contained groups 1,2,6; dive 1345 contained the majority of the clusters (3,4,5,7,8); dives 1342,1343 and 1346 didn't contain any clusters of concentrations of megafauna (Fig. 4-27).

The BPI variables F300 and B500 (which are large scale 300m and 500m depth-slope variables) and slope were most accurate on OS and SE OK, where depth and fine sediment at Eastern OK were the most accurate at predicting abundance through notable changes in community diversity (Fig. 4-28).

Abundant species on OS (D1340) and SE OK (D1341) that are best predicted by slope (at various scales 100m, 300m and 500m) were Hexactinellidae, *Acanthogorgia* spp., *Ceriantharia*, *Chrysogorgia* spp., Porifera and Ophiuroidea (order dictating most accurate predictive response) (Fig. 4-27). Abundant species on East OK (D1345) that are best predicted by depth and fine sediment were *Gersemia* spp., Crinoidea, Pennatulacea (Fig. 4-28).

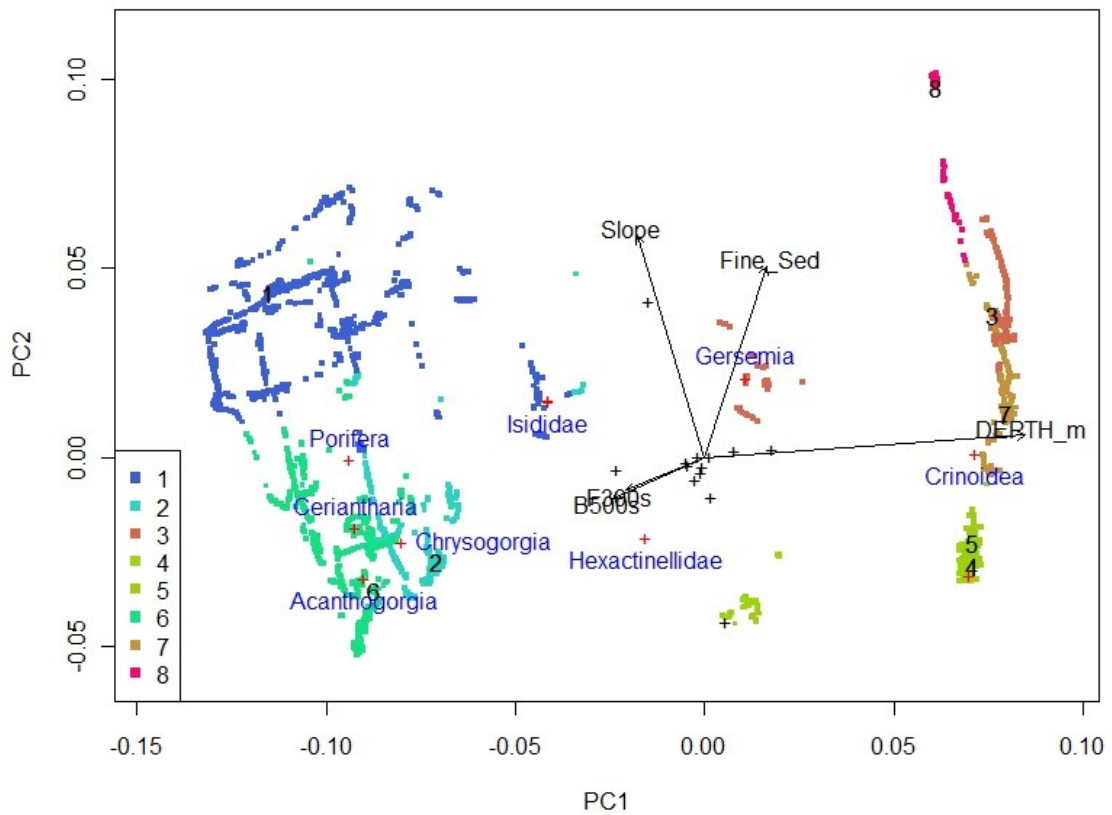


Figure 4-27. Principal Components Analysis of the first two dimensions and the most important predictors as vectors; red crosses identify the most responsive coral fauna; colored and numbered clusters represent inferred assemblages, rather than a continuous representation of concentrations (>20% area coverage) biodiversity at Orphan Seamount and Orphan Knoll.

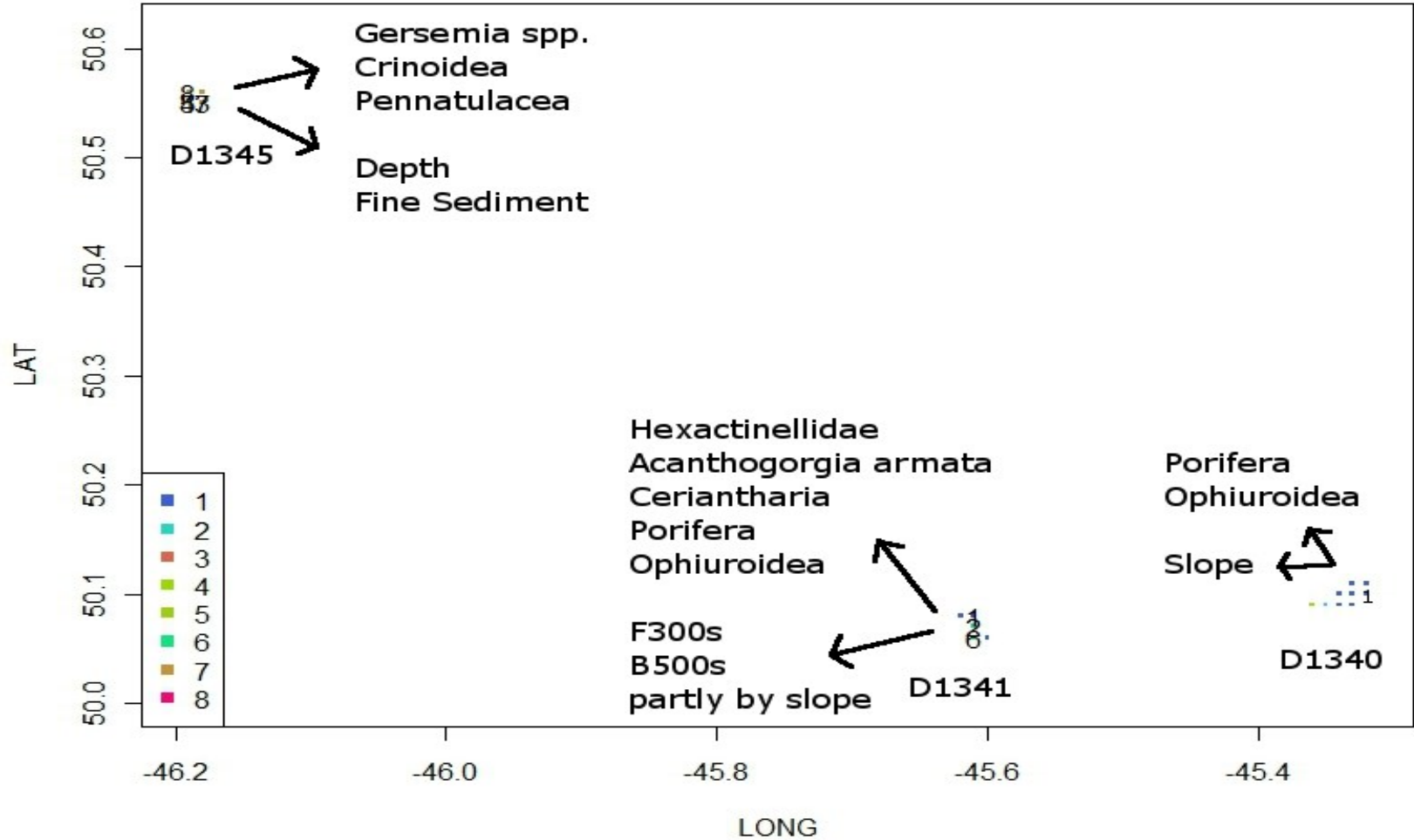


Figure 4-28. Geospatial cluster occurrences of PCA scores. Dive ID (e.g. D1340) is shown below the actual dive location; Arrows are not vectors, but rather labeling arrows for the most responsive concentrations (>20% area coverage) megafauna and the most important environmental drivers relative to a specific dive site.

## 4.5 Discussion

This study presents a detailed examination of megafaunal species abundance and distribution for three unique offshore habitat types in the Northwest Atlantic: Seamounts, knoll mounds and knoll flats. The study was novel by using an ROV, to explore Northwest Atlantic submarine knoll and seamount at Bathyal – Abyssal depths, for discovering deep sea megafaunal species and investigating the relative deep sea habitats and what mechanisms are driving these megafaunal communities. The novel analytical approach compared the relative importance of bathymetric, oceanographic, and geological drivers in megafaunal species' distributions and abundances.

The megafaunal distribution maps and community turnover analysis presented contribute to the NW Atlantic ocean knowledge of deep-sea megafaunal distribution and community drivers of change. These data are the first efforts to identify *in-situ* species distribution for this 'new' eastern extent of the Canadian continental margin (Canadian UNCLOS submission pending), whereby, the community turnover and changes in community abundance were analyzed to better understand how changes of environmental drivers could affect community turnover in a changing climate.

## 4.5.1 Environmental Mechanisms Driving Deep-Sea Megafaunal Abundance and Distribution

The Orphan Knoll megafauna varied among the habitat types found on the knoll (e.g. slopes, flats, exposed bedrock and fine sediment). gradientForest analysis showed that differences in faunal composition were driven by bathymetry, water column properties, and surficial geology, in decreasing order of importance.

### ***4.5.1.1 Bathymetry (Depth, Slope, Aspect)***

#### **Depth**

The principal driver of changes in megafaunal species composition was bathymetry. Depth was identified as the most accurate predictor of changes in community turnover for almost all species in almost all of the habitats examined. Even though depth is often considered an indirect predictor for community turnover, it was most accurate at identifying changes in overall community turnover, as observed in several other deep-sea biodiversity analyses from both the Northwest and Northeast Atlantic (Howell et al. 2010; Baker et al. 2012; Buhl-Mortensen et al. 2012; Gonzalez-Mirelis & Buhl-Mortensen 2015; Davies et al. 2015).

## Slope

On the Orphan Seamount (OS) slopes, slope, itself being a 1<sup>st</sup> derivative of depth, was found to be a reliable predictor of megafaunal composition, as observed on other deep-sea submarine features (Bryan & Metaxas 2007; Heindel et al. 2010; Neves et al. 2014). When the individual species CI plots were examined it was seen that some species saw turnover at different degrees of slope. Sponges were found throughout the seamount and no one species type was restricted to specific depth or substrate types. Slope was the principal variable indicating sponge abundance and distribution, as observed off the coast of Norway (Gonzalez-Mirelis & Buhl-Mortensen 2015).

## Aspect

In the case of Orphan Knoll (OK) flats, aspect (orientation of surface) provided insight into *D.dianthus* and *Bathypathes* spp. distributions, at the transition between flat – sloping (Southern Orphan Knoll). The examination of the individual CI plots identified that some coral species appear to respond more strongly to changes in depth and slope in relation to their orientation. For example, *Desmophyllum dianthus* showed the strongest response to slope at 5-8° slope (and 300° aspect – opposite to the prevailing current) and *Acanella* spp. (225° aspect – normal to current). Dominant changes in abundance in relation to slope occurred at 15-18° slope for *Anthomastus* spp. (125° aspect – into current), 18-25° slope for Isididae (50-60° aspect) and 18-25° slope for Zoantharia (90-100° aspect) indicate that the combination of slope and aspect seemed to influence individual species distributions.

Curiously, *D. dianthus*, which typically grows on vertical or overhanging bedrock faces (Försterra et al. 2005; Baker et al. 2012), was not restricted to the highest slope features, where slope was measured from ship-based multibeam bathymetry at 100 m grid size. This discrepancy indicates the importance of observational scale in analysis: habitat can be described at the oceanographic scale of  $10^1$ - $10^2$  - $10^3$ m, while attachment substrate is often describable only at the 1m scale from video analysis (Miles et al. 2015).

#### **4.5.1.2 Oceanography**

Another mechanism of deep-sea distribution is water circulation on seamounts and submarine bathymetric highs (knolls or seamounts), which move in an anti-cyclonic motion in the northern hemisphere (Christiansen & Wolff 2009; Greenan et al. 2010; Davies et al. 2015). These Taylor columns over bathymetric highs influence the dispersion of food (Particulate Organic Carbon - POC) and sediment flux (Stein 2007; Christiansen & Wolff 2009). This effect can be seen in the increased abundance of *Anthomastus* spp. and Pennatulacea on the edges of the West and Eastern Orphan Knoll flats (Table 4-1, Fig. 4-9), relative to the centre of the knoll. The effects of the Taylor Column (strongest currents at the margins of the feature, least water movement in center) leave the center of OK with less abundant megafaunal species, but the diversity of megafauna remained surprisingly moderate. Increased biodiversity on the OK slope and on the slopes of OS was not surprising however, a higher biodiversity of hard cold-water corals (CCW) near the center of OK was surprising and found to occur on the exposed winnowed sedimentary mounds, providing the hard sloped substrates colonized by slope

capable species as observed by other stony corals on other submarine sloping terrain (O'Hara et al. 2008; Buhl-Mortensen, Buhl-Mortensen, et al. 2009; Howell et al. 2010; Baker et al. 2012; Davies et al. 2015). Low sedimentation rates near the centre of the knoll may also help to explain the very old ages of subfossil corals observed in the coral graveyard on the Orphan Knoll NE mounds, where the oldest coral collected was 181 ka (Menabreaz 2015).

*Table 4-1. Synthesis of Spatial PCA plots of gradientForest separated by Habitat and BioType ('inverts' are non-coral and non-sponge, 'concen' are >20% area coverage of any one abbreviated faunal types: Antho=Anthomastus spp., Zoan=Zoantharia, Porif=Porifera, Euplec=Euplectella, Aster=Asteroidea, Mysid=Mysidae spp., Oph=Ophiuriodea, Ceri=Ceriantharia, Vaug=Vaughnella spp., Penn=Pennatulacea, Hexa=Hexactinellidae, Acanth=Acanthogorgia spp., Desmo=Desmophyllum dianthus, Bathy=Bathypathes spp., Poly=Polymastia, Echin=Echinodermata, Pycno=Pycnogonidae spp., Crin=Crinoidea, Enter=Enteropneusta spp., Gers=Gersemia spp., Holo= Holothuroidea)*

Dive	Habitat	BioType	Driving Variables	Species Affected by Change in Magnitude of Drivers	PCA Clusters
1340	OS	coral	Slope	Antho, Zoan	1,2,3
1340	OS	sponge	Slope, Density	Porif, Euplec	1,2,5
1340	OS	inverts	Slope	Aster, Mysid, Oph	1,2,5
1340	OS	concen	Slope	Porif, Oph	1
1341	SE mound	coral	Depth	Ceri, Vaughn	5, 6
1343	NE mound	coral	Conductivity	Antho, Penn	8
1341	SE mound	sponge	Density	Porif	3
1343	NE mound	sponge	Depth	Hexa	6
1341	SE mound	inverts	Density	Actin, Holo, Enter	3,7
1343	NE mound	inverts	Density	Enter	7
1341	SE mound	concen	Depth-Slope	Hex, Acanth, Ceri, Porif, Oph	1,2,6
1343	NE mound	concen	na	Na	Na
1342	S flat	coral	Aspect	Desmo, Bathy	7,4
1346	W flat	coral	Conductivity	Antho, Penn	8
1345	E flat	coral	Conductivity	Antho, Penn	8
1342	S flat	sponge	Depth	Polym	7, 8
1346	W flat	sponge	Depth	Hexa	6
1345	E flat	sponge	Depth	Hexa	6
1342	S flat	inverts	Depth	Echn,Pycn, Crin	6
1346	W flat	inverts	Aspect	Enter	4
1345	E flat	inverts	Aspect	Enter	8
1342	S flat	concen	na	Na	Na
1346	W flat	concen	Depth,Fine Sed	Gers, Crin, Penn	3,5,7,8
1345	E flat	concen	na	Na	Na

### 4.5.1.3 *Surficial Geology*

The importance of surficial geology as an accurate predictor of community turnover, was always less accurate than bathymetry or oceanography. However, surficial geology does play a role in distribution of sessile megafaunal species, such as cold-water corals (CWC's), most of which require a hard substrate to form a holdfast to support its colony growth and effectively compete for access to food (O'Hara et al. 2008; Baker et al. 2012). The surficial geology indicates hard or soft substrates, thereby helping to determine distribution of megafaunal species such as CWC's. This is seen in the distribution of hard CWC on boulders and sloped hard substrate (IRD, cobbles, walls) on the Orphan Knoll NE mounds and the slopes of Orphan Seamount, as also observed on other seamounts and other sloped habitat (i.e. canyon walls) (Heindel et al. 2010; Davies & Guinotte 2011; Baker et al. 2012). Some types of soft corals, such as Pennatulaceans (sea pens) and some small bamboo coral such as *Acanella arbuscula* have the ability to anchor their colony structure within a variety of substrate types (predominantly fine sediment), and are also found periodically in depressions of fine sediment within hard substrate on the Orphan Seamount. The seamount slopes were a varied geology with bedrock outcrops throughout the seamount, boulders near the top and bottom of the seamount, and cobbles, granules and fine sediment draped over the slopes, most predominant at the medium-upper depths of the seamount.

On the Orphan Knoll flats (D1345, D1346), an increase in fine sediment with a decrease in depth indicated a change in community turnover for large abundances of *Gersemia* spp., Crinoidea and Pennatulacea. This change was seen primarily on the

Western OK (D1346) where a decrease in depth along the borders of OK would align these species with a higher speed northerly current, thus bringing more food. The depth and orientation to food sources observations are analogous to previous studies for coral and sponge distributions (Bryan & Metaxas 2006; Watanabe et al. 2009; Baillon et al. 2014).

#### ***4.5.1.4 Not a Typical Continental Margin***

One other pattern influencing distributions of deep-sea megafauna is geographical distance from land. The continental margin habitats are subject to processes such as wave-activated sediment transport and terrigenous sedimentation resulting in active sediment resuspension and much higher rates of sediment accumulation at continental slope depths than observed in mid-ocean benthic habitats (King et al. 1985; Amos & Judge 1991; Greenan et al. 2010). By contrast, the Orphan Knoll and Orphan Seamount are separated from the continental margin and are not affected by the same sedimentary input from terrigenous sources (Piper 2005; Xu et al. 2009). Instead, the main sources of sediment on the OS and OK are fine-grained hemipelagic (biogenic) sediment and coarse-grained ice-rafted debris (IRD). The ubiquitous ice-rafted debris occurring on all bottom-types at OS and OK may also help to reduce the variation in species composition between surficial geology bottom types, as IRD can provide hard substrates within otherwise fine-grained facies. This abundance of IRD, not buried by hemipelagic sedimentation, contrasts strongly with the predominant abundance of mud along the continental slope of most continental margin environments in the Northwest Atlantic (Edinger et al. 2011).

The distance from land and great depth has created a relatively stable habitat, where steep slopes facing into to the slow predominant deep water current, promote some particle resuspension on the tops of Orphan Knoll (up-welling and down-welling) (Davies et al. 2009). The OK and Orphan Seamount are on the eastern limit of the continental margin and are deep bathymetric features with sloped edges. Depending on the speed of the water currents and the orientation of the megafauna to the predominant water current, Orphan Seamount slopes and the ice-rafted debris (IRD) on Orphan Knoll, might have provided a suitable habitat for slope-capable species during previous glacial cycles (excessive sedimentation and changing environmental conditions). These environmental mechanisms may help explain the megafaunal distributions on OK and OS (i.e. natural selection of slope capable species) (Yasuhara et al. 2008).

Changes in primary productivity over glacial cycles may have altered abundance and distribution of corals in these offshore environments, which may help explain why *Desmophyllum dianthus* on the Orphan Knoll Northeast mounds appear to have been absent or present in extremely low abundance during Quaternary glaciations, and present (or more abundant) during interstadials (MIS 7, 5c, and 1;(Menabreaz 2015)).

The OK and OS share a similar shape, depth and orientation to the predominant deep NE Atlantic water mass moving west over the OK and OS. This results in similar oceanographic drivers for habitats with exposed slope and aspect to the current's flow, regardless of the difference in size (OK is much larger than OS). When examining the drivers of change in megafaunal community diversity on Orphan Seamount, OK mounds

and OK flats, increasing slope, depth and aspect slightly indicated increases in community turnover for all megafauna on OS.

The mound habitats appear to be most affected by changes in water chemistry, where small density and conductivity increases showed increase community turnover in Actinaria, Holothuroida, Enteronusta, Porifera, *Anthomastus* spp. and Pennatulacea, Deep-sea megafaunal sensitivities to oceanographic drivers were also documented on other mounds (Roberts et al. 2003; Roberts et al. 2006).

For filter-feeding deep-sea coral species, access to deep food rich water is essential (Bryan & Metaxas 2006; Hall-spencer et al. 2007; O'Hara et al. 2008; Gilkinson & Edinger 2009). The mechanism by which the combination of slope and aspect become important to faunal distribution may be through access to food. This combination may be seen in the distribution of megafauna on OK and OS and in the examination of the changes in magnitude of their community turnover.

The deep NE Atlantic water mass forms a stable oceanographic environment (temperature avg.  $3^{\circ}\text{C} \pm 0.2^{\circ}\text{C}$ , salinity 34.9 PSU,  $\text{DO}_2$  8-8.4 mg /L: (Greenan et al. 2010)). This stable current allows for consistent growing conditions, affecting megafaunal distribution and community turnover for *Anthomastus* spp. and Pennatulacea, with respect to the western and eastern edges of the Orphan Knoll. The predominant current (food supply) is supplemented from the overlaying Denmark Strait water mass (Greenan et al. 2010). Additionally, the Denmark Strait water mass also brings Particulate Organic Carbon (POC), Dissolved Inorganic Carbon (DIC) and Ice-Rafted Debris through transportation of Labrador Sea ice, providing additional habitat for some hard CCW (i.e.

*D. dianthus*, *Bathypathes* spp. and *Zoantharia*) and food for all megafaunal species on the OK and OS. Down welling and upwelling patterns of water movement as delivery methods of food and reproduction have also been observed in the deep North Atlantic (Stein 2007; Han et al. 2008; Miles et al. 2015).

#### **4.5.1.5 Community Ecology Analysis**

Recent advances in statistical processing and advancing technologies now allow for comprehensive community analysis. One such method is community analysis through gradientForest and the statistical software R, which is especially helpful when examining a multitude of variables from various sites possibly affecting multiple species.

gradientForest was effective at discerning drivers of community turnover, which then demonstrated a variable's importance in its accuracy to model the magnitude of change in species abundance (Ellis et al. 2012). Examining the effects of surficial geology, oceanographic, bathymetric and biological presence data, was done through combining all the different data sets and analyzing the data in R, through the gradientForest analysis package. The analysis of NW Atlantic coral, sponge, and other benthic megafaunal species distributions on a continental margin (Baker et al. 2012) and at offshore sites could yield more insights (Miles et al. 2015), though a broad comprehensive study of this scale is beyond the scope of this study.

Community turnover examination, such as the work presented, at a species level are not seen in the overall CI plot, which may be helpful in explaining the megafaunal groups as a whole, but the ability of the individual CI plots were shown to be effective

indicators of species sensitivities to their physical surroundings. This addresses the issues of analysis and the scale at which the interpretation occurs, as observed off the coast of Norway (Gonzalez-Mirelis & Buhl-Mortensen 2015). Therefore, bathymetry, oceanography and geology datasets are used in habitat models to create ‘informed’ investigations of several predictors, to help reduce the effects of bathymetric predictor bias, when interpreting cumulative and overall importance plots of community turnover for deep-sea megafauna.

These findings confirm the importance of field data in habitat modeling. Comprehensive field studies help create ‘informed’ models that show the importance of good bathymetric, oceanographic and geological data in relation to creating habitat modeling at seamounts and other deep-sea bathymetric highs (Buhl-Mortensen, Buhl-Mortensen, et al. 2009; Buhl-Mortensen, Dolan, et al. 2009; Davies & Guinotte 2011; Buhl-Mortensen et al. 2012; Gonzalez-Mirelis & Buhl-Mortensen 2015).

## 4.6 Conclusions

Oceanographic , Bathymetric and Geological datasets combined can help explain the magnitude of change of species level community turnover, gaining insight into changes along the gradient which can identify preferred depths, slope, aspect, density, etc, conditions for increased abundance and distribution of deep-sea megafauna.

Megafaunal species on the periphery of a Taylor Column will be exposed to greater current and thus food supply and increased sediment removal, best inhabited by low-lying megafauna, not unlike observations at other seamounts (O'Hara et al. 2008).

The Orphan Seamount is a biological hotspot, not unlike other deep-sea seamounts, with abundant megafauna distributed throughout the seamount (Hall-spencer et al. 2007; O'Hara et al. 2008; Howell et al. 2010). Sponge communities on OS showed some sensitivity to density changes but were found throughout the dive transects.

This was one of the first studies of coral and sponge distributions in a deep-sea environment not previously affected by fishing activity. This study identifies some sensitivities of easily collected variables that drive change within community turnover in the deep sea. For the Orphan Knoll and Orphan Seamount, the deep-sea species that are slope capable, which apparently are many, will have the best chance at survival in the deep sea.

## 4.7 Bibliography

- Alt, J., 1988. Hydrothermal oxide and nontronite deposits on seamounts in the eastern Pacific. *Marine Geology*, 81(1–4), pp.227–239.
- Althaus, F. et al., 2009. Impacts of bottom trawling on deep-coral ecosystems of seamounts are long-lasting. *Marine Ecology Progress Series*, 397, pp.279–294. Available at: <http://www.int-res.com/abstracts/meps/v397/p279-294/>.
- Amos, C. & Judge, J., 1991. Sediment transport on the eastern Canadian continental shelf. *Continental Shelf Research*, 11(8–10), pp.1037–1068. Available at: <http://linkinghub.elsevier.com/retrieve/pii/027843439190090S>.
- Austin, M., 2002. Spatial prediction of species distribution: an interface between ecological theory and statistical modelling. *Ecological Modelling*, 157(2–3), pp.101–118. Available at: <http://linkinghub.elsevier.com/retrieve/pii/S0304380002002053>.
- Bailey, W. et al., 2003. The spatial distributions of fault and deep sea carbonate mounds in the Porcupine Basin, offshore Ireland. *Marine and Petroleum Geology*, 20, pp.509–522.
- Baillon, S., Hamel, J.-F. & Mercier, A., 2014. Diversity, distribution and nature of faunal associations with deep-sea pennatulacean corals in the northwest atlantic. *PloS one*, 9(11), p.16. Available at: <http://dx.plos.org/10.1371/journal.pone.0111519>.
- Baker, K. et al., 2012. Distributional patterns of deep-sea coral assemblages in three submarine canyons off Newfoundland, Canada. *Marine Ecology Progress Series*, 445, pp.235–249. Available at: <http://www.int-res.com/abstracts/meps/v445/p235-249/>.
- Barrett, T. et al., 1988. Geochemical aspects of hydrothermal sediments in the eastern Pacific Ocean; an update. *Canadian Mineralogist*, 26(3), p.841.
- Barrie, J. & Conway, K., 2008. Surficial geology: The third dimension in habitat mapping. In J. Reynolds & H. Greene, eds. *Marine Habitat Mapping Technology for Alaska*. Fairbanks, AK: University of Alaska Fairbanks, pp. 91–97.
- Beazley, L. et al., 2015. Drivers of epibenthic megafaunal composition in the sponge grounds of the Sackville Spur, northwest Atlantic. *Deep Sea Research Part I: Oceanographic Research Papers*, 98, pp.102–114.
- Bellier, J.-P., Mathieu, R. & Granier, B., 2010. Short Treatise on Foraminiferology (Essential on modern and fossil Foraminifera). In *Carnets de Geologie*. p. 106.
- Berggren, W. & Aubert, J., 1976. Eocene benthonic foraminiferal biostratigraphy and paleobathymetry of Orphan Knoll (Labrador Sea). *Micropaleontology*, 22(3), pp.327–346.
- Blow, W., 1956. Origin and Evolution of the Foraminiferal Genus *Orbulina* d'Orbigny. *Micropaleontology*, 2(1), pp.57–70. Available at: <http://www.jstor.org/stable/1484492>.

- Bluhm, B., Iken, K. & Hopcroft, R., 2010. Observations and exploration of the Arctic's Canada Basin and the Chukchi Sea: The Hidden Ocean and RUSALCA expeditions. *Deep Sea Research Part II: Topical Studies in Oceanography*, 57(1–2), pp.1–4. Available at: <http://linkinghub.elsevier.com/retrieve/pii/S0967064509002446> [Accessed February 18, 2011].
- Bolton, B. et al., 1988. Geochemistry and mineralogy of seafloor hydrothermal and hydrogenetic Mn oxide deposits from the Manus Basin and Bismarck Archipelago region of the southwest Pacific Ocean. *Marine Geology*, 85(1), pp.65–87.
- Boutillier, J. et al., 2008. Status of Cold-Water Coral Communities of the World: A Brief Update. In T. Hourigan, ed. *Status of Coral Reefs of the World*. Australian Institute of Marine Science, pp. 58–66.
- Breeze, H. et al., 1997. Distribution and Status of Deep Sea Corals off Nova Scotia. *Ecology & Action*, (1), pp.1–40. Available at: [http://www.ecologyaction.ca/files/images/file/Marine/Distribution and Status of Deep Sea Coral off Nova Scotia Part 1.pdf](http://www.ecologyaction.ca/files/images/file/Marine/Distribution%20and%20Status%20of%20Deep%20Sea%20Coral%20off%20Nova%20Scotia%20Part%201.pdf).
- Bronner, A. et al., 2011. Magmatic breakup as an explanation for magnetic anomalies at magma-poor rifted margins. *Nature Geoscience Letters*, 4(8), pp.549–553. Available at: <http://dx.doi.org/10.1038/ngeo1201>.
- Brown, C. et al., 2011. Benthic habitat mapping: A review of progress towards improved understanding of the spatial ecology of the seafloor using acoustic techniques. *Estuarine, Coastal and Shelf Science*, 92(3), pp.502–520. Available at: <http://linkinghub.elsevier.com/retrieve/pii/S0272771411000485> [Accessed March 16, 2012].
- Bryan, T. & Metaxas, A., 2006. Distribution of deep-water corals along the North American continental margins: Relationships with environmental factors. *Deep Sea Research Part I: Oceanographic Research Papers*, 53(12), pp.1865–1879. Available at: <http://linkinghub.elsevier.com/retrieve/pii/S0967063706002378>.
- Bryan, T. & Metaxas, A., 2007. Predicting suitable habitat for deep-water gorgonian corals on the Atlantic and Pacific Continental Margins of North America. *Marine Ecology Progress Series*, 330, pp.113–126. Available at: <http://www.int-res.com/abstracts/meps/v330/p113-126/>.
- Buhl-Mortensen, L. et al., 2010. Biological structures as a source of habitat heterogeneity and biodiversity on the deep ocean margins. *Marine Ecology*, 31(1), pp.21–50. Available at: <http://blackwell-synergy.com/doi/abs/10.1111/j.1439-0485.2010.00359.x>.
- Buhl-Mortensen, L. et al., 2012. Habitat complexity and bottom fauna composition at different scales on the continental shelf and slope of northern Norway. *Hydrobiologia*, 685(1), pp.191–219.
- Buhl-Mortensen, P., Buhl-Mortensen, L., et al., 2009. Megafaunal diversity associated with marine landscapes of northern Norway: A preliminary assessment. *Norsk Geologisk Tidsskrift*, 89(1–2), pp.163–171.

- Buhl-Mortensen, P., Dolan, M. & Buhl-Mortensen, L., 2009. Prediction of benthic biotopes on a Norwegian offshore bank using a combination of multivariate analysis and GIS classification. *ICES Journal of Marine Science*, 66(9), pp.2026–2032. Available at: <http://icesjms.oxfordjournals.org/content/66/9/2026.short>.
- Burton-Ferguson, R., Enachescu, M. & Hiscott, R., 2006. Preliminary Seismic Interpretation and Maps for the Paleogene-Neogene (Tertiary) Succession, Orphan Basin. *Recorder*, 31(7), pp.28–32.
- Burton, E. & Lundsten, L., 2008. Davidson Seamount taxonomic guide. *Marine sanctuaries conservation series ; ONMS-08-08*, pp.1–160. Available at: <http://sanctuaries.noaa.gov/science/conservation/pdfs/taxonomic.pdf>.
- Carlson, A. et al., 2007. Geochemical proxies of North American freshwater routing during the Younger Dryas cold event. *Proceedings of the National Academy of Sciences*, 104(16), pp.6556–6561. Available at: <http://www.pubmedcentral.nih.gov/articlerender.fcgi?artid=1871824&tool=pmcentrez&rendertype=abstract>.
- Carmack, E. & Wassmann, P., 2006. Food webs and physical-biological coupling on pan-Arctic shelves: Unifying concepts and comprehensive perspectives. *Progress in Oceanography*, 71(2–4), pp.446–477.
- Carpenter, K. et al., 2008. One-Third of Reef-Building Corals Face Elevated Extinction Risk from Climate Change and Local Impacts. *Science*, 321(5888), pp.560–563. Available at: <http://www.sciencemag.org/content/321/5888/560.abstract>.
- Channell, J. et al., 2006. IODP Expeditions 303 and 306 Monitor Miocene-Quaternary Climate in the North Atlantic. *Scientific Drilling*, 2, pp.4–10.
- Chian, D., Reid, I. & Jackson, H., 2001. Crustal structure beneath Orphan Basin and implications for nonvolcanic continental rifting. *Journal Geophysical Research*, 106(B6), pp.10923–10940. Available at: <http://dx.doi.org/10.1029/2000JB900422>.
- Christiansen, B. & Wolff, G., 2009. The oceanography, biogeochemistry and ecology of two NE Atlantic seamounts: The OASIS project. *Deep Sea Research Part II: Topical Studies in Oceanography*, 56(25), pp.2579–2581. Available at: <http://linkinghub.elsevier.com/retrieve/pii/S0967064508004451> [Accessed September 2, 2010].
- Coles, G. et al., 1996. Foraminifera and Ostracoda from Quaternary carbonate mounds associated with gas seepage in the Porcupine Basin, offshore Western Ireland. *Revista Española de Micropaleontología*, XXVIII(2), pp.113–151.
- Colman, J. et al., 2005. Carbonate mounds off Mauritania, Northwest Africa: status of deep-water corals and implications for management of fishing and oil exploration activities. In A. Freiwald & J. M. Roberts, eds. Erlangen Earth Conference Series. Springer Berlin Heidelberg, pp. 417–441. Available at: [http://dx.doi.org/10.1007/3-540-27673-4\\_21](http://dx.doi.org/10.1007/3-540-27673-4_21).
- Compton, R., 1985. *Geology in the Field* 1st ed., John Wiley & Sons, Inc.

- Costello, M., 2009. Distinguishing marine habitat classification concepts for ecological data management. *Marine Ecology Progress Series*, 397, pp.253–268. Available at: <http://www.int-res.com/abstracts/meps/v397/p253-268/> [Accessed July 27, 2010].
- Cronan, D., Rothwell, G. & Croudace, I., 2010. An ITRAX Geochemical Study of Ferromanganiferous Sediments from the Penrhyn Basin, South Pacific Ocean. *Marine Georesources & Geotechnology*, 28(3), pp.207–221. Available at: <http://search.ebscohost.com/login.aspx?direct=true&db=aph&AN=53155598&site=ehost-live&scope=site>.
- Curewitz, D. & Karson, J., 1997. Structural settings of hydrothermal outflow: Fracture permeability maintained by fault propagation and interaction. *Journal of Volcanology and Geothermal Research*, 79(3–4), pp.149–168. Available at: <http://www.sciencedirect.com/science/article/pii/S0377027397000279>.
- Danovaro, R. et al., 2001. Deep-sea ecosystem response to climate changes: the eastern Mediterranean case study. *Trends in Ecology & Evolution*, 16(9), pp.505–510.
- Danovaro, R. et al., 2008. Exponential decline of deep-sea ecosystem functioning linked to benthic biodiversity loss. *Current Biology*, 18(1), pp.1–8. Available at: <http://www.sciencedirect.com/science/article/pii/S0960982207023421> [Accessed March 9, 2012].
- Davies, A. et al., 2009. Downwelling and deep-water bottom currents as food supply mechanisms to the cold-water coral *Lophelia pertusa* (Scleractinia) at the Mingulay Reef complex. *Limnology and Oceanography*, 54(2), pp.620–629. Available at: <http://hdl.handle.net/10242/44685>.
- Davies, A. et al., 2008. Predicting suitable habitat for the cold-water coral *Lophelia pertusa* (Scleractinia). *Deep Sea Research Part I: Oceanographic Research Papers*, 55(8), pp.1048–1062. Available at: <http://linkinghub.elsevier.com/retrieve/pii/S0967063708000836> [Accessed February 11, 2011].
- Davies, A., Roberts, M. & Hall-Spencer, J., 2007. Preserving deep-sea natural heritage: Emerging issues in offshore conservation and management. *Biological Conservation*, 138(3–4), pp.299–312. Available at: <http://www.sciencedirect.com/science/article/pii/S0006320707002285>.
- Davies, A.J. & Guinotte, J.M., 2011. Global habitat suitability for framework-forming cold-water corals. *PloS one*, 6(4), pp.1–15. Available at: <http://www.pubmedcentral.nih.gov/articlerender.fcgi?artid=3078123&tool=pmcentrez&rendertype=abstract> [Accessed March 18, 2012].
- Davies, J. et al., 2015. Benthic Assemblages of the Anton Dohrn Seamount (NE Atlantic): Defining Deep-Sea Biotopes to Support Habitat Mapping and Management Efforts with a Focus on Vulnerable Marine Ecosystems. *PloS one*, 10(5), p.33. Available at: <http://www.pubmedcentral.nih.gov/articlerender.fcgi?artid=4436255&tool=pmcentrez&rendertype=abstract>.
- Dowsett, H. & Robinson, M., 2007. Mid-Pliocene planktic foraminifera assemblage of

- the North Atlantic Ocean. *Micropaleontology*, 53(1–2), pp.105–126. Available at: <http://micropal.geoscienceworld.org/cgi/content/abstract/53/1-2/105>.
- Dronov, A., 1993. Middle paleozoic waulsortian-type mud mounds in Southern Fergana (Southern Tien-Shan, commonwealth of independent states): The shallow-water atoll model. *Facies*, 28(1), pp.169–180. Available at: <http://dx.doi.org/10.1007/BF02539735>.
- Durán Muñoz, P. & Sayago-Gil, M., 2011. An overview of cold-water coral protection on the high seas: The Hatton bank (NE Atlantic)—A case study. *Marine Policy*, 35(5), pp.615–622. Available at: <http://www.sciencedirect.com/science/article/pii/S0308597X11000248>.
- Edinger, E. et al., 2011. Geological features supporting deep-sea coral habitat in Atlantic Canada. *Continental Shelf Research*, 31(2, Supplement), pp.S69–S84. Available at: <http://www.sciencedirect.com/science/article/pii/S0278434310002220>.
- Elith, J. et al., 2010. A statistical explanation of MaxEnt for ecologists. *Diversity and Distributions*, 17(1), p.no-no. Available at: <http://doi.wiley.com/10.1111/j.1472-4642.2010.00725.x> [Accessed November 25, 2010].
- Ellis, N., Smith, S. & Pitcher, R., 2012. Gradient forests: calculating importance gradients on physical predictors. *Ecological Society of America*, 93(1), pp.156–168.
- Enachescu, M., 2004. Conspicuous deepwater submarine mounds in the northeastern Orphan Basin and on the Orphan Knoll, offshore Newfoundland. *The Leading Edge*, 23(12), pp.1290–1294. Available at: <http://link.aip.org/link/LEEDFF/v23/i12/p1290/s1&Agg=doi>.
- Enachescu, M., 2009. *Investigating basin architecture and evolution of the Orphan Basin by use of reflection, refraction, heatflow and potential filed transects*, St. John's, NL.
- Enachescu, M., 2005. Offshore Newfoundland and Labrador - An Emerging Energy Powerhouse. In *Offshore Technology Conference*. Houston ,TX: Offshore Technology Conference, pp. 1–8. Available at: <http://www.onepetro.org/mslib/servlet/onepetropreview?id=OTC-17570-MS&soc=OTC>.
- Etnoyer, P., 2005. Seamount resolution in satellite-derived bathymetry. *Geochemistry Geophysics Geosystems*, 6(3), pp.311–312. Available at: <http://www.agu.org/pubs/crossref/2005/2004GC000833.shtml> [Accessed February 11, 2011].
- Farrand, W. & Lane, M., 2007. New observations of enigmatic landforms and surface terrains on the northern plains of Mars. In *Geological Society of America Annual Meeting*. Denver, CO: Geological Society of America. Available at: [https://gsa.confex.com/gsa/2007AM/finalprogram/abstract\\_129996.htm](https://gsa.confex.com/gsa/2007AM/finalprogram/abstract_129996.htm).
- Ferrier, S. et al., 2006. Novel methods improve prediction of species ' distributions from occurrence data. *Ecography*, 29, pp.129–151.
- Ferrier, S. et al., 2007. Using generalized dissimilarity modelling to analyse and predict

- patterns of beta diversity in regional biodiversity assessment. *Diversity and Distributions*, 13(3), pp.252–264. Available at: <http://blackwell-synergy.com/doi/abs/10.1111/j.1472-4642.2007.00341.x>.
- Fischer, J. & Schott, F., 2002. Labrador Sea Water Tracked by Profiling Floats—From the Boundary Current into the Open North Atlantic. *Journal of Physical Oceanography*, 32(2), pp.573–584. Available at: [http://journals.ametsoc.org/doi/abs/10.1175/1520-0485\(2002\)032%3C0573:LSWTBP%3E2.0.CO;2](http://journals.ametsoc.org/doi/abs/10.1175/1520-0485(2002)032%3C0573:LSWTBP%3E2.0.CO;2).
- Fitzgerald, C. & Gillis, K., 2006. Hydrothermal manganese oxide deposits from Baby Bare seamount in the northeast Pacific Ocean. *Marine Geology*, 225(1–4), pp.145–156.
- Ford, D. & Williams, P., 1989. *Karst geomorphology and hydrology* 1st ed., London and Boston: Springer.
- Försterra, G. et al., 2005. Shallow-water *Desmophyllum dianthus* (Scleractinia) from Chile: characteristics of the biocoenoses, the bioeroding community, heterotrophic interactions and (paleo)-bathymetric implications. In A. Freiwald & J. M. Roberts, eds. *Cold-Water Corals and Ecosystems*. Erlangen Earth Conference Series. Berlin Heidelberg: Springer Berlin Heidelberg, pp. 937–977. Available at: [http://dx.doi.org/10.1007/3-540-27673-4\\_48](http://dx.doi.org/10.1007/3-540-27673-4_48).
- Fryer, P. & Fryer, G., 1987. Origins of Nonvolcanic Seamounts in a Forearc Environment. In *Seamounts, Islands, and Atolls*. American Geophysical Union, pp. 61–72.
- Genin, A. et al., 1986. Corals on seamount peaks provide evidence of current acceleration over deep-sea topography. *Nature*, 322(6074), pp.59–61. Available at: <http://dx.doi.org/10.1038/322059a0>.
- Gianni, M. et al., 2011. *Unfinished business: a review of the implementation of the provisions of UNGA resolutions 61/105 and 64/72 related to the management of bottom fisheries in areas beyond national jurisdiction*, Available at: [http://scholar.google.ca/scholar?hl=en&q=Unfinished+business:+a+review+of+the+implementation+of+the+provisions+of+UNGA+resolutions+61/105+and+64/72+related+to+the+management+of+bottom+fisheries+in+areas+beyond+national+jurisdiction&btnG=Search&as\\_sdt=1,5&](http://scholar.google.ca/scholar?hl=en&q=Unfinished+business:+a+review+of+the+implementation+of+the+provisions+of+UNGA+resolutions+61/105+and+64/72+related+to+the+management+of+bottom+fisheries+in+areas+beyond+national+jurisdiction&btnG=Search&as_sdt=1,5&).
- Gilkinson, K. & Edinger, E., 2009. *The Ecology of Deep-Sea Corals of Newfoundland and Labrador Waters : Biogeography, Life History, Biogeochemistry, and Role as Critical Habitat*, St.John's, NL.
- Glasby, G., 1978. Deep-sea manganese nodules in the stratigraphic record: Evidence from DSDP cores. *Marine Geology*, 28(1–2), pp.51–64. Available at: <http://www.sciencedirect.com/science/article/pii/0025322778900968>.
- Gonzalez-Mirelis, G. & Buhl-Mortensen, P., 2015. Modelling benthic habitats and biotopes off the coast of Norway to support spatial management. *Ecological Informatics*. Available at: <http://www.sciencedirect.com/science/article/pii/S1574954115000953>.

- Greenan, B. et al., 2010. *Serial No. N5774 NAFO SCR Doc. 10/19 SCIENTIFIC COUNCIL MEETING--JUNE 2010*,
- Guisan, A. et al., 2007. Sensitivity of predictive species distribution models to change in grain size. *Diversity and Distributions*, 13(3), pp.332–340. Available at: <http://dx.doi.org/10.1111/j.1472-4642.2007.00342.x>.
- Hall-spencer, J. et al., 2007. Deep-sea coral distribution on seamounts , oceanic islands , and continental slopes in the Northeast Atlantic. *Bulletin of Marine Science*, 81(1), pp.135–146. Available at: <http://www.ingentaconnect.com/contentone/umrsmas/bullmar/2007/00000081/A00103s1/art00013>.
- Han, G. et al., 2008. Seasonal variability of the Labrador Current and shelf circulation off Newfoundland. *Journal of Geophysical Research*, 113(C10013), pp.1–23. Available at: <http://www.agu.org/pubs/crossref/2008/2007JC004376.shtml> [Accessed February 18, 2011].
- Hart, B., 1977. The mid-Cretaceous succession of Orphan Knoll (northwest Atlantic): micropaleontology and palaeo-oceanographic implications. *Deep Sea Research*, 24(3–4), pp.272–272. Available at: <http://linkinghub.elsevier.com/retrieve/pii/0146629177902958>.
- Hart, M., 1976. The mid-Cretaceous succession of Orphan Knoll (northwest Atlantic): micropalaeontology and palaeo-oceanographic implications. *Canadian Journal of Earth Sciences*, 13(10), pp.1411–1421.
- Haworth, R. & Keen, C., 1979. The Canadian Atlantic Margin: A Passive Continental Margin Encompassing an Active Past. *Tectonophysics*, 59, pp.83–126.
- Heindel, K. et al., 2010. The sediment composition and predictive mapping of facies on the Propeller Mound—A cold-water coral mound (Porcupine Seabight, NE Atlantic). *Continental Shelf Research*, 30(17), pp.1814–1829. Available at: <http://linkinghub.elsevier.com/retrieve/pii/S0278434310002645> [Accessed March 18, 2012].
- Henriet, J.P. et al., 2010. Mounds and sediment drift in the Porcupine Basin, west of Ireland. In *European Margin Sediment Dynamics*. Springer Verlag. Available at: <http://eprints.soton.ac.uk/55535/>.
- Heywood, W. & Sanford, B., 1976. *Geology of Southampton, Coats and Mansel Islands, District of Keewatin, Northwest Territories*, Dartmouth, NS.
- van Hinte, J. et al., 1995. Palaeozoic microfossils from Orphan Knoll, NW Atlantic Ocean. *Scripta Geologica*, 109, pp.1–63. Available at: <http://www.narcis.nl/publication/RecordID/oai:naturalis.nl:317524> [Accessed October 26, 2011].
- Hoffmann, M. et al., 2010. The Impact of Conservation on the Status of the World's Vertebrates. *Science*, 330(6010), pp.1503–1509. Available at: <http://www.sciencemag.org/content/330/6010/1503.abstract>.

- Hovland, M., Croker, P. & Martin, M., 1994. Fault-associated seabed mounds(carbonate knolls?) off western Ireland and north-west Australia. *Marine and Petroleum Geology*, 11(2), pp.232–246.
- Howell, K., Davies, J. & Narayanaswamy, B., 2010. Identifying deep-sea megafaunal epibenthic assemblages for use in habitat mapping and marine protected area network design. *Journal of the Marine Biological Association of the United Kingdom*, 90, p.33. Available at: [http://www.journals.cambridge.org/abstract\\_S0025315409991299](http://www.journals.cambridge.org/abstract_S0025315409991299).
- Huuse, M. & Feary, D., 2005. Seismic inversion for acoustic impedance and porosity of Cenozoic cool-water carbonates on the upper continental slope of the Great Australian Bight. *Marine Geology*, 215(3–4), pp.123–134. Available at: <http://www.sciencedirect.com/science/article/pii/S002532270400355X>.
- Huvenne, V.A.I. et al., 2009. Sediment dynamics and palaeo-environmental context at key stages in the Challenger cold-water coral mound formation; clues from sediment deposits at the mound base. *Deep-Sea Research Part I: Oceanographic Research Papers*, 56(12), pp.2263–2280. Available at: <http://ezproxy.library.dal.ca/login?url=http://search.proquest.com/docview/877398895?accountid=10406>.
- ICES, 2007. *Report of the Working Group on Deep-eater Ecology (WGDEC)*,
- Immenhauser, A. & Rameil, N., 2011. Interpretation of ancient epikarst features in carbonate successions — A note of caution. *Sedimentary Geology*, 239(1–2), pp.1–9. Available at: <http://www.sciencedirect.com/science/article/pii/S0037073811001503> [Accessed March 10, 2012].
- Jauer, C. & Budkewitsch, P., 2010. Old marine seismic and new satellite radar data: Petroleum exploration of north west Labrador Sea, Canada. *Marine and Petroleum Geology*, 27(7), pp.1379–1394. Available at: <http://linkinghub.elsevier.com/retrieve/pii/S0264817210000620> [Accessed October 27, 2010].
- Keen, C. et al., 1987. Deep crustal structure and evolution of the rifted margin northeast of Newfoundland: results from LITHOPROBE East. *Canadian Journal of Earth Sciences*, 24(8), pp.1537–1549. Available at: <http://dx.doi.org/10.1139/e87-150>.
- King, L. et al., 1985. Occurrence and regional geological setting of Paleozoic rocks on the Grand Banks of Newfoundland. *Canadian Journal of Earth Sciences*, 23, pp.504–526.
- Land, L., Paull, C. & Hobson, B., 1995. Genesis of a submarine sinkhole without subaerial exposure: Straits of Florida. *Geology*, 23(10), pp.949–951. Available at: <http://geology.gsapubs.org/cgi/content/abstract/23/10/949>.
- Laughton, A. et al., 1972. Site 111. *International Deep Sea Drilling Project*, (12), pp.33–159.
- Leaper, R. et al., 2011. Predictions of beta diversity for reef macroalgae across



- Marine Ecology Progress Series*, 339(3), pp.313–314. Available at: <http://www.int-res.com/abstracts/meps/v339/p313-314/>.
- Miles, L., Edinger, E. & Piper, D., 2015. Investigating the relationship between cold-water corals distribution and surficial geology. In *14th Deep-Sea Biology Symposium*. Aveiro, Portugal: DSBS, p. 1.
- Miller, K. et al., 2011. Out of their depth? Isolated deep populations of the cosmopolitan coral *Desmophyllum dianthus* may be highly vulnerable to environmental change. *PloS one*, 6(5), pp.1–10. Available at: [http://apps.webofknowledge.com.proxy-ub.rug.nl/full\\_record.do?product=UA&search\\_mode=GeneralSearch&qid=1&SID=T15EYVKBZuXIHfTAVsm&page=9&doc=87&cacheurlFromRightClick=no](http://apps.webofknowledge.com.proxy-ub.rug.nl/full_record.do?product=UA&search_mode=GeneralSearch&qid=1&SID=T15EYVKBZuXIHfTAVsm&page=9&doc=87&cacheurlFromRightClick=no).
- Miller, K. & Fairbanks, R., 1983. Evidence for Oligocene-Middle Miocene abyssal circulation changes in the western North Atlantic. *Nature*, 306(5940), pp.250–253. Available at: <http://dx.doi.org/10.1038/306250a0>.
- Monk, J. et al., 2010. Habitat suitability for marine fishes using presence-only modelling and multibeam sonar. *Marine Ecology Progress Series*, 420, pp.157–174. Available at: <http://www.int-res.com/abstracts/meps/v420/p157-174/> [Accessed March 18, 2012].
- Moore, J., Clague, D. & Normark, W., 1982. Diverse basalt types from Loihi seamount, Hawaii. *Geology*, 10(2), p.88.
- Mortensen, P. et al., 2006. *Deep-Water Corals In Atlantic Canada: A Summary Of ESRF-Funded Research (2001-2003)*, Report No. 143. Calgary, AB: Environmental Studies Research Funds.
- Moscardelli, L. et al., 2013. Seismic geomorphological analysis and hydrocarbon potential of the Lower Cretaceous Cromer Knoll Group, Heidrun field, Norway. *AAPG Bulletin*, 97(8), pp.1227–1248.
- Mullineau, L. & Mills, S., 1997. A test of the larval retention hypothesis in seamount-generated flows. *Deep Sea Research Part I: Oceanographic Research Papers*, 44(5), pp.745–770. Available at: [http://dx.doi.org/10.1016/S0967-0637\(96\)00130-6](http://dx.doi.org/10.1016/S0967-0637(96)00130-6) [Accessed March 9, 2011].
- NAFO, 2015. *NAFO Conservation and Enforcement Measures 2015*, Dartmouth, Nova Scotia, Canada B2Y 3Y9 Tel.: (902) 468-5590. Available at: [www.nafo.int](http://www.nafo.int).
- NAFO SCS, 2008. *Report of the NAFO Scientific Council Working Group on Ecosystem Approach to Fisheries Management (WGEAFM)*, Dartmouth, Canada.
- Neves, B., Du Preez, C. & Edinger, E., 2014. Mapping coral and sponge habitats on a shelf-depth environment using multibeam sonar and ROV video observations: Learmonth Bank, northern British Columbia, Canada. *Deep-Sea Research Part II: Topical Studies in Oceanography*, 99, pp.169–183. Available at: <http://dx.doi.org/10.1016/j.dsr2.2013.05.026>.
- O'Hara, T. et al., 2008. Cold-water coral habitats on seamounts: do they have a specialist fauna? *Global Ecology and Biogeography*, 14(6), pp.925–934. Available at:

- <http://blackwell-synergy.com/doi/abs/10.1111/j.1472-4642.2008.00495.x> [Accessed August 20, 2010].
- Paduan, J., Clague, D. & Davis, A., 2007. Erratic continental rocks on volcanic seamounts off the US west coast. *Marine Geology*, 246(1), pp.1–8.
- Parson, L. et al., 1984. Remnants of a submerged pre-Jurassic ( Devonian?) landscape on Orphan Knoll , offshore eastern Canada. *Canadian Journal of Earth Sciences*, 21(1), pp.61–66.
- Pautot, G., Auzende, J.-M. & Le Pichon, X., 1970. Continuous Deep Sea Salt Layer along North Atlantic Margins related to Early Phase of Rifting. *Nature*, 227(5256), pp.351–354. Available at: <http://dx.doi.org/10.1038/227351a0>.
- Pe-Piper, G. et al., 2013. Petrology and tectonic significance of seamounts within transitional crust east of Orphan Knoll, offshore eastern Canada. *Geo-Marine Letters*, 33(6), pp.433–447. Available at: <http://dx.doi.org/10.1007/s00367-013-0342-2>.
- Pettit, R., 2011. Culturability and Secondary Metabolite Diversity of Extreme Microbes: Expanding Contribution of Deep Sea and Deep-Sea Vent Microbes to Natural Product Discovery. *Marine Biotechnology*, 13(1), pp.1–11. Available at: <http://dx.doi.org/10.1007/s10126-010-9294-y>.
- Piper, D., 2005. *Hudson 2004-024 Cruise Report: Geohazards on the continental margin off Newfoundland*, Dartmouth, NS.
- Pitcher, C. et al., 2016. *Implications of current spatial management measures for AFMA ERAs for habitats - FRDC Project No 2014/204*, Brisbane.
- Pitcher, R. et al., 2012. Exploring the role of environmental variables in shaping patterns of seabed biodiversity composition in regional-scale ecosystems. *Journal of Applied Ecology*, 49(3), pp.670–679. Available at: <http://dx.doi.org/10.1111/j.1365-2664.2012.02148.x>.
- Pitcher, R., Ellis, N. & Smith, S., 2011. *Example analysis of biodiversity survey data with R package gradientForest*, Available at: <http://gradientforest.r-forge-project.org/biodiversity-survey.pdf>.
- Pohlman, J. et al., 2009. Methane sources in gas hydrate-bearing cold seeps: Evidence from radiocarbon and stable isotopes. *Marine Chemistry*, 115(1–2), pp.102–109. Available at: <http://linkinghub.elsevier.com/retrieve/pii/S0304420309000966> [Accessed November 19, 2010].
- Poirier, A. et al., 2011. Osmium isotopes in manganese nodules from the Labrador Sea. *Goldschmidt*, p.1. Available at: [www.minersoc.org](http://www.minersoc.org).
- Quilty, P., 1997. Eocene and younger biostratigraphy and lithofacies of the Cascade Seamount, East Tasman Plateau, southwest Pacific Ocean. *Australian Journal of Earth Sciences*, 44(5), pp.655–665.
- Reidenbach, M. et al., 2006. Boundary layer turbulence and flow structure over a fringing

- coral reef. *Limnology and Oceanography*, 51(5), pp.1956–1968. Available at: [http://www.aslo.org/lo/toc/vol\\_51/issue\\_5/1956.html](http://www.aslo.org/lo/toc/vol_51/issue_5/1956.html).
- Richer-de-Forges, B., Koslow, A. & Poore, G., 2000. Diversity and endemism of the benthic seamount fauna in the southwest Pacific. *Nature*, 405(6789), pp.944–947. Available at: <http://dx.doi.org/10.1038/35016066>.
- Roark, B. et al., 2009. Extreme longevity in proteinaceous deep-sea corals. *Proceedings of the National Academy of Sciences*, 106(13), pp.5204–5208. Available at: <http://www.pnas.org/content/106/13/5204.abstract>.
- Roberts, C., 2002. Deep impact: the rising toll of fishing in the deep sea. *Trends in Ecology & Evolution*, 17(5), pp.242–245. Available at: <http://www.sciencedirect.com/science/article/pii/S0169534702024928>.
- Roberts, M. et al., 2003. The cold-water coral *Lophelia pertusa* (Scleractinia) and enigmatic seabed mounds along the north-east Atlantic margin: are they related? *Marine Pollution Bulletin*, 46(1), pp.7–20. Available at: <http://www.sciencedirect.com/science/article/pii/S0025326X0200259X>.
- Roberts, M., Wheeler, A. & Freiwald, A., 2006. Reefs of the deep: the biology and geology of cold-water coral ecosystems. *Science*, 312(5773), pp.543–547. Available at: <http://www.ncbi.nlm.nih.gov/pubmed/16645087>.
- Roberts, S. & Nunn, J., 1995. Episodic fluid expulsion from geopressed sediments. *Marine and Petroleum Geology*, 12(2), pp.195–204. Available at: <http://www.sciencedirect.com/science/article/pii/0264817295928390>.
- Rodríguez-Martínez, M., 2011. Mud Mounds. In J. Reitner & V. Thiel, eds. *Encyclopedia of Geobiology*. Encyclopedia of Earth Sciences Series. Springer Netherlands, pp. 667–675. Available at: [http://dx.doi.org/10.1007/978-1-4020-9212-1\\_153](http://dx.doi.org/10.1007/978-1-4020-9212-1_153).
- Ruffman, A., 1989. First report of Ordovician (Caradoc-Ashgill) palynomorphs from Orphan Knoll, Labrador Sea: Discussion. *Canadian Journal of Earth Sciences*, 26(12), pp.2749–2751. Available at: [http://www.nrc.ca/cgi-bin/cisti/journals/rp/rp2\\_abst\\_e?cjes\\_e89-239\\_26\\_ns\\_nf\\_cjes26-89](http://www.nrc.ca/cgi-bin/cisti/journals/rp/rp2_abst_e?cjes_e89-239_26_ns_nf_cjes26-89).
- Ruffman, A., 2011. Orphan Knoll as a Window on the Palaeozoic : Seemingly ignored by the petroleum industry for 40 years. In *Recovery - CSPG CSEG CWLS Convention*. pp. 1–5.
- Ruffman, A. & van Hinte, J., 1973. Orphan Knoll—a“ chip” off the North American" plate. In *Earth Science Symposium on Offshore Eastern Canada*. Dartmouth, NS: Geological Survey of Canada (Atlantic), pp. 23–71.
- Rüggeberg, A. et al., 2005. Sedimentary patterns in the vicinity of a carbonate mound in the Hovland Mound Province, northern Porcupine Seabight. In A. Freiwald & J. M. Roberts, eds. Erlangen Earth Conference Series. Springer Berlin Heidelberg, pp. 87–112. Available at: [http://dx.doi.org/10.1007/3-540-27673-4\\_5](http://dx.doi.org/10.1007/3-540-27673-4_5).
- Santos, R.-S. et al., 2009. Toward the conservation and management of Sedlo Seamount: A case study. *Deep Sea Research Part II: Topical Studies in Oceanography*, 56(25),

- pp.2720–2730. Available at:  
<http://linkinghub.elsevier.com/retrieve/pii/S0967064508004578>.
- Shaw, J. et al., 2006. A conceptual model of the deglaciation of Atlantic Canada. *Quaternary Science Reviews*, 25(17–18), pp.2059–2081. Available at:  
<http://linkinghub.elsevier.com/retrieve/pii/S0277379106001326> [Accessed July 5, 2010].
- Sherwood, O. & Edinger, E., 2009. Ages and growth rates of some deep-sea gorgonian and antipatharian corals of Newfoundland and Labrador. *Canadian Journal of Fisheries Aquatic Science*, 66(1), pp.142–152. Available at:  
<http://dx.doi.org/10.1139/F08-195>.
- Shester, G. & Ayers, J., 2005. A cost effective approach to protecting deep-sea coral and sponge ecosystems with an application to Alaska’s Aleutian Islands region. In A. Freiwald & J. M. Roberts, eds. Erlangen Earth Conference Series. Springer Berlin Heidelberg, pp. 1151–1169. Available at: [http://dx.doi.org/10.1007/3-540-27673-4\\_59](http://dx.doi.org/10.1007/3-540-27673-4_59).
- Sibuet, J.-C., 1992. New constraints on the formation of the non-volcanic continental Galicia-Flemish Cap conjugate margins. *The Geological Society*, 149(5), pp.829–840. Available at: <http://jgs.lyellcollection.org/cgi/content/abstract/149/5/829>.
- Smee, J. et al., 2003. Orphan Basin , Offshore Newfoundland : New seismic data and hydrocarbon plays for a dormant Frontier Basin. In *Offshore Technology Conference*.
- Smith, J. et al., 1997. Rapid climate change in the North Atlantic during the Younger Dryas recorded by deep-sea corals. *Nature*, 386, pp.818–820. Available at:  
<http://www.nature.com/nature/journal/v386/n6627/abs/386818a0.html>.
- Srivastava, S. et al., 2000. Magnetic evidence for slow seafloor spreading during the formation of the Newfoundland and Iberian margins. *Earth and Planetary Science Letters*, 182(1), pp.61–76. Available at:  
<http://www.sciencedirect.com/science/article/pii/S0012821X00002314>.
- Stein, M., 2007. Oceanography of the Flemish Cap and Adjacent Waters. *Journal of Northwest Atlantic Fisheries Science*, 37(February), pp.135–146. Available at:  
<http://journal.nafo.int/37/stein/12-stein.pdf> [Accessed February 18, 2011].
- Tankard, A. & Balkwill, H., 1989. Extensional tectonics and stratigraphy of the North Atlantic margins. In *Extensional Tectonics and Stratigraphy of the North Atlantic Margins*. Calgary, AB: American Association of Petroleum Geologists, pp. 1–6.
- Thomson, R. et al., 2014. Congruence in demersal fish, macroinvertebrate, and macroalgal community turnover on shallow temperate reefs. *Ecological Applications*, 24(2), pp.287–299. Available at: <http://doi.wiley.com/10.1890/12-1549.1> [Accessed January 9, 2017].
- Thornburg, C., Zabriskie, M. & McPhail, K., 2010. Deep-Sea Hydrothermal Vents: Potential Hot Spots for Natural Products Discovery? *J. Nat. Prod.*, 73(3), pp.489–499. Available at: <http://dx.doi.org/10.1021/np900662k>.

- Toews, M. & Piper, D., 2002. *Recurrence interval of seismically triggered mass-transport deposition at Orphan Knoll , continental margin off Newfoundland and Labrador*, Dartmouth, NS.
- Tucholke, B., Sawyer, D. & Sibuet, J.-C., 2007. Breakup of the Newfoundland–Iberia rift. *Geological Society, London, Special Publications*, 282(1), pp.9–46. Available at: <http://sp.lyellcollection.org/content/282/1/9.abstract>.
- Via, R. & Thomas, D., 2006. Evolution of Atlantic thermohaline circulation: Early Oligocene onset of deep-water production in the North Atlantic. *Geology*, 34(6), pp.441–444. Available at: <http://geology.gsapubs.org/cgi/content/abstract/34/6/441>.
- Waller, R. et al., 2007. Anthropogenic impacts on the Corner Rise seamounts, north-west Atlantic Ocean. *Journal of the Marine Biological Association of the United Kingdom*, 87(5), pp.1075–1076. Available at: [http://www.journals.cambridge.org/abstract\\_S0025315407057785](http://www.journals.cambridge.org/abstract_S0025315407057785) [Accessed February 18, 2011].
- Wareham, V. & Edinger, E., 2007. Distribution of deep-sea corals in the Newfoundland and Labrador region , Northwest Atlantic Ocean. In R. Y. George & S. D. Cairns, eds. *Conservation and adaptive management of seamount and deep-sea coral ecosystems*. Miami: Rosentiel School of Marine and Atmosphere Science, University of Miami, pp. 289–313.
- Watanabe, S. et al., 2009. Patterns in abundance and size of two deep-water gorgonian octocorals, in relation to depth and substrate features off Nova Scotia. *Deep Sea Research Part I: Oceanographic Research Papers*, 56(12), pp.2235–2248. Available at: <http://linkinghub.elsevier.com/retrieve/pii/S0967063709001769> [Accessed February 18, 2011].
- Welford, K. et al., 2010. Structure across the northeastern margin of Flemish Cap, offshore Newfoundland from Erable multichannel seismic reflection profiles: evidence for a transtensional rifting environment. *Geophysical Journal International*, 183(2), pp.572–586. Available at: <http://dx.doi.org/10.1111/j.1365-246X.2010.04779.x>.
- Wendt, J. et al., 1997. The world’s most spectacular carbonate mud mounds (Middle Devonian, Algerian Sahara). *Journal of Sedimentary Research*, 67(Section A and B), pp.424–436.
- Wielens, H., MacRae, A. & Shimeld, J., 2002. Geochemistry and sequence stratigraphy of regional Upper Cretaceous limestone units, offshore eastern Canada. *Organic Geochemistry*, 33(12), pp.1559–1569. Available at: <http://www.sciencedirect.com/science/article/pii/S0146638002001031>.
- Wilson, M. et al., 2007. Multiscale Terrain Analysis of Multibeam Bathymetry Data for Habitat Mapping on the Continental Slope. *Marine Geodesy*, 30(1), pp.3–35. Available at: <http://www.informaworld.com/openurl?genre=article&doi=10.1080/01490410701295962&magic=crossref%7C%7CD404A21C5BB053405B1A640AFFD44AE3>.

- Workum, R., Bolton, T. & Barnes, C., 2011. Ordovician geology of Akpatok Island, Ungava Bay, District of Franklin. *Can. J. Earth Sci.*, 13(1), pp.157–178. Available at: <http://dx.doi.org/10.1139/e76-015>.
- Wright, D. & Goodchild, M., 1997. Data from the deep: implications for the GIS community. *International Journal of Geographical Information Science*, 11(6), pp.523–528. Available at: <http://www.ingentaconnect.com/content/tandf/tgis/1997/00000011/00000006/art00001>.
- Xu, Y., Eyles, N. & Simpson, M.J., 2009. Terrigenous organic matter sources in mid-pleistocene sediments from the orphan knoll, Northwest Atlantic Ocean. *Applied Geochemistry*, 24(10), pp.1934–1940. Available at: <http://www.sciencedirect.com/science/article/B6VDG-4WV77VG-1/2/7e4c6095d4f3c7f42008062fbd5e9664>.
- Yasuhara, M. et al., 2008. Abrupt climate change and collapse of deep-sea ecosystems. *Proceedings of the National Academy of Sciences*, 105, pp.1556–1560.
- Yesson, C. et al., 2011. The global distribution of seamounts based on 30 arc seconds bathymetry data. *Deep Sea Research Part I: Oceanographic Research Papers*, 58(4), pp.442–453. Available at: <http://www.sciencedirect.com/science/article/pii/S0967063711000392>.

## 4.8 Appendices

*Appendix 4-1. Potential habitat classification categories used for the Benthic Terrain Modeller (BTM) to make macro-habitat 'zones' and micro-habitat 'structures'.*

### Zones Categories

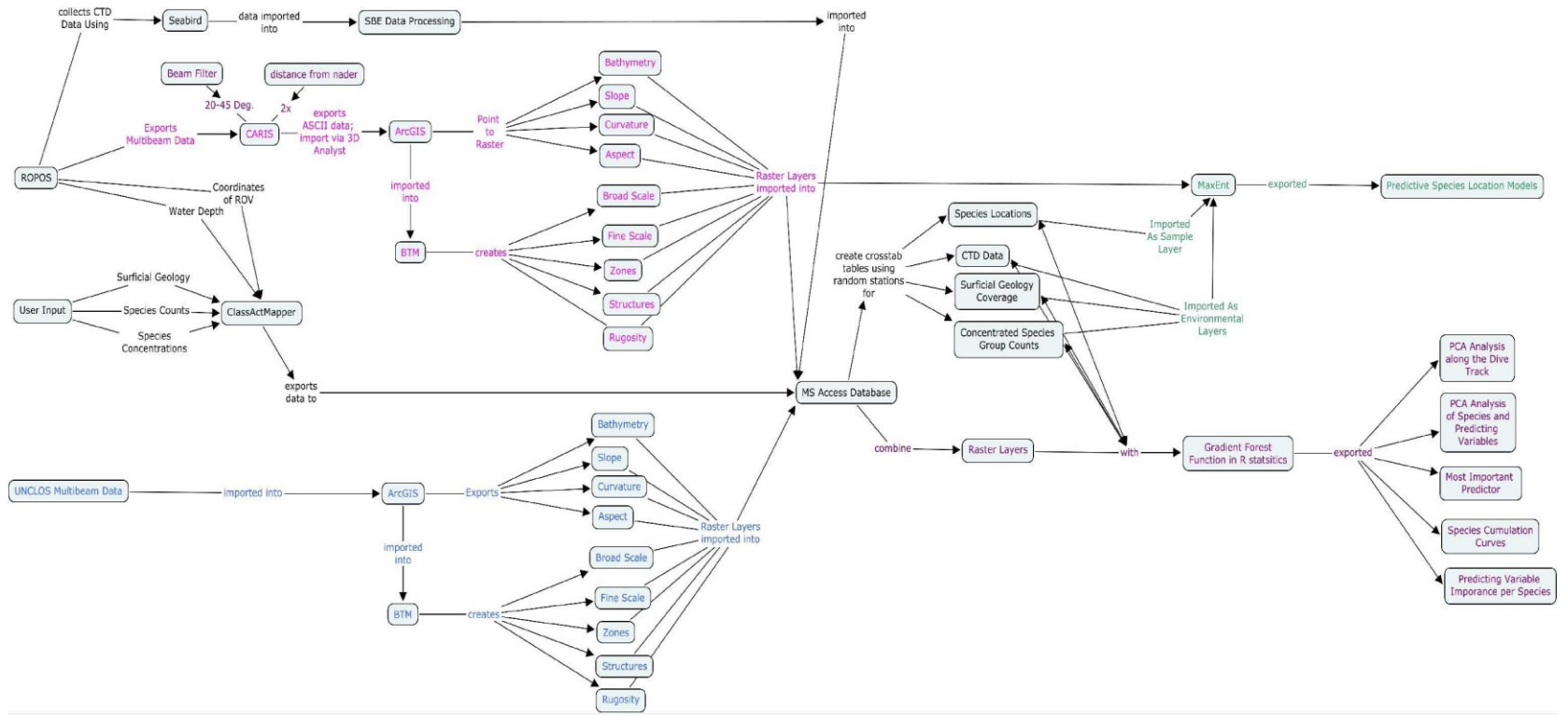
- 1 - Crests
- 2 - Depressions
- 3 - Flats
- 4 - Slopes

### Structures Categories

- 1 - Narrow Depression
- 2 - Depression on Flat
- 3 - Midslope Depression
- 4 - Depression on Crest
- 5 - Open Depression
- 6 - Broad Flat
- 7 - Shelf
- 8 - Escarpment
- 9 - Crest in Depression
- 10 - Crest on Flat
- 11 - Midslope Crest
- 12 - Narrow Crest
- 13 - Near Vertical Wall
- 14 - Broad Crest
- 15 - Deep Shelf (not detected)



### Appendix 4-2. Biological Data Extraction and Processing Flow Diagram







*Appendix 4-4. Coral megafauna recorded on Orphan Knoll and Orphan Seamount (D1340). O = order, G = genus, F = family, C = class. rF\_Overall\_Perf indicates which coral fauna performed well enough during RandomForest (rF) analysis to be used for gradientForest analysis.*

All_Sites	D1340	D1341	D1342	D1343	D1345	D1346	rF_Overall_Perf
Acanella_arbuscula	Acanella_arbuscula	Acanella_arbuscula	Acanella_arbuscula	Acanella_arbuscula	Acanella_arbuscula		Acanella_arbuscula
Acanthogorgia_armata	Acanthogorgia_armata	Acanthogorgia_armata			Acanthogorgia_armata		
Anthomastus_grandiflorus	Anthomastus_grandiflorus	Anthomastus_grandiflorus	Anthomastus_grandiflorus	Anthomastus_grandiflorus	Anthomastus_grandiflorus	Anthomastus_grandiflorus	
Anthoptilium_grandiflorum	Anthoptilium_grandiflorum						
Antipatharia_O	Antipatharia_O						
Bathypathes_G	Bathypathes_G	Bathypathes_G		Bathypathes_G	Bathypathes_G	Bathypathes_G	Bathypathes_G
Ceriantharia_O	Ceriantharia_O	Ceriantharia_O	Ceriantharia_O				
Chrysogorgia_spp	Chrysogorgia_spp	Chrysogorgia_G			Chrysogorgia_G	Chrysogorgia_G	Chrysogorgia_G
Desmophyllum_dianthus				Desmophyllum_dianthus			Desmophyllum_dianthus
Flabellum_spp	Flabellum_spp			Flabellum_G	Flabellum_G	Flabellum_G	Flabellum_G
Gersemia_spp	Gersemia_spp	Gersemia_G					
Isididae_F	Isididae_F	Isididae_F	Isididae_F	Isididae_F		Isididae_F	Isididae_F
Keratoisis_ornata	Keratoisis_ornata						Keratoisis_ornata
Paramuricea_clavata	Paramuricea_clavata						
Pennatula_aculeata	Pennatula_aculeata						
Pennatulacea_O	Pennatulacea_O	Pennatulacea_O		Pennatulacea_O			Pennatulacea_O
Stauropathes_arctica		Stauropathes_arctica	Stauropathes_arctica	Stauropathes_arctica			
Umbellula_encrinus	Umbellula_encrinus	Umbellula_encrinus		Umbellula_encrinus	Umbellula_encrinus		
Vaughanella_margaritata	Vaughanella_margaritata	Vaughanella_margaritata		Vaughanella_margaritata	Vaughanella_margaritata		Vaughanella_margaritata
Zoantharia_O	Zoantharia_O	Zoantharia_O		Zoantharia_O			Zoantharia_O



*Appendix 4-5. Sponge megafauna recorded on Orphan Knoll and Orphan Seamount (D1340). O = order, G = genus, F = family, C = class. rF\_Overall\_Perf indicates which coral fauna performed well enough during RandomForest (rF) analysis to be used for gradientForest analysis.*

All_Sites	D1340	D1341	D1342	D1343	D1345	D1346	rF_Overall_Perf
Euplectellidae_F	Euplectellidae_F	Euplectellidae_F		Euplectellidae_F	Euplectellidae_F	Euplectellidae_F	Euplectellidae_F
Hexactinellida_C							
Polymastia_G	Polymastia_G	Polymastia_G		Polymastia_G	Polymastia_G	Polymastia_G	Polymastia_G
Porifera_P	Porifera_P	Porifera_P		Porifera_P	Porifera_P	Porifera_P	Porifera_P

*Appendix 4-6. Other non-coral nor sponge megafauna recorded on Orphan Knoll and Orphan Seamount (D1340). O = order, G = genus, F = family, C = class. rF\_Overall\_Perf indicates which coral fauna performed well enough during RandomForest (rF) analysis to be used for gradientForest analysis.*

All_Sites	D1340	D1341	D1342	D1343	D1345	D1346	rF_Overall_Perf
Actinaria_O	Actinaria_O	Actinaria_O	Actinaria_O	Actinaria_O	Actinaria O	Actinaria_O	Actinaria_O
Asteroidea_C	Asteroidea_C	Asteroidea_C		Asteroidea_C	Asteroidea C	Asteroidea_C	
Crinoidea_C	Crinoidea_C	Crinoidea_C		Crinoidea_C	Crinoidea C	Crinoidea_C	Crinoidea_C
Echinoidea_C	Echinoidea_C			Echinoidea_C	Echinoidea C	Echinoidea_C	
Enteropneusta_C	Enteropneusta_C	Enteropneusta_C	Enteropneusta_C	Enteropneusta_C	Enteropneusta C	Enteropneusta_C	Enteropneusta_C
Holothuroidea_C	Holothuroidea_C	Holothuroidea_C	Holothuroidea_C	Holothuroidea_C	Holothuroidea C	Holothuroidea_C	Holothuroidea_C
Munidopsis_G	Munidopsis_G			Munidopsis_G	Munidopsis G	Munidopsis_G	
Mysidacea_O	Mysidacea_O	Mysidacea_O		Mysidacea_O	Mysidacea O	Mysidacea_O	
Ophiuroidea_C	Ophiuroidea_C	Ophiuroidea_C		Ophiuroidea_C	Ophiuroidea C	Ophiuroidea_C	Ophiuroidea_C
Pycnogonida_C	Pycnogonida_C	Pycnogonida_C		Pycnogonida_C	Pycnogonida C	Pycnogonida_C	



*Appendix 4-7. Grouped concentrations of megafauna recorded on Orphan Knoll and Orphan Seamount (D1340). O = order, G = genus, F = family, C = class. rF\_Overall\_Perf indicates which coral fauna performed well enough during RandomForest (rF) analysis to be used for gradientForest analysis.*

All_Sites	D1340	D1342	D1341	D1343	D1345	D1346	rF_Overall_Perf
Acanthogorgia_armata			Acanthogorgia_armata				Acanthogorgia_armata
Ceriantharia_O			Ceriantharia_O				Ceriantharia_O
Chrysogorgia_spp	Chrysogorgia_spp		Chrysogorgia_spp				Chrysogorgia_spp
Crinoidea_C				Crinoidea_C			Crinoidea_C
Gersemia_spp	Gersemia_spp						Gersemia_spp
Hexactinellida_C	Hexactinellida_C		Hexactinellida_C	Hexactinellida_C			Hexactinellida_C
Isididae_F	Isididae_F						Isididae_F
Ophiuroidea_C	Ophiuroidea_C						Ophiuroidea_C
Pennatulacea_O				Pennatulacea_O			Pennatulacea_O
Porifera_P	Porifera_P		Porifera_P				Porifera_P

## **5 Concluding Statements**

### **5.1 Physical Characterization of Orphan Knoll and Orphan Seamount**

Deep sea mounds could have a variety of origins. Carbonate mounds have been thoroughly studied in both the Atlantic and Pacific oceans and tend to be formed through coral reef development, hydro-thermal activity, cold seeps and oceanic ridges. The mounds of Orphan Knoll are none of these. The mystery of the Orphan Knoll mounds continues but only because the bedrock samples couldn't be 100% confirmed that the samples collected weren't just remnants of erosion, IRD and underlying bedrock. With that being said, the previously collected seismic data confirms one of the hypothetical situations; that the OK mounds are sections of listrically faulted blocks from a failed rift event, which could have been re-activated at any point in the Cenozoic to their present orientation. This research has eliminated several biogeochemical theories concerning the origins of the Orphan Knoll mound origins.

Future evidence concerning the provenience of the OK mounds could be verified with deeper bedrock samples into the exposed mounds of OK. It would most likely come from the NE mound field as the mound slopes down towards the abyssal plain east of Orphan Knoll. The presence of Fe-Mn nodules at the base of the SE Orphan Knoll mounds was a nice find, though not completely unexpected considering its proximity to oceanic crust and a seamount.

The Orphan Seamount proved to be as expected, a volcanic seamount. The basalt samples, though highly weathered, still provided some data for a chemical analysis (see associated publication (Pe-Piper et al. 2013)). The presence of lava tubes and the abundance of boulders, bedrock, cobbles have provided ample substrate for hard cold-water corals.

## **5.2 Deep-Sea Megafaunal Community Analysis**

Community ecology analysis methods are becoming more advanced as statistical packages such as gradientForest become easier to use and can identify changes in predicting variable gradients, that historically, wouldn't have been examined with such ease.

The Orphan Knoll and Orphan Seamount habitats were separated into three possible environments (seamount, knoll flats and knoll mounds / pinnacle type substrates).

The different variables showing higher accuracy in predicting changes in community turnover were different for various species of megafauna, but overall bathymetry out-performed oceanographic and surficial geology variables. Using the community turnover analysis, gradientForest identified changes in turnover on a species level by examination of the variables' gradients. All models have their limitations and when examining habitat and their drivers, having several predicting variables can be an advantage when trying to discover the restrictions of deep-sea distribution and abundance. Habitat models and community analysis continue to also be useful in helping identify

predicting variable importance and what variables would need to be managed in-order to better preserve sensitive marine habitats.

## **5.3 Emerging Issues**

### **5.3.1 Climate Change and the Deep-Sea**

Studies such as this one are rarities due to the high cost of deep-sea research. The data and samples collected in these areas of the deep sea have proven to be useful baseline datasets to better understand the different factors that drive community change within the megafaunal communities across various habitat types, not uncommon throughout the world's oceans. These data and analytical models such as gradientForest have identified Depth, Slope, Aspect, Conductivity, Density and substrate as the driving mechanisms that have created a baseline dataset allowing better understanding concerning which deep sea species are where and what factors or habitats may need protection in a changing climate.

### **5.3.2 Conservation and Preservation**

Present efforts to conserve the Orphan Knoll and Orphan Seamount include a fishing ban, until 2020. In a changing climate, motile megafauna might need to relocate (latitudinal or bathymetric) and the less motile species, if not already on deep slopes, could potentially be removed from their habitat by anthropogenic forcing (Danovaro et al. 2001; Yasuhara et al. 2008). An examination of ecologically and biologically sensitive marine areas should be continued, possibly in the form of predictive habitat models, using

a variety of explanatory variables. The decisions to protect and conserve marine biodiversity and marine habitat could benefit from doing community analysis through the integration of actual sample data (such as presented in this thesis) along with continuous oceanographic data.

On that same note of using multiple variables within community analysis models, the addition of anthropogenic forcings to the models such as fishing pressure, could improve management efforts in the world's oceans (Roberts 2002; Shester & Ayers 2005; Davies et al. 2007). Further management efforts using this dataset could benefit from using a variety of spatial habitat modeling, such as MaxEnt. Several countries' habitat protection organizations (e.g. CSIRO, NOAA, DFO, etc.) have already moved to using predictive spatial models such as MaxEnt (spatial predictions), MARXAN (spatial planning), gradientForest (community turnover analysis), GDM (biodiversity), etc., in an effort to better spatially understand the drivers of deep-sea biodiversity and in doing so, help protect and conserve these unique habitats (Ferrier et al. 2006; Ferrier et al. 2007; Guisan et al. 2007; Metaxas & Bryan 2007; Elith et al. 2010; Pitcher et al. 2011).